Canadian
Journal of Chemistry

ELECTROPHORESIS OF RESIN EMULSIONS
II. THE EFFECT OF ELECTROLYTE CONCENTRATION ON THE MOBILITIES AND ZETA POTENTIALS[1]

BY L. A. MUNRO AND F. H. SEXSMITH

ABSTRACT

Electrolyte concentration, rather than pH, concentration of resin particles, or dispersity, is the most significant variable affecting the mobility of polyvinyl acetate emulsions. The mobility–electrolyte concentration curves for latices prepared with nonionic and mixed nonionic and anionic emulsifiers, indicate micelle formation at low electrolyte concentrations. Zeta potentials calculated for a typical latex show the potential drop in the double layer to be of the order of 10^{-7} volts for a variation of thickness of the ionic atmosphere from 10^{-5} to 10^{-6} cm. over the range of salt concentration used.

INTRODUCTION

In a previous paper the effect of the chemical nature of the emulsifying agent on the mobility and sign of polyvinyl acetate emulsions was reported. It was noted that electrolyte concentration, rather than pH, concentration of resin particles, or dispersity, was the most significant variable affecting the mobility of any one emulsion.

The present paper describes the divergent effects of increasing electrolyte content on the mobilities of various emulsions and the zeta potential curve calculated for a very uniform latex.

EXPERIMENTAL

Incremental Salt Addition

A 3 liter stock suspension was prepared by diluting the given latex to an appropriate total solids content. Fifty-milliliter samples of each stock solution were then mixed with exactly equivalent volumes of pure, rigorously standardized solutions of sodium chloride. For each study at least 12 samples varying in salt concentration from 0 to 0.01 M were used. For salt concentrations below 2.57×10^{-4} M the electrolyte concentration of the samples was checked conductimetrically. It is in this low range that the effect of the salt on mobility is most significant.

The samples of latex with added electrolyte, after vigorous shaking, were allowed to stand for approximately twelve hours before the mobilities were
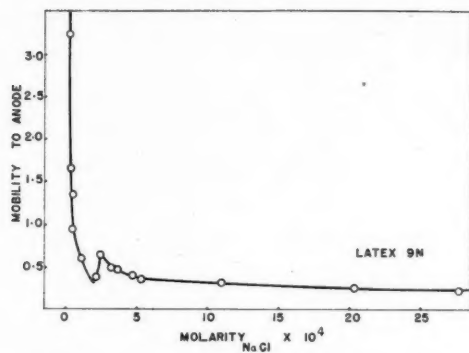
FIG. 1. Mobility curve for latex prepared with nonionic emulsifier.

FIG. 2. Mobility curve for a very uniform latex prepared with a nonionic emulsifier.
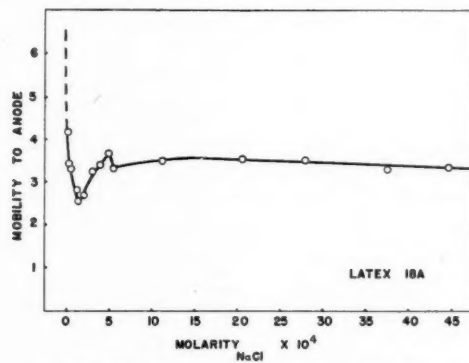
FIG. 3. Mobility curve of typical anionic latex.

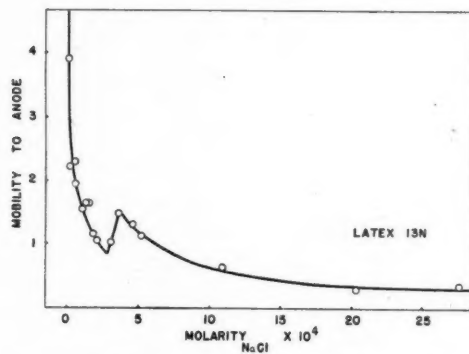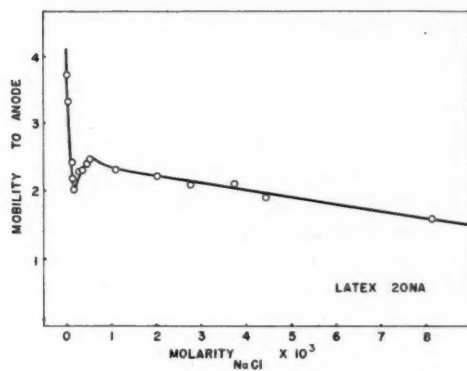FIG. 4. Mobility curve for a latex prepared with mixed nonionic and anionic emulsifiers.
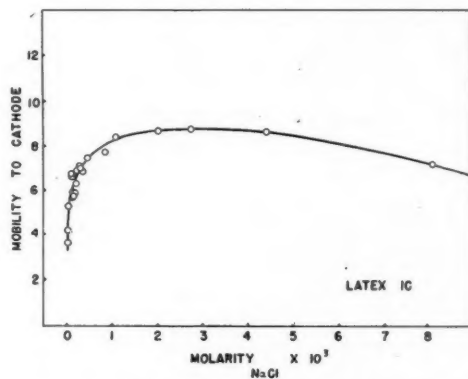
FIG. 5. Mobility curve for a latex prepared with a cationic emulsifier.
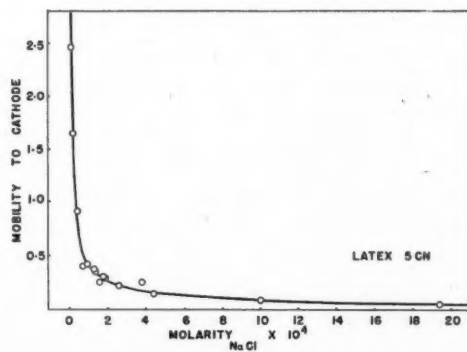
FIG. 6. Mobility curve for a latex prepared with mixed cationic and nonionic emulsifiers.

measured. The apparatus and technique were the same as previously described (12).

EXPERIMENTAL RESULTS

The experimental results for the emulsions described are shown graphically in Figs. 1–6. Figs. 1 and 2 are for two specimens prepared with nonionic emulsifying agents (9N213N), Fig. 3 represents the results using a latex prepared with an anionic agent (18A), Fig. 4 mixed nonionic and anionic emulsifiers (20NA) while Figs. 5 and 6 refer to emulsions prepared with cationic (1C) and mixed cationic and nonionic agents (5CN) respectively.

DISCUSSION

The most striking results of the electrophoretic investigations lie in the irregularities in the curves of mobility vs. concentration of sodium chloride. Similar irregularities in surface tension, interfacial tension, viscosity, light scattering, foaming characteristics with increasing concentration of surfactant or emulsifying agent have been reported in the literature (3, 18). The concentration at which such changes in direction of the curve take place has been termed the "critical concentration for the formation of micelles" or C.M.C.

The critical micelle concentration is an important factor in the mechanism of emulsion polymerization (6, 21). It is believed the C.M.C. represents the limit where solubilized colloidal salt or emulsifying agent begins to form a new phase of minute spherical droplets or micelles. Hartley (7) visualized these globules as being two ion lengths in diameter with polar heads outward in water and the long chains forming a hydrophobic interior. McBain (11) has postulated a lamellar micelle consisting of two layers of surface active molecules arranged side by side, the adjacent long chains forming a hydrophobic layer. The electron micrograph of a resin emulsion in which micelles of emulsifier are probably present (Fig. 7) would seem to confirm the postulated spherical shape.

The minima and maxima in our experimental curves are attributed respectively to the critical micelle concentration and to an increasing rate of removal of charge by added sodium chloride. The minima represent alterations in the distribution of soluble capillary-active substance between the bulk of the sol and the surface of the polyvinyl acetate particles. The total amount of emulsifying agent is constant in each latex system. In the absence of salt no micelles are present. When the proper amount of salt is added micelles begin to form and the mobility of the latex increases. This is effectively a lowering of the C.M.C. by added salt. The same situation could be promoted by adding additional quantities of the emulsifying agent used in the emulsion formulation as evidenced by the experiments of Powney and Wood (16, 17).

It is possible that the emulsifying layer increased in size by adsorption to a maximum, and being itself charged contributed a finite amount to the electrical density of each particle, increasing the mobility. Thereupon discrete

micelles began to form in the aqueous media. Although increasing concentration of salt steadily diminished the amount of solubilized colloid, it also had the effect of enhancing the retarding force of the Gouy ionic atmosphere around the particle. This explains the ultimate falling off in electrophoretic mobility. The "nonionic" emulsions which displayed C.M.C. may be assumed to be partially anionic.

Neither of the positively charged latices evidenced C.M.C. irregularities comparable with the mobility curves for nonionic and anionic emulsions. Latex 1C (Fig. 5) is known to have been made with an excess of cationic material. It is quite possible that the amount of detergent inherently present in the diluted samples was alone sufficient to exceed the C.M.C. Addition of salt immediately promoted micellar migration to the resin particle interfaces with attendant increase in positive electrophoretic mobility up to relatively high concentration of sodium chloride.
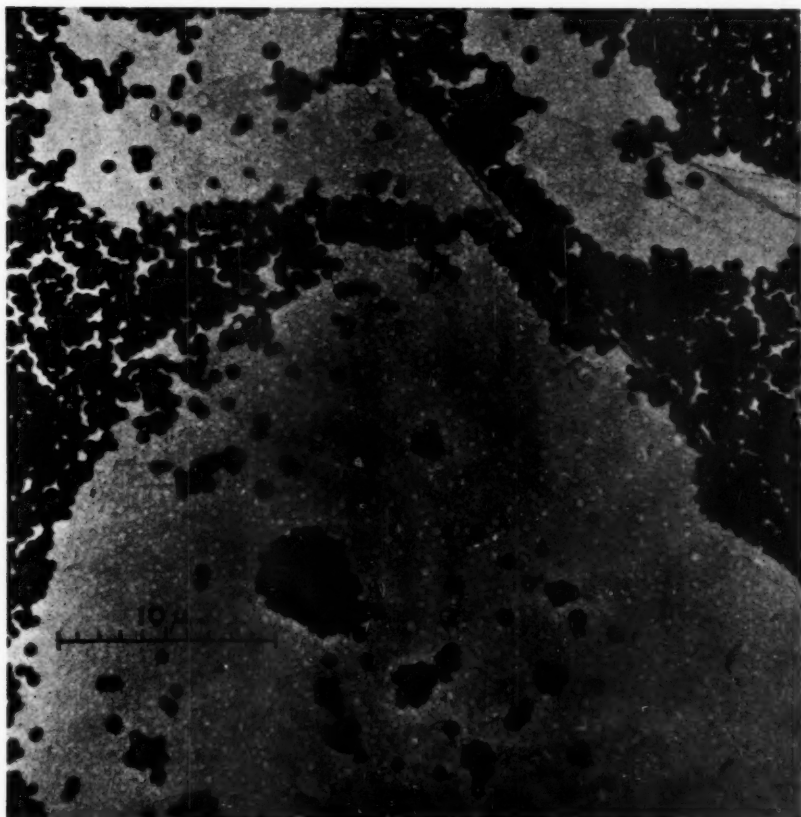
FIG. 7. Electron-micrograph of latex 13N.

Doscher has stated (4) that cationic materials above the critical concentration in general exhibit a strong tendency to be sorbed on surfaces as charged aggregates or micelles rather than as simple ions. This characteristic was used to explain the inability of cationic agents to effect suspension and their inefficiency as detergents (4). The sorption of these aggregates evidently results in a hydrophobic exterior regardless of the substrate to which they are attached. From this point of view the behavior of Latex 1C under salt addition is more easily explained.

On the other hand, emulsion 5CN was formulated using a minimum of emulsifying agent, a large percentage of which was nonionic material. The salt addition graph (Fig. 6) executed almost an exponential drop. Possibly any micellar phenomena were not revealed in electrophoresis owing to the combined effect of different protective colloids. This is proposed in view of the possible anionic character of the 'nonionic' agent used for emulsification. Another possibility is that dilution of the latex resulted in a low concentration of solubilized colloidal electrolyte. Hence, upon addition of salt, the micellar aggregation was of insufficient magnitude to affect the electrophoretic mobility.

It has already been shown by previous investigators that the mechanism of micelle formation from anionic colloids differs from anything observed with invert soaps or cationic materials. Schulman and Cocbain stated in contrast with the views of Doscher (4) that long chain quaternary ammonium compounds are too soluble in water and too highly ionized to form other than highly expanded vaprous films at oil–water interfaces (19). While investigating the electrophoretic mobility of oil drops in detergent solutions, Powney and Wood observed no C.M.C. irregularity when the colloidal addend was dodecylpyridinium chloride. Cassie and Palmer noted that their theories relating to the C.M.C. did not appear to apply even qualitatively for cationic surfactants (2).

It will be noted that the difference between the maximum and minimum mobilities near the critical micelle concentration increases as the character of the protective colloid becomes more anionic. The limiting mobility value follows the same trend.

The concept of a limiting mobility value has been suggested by Ham and Dean (5), who studied the effect of added salts on the mobility of octadecane dispersions. The mobility did not fall to zero, but decreased logarithmically, tending toward limiting values dependent on the valency of the added salt. The results of Ham and Dean inferred strongly that there was a limit beyond which salt addition could have no further electrokinetic effect.

ZETA POTENTIAL

The zeta potential of a typical latex was calculated by use of the Henry modification of the Smoluchowski equation (20). Henry's (8) equation also affords an estimate of the dimensions of the ionic layer of the latex particles. Various slight improvements have been suggested (1, 9, 10, 13, 14, 15) but none of the modifications gives corrections of more than negligible magnitude.

The Henry equation is: $U = \epsilon E \zeta F(b)/4\pi\eta$

where U = mobility

ϵ = dielectric constant

E = field strength

η = viscosity

The quantity (b) is directly related to the thickness of the ionic atmosphere. It has been equated to $\kappa(a)$ where $\kappa(a)$ is the radius of the colloidal particle independent of the double layer, and κ is the Debye-Huckel factor for the reciprocal of the ionic atmosphere thickness.

Table I gives the values for the quantities in the Henry–Smoluchowski equation for emulsion 13N at different concentrations of salt. $\kappa(a)$ values were derived from the experimental data. The large original electron micrograph from which Fig. 7 is reproduced served for determining particle size of latex 13N. This uniform latex had an average particle radius of 2.40×10^{-5} cm.

The $F(b)$ values were obtained from Henry's graph, except in three cases where $b > 25$. The latter were calculated from the appropriate equation (9). By these methods each correction was determined to three significant figures.

TABLE I

QUANTITIES IN HENRY–SMOLUCHOWSKI EQUATION FOR DIFFERENT CONCENTRATION OF SALT
(Emulsion 13N)

Salt conc., $M \times 10^{-5}$	Mobility, μ/sec./volt/ cm.	κ, cm.$^{-1} \times 10^{-5}$	$\kappa(a)$	$F(b)$	ζ, volts $\times 10^{7}$	Q, coulombs $\times 10^{9}$
0.838	3.90	0.951	2.28	0.708	8.73	5.50
1.59	2.23	1.31	3.15	0.727	4.87	3.86
5.00	2.30	2.33	5.58	0.764	4.77	6.04
5.13	1.95	2.36	5.65	0.767	4.02	5.13
10.6	1.55	3.39	8.13	0.800	3.08	5.32
13.0	1.63	3.76	9.01	0.813	3.19	6.14
15.5	1.64	4.09	9.83	0.828	3.14	6.52
18.3	1.15	4.45	10.67	0.838	2.17	4.85
20.5	1.05	4.71	11.29	0.844	1.97	4.66
30.8	1.02	5.77	13.83	0.865	1.88	5.35
36.1	1.47	6.25	14.98	0.875	2.66	8.17
46.3	1.31	7.07	16.95	0.886	2.34	8.07
52.2	1.12	7.51	18.00	0.891	1.99	7.26
109	0.622	10.9	26.02	0.919	1.09	5.68
203	0.275	14.8	35.58	0.931	0.49	3.50
276	0.339	17.3	41.40	0.939	0.57	4.68

Note: Viscosity measurements showed that the electroviscous effect was of no significance with the above samples.

Table I lists the mobility in cm. per sec. per volt per $\times 10^{4}$, molarity of sodium chloride $\times 10^{5}$, κ in cm. $^{-1} \times 10^{-5}$, ζ in volts $\times 10^{7}$, Q the particle charge in coulombs $\times 10^{9}$.

There is no regular trend in charge variation with electrolyte concentration. This is not unexpected particularly with nonionogenic emulsifiers.

Fig. 8 is a plot of the zeta potential versus salt concentration for emulsion 13N. This curve is very similar to the mobility curve, Fig. 2, showing the same minimum and maximum.
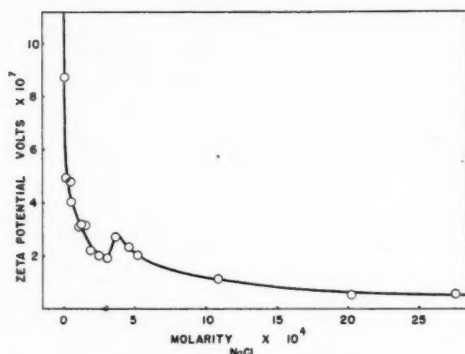
FIG. 8. The zeta potential for latex 13N at increasing concentration of salt.

In view of the opposing ideas as to whether there is any relation between the zeta potential and stability, a study of the stability of an emulsion with such a characteristic potential curve would be of interest.

ACKNOWLEDGMENTS

REFERENCES

 1. Booth, F.   Proc. Roy. Soc. (London), A, 203: 514.   1950.
 2. Cassie, A. B. and Palmer, R. C.   Trans. Faraday Soc. 43: 467.   1947.
 3. Corrin, M. L.   J. Colloid Sci. 3: 333.   1948.
 4. Doscher, T. M.   J. Colloid Sci. 5: 100.   1950.
 5. Ham, J. J. and Dean, E. M. D.   Trans. Faraday Soc. 36: 52.   1940.
 6. Harkins, W. D.   J. Polymer Sci. 5: 217.   1950.
 7. Hartley, G. S.   Kolloid-Z. 88: 22.   1939.
 8. Henry, D. C.   Proc. Roy. Soc. (London), A. 133: 106.   1931.
 9. Henry, D. C.   Trans. Faraday Soc. 44: 1021.   1948.
10. Hermans, J. J.   Phil. Mag. 7 (26): 650.   1938.
11. McBain, J. W.   J. Phys. Colloid Chem. 53: 39.   1949.
12. Munro, L. A. and Sexsmith, F. H.   Can. J. Chem. 31: 287.   1953.
13. Nakagaki, M.   J. Chem. Soc. Japan. 72: 113.   1951.
14. Overbeek, J. Th. G.   Kolloid-Beih. 54: 283.   1943.
15. Overbeek, J. Th. G.   Phillips Research Rep. !: 313.   1945.
16. Powney, J. E. and Wood, L. J.   Trans. Faraday Soc. 36: 57.   1940.
17. Powney, J. E. and Wood, L. J.   Trans. Faraday Soc. 37: 152.   1941.
18. Reichenberg, D.   Trans. Faraday Soc. 43: 467.   1947.
19. Schulman, J. H. and Cocbain, E. C.   Trans. Faraday Soc. 36: 662.   1940.
20. Smoluchowski, M.   Z. Physik Chem. 93: 129.   1918.
21. Staudinger, J. P. P.   Chemistry and Industry, 563.   1948.

A NOTE ON THE VALIDITY OF THE GIBBS-DALTON LAW AS APPLIED TO DILUTE MIXTURES OF WATER VAPOR WITH HYDROGEN, HELIUM, AND ARGON AT ROOM TEMPERATURES[1]

By E. A. Flood

ABSTRACT

Water vapor at room temperature and at pressures in the neighborhood of 10 mm. Hg behaves as a vacuum to each of the three gases hydrogen, helium, and argon, at pressures up to about 100 mm. Hg. The thermodynamic potentials of constituent gases in such mixtures of water vapor and hydrogen, water vapor and helium, etc. probably do not differ from those of the pure components, at equal volume concentrations, by more than 0.3%. Thus these gas mixtures obey the Gibbs–Dalton Law very closely and accordingly must also obey Dalton's Law. Velocity distribution functions of these gases under our experimental conditions are essentially Maxwellian.

INTRODUCTION

Gases which obey the ideal gas laws quite closely and whose mixtures obey Dalton's Law may interact with one another in a variety of ways and the gas mixtures thus deviate considerably from the Gibbs–Dalton Law (1). However, when the Gibbs–Dalton Law is obeyed Dalton's Law is necessarily obeyed, the former being a special case of the latter.

While the range of validity of Dalton's Law, as applied to mixtures of the more common gases and vapors, is fairly well known, there are comparatively few data available concerning the validity of the Gibbs–Dalton Law. McHaffie (3) has shown that air at 25 atmospheres exerts a very considerable positive solvent action on water vapor while exerting both a negative and positive solvent action at still higher pressures. Gillespie (2) has shown that both hydrogen and nitrogen at higher pressures exert a considerable solvent action of ammonia. In view of these data, it is hardly permissible to assume that such effects vanish entirely at pressures below one atmosphere. It may be remarked that there are a good many standard methods of measurement dependent on the assumption that the hydrogen, nitrogen, etc. behave as perfect vacua to various vapors. Thus the determination of the density of adsorbates by helium displacement and many dynamic methods of determining vapor pressure are entirely dependent on the assumption that the Gibbs–Dalton Law holds accurately as applied to the systems concerned.

From a purely theoretical point of view, the validity of the Gibbs–Dalton Law is of interest as providing a fairly sensitive test of the validity of the Maxwellian distribution. It is easily shown that kinetic theory model gases having velocity distribution functions only slightly different from the Maxwellian cannot behave as thermodynamically independent of one another, cannot have equal mean translational kinetic energies, and cannot obey the Gibbs–Dalton Law if their molecular weights differ appreciably.

Accordingly it seemed worth while to ascertain whether any departures from the Gibbs–Dalton Law could be detected in the case of mixtures of water vapor with such inert gases as helium, hydrogen, and argon in pressure regions where Dalton's Law might be expected to hold fairly accurately.

EXPERIMENTAL

When the Gibbs–Dalton Law holds for a gas mixture, the thermodynamic potentials of constituent gases are mutually independent. Thus, if water vapor and helium obey this law, the potential of the water in a given volume is not altered by the addition of helium. Since the interiors of simple ionic crystals such as NaBr and NaBr.$2H_2O$ will not be appreciably influenced by helium at lower hydrostatic pressures, the potential of water vapor in equilibrium with these salts will be constant at constant temperature. Accordingly, if helium influences the potential of water vapor, the concentration of water vapor in a mixture of helium and water vapor in equilibrium with these salts will depend on the helium concentration. The salt system thus behaves like a volume of pure water vapor at constant pressure separated from the gas mixture by a semipermeable membrane. Accordingly the experimental method used was to provide a large volume that could be opened to, or closed from, a small volume containing NaBr–NaBr.$2H_2O$, and to determine weights of water vapor contained within the large volume when equilibria had been established with the salt system, the equilibrations being carried out both in the presence and absence of diluent gases.
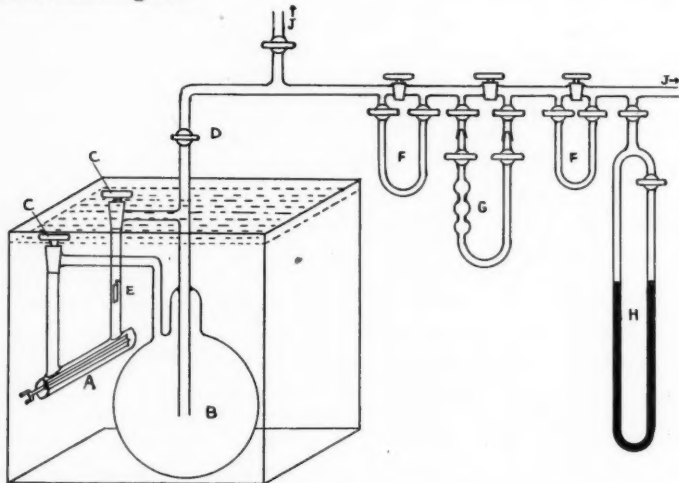
FIG. 1. A. Tube containing NaBr–NaBr.$2H_2O$ mixture and mechanical stirring device.
          B. 13 liter flask (13,060 ml. collection volume).
          C, C, D. Stopcocks.
          E. Vibratory circulator operated by electromagnet (not shown).
          F. Collecting traps containing brass wire to remove mercury.
          G. Weighing trap.
          H. Manometer.
          J. To pumping system, flowmeter, etc.
N.B. The drawing is not to scale.

The apparatus used is indicated diagrammatically in Fig. 1 and described in the legend.

The small salt-containing vessel (A) as well as the 13 liter flask (B) were immersed in a water thermostat whose temperature was maintained constant to within about ±0.005°C. During most of the experiments the temperatures were constant to within ±0.002°C. and were probably within ±0.01 of the mean temperature of all experiments, namely 26.2°C.

The procedures used were as follows: With the 13 liter flask (B) evacuated and cock (D) closed, cocks (C) were opened very slowly allowing water vapor to flow into the empty flask. The stirring device in (A) was then set in operation (the stirring device turned over about one-half of the total salt mixture once in every one or two seconds). After 48 hr. the stirring was discontinued, the systems allowed to stand for about one hour and the cocks (C) closed. The vapor contained in the 13 liter flask between cocks (C) and (D) was then removed by evacuation through liquid air traps, the traps containing brass wire coils to remove mercury. (Brass wire was found to be somewhat better than gold foil under our experimental conditions.) The water collected in the traps was distilled into a small weighing tube and finally the weight of water was obtained by comparison with the weight of duplicate counterpoise tube. The weights of water collected in this way, after a standardized procedure was adopted, are shown in the upper part of Table I following the legend "equilibria approached from zero water pressure".

TABLE I

WEIGHTS (GM.) OF WATER COLLECTED

Equilibria approached from zero H_2O pressure	0.1170 0.1173 0.1170	0.1167 0.1172 0.1167	0.1171 0.1168 0.1169 Mean 0.1170
Equilibria approached from H_2O pressure in mm. Hg as shown in parenthesis	0.1168 (12) 0.1173 (12) 0.1168 (13)	0.1171 (15) 0.1170 (15) 0.1178 (16)	0.1183 (18) 0.1181 (22) Mean 0.1174

A second series of experiments was carried out in which water vapor was introduced into the 13 liter (B) flask at pressures greater than the equilibrium pressure. The results are recorded in the lower part of Table I. Possibly, the values at higher initial water vapor pressure 18 and 22 mm. are significantly higher than the mean. Of course, higher values are to be expected, in general, when equilibria are approached from higher values and in this case appreciable adsorption effects are also to be expected at vapor pressures above 50% of saturation.

In order to determine what effect a diluent gas would have on the collection procedure and on introducing errors due to adsorption or desorption from the glass walls, etc., a series of experiments were carried out in which the equilibration procedures were essentially the same as in the first series, but where hydrogen at various pressures was introduced into the 13 liter flask (B) after

equilibrium concentration of water vapor had been attained therein, and the cocks (C) closed. The hydrogen pressures were calculated from Dalton's Law. (It may be remarked that previous experiments had shown that within our experimental error, Dalton's Law was obeyed for mixtures of water vapor at about 10 mm. and various pressures of hydrogen, helium, and argon. The experimental error in pressure readings was probably not more than 8%.) The mixture of water vapor and hydrogen was then removed from the 13 liter flask and the water collected as in the previous experiments. The weights of water so obtained are recorded in Table II. The data in Tables I and II thus

TABLE II

WEIGHTS OF H_2O COLLECTED (GM.). HYDROGEN AT PRESSURES (MM. Hg) SHOWN ADDED AFTER EQUILIBRATION. EQUILIBRATIONS APPROACHED FROM ZERO WATER PRESSURES EXCEPT WHERE SHOWN

0.1175 (8.0)	0.1169 (21.7)	0.1165 (44.5)
0.1171 (17.7)	0.1170 (28.5)	0.1169 (46.6)
0.1163 (17.7)	0.1172 (29.9)	0.1170 (50.0)
		Mean 0.1169
0.1184* (20.3)		
0.1168* (21.0)		
0.1187**(32.0)		
		Mean 0.1180

*Equilibrations approached from 11 mm.
**Equilibrations approached from 14 mm.

establish the weight of water vapor contained within the flask under equilibrium conditions as well as establishing some measure of the experimental error involved. The mean of all the control experiments is 0.1172 ± 0.0004. The exceptionally high figures are probably due to desorption errors. If these are excluded, the mean value is close to 0.1170 ± 0.0001.

In the final series of experiments, diluent gases were present in both the salt containing tube and the 13 liter flask during the equilibration period. The approach to equilibrium could be observed by cathetometer readings of the pressure changes involved. When the diluent gas pressures were less than 10 mm., equilibrium was attained quite rapidly. However, in all of these experiments equilibrations were carried out over periods from one to two weeks. It may be remarked that in the case of argon at pressures of 100 mm. or greater, equilibrium was not attained even after three weeks. While it was hoped that reliable results with diluent gas pressures up to one atmosphere could be obtained with this equipment (a vibrating 'reed' gas circulator (E) was provided with this end in view) it soon became apparent that in the presence of diluent gases at pressures near atmospheric, the times required for attainment of equilibria would be entirely impracticable. It may be remarked that the vibrating 'reed' type circulating pump that was installed in the equilibration system had been previously tested in a similar apparatus and was found to be capable of pumping air at atmospheric pressure at the rate of almost 4 liters per minute. Possibly the presence of diluent gas at higher pressures interferes with the dynamic equilibrium existing between interfaces of salt and its hydrate.

The weights of water collected when equilibrations were carried out in the presence of hydrogen, helium, and argon are recorded in Table III. Evidently the diluent gases do not change the thermodynamic potential of the water vapors. Some casual experiments were carried out using nitrogen and methane

TABLE III

WEIGHTS OF WATER COLLECTED (GM.)

Equilibration in Presence of Gases.—Weights of water collected. Equilibrium values approached from zero water pressures except where indicated. Initial diluent gas pressures in mm. Hg given in parentheses. V.P. H_2O 9.27 mm. Hg

Hydrogen	0.1172 (0.9)	0.1171 (3.0)	0.1168 (34.1)
	0.1168 (1.3)	0.1178* (12.7)	0.1171 (82.6)
	0.1169 (4.9)	0.1168 (13.4)	0.1170 (83.1)
			Mean 0.1171
Argon	0.1178 (3.1)	0.1181 (10.0)	0.1168 (22.0)
	0.1168 (4.9)	0.1167 (10.3)	0.1168 (56.4)
	0.1168 (6.1)	0.1169 (21.8)	0.1168** (56.8)
			Mean 0.1171
Helium	0.1170 (10.6)	0.1165 (113.6)	
	0.1168 (10.6)	0.1173 (229.8)	
	0.1170 (20.3)		
			Mean 0.1169

*Equilibrium approached from 11 mm. H_2O pressure.
**Equilibrium approached from 9.5 mm. H_2O pressure.

at pressures of about 2 cm. The weights of water collected were essentially the same. The equilibrium pressure of water vapor over NaBr–NaBr.2H_2O was found to be 9.27 mm. ±0.05 mm. at 26.2°C.

CONCLUSION

Water vapor at room temperature and at pressures in the neighborhood of 10 mm. Hg behaves as a vacuum to each of the three gases hydrogen, helium, and argon, at pressures up to about 100 mm. Hg. The thermodynamic potentials of constituent gases in such mixtures of water vapor and hydrogen, water vapor and helium, etc., probably do not differ from those of the pure components, at equal volume concentrations, by more than 0.3%. Thus these gas mixtures obey the Gibbs–Dalton Law very closely and accordingly must also obey Dalton's Law. Velocity distribution functions of these gases under our experimental conditions are essentially Maxwellian.

REFERENCES

1. FLOOD, E. A. and BENSON, G. C. Can. J. Research, B, 27: 988. 1949.
2. GILLESPIE, L. Phys. Rev. 36: 121. 1930.
3. McHAFFIE, I. R. Phil. Mag. 1: 561. 1926.

NOTE ON THE DIELECTRIC CONSTANTS OF ETHYL CHLORIDE AND n-BUTANE ADSORBED ON NONPOROUS TiO$_2^1$

BY M. H. WALDMAN,[2] J. A. SNELGROVE,[3] AND R. MCINTOSH[4]

ABSTRACT

The dielectric constants of ethyl chloride and n-butane adsorbed on nonporous TiO$_2$ were measured. The plot of capacity change versus volume adsorbed was found to reveal two linear sections in the case of ethyl chloride with an abrupt change in the slope of the plot occurring at the V_m value calculated using the B.E.T. or Hüttig adsorption equations. With n-butane the plot was linear beyond V_m. For ethyl chloride on rutile a slight temperature dependence in the polarization was observed for the volume of gas adsorbed above V_m, while a negligible temperature dependence was noted for the portion below V_m. It is postulated that the observations with the polar gas on the nonporous rutile can be explained by a change from oscillatory to rotational motion of the adsorbed molecule after the monolayer is complete. It was noted that gases adsorbed on nonporous TiO$_2$ behaved differently from gases adsorbed on porous silica gel. This appears to lead to the necessity of postulating changes of density for the adsorbed phase on silica gel.

INTRODUCTION

In earlier work the dielectric properties of gases adsorbed on porous gels have been examined. Because of the relatively large quantities which can be adsorbed on porous adsorbents, the measurements are more readily carried out, but the porous structure of the adsorbent complicates the adsorption process and renders any correlation of the electrical data with adsorption theories very difficult to make. Thus it has not yet been established whether the discontinuities of the slopes of the plots of capacity change of test cell versus volume of gas adsorbed, observed by Higuti (3), Kurbatov (5), and in this laboratory (6, 8), are associated with the completion of the unimolecular layer, variations of the density of the adsorbate, or interactions which influence the rotational or oscillatory motions of the adsorbed molecules. In an attempt to distinguish among these possibilities, the dielectric properties of ethyl chloride and n-butane, adsorbed on TiO$_2$ (rutile) of specific surface to nitrogen equal to 85 sq. meters, have been determined. The adsorbent is believed to be nonporous. Owing to the comparatively small specific surface, the electrical data are less precisely defined than when activated silica gel was employed. Nevertheless, typical data given below indicate that:

(1) On a nonporous adsorbent a polar adsorbate may exhibit a sudden change of electrical properties at some critical quantity of adsorbed matter.

(2) This change was not observed using the nonpolar adsorbate.

(3) The critical quantity of the polar adsorbate agrees remarkably well with the volume required to complete the unimolecular layer (V_m) when this volume is computed by either the B.E.T. (1) or Hüttig adsorption equations (4).

998

(4) Certain distinctions between the behavior of adsorbates on porous and nonporous adsorbents are clear, and presumably may be accounted for on the basis of the structures of the adsorbents.

In this preliminary report no attempt will be made to discuss all the observed phenomena. The difference of behavior of the polar and nonpolar adsorbates on the nonporous adsorbent is of fundamental importance, however, as it seems to show that the type of discontinuity to be described below is attributable to the polar character of the adsorbate, and not to the density of the adsorbed film.

EXPERIMENTAL

The experimental procedures were essentially those previously described (6, 8). Mercury cutoffs were used instead of stopcocks in order to prevent
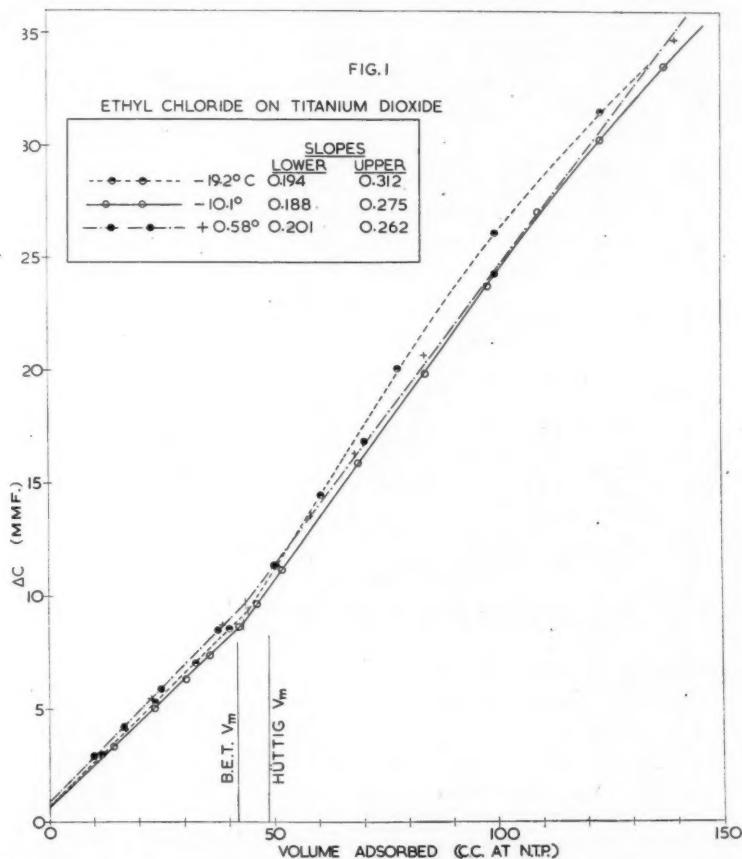
FIG. 1. Plots of capacitance change versus volume adsorbed for ethyl chloride on rutile at various temperatures.

errors in the quantity adsorbed due to the solubility of the gases in the stop-cock grease. All electrical measurements were made at the single frequency of 3.70 mc. per sec. since no Debye type dispersion was apparent up to that frequency.

The solid adsorbent was obtained from Dr. J. A. Morrison, of the National Research Council. Its preparation and some of its properties have been reported by Morrison, Los, and Drain (7).

RESULTS

Typical results using ethyl chloride are shown in Fig. 1. The sudden change of slope, which occurs at the computed $V_m{}^*$ value, should be noted. Fig. 2
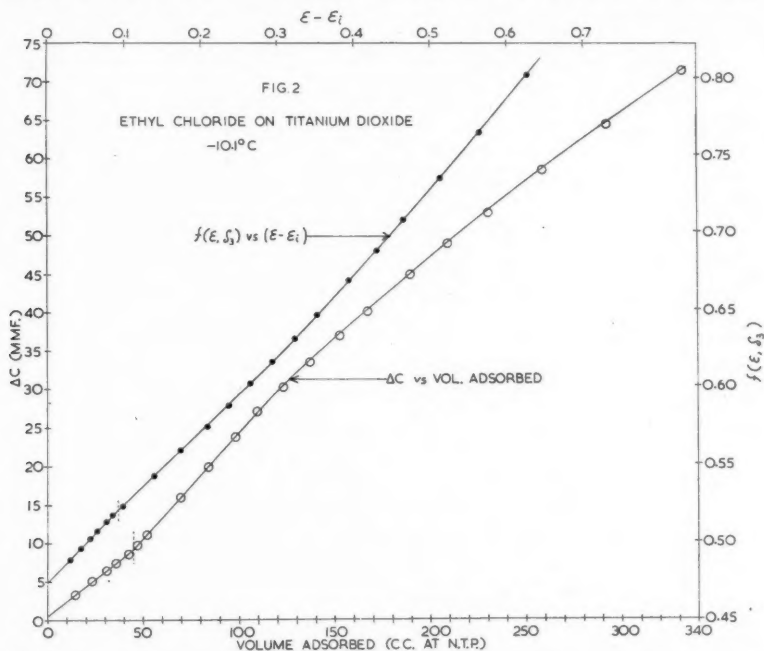
FIG. 2. (a) Plot of capacitance change versus volume adsorbed for ethyl chloride on rutile at $-10.1°C$. (b) Plot of $f(\epsilon, \delta_3)$ versus $(\epsilon - \epsilon_i)$ for ethyl chloride on rutile at $-10.1°C$.

shows results at $-10.1°C$. in greater detail to emphasize the sharpness of the discontinuities of the slopes in both the plot of the primary data and in that of the functional plot from which the polarization is calculated (6). It should also be noted that the material adsorbed beyond V_m has a higher polarizability than that adsorbed before V_m. This is in contrast with results obtained when the adsorbent was activated silica gel (6).

As shown in Table I, the polarization of the material adsorbed is approximately the same as that of bulk liquid for the first material adsorbed on silica

*B.E.T. $V_m = 41.9$ cc.; Hüttig $V_m = 47.8$ cc.

TABLE I

DIELECTRIC CONSTANTS AND POLARIZATIONS FOR ETHYL CHLORIDE AND
n-BUTANE ADSORBED ON TiO_2 AND SILICA GEL

	Dielectric constant			Polarization per cc.			
	Section 1	Section 2	By Onsager formula	Section 1	Section 2	By Onsager formula	Temp.,°C.
Ethyl chloride on TiO_2	5.70	11.14	12.31	0.61	0.77	0.79	−19.2
	5.84	8.65	11.68	0.62	0.72	0.78	−10.1
	6.30	7.82	11.00	0.64	0.69	0.77	0.58
	6.16	7.77	11.00	0.63	0.69	0.77	0.60
Ethyl chloride on silica gel	8.66	4.36	10.9	0.72	0.53	0.77	0.1
	7.89	4.14	10.0	0.70	0.51	0.75	15.0
			By R.I.			By R.I.	
Butane on TiO_2	2.05	. .	1.80	0.26	. .	0.21	5.3
Butane on silica gel	1.80	1.61	1.79	0.21	0.17	0.21	0.1
	1.78	1.58	1.79	0.21	0.16	0.21	15.0

R.I. = Refractive Index.

gel. In the case of ethyl chloride on rutile this is so for the adsorbate taken up after the unimolecular layer is completed. Thus the two cases are distinct in that the change of polarizability with amount adsorbed is from higher to lower values on silica, but from lower to higher values on rutile.
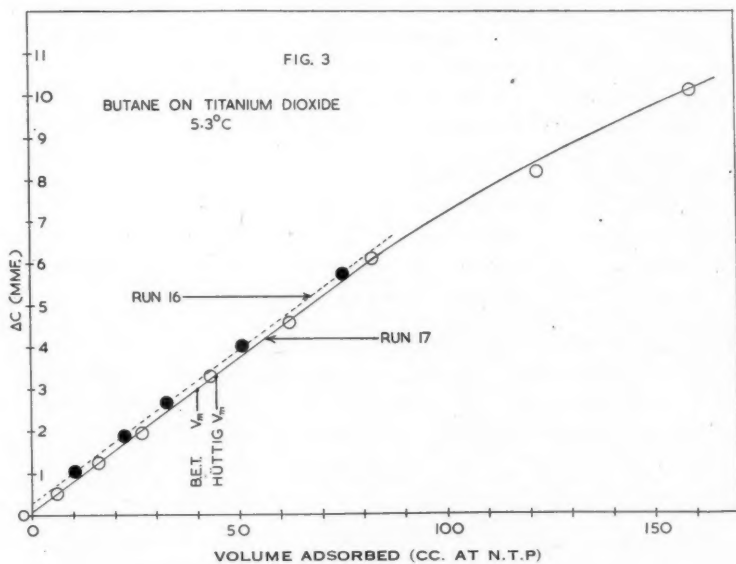
FIG. 3. Plot of capacitance change versus volume adsorbed for n-butane on rutile at 5.3°C.

The existence of a temperature coefficient of polarizability for ethyl chloride beyond V_m seems established, while a very small or possibly zero temperature coefficient is observed before the V_m value. This is again opposite to the observations made when silica gel was used as the adsorbent.

In Fig. 3 are shown two experiments using butane. Within the limits of the reproducibility of the measurements the plots are linear to volumes adsorbed well above V_m, and thus no change of electrical properties is observed. A discontinuous change to a lower value was observed on silica gel, however. This result very strongly suggests that density variations associated with the porous structure of the silica gel are required to explain the results found using silica, and that the behavior found using ethyl chloride on rutile is not caused by such factors.

The values of polarization given in the table are based on the use of the density of the liquid state to evaluate the volume of the dielectric occupied by adsorbed matter. The somewhat greater value of the polarization of butane than is calculated using known refractive index data (2) suggests that the packing is somewhat closer than for the bulk liquid state. However, the increase of capacity of the test cell caused by the adsorption of butane is comparatively small, and until the value of the polarization reported here is thoroughly established, comment on this point is not warranted.

CONCLUSIONS

Snelgrove and McIntosh (9) have shown that a negligible temperature coefficient would signify oscillatory motion while a negative temperature coefficient would suggest rotational motion of the adsorbed molecule. Therefore, since a negligible temperature coefficient below V_m and a negative temperature coefficient above V_m was observed, the data for ethyl chloride can apparently be accounted for by postulating that the molecules are oscillators when adsorbed into the first layer, and may rotate, showing the dielectric properties of the bulk liquid in higher layers. Since the isosteric heat of adsorption is high (9500–7000 cal. per mole) for quantities adsorbed less than V_m, it is to be expected that the first layer would be substantially complete before adsorption into higher layers is appreciable. Thus the agreement found between the V_m values by adsorption and the V_m values obtained from the position of the discontinuity seems reasonable, and for such systems the electrical data yield a value of V_m.

Since no changes of the properties of butane are observed as the amount adsorbed passes through V_m, there is no suggestion that variations of the density of the film occur. This must also mean that the results with butane and silica gel are explicable on the basis of the density of the adsorbate.

ACKNOWLEDGMENT

REFERENCES

1. BRUNAUER, S., EMMETT, P. H., and TELLER, E. J. Am. Chem. Soc. 60: 309. 1938.
2. GROSSE, A. V. J. Am. Chem. Soc. 59: 2739. 1937.
3. HIGUTI, I. Bull. Inst. Phys. Chem. Research, (Tokyo), 20: 489. 1941.
4. HUTTIG, G. F. Monatsh. 78: 177. 1948.
5. KURBATOV, L. N. Doklady Akad. Nauk. S.S.S.R. 63: 557. 1948. (From translation of Scientific Information Service, Defence Research Board, Ottawa, by E. Hope.)
6. McINTOSH, R., RIDEAL, E. K., and SNELGROVE, J. A. Proc. Roy. Soc. (London), A, 208: 292. 1951.
7. MORRISON, J. A., LOS, J. M., and DRAIN, L. E. Trans. Faraday Soc. 47: 1023. 1951.
8. SNELGROVE, J. A., GREENSPAN, H., and McINTOSH, R. Can. J. Chem. 31: 72. 1953.
9. SNELGROVE, J. A. and McINTOSH, R. Can. J. Chem. 31: 84. 1953.

THE INFRARED SPECTRA OF ALPHA AND BETA OXIMES[1]

By Ann Palm[2] and Harold Werbin[3]

ABSTRACT

The spectra of several isomeric oximes in the solid state were examined in the range 700–3600 cm^{-1}. The associated OH stretching frequency near 3250 cm.$^{-1}$ in the α oximes is displaced towards lower frequency in the β oximes. The region of the OH stretching mode of several oximes was also studied in benzene and chloroform solutions. The frequencies near 1300 cm.$^{-1}$ and 920 cm.$^{-1}$ are tentatively assigned to the OH deformation and the N-OH stretching modes, respectively. No consistent differences are observed between the α and the β oximes with respect to these vibrations. The band at approximately 1640 cm.$^{-1}$ ascribed to the $C=N$ vibration remains essentially unchanged in the spectra of the two isomeric forms.

Although the infrared spectra of several oximes that are of value as analytical reagents have been reported (10, 23), a review of the literature indicates that no serious attempts have been made to compare the infrared spectra of the α and β oximes. The 7000 cm.$^{-1}$ region (first overtone of the OH stretching frequency) of dilute carbon tetrachloride solutions of α and β benzilmonoximes (16) were found to be identical while α benzoinoxime acetate showed two weak bands that did not appear in the β form (24).

The spectra of α and β oximes are not expected to be identical since the arrangement and bonding of the atoms in the molecule give rise to characteristic absorption bands. The present investigation was undertaken, therefore, in order to determine possible differences in the infrared spectra of the two isomeric forms. The data presented in this report on 15 oximes in the solid state, 10 of which are geometric isomers, demonstrate that one can distinguish between the α and β compounds on the basis of the position of the OH stretching frequency.

EXPERIMENTAL

Infrared Spectra

The spectra were recorded in the region 700–3600 cm.$^{-1}$ with a Perkin-Elmer Model 21 double-beam spectrometer. The crystalline compounds were dried over phosphorus pentoxide, ground to a fine powder to reduce the scattering effect, and measured between two salt plates as Nujol mulls. The solutions (about 0.02 M) were examined in sodium chloride cells of 0.03 mm. thickness. The instrument was set at a slit schedule of 4 and speed 3 for each run. Duplicate spectra of the same compound did not differ by more than ± 10 cm.$^{-1}$ at 3000 cm.$^{-1}$ and ± 5 cm.$^{-1}$ at 1500 cm^{-1}.

Materials

The following oximes were commercial samples and, with the exception of α-benzaldoxime which was used directly, were recrystallized until the melting

points agreed with those reported in the literature: α-benzilmonoxime, benzophenone oxime, cyclohexanone oxime, acetophenone oxime, and N-benzylidineaniline. The α- and β-*p*-chloro- and α-*o*-chlorobenzaldoximes were prepared according to Erdmann and Schwechten (11). The β-benzilmonoxime, m.p. 112°C., was prepared by following the directions of Taylor and Marks (21), but it required repeated recrystallization from benzene to reach that melting point. β-Benzaldoxime melted at 128°C. after being recrystallized twice from petroleum ether (4). The α-nitrobenzaldoximes were prepared in the usual manner (13). The methods of Forster and Dunn (12) were employed in the preparation of β-*o*- and *p*-nitrobenzaldoximes which melted at 145° and 174°, respectively. They reported 154° and 184°, while others have found 143–145° for the *o*-nitro oxime and 177° for the *p*-nitro oxime (6, 17). An attempt was made to convert the α-*m*-nitrobenzaldoxime, m.p. 121°, into the β isomer by the above procedure (12). The resulting compound melting at 119° (Forster and Dunn obtained 123°) was believed to be the β oxime; however, the infrared spectrum was identical with that of the α oxime, indicating that the β oxime had not been made.

Analytical reagent grade benzene and chloroform were used for the solution studies. The solvents were dried and distilled before use.

RESULTS AND DISCUSSION

In Fig. 1 is summarized an abbreviated form of the infrared spectra of the α and β oximes in the solid state. The 1700–2900 cm.$^{-1}$ region is omitted in the diagram. The absorption bands due to OH stretching, OH deformation, and
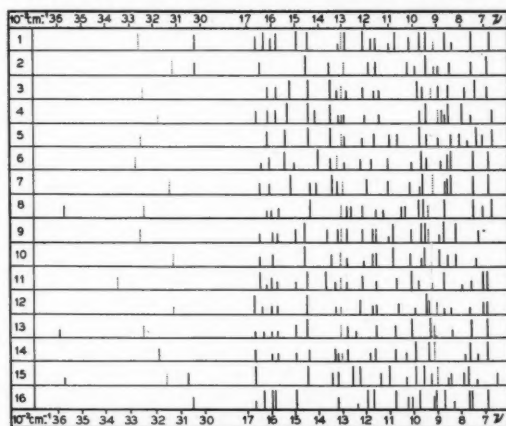
FIG. 1.   Infrared spectra of:
1. α-Benzaldoxime
2. β-Benzaldoxime
3. α-*o*-Nitrobenzaldoxime
4. β-*o*-Nitrobenzaldoxime
5. α-*m*-Nitrobenzaldoxime
6. α-*p*-Nitrobenzaldoxime
7. β-*p*-Nitrobenzaldoxime
8. α-*o*-Chlorobenzaldoxime
9. α-*p*-Chlorobenzaldoxime
10. β-*p*-Chlorobenzaldoxime
11. α-Benzilmonoxime
12. β-Benzilmonoxime
13. Acetophenone oxime
14. Benzophenone oxime
15. Cyclohexanone oxime
16. N-Benzylideneaniline

N–OH stretching vibrations occurring at about 3200, 1300, and 920 cm.$^{-1}$, respectively, which appear to differ the most, are represented by dotted lines. The height of the line gives an indication of the intensity of the band represented.

The OH stretching mode could be assigned unambiguously, while the $C = N$, the OH deformation, and the N–OH vibrations were located with less certainty because of interfering bands due to C–H vibrations.

In the spectra of the α oximes the OH absorption band is found at about 3250 cm.$^{-1}$, whereas it appears near 3115 cm.$^{-1}$ in the β oximes. This frequency shift is noted in the spectra of each pair of isomeric oximes. It would indicate that the OH vibrations are more strongly bonded in the β isomers (1, 2). This increase in the strength of the hydrogen bridge is in line with the higher melting points of the β oximes (with the exception of β-benzilmonoxime), their larger conductivities (18) and previous studies on carboxylic acids which demonstrate that an increase in acidity is accompanied by a shift in the OH stretching vibration to lower frequency (9, 22).

Reference to Table I suggests that the oximes are associated both in the crystalline state and to a somewhat lesser extent in solution. The spectra of the

TABLE I
O–H ABSORPTION BANDS (FREQUENCIES IN CM.$^{-1}$)

Compound	In Nujol		In benzene		In chloroform	
	α	β	α	β	α	β
Benzilmonoxime	3345(m)	3110(w,bd)	3250(w)	3485(m)	3520(w) 3250(w,bd)	3570(w) 3200(w)
Benzaldoxime	3260(s,bd)	3115(m,bd)	*n.m.*	3520(w) 3240(w,bd)	*n.m.*	3570(w) 3270(m,bd)
o-Nitro- benzaldoxime	3240(m)	3175(w,bd)	3515(s) 3300(w)	3420(w)	3560(w) 3260(w)	*n.m.*
m-Nitro- benzaldoxime	3250(m,bd)	a	3500(m)	a	3560(m) 3280(w)	a
p-Nitro- benzaldoxime	3270(m)	3120(s)	3500(m)	*n.m.*	3550(m) 3280(w)	3260(w)
o-Chloro- benzaldoxime	3572(m) 3235(m,bd)	b	3510(s) 3270(s)	b	3555(m) 3280(w,bd)	b
p-Chloro- benzaldoxime	3260(m,bd)	3110(m,bd)	3510(m)	3495(m)	3300(w)	3280(w)
Acetophenone oxime	3590(w) 3240(m,bd)		3520(w) 3250(w,bd)		3560(m) 3260(m,bd)	
Benzophenone oxime	3170(m)					
Cyclohexanone oxime	3570(w) 3140(m)					

$a = An\ attempted\ synthesis\ was\ unsuccessful.$
$b = This\ compound\ was\ not\ prepared.$
$n.m. = Not\ measured.$
$Intensities:\ weak\ (w),\ medium(m),\ broad\ band\ (bd),\ and\ strong(s).$

α oximes as solids or in solutions (benzene and chloroform) show the bonded OH at essentially the same position, around 3250 cm.$^{-1}$ However, the OH band of the β oximes occurs near 3115 cm.$^{-1}$ in the solid spectra and at approximately 3250 cm.$^{-1}$ in the solution spectra. Thus it seems that one can distinguish the α from the corresponding β compounds on the basis of the OH stretching frequency in the solid state only. The spectra of the benzene and chloroform solutions of some oximes (see Table I) have an unassociated OH valence vibration at 3500 cm.$^{-1}$ and 3550 cm.$^{-1}$, respectively. This difference of about 50 cm.$^{-1}$ is due to a slightly larger solvation effect in the former solvent. The 'free' OH absorption band is well defined in contrast to the hydrogen-bonded OH band which is broad and diffuse, as is commonly observed.

The association of oximes through hydrogen bonds has been observed by several groups (3, 7). From the present studies, as well as the previous ones, it cannot be determined whether the hydrogen bonds are of the N—H–O or O—H–O type. In the case of acetoxime, X-ray diffraction data have shown that the molecules form sheets of planar trimers held together by N—H–O bonds (5).

Benzophenone and cyclohexanone oximes which exist in one form only, have an OH stretching vibration in the region comparable to that of the β oximes, around 3150 cm^{-1}. This is also true for acetoxime (8). The results of the Beckmann rearrangement of acetophenone oxime suggest that it exists as the α isomer (14). The present investigation also provides evidence for the α configuration because the OH stretching frequency appears at 3240 cm^{-1}.

It is known that the OH deformation mode occurs in the range 1274–1595 cm.$^{-1}$ (19). Since this vibration is at least as sensitive to neighboring atoms as the OH stretching mode (20), it would be expected to exist at different positions and with varying intensities in the spectra of the α and β oximes. Most of the compounds studied show (see Fig. 1) a fairly intense band around 1300 cm.$^{-1}$ which may possibly be attributed to the OH deformation vibration since it is absent from the spectra of the corresponding aldehydes. However, no consistent shift is observed in the position of the OH bending mode as in the case of the OH stretching vibration.

Frequencies occurring near 900 cm.$^{-1}$ are ascribed to the N–OH stretching vibration (15). The fact that these maxima are not found in the spectra of the corresponding aldehydes lends support to the correctness of this assignment. Fig. 1 shows that each pair of isomeric oximes exhibits differences in the absorption bands in that region. As for the OH bending mode, no consistent distinguishing features are discernible for the N–OH frequencies.

Aliphatic oximes have an absorption band near 1670 cm.$^{-1}$ which is attributed to the $C=N$ vibration (19). A displacement of 30–40 cm.$^{-1}$ towards lower frequency, the usual concomitant of conjugation with a phenyl group, is noticed in the present studies also. Since the spectra of some oximes revealed rather weak $C=N$ maxima, only approximate band positions could be located. A possible explanation for the low intensities may be the existence of ionic resonating forms as suggested by Goubeau (15). As seen in Table II, the $C=N$ frequencies are independent of ring substitution. Again, no consistent

TABLE II
C = N FREQUENCIES OF SOLID OXIMES

Compound	Cm.$^{-1}$	Compound	Cm.$^{-1}$
α-Benzaldoxime	1630(s)	β-Benzaldoxime	1645(m)
α-o-Nitrobenzaldoxime	1614(m)	β-o-Nitrobenzaldoxime	1618(m)
α-p-Nitrobenzaldoxime	1640(w)	β-p-Nitrobenzaldoxime	1643(m)
α-p-Chlorobenzaldoxime	1650(m)	β-p-Chlorobenzaldoxime	1645(m)
α-Benzilmonoxime	1620(w)	β-Benzilmonoxime	1640(w)
α-m-Nitrobenzaldoxime	1619(m)	Cyclohexanone oxime	1662(s)
α-o-Chlorobenzaldoxime	1618(w)	Acetophenone oxime	1630(vw)
		N-benzylideneaniline*	1630(s)

*Included for comparative purposes.
  Intensities are represented by the same symbols as in Table I.

differences are noted in the position and intensity of the C = N band between
the α and β oximes examined in these studies.

REFERENCES

1. BADGER, R. M.   J. Chem. Phys. 8: 288. 1940.
2. BADGER, R. M. and BAUER, S. H.   J. Chem. Phys. 5: 839. 1937.
3. BARER, R., COLE, A. R. H., and THOMPSON, H. W.   Nature, 163: 198. 1949.
4. BECKMANN, E.   Ber. 23: 1684. 1890.
5. BIERLEIN, T. K. and LINGAFELTER, E. C.   Acta Cryst. 4: 450. 1951.
6. BRADY, O. L. and GOLDSTEIN, R. F.   J. Chem. Soc. 1918. 1926.
7. BUSWELL, A. M., RODEBUSH, W. H., and ROY, M. F.   J. Am. Chem. Soc. 60: 2444. 1938.
8. CAUGHLAN, C. N., TARTAR, H. V., and LINGAFELTER, E. C.   J. Am. Chem. Soc. 73: 1180.
      1951.
9. DAVIES, M. M. and SUTHERLAND, G. B. B. M.   J. Chem. Phys. 6: 755. 1938.
10. DUYCKAERT, G.   Bull. soc. roy. sci. Liège. 4–5: 196. 1952.
11. ERDMANN, H. and SCHWECHTEN, E.   Ann. 260: 53. 1890.
12. FORSTER, M. O. and DUNN, F. D.   J. Chem. Soc. 430. 1909.
13. GABRIEL, S.   Ber. 16: 520. 1893.
14. GILMAN, H.   Organic chemistry. Vol. I. John Wiley and Sons, Inc., New York. 1943.
15. GOUBEAU, J. and FROMME, I.   Z. anorg. Chem. 258: 18. 1949.
16. HILBERT, G. E., WULF, O. R., HENDRICKS, S. B., and LIDDEL, U.   J. Am. Chem. Soc.
      58: 548. 1936.
17. MEISENHEIMER, J. and DORNER, O.   Ann. 502: 156. 1933.
18. PATWARDHAM, N. K. and DESHAPANDE, S. S.   J. Indian Chem. Soc. 21: 135.   1944.
19. RANDALL, H. M., FOWLER, R. G., FUSON, N., and DANGL, J. R.   Infrared determinations
      of organic structures. D. Van Nostrand Co., New York.   1949.
20. SUTHERLAND, G. B. B. M.   Discussions Faraday Soc. 9: 275.   1950.
21. TAYLOR, T. W. J. and MARKS, M. S.   J. Chem. Soc. 2302.   1930.
22. VENKATESWARAN, C. S.   Proc. Indian Acad. Sci. A, 7: 13.   1938.
23. VOTER, R. C., BANKS, C. W., FASSEL, V. A., and KEHRES, P. W.   Anal. Chem. 23: 1730.
      1951.
24. WULF, O. R. and LIDDEL, U.   J. Chem. Phys. 6: 702.   1938.

THE ELECTRICAL CONDUCTIVITY OF MOLTEN OXIDES[1]

By A. E. van Arkel[2], E. A. Flood, and Norman F. H. Bright[3]

ABSTRACT

Electrical conductivities of some molten oxides have been determined. In order of decreasing equivalent conductances at their melting points the oxides investigated were: Li_2O, PbO, TeO_2, MoO_3, Bi_2O_3, V_2O_5, Sb_2O_3, and CrO_3. The variation of the observed values of the specific conductivities, K, with the absolute temperature, T, can be described by an equation of the form,

$$\log K = A + BT^{-1} + CT^{-2} \ldots,$$

where A, B, C, etc. are constants. While the experimental data are adequately described by an equation of this form containing only the constants A and B, a slightly better fit is obtained using three constants. The conductivities of the molten oxides follow a pattern of variation from element to element which is substantially the same as that of the molten halides. For elements giving more than one oxide stable in the molten state, the oxide corresponding to the highest state of valency has the lowest conductivity.

INTRODUCTION

A good deal of information is available in the scientific literature concerning the electrical conductivities of the molten halides of the various elements of the Periodic System. The following are some general trends:

(i) Compounds of the lighter halogens usually have better conductivities than the corresponding compounds of the heavier halogens.

(ii) In the alkali metal group the conductivities for each molten halide decrease with increasing size of the positive ion. (The liquid hydrogen halides are, of course, all poor conductors.)

(iii) In groups other than the alkali metal group the conductivities of the molten halides increase with increasing size of the positive ion; thus molten beryllium chloride is a poor conductor whereas magnesium, calcium, strontium, and barium chlorides are all good and increasingly so in that order.

(iv) As one goes across the Periodic System from Group I to Group VII, the further down each Group it is necessary to go before good conductors are reached; thus, in Group I the chloride of the lightest member, lithium chloride, conducts well whereas in Group VI, tungsten chloride is a poor conductor and it is only the heaviest member of the group, uranium, that yields a chloride having a good conductivity in the molten state.

(v) In the case of an element which forms more than one stable molten halide with any given halogen, the compound corresponding to the highest state of stoichiometric valency usually has the lowest conductivity. Tin and indium chlorides furnish good examples of this tendency.

While there are some striking contrasts between the trends of the conductivities of the molten halides and the trends of the conductivities of their aqueous solutions, in general, the former are qualitatively consistent with

TABLE I

Element	Oxide	Reference number	Information available
Hydrogen	H_2O	18	Specific conductivity at $0°C. = 1.5 \times 10^{-8}$ ohm^{-1} cm.$^{-1}$; at $15°C. = 0.85 \times 10^{-7}$ ohm^{-1} cm.$^{-1}$
Beryllium	BeO	19	Can be fused and distilled in the electric arc furnace, so presumably the melt is conducting
Boron	B_2O_3	(i) 27	Stated to be a nonconductor
		(ii) 1	Specific conductivity varies from 7×10^{-6} ohm^{-1} cm.$^{-1}$ at $800°C.$ to 46×10^{-6} ohm^{-1} cm.$^{-1}$ at $1000°C.$
Carbon	CO_2	7	Stated by various workers to be a nonconductor
Nitrogen	N_2O_3	29	Liquid will not conduct across a narrow gap
	NO_2	(i) 11	Stated to be a poor conductor in the liquid state
		(ii) 15	Specific conductivity varies from 1.16×10^{-8} ohm^{-1} cm.$^{-1}$ at $-10°C.$ to 14.2×10^{-8} ohm^{-1}cm.$^{-1}$ at $20°C.$
Magnesium	MgO	23	Fusible in the electric arc furnace (Much information is available on the conductivity of the solid oxide under various conditions)
Aluminum	Al_2O_3	23	As for magnesium oxide
Silicon	SiO_2	10	Specific conductivity of liquid at melting point (ca. $1625°C.$) $= 10^{-5}$ ohm^{-1} cm.$^{-1}$
Phosphorus	P_2O_3	25	Specific conductivity at $25°C.$, less than 1.2×10^{-7} ohm^{-1} cm.$^{-1}$
Sulphur	SO_2	(i) 4	Stated to be a nonconductor
		(ii) 9	Specific conductivity at $-15°C. = 0.85 \times 10^{-7}$ ohm^{-1} cm.$^{-1}$
		(iii) 28	Specific conductivity at $0°C. = 0.90 \times 10^{-7}$ohm^{-1}cm.$^{-1}$
	SO_3	21, 13	Stated by various workers that the liquid was either a poor or a nonconductor
Potassium	$K_2O(?)$	11	Faraday stated that molten "potassa" conducted
Calcium	CaO	23	As for magnesium oxide
Titanium	TiO_2	23	As for magnesium oxide
Vanadium	V_2O_5	6	Stated to be a fairly good conductor
Chromium	Cr_2O_3	23	As for magnesium oxide
	CrO_3	(i) 23	Stated by some workers to be a good conductor
		(ii) 3	Stated to be a nonconductor if pure, but to conduct well when it has absorbed water
Manganese	MnO	23	As for magnesium oxide
	MnO_2	22	Fusible in the electric arc but decomposes
	Mn_2O_7	20	Stated to have an immeasurably low conductivity
Iron	Fe_2O_3	22	As for manganese dioxide
Cobalt	CoO	23	As for magnesium oxide
Nickel	NiO	23	As for magnesium oxide; gives a green crystalline material on cooling
Copper	CuO	22	As for manganese dioxide
Zinc	ZnO	23	Fusible in the electric arc but immediately volatilizes
Arsenic	As_2O_3	3	Stated to be a good conductor, but volatile
Strontium	SrO	23	As for magnesium oxide
Zirconium	ZrO_2	23	As for magnesium oxide
Molybdenum	MoO_3	14	Stated to be a good conductor and could be electrolyzed
Ruthenium	RuO_4	20	Stated to have immeasurably low conductivity at its melting point $(25.5°C.)$
Tin	SnO_2	23	As for magnesium oxide but volatilizes in the arc
Antimony	Sb_2O_3	(i) 11	Stated by Faraday to conduct well when molten
		(ii) 27	Stated to be a nonconductor in the liquid condition when dry
	Sb_2O_5	11	Stated by Faraday to conduct well, but this is doubtful owing to decomposition
Iodine	I_2O_5	8	Stated to decompose no more when a potential is applied across the melt than it does thermally, and concluded from this that the liquid does not conduct
Barium	BaO	23	As for magnesium oxide
Cerium	CeO_2	23	As for magnesium oxide
Osmium	OsO_4	4, 5	Stated by various workers to be a very poor conductor in both solid and liquid states
Lead	PbO	12	Faraday stated it to be a good conductor
Bismuth	Bi_2O_3	11	Stated to be a good conductor

what is known concerning the structures of these substances, the natures of the bonds involved, the ion sizes, and charge ratios, the ion coordination numbers in the various melts, the deformabilities of the ions, etc.

It was considered of interest to determine whether the molten oxides exhibited the same trends and pattern of variation of conductivity as do the molten halides. What little information is available in the literature concerning the conductivity of the fused oxides is summarized in Table I. The table gives the conductivity, in general terms, of the various oxides in the molten state, together with the sources of the information.

SPECIFIC AND EQUIVALENT CONDUCTANCES

Substance	Melting point, °C.	Specific conductivity at melting point, ohm^{-1} cm.$^{-1}$	Density of solid, gm./cc.	Assumed density of liquid (75% of solid), gm./cc.	Equivalent conductance, ohm^{-1} cm.$^{-2}$
MgO	2800	35	3.6	2.70	261
CaO	2580	40	3.3	2.48	453
TiO$_2$*	1650	10	4.2	3.15	63
ZrO$_2$	2600	15	5.7	4.28	108
ThO$_2$	3050	8	9.7	7.28	73
Cr$_2$O$_3$	2275	65	5.2	3.90	844
Al$_2$O$_3$	2050	15	3.9	2.93	175

Titanium dioxide is generally assigned the formula $TiO_{1.90 \rightarrow 1.98}$ and might be expected to be a semiconductor.

It will be seen from this table that there are only a very few oxides for which there are any quantitative data, and of these only four are applicable over a range of temperatures, viz., H_2O, B_2O_3, NO_2, and SO_2. These are all poor conductors and there would not appear to be any quantitative determinations of the conductivities of molten metallic oxides. There are a considerable number of qualitative observations concerning the possibility of striking and maintaining an electric arc under various molten metallic oxides, and it has been assumed that where this is possible the molten oxides concerned must be conducting.

Various oxides are handled commercially by the electric arc furnace technique. These include the following materials: MgO, CaO, TiO_2, ThO_2, ZrO_2, Cr_2O_3, Al_2O_3, UO_2, and U_3O_8. Semiquantitative figures for the conductivity of some of these oxides have been supplied to the authors in a private communication by the Norton Company, Chippawa, near Niagara Falls, Ont., to whom we are indebted for them. These figures are probably not reliable to better than ±50% owing to the indirect means necessary to obtain them.

In view of the scarcity of quantitative information it was felt desirable to augment the observations by direct experimental measurements of the electrical conductivity of some molten oxides over a range of temperatures. Consideration showed that the number of oxides available for convenient investigation is limited by several factors such as instability, volatility, and difficulty in finding suitable container and electrode materials.

EXPERIMENTAL

The oxides which have been studied in the molten state are lithium oxide, molybdenum trioxide, antimony trioxide, bismuth trioxide, vanadium pentoxide, tellurium dioxide, lead monoxide, and chromium trioxide (CrO_3).

In the case of lithium oxide a reasonably suitable material for the cell was found to be synthetic fused magnesia in the form of large single crystals* from which crucibles and lids could be conveniently, though laboriously, drilled. Molten lithium oxide has a quite remarkable solvent action on almost all the known refractory materials and, in addition, readily attacks most high-melting metals in both inert and active atmospheres; even platinum is readily attacked by it *in vacuo* with the probable production of an alloy of platinum and lithium. The alloy of 40% of rhodium with 60% of platinum, however, appears to be able to withstand the action of molten lithium oxide reasonably well and this was the material adopted for fabrication of the electrodes. The oxide was prepared by heating pure hydroxide, available commercially, to 1000°C. for several hours *in vacuo* in a platinum crucible. There is no appreciable attack on the platinum at this temperature. The oxide was subsequently handled in an atmosphere dried over phosphorus pentoxide. The cell, whose design is shown in Fig. 1, was loaded with finely ground lithium oxide and was heated inside a larger graphite crucible, placed in a surrounding quartz tube. Atmospheric pressure of argon gas was used in the heating tube. Induction heating was employed and the temperature estimated by means of an optical pyrometer sighted through the top window of the outer vessel. The lithium oxide was found to melt quite sharply at 1570°C. The resistance of the cell was measured on a simple a-c. bridge circuit at a frequency of 1000 c.p.s. The measured resistance dropped from a figure of over 10^5 ohms while the oxide was still solid to about 30–40 ohms on melting corresponding, in this case, to a specific conductivity of 7 ohm^{-1} cm.$^{-1}$. It was found by trial that, within the limits of measurement employed herein, it made no difference what frequency was used for the a-c. bridge circuit, within the range 2000 c.p.s. to the lowest audible limit; accordingly, 1000 c.p.s. was chosen as a convenient working frequency.

The cell was filled with just the required amount of material, previously determined by volume measurements, to ensure that the melt rose sufficiently far up the narrow holes in the lid that electrical contact was made with the platinum/rhodium electrodes.

The cell constant had previously been determined, using molten potassium chloride, whose conductivity is well established from the data of Jaeger and Kapma (17) and of Biltz and Klemm (2). It was found that the resistance of the cell, calculated from its dimensions and the known conductivity of molten potassium chloride, agreed well with the directly measured value.

The magnesium oxide of the crucible was attacked to a considerable extent by the lithium oxide (to about 20% of the lithium oxide weight). Accordingly an attempt was made to determine the conductivity as a function of concentration of magnesium oxide and thus determine by extrapolation the conduc-

Supplied through the courtesy of the Norton Company, Chippawa, Ont.
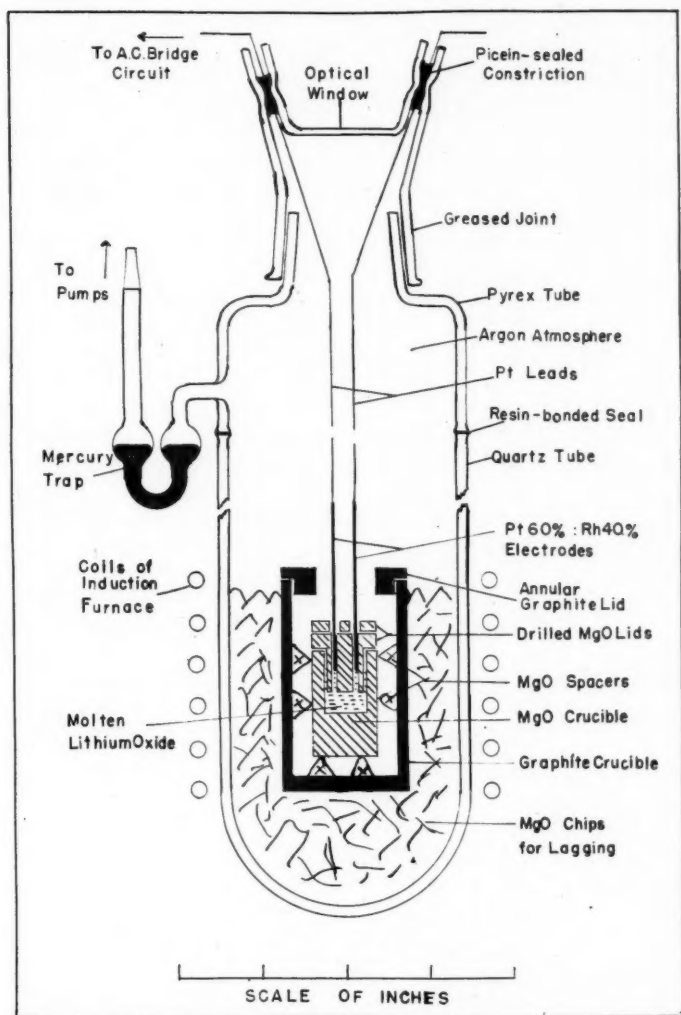
Fig. 1

tance of pure lithium oxide. To this end the conductivities of synthetic mixtures of magnesium and lithium oxides were determined and it was found that the conductivity was practically independent of magnesium oxide concentration from zero to 20% magnesium oxide by weight.

The equivalent conductance of fused lithium oxide at its melting point was found to be 108 ohm^{-1} cm^{-2}. It is considered that this figure may be taken as representing the conductivity of molten lithium oxide at its melting point to within $\pm20\%$.

TABLE II

DETAIL EXPERIMENTAL RESULTS

Temperatures (t) are given in degrees Centigrade. Specific conductivities (K) are given in ohm^{-1} cm^{-1}. All the readings quoted below are given in the order in which they were obtained experimentally for each individual oxide.

Bismuth trioxide (Bi$_2$O$_3$)			Tellurium dioxide (TeO$_2$)			Lead monoxide (PbO)			Molybdenum trioxide (MoO$_3$)			Vanadium pentoxide (V$_2$O$_5$)			Chromium trioxide (CrO$_3$)			Antimony trioxide (Sb$_2$O$_3$)		
Cell	t	K	Cell	t	K	Cell	t	K	Cell	t	K	Cell	t	K	Cell	t	K	Cell	t	K
A	933	1.416	B	911	2.330	D	891	1.030	F	858	1.50	H	867	0.0969	I	218	2.958×10^{-6}	J	842	0.1004
	929	1.217		932	2.532		914	1.523		895	2.58		884	0.1348		228	1.479×10^{-7}		828	0.0792
	880	0.716		948	2.773		939	1.843		950	4.65		888	0.1444		235	3.697×10^{-1}			
	871	0.591		952	2.841		957	2.189	G	847	0.99		899	0.1590		240	1.479×10^{-3}	K	854	0.1161
	860	0.495		941	2.588	E	897	1.251	F	840 (solid)	0.141		924	0.1993		245	2.958×10^{-3}		864	0.1231
	848	0.420		873	2.080		918	1.523		809 ''	0.086		937	0.2359		252	5.916×10^{-3}		870	0.1286
	833	0.302		843	1.879		941	1.751		822 ''	0.105		949	0.2483		262	8.964×10^{-3}		888	0.1442
	829	0.222		814	1.664		953	2.189		841	0.150		964	0.2888						
	837	0.377		789	1.493		987	2.694		857	1.41									
	849	0.435		773	1.420					862	1.79									
	872	0.609		750	1.213															
	888	0.742	C	812	1.713															
	904	0.846		840	1.879															
	908	0.937		868	2.080															
	911	1.068		908	2.377															
	920	1.269		930	2.532															
	930	1.353		941	2.647															
	955	1.450		960	2.841															

Cell constants in cm^{-1}

A	609
B	582
C	583
D	35
E	35
F	465
G	445
H	1415
I	29.6
J	550
K	714

It may be remarked that although nothing can be said of the nature of the carriers responsible for the conduction, such a high specific conductivity suggests the presence of a simple ionic melt, i.e., an arrangement of ions of small and comparable sizes, in an approximately close-packed configuration, analogous to that in the crystalline oxide.

The other oxides were all of much lower melting point and their conductivities were studied over a range of temperatures. In most cases the quartz capillary tube conductivity cell was heated by means of a bath of molten sodium chloride, and temperatures were measured by means of a Pt:Pt/Rh thermocouple. In the case of lead monoxide, which attacks quartz very readily, a platinum crucible containing a suitably drilled piece of polycrystalline magnesium oxide with a platinum electrode was used, the crucible itself acting as the other electrode. In all cases, care was taken to maintain the oxide under investigation free from any lower oxide whose presence might well lead to the intrusion of semiconductivity. In most cases conductivity measurements were made with both rising and falling temperatures, yielding concordant results; with vanadium pentoxide, however, the onset of decomposition at the highest temperatures investigated prohibited this procedure. In determining the cell constants for the quartz capillary cells, aqueous $N/1$ and $N/10$ potassium chloride solutions at a measured room temperature were used, employing the conductivity data of Parker and Parker (24), quoted by the International Critical Tables. Allowance was made for the temperature of the potassium chloride solution in determining the cell constant, but no account was taken of possible variation of the cell constant with temperature during the oxide conductivity determinations.

It is not considered that any variations of temperature within the oxide melts themselves, in either the lithium oxide experiments or those in the capillary U-tube cells, would have been sufficient to have caused variations in the measured conductivities which would have been significant in these comparatively crude experiments.

The results obtained with the various oxides other than lithium oxide, which has already been dealt with, are shown in Table II. The expression of the conductivity, K, as a function of absolute temperature, T, in the form,

$$\log K = A + B/T$$

will give a quantity, B, which when expressed in the proper units will be proportional to an 'activation energy'. However, when $\log K$ is plotted against $1/T$, it is apparent that in most cases there is an appreciable departure from linearity, and it would appear possible that it might be better to express $\log K$ as a quadratic function of $1/T$, thus,

$$\log K = A + B/T + C/T^2.$$

In this case, the 'activation energy' will itself be temperature dependent. An attempt has been made to determine by statistical means which is the more justifiable form to take as representing the experimental results. The best linear and quadratic equations connecting $\log K$ and $1/T$ were worked out by the usual least square methods, and from them the standard deviations of a single determination of $\log K$. In every case this quantity was less for the

quadratic plot than for the linear as, of course, it should be since an extra parameter, C, has been introduced. Often, however, the improvement obtained with the more complex form was slight.

As an additional test of the relative validity of the two forms of temperature dependence, correlation coefficients* were determined and appear together with other relevant data in Tables III and IV.

It will be noted that the correlation coefficients appearing in Tables III and IV show no significant difference as between the linear and the quadratic plots. However, it has recently been shown by Spooner and Wetmore (26) that the variation of the conductivity of molten silver nitrate with temperature is much better expressed by a quadratic plot than by a linear plot.

DISCUSSION

In view of the double charge carried by the oxygen ion and the rather striking differences which exist as between the melting points of halides and of oxides, the molten oxides might be expected to exhibit marked and systematic differences in conductance behavior as compared with the corresponding halides. In the case of lithium oxide, it was thought that the strong fields about the oxygen and lithium ions might lead to a melt containing rather large ion clusters or to a melt having considerable covalent character, and thus be a poor conductor in comparison with fused lithium chloride or fluoride. However, the conductivity of fused lithium oxide, while somewhat lower than that of lithium fluoride, is quite comparable with the conductivity of the molten chloride, and is considerably greater than that of fused potassium chloride.

It may be pointed out that, in cases where the temperature coefficients of conductivity are comparatively large, the oxides were observed to form rather viscous liquids on melting, while where the temperature coefficients are small, it was noticed that the oxides melt sharply yielding comparatively mobile liquids. This suggests that in the former case, ion clusters of appreciable size having, perhaps, considerable covalent character are present in the melts, while in the latter case, the crystals melt to form liquids where the ion coordinations are essentially similar to those of simple ionic crystals. In Table V we present in diagrammatic form a summary of the information available to date concerning the conductivities of the fused oxides.

This quantity is defined as follows:

Let $\log K$ be denoted by y and $1/T$ by x. Then the experimentally determined points will be $R^2 = 1 - (x_1, y_1),(x_2, y_2), (x_3, y_3) \ldots (x_n, y_n)$. The correlation coefficient, R, is defined by the equation,
$$R^2 = 1 - U/n\sigma_y^2$$
where n = number of experimental observations.

     σ_y = standard deviation of y.

     U = sum of squares of residuals (differences between the observed values of y and those calculated from the best linear or quadratic equation, as the case may be).

Thus for the linear equation

$$R^2 = 1 - \left(\sum_n(y_1^2) - A\sum_n(y_1) - B\sum_n(x_1y_1)\right) \Big/ \left(\sum_n(y_1^2) - \frac{1}{n}[\sum_n(y_1)]^2\right).$$

and for the quadratic equation

$$R^2 = 1 - \left(\sum_n(y_1^2) - A\sum_n(y_1) - B\sum_n(x_1y_1) - C\sum_n(x_1^2y_1)\right) \Big/ \left(\sum_n(y_1^2) - \frac{1}{n}[\sum_n(y_1)]^2\right).$$

cf. Udny Yule, G. and Kendall, M. G. *An Introduction to the theory of statistics.* C. Griffin and Co. Ltd., London. 1947. pp. 328–330.

TABLE III
SUMMARY OF RESULTS CALCULATED ACCORDING TO LINEAR PLOT

| Oxide | Melting point, °C. | Range studied, °C. | $\mathrm{Log_{10}}\,K = A + B/T$ | | Standard deviation of log$K$ | Correlation coefficient | Extrapolated K at m.p., ohm^{-1} cm.$^{-1}$ | Equivalent conductance at m.p. | Activation energy, kcal./mole |
			A	B					
Bi$_2$O$_3$	828	829–955	7.057	−8,354	0.0471	0.981	0.29	5.15	38.2
TeO$_2$	730	750–960	2.162	−2,109	0.0088	0.997	1.14	7.75	9.65
PbO	888	891–987	5.245	−6,041	0.0237	0.983	1.10	12.89	27.6
MoO$_3$	847	847–950	7.309	−8,089	0.0552	0.973	1.22	6.51	37.0
V$_2$O$_5$	690	867–964	4.670	−6,427	0.0234	0.989	0.00988	0.107	29.4
CrO$_3$	196	218–262	27.828	−15,838	0.1821	0.980	1.16×10^{-6}	6.9×10^{-6}	72.5
Sb$_2$O$_3$	656	828–888	3.800	−5,364	0.0206	0.973	0.011	0.18	24.5

TABLE IV
SUMMARY OF RESULTS CALCULATED ACCORDING TO QUADRATIC PLOT

| Oxide | $\log_{10}K = A + B/T + C/T^2$ | | | Standard deviation of log$K$ | Correlation coefficient | Extrapolated K at m.p., ohm^{-1} cm.$^{-1}$ | Equivalent conductance at m.p. | Activation energy, in kcal./mole | | |
	A	B	C					T_1	T_2	T_3
Bi$_2$O$_3$	−24.039	63,729	-41.729×10^{-6}	0.0380	0.988	0.26	4.57	55.2	33.9	20.6
TeO$_2$	1.418	−425	-0.950×10^{-6}	0.0085	0.997	1.12	7.60	10.6	9.69	9.05
PbO	5.499	−6,646	$+0.361 \times 10^{-6}$	0.0238	0.984	1.10	12.89	27.6	27.7	27.8
MoO$_3$	−5.476	21,898	-17.561×10^{-6}	0.0490	0.978	1.19	6.35	43.3	36.8	31.2
V$_2$O$_5$	−26.368	67,313	-43.767×10^{-6}	0.0164	0.996	0.000217	0.00235	107.9	33.4	19.5
CrO$_3$	−136.885	152,997	-43.234×10^{-6}	0.1231	0.991	6.2×10^{-8}	3.7×10^{-7}	143.3	86.3	35.2
Sb$_2$O$_3$	−59.006	136,614	-80.214×10^{-6}	0.0071	0.996	1.27×10^{-5}	2.17×10^{-4}	165.0	28.6	0.7

N.B. T_1, T_2, T_3 in Table IV refer to the melting point, middle, and upper end respectively of the temperature range investigated.

The interpretation of the behavior pattern in terms of the natures of the bonds involved, ion sizes, etc. is of course obscured by the large differences in temperature at which the various measurements were made. However, it is a rather striking fact that the molten oxides—like the halides—are usually either fairly good conductors or insulators. For example, molten TiO$_2$ is a fairly good conductor while molten SiO$_2$ is virtually an insulator, the melting points of the two oxides being not very different.

It is also observable that there is a tendency in the case of elements which give more than one oxide which is stable in the molten state for the oxide corresponding to the highest state of valency of the element to have the lowest conductivity; chromium and manganese furnish good examples of this tendency.

TABLE V

SUMMARY OF INFORMATION ON CONDUCTIVITY OF MOLTEN OXIDES

Group I	Group II	Group III	Group IV	Group V	Group VI	Group VII	Group VIII
H_2O**	—	—	—	—	—	—	—
Li_2O*	BeO	B_2O_3**	CO_2	N_2O_3 NO_2**	O_2		
	MgO*	Al_2O_3*	SiO_2*	P_2O_2*	SO_2* SO_3		
K_2O(?)	CaO*		TiO_2*	V_2O_6**	CrO_3**	Mn_2O_7 MnO_2	Fe_2O_3 CoO
					Cr_2O_3*	MnO	NiO
CuO	ZnO			As_2O_3			
	SrO		ZrO_2* SnO_2	Sb_2O_3**	MoO_3** TeO_2**	I_2O_5	RuO_4
	BaO		CeO_2 PbO**	Bi_2O_3**			OsO_4
			ThO_2*		UO_2 U_3O_8		

Data in italics: Nonconducting oxides.
Data in roman: Conducting oxides.
*Isolated quantitative data available.
**Data available over a range of temperature.

While the picture is by no means as complete as that for the halides, it is evident that the conductivities of the molten oxides of the elements of the Periodic System exhibit essentially the same general pattern of behavior as do the molten halides.

ACKNOWLEDGMENTS

REFERENCES

1. ARNDT, K. and GESSLER, A. Z. Elektrochem. 14: 662. 1908.
2. BILTZ, W. and KLEMM, W. Z. physik. Chem. 110: 318. 1924.
3. BLEEKRODE, L. Proc. Roy. Soc. (London), 25: 322. 1877.
4. BLEEKRODE, L. Phil. Mag. (5) 5: 375. 1878.
5. BUFF, H. Liebigs Ann. Chem. 110: 257. 1859.
6. BUFF, H. Liebigs Ann. Chem. 110: 277. 1859.
7. CAILLETET, L. P. Compt. rend. 75: 1271. 1872.
8. CONNELL, A. Edinburgh New Phil. J. 10: 93 and 337. 1831; 11: 72. 1831; 13: 284. 1832.
9. DUTOIT, P. and GYR, E. J. J. chim. phys. 7: 189. 1909.
10. ENDELL, K. and HELLBRUGGE, J. Naturwiss. 30: 421. 1942.
11. FARADAY, M. Phil. Trans. 123: 507. 1833.
12. FARADAY, M. Phil. Trans. 124: 77. 1834.
13. GEUTHER, A. Liebigs Ann. Chem. 109: 129. 1859.
14. GUICHARD, M. Ann. chim. (7) 23: 516. 1901.
15. HEBERLEIN, R. Recherches sur les conductibilités électriques. Geneva. 1926.
16. HITTORF, J. W. Wied. Ann. 4: 403. 1878.
17. JAEGER, F. M. and KAPMA, B. Z. anorg. Chem. 113: 27. 1920.

18. KOHLRAUSCH, F. and HEYDWEILLER, A.   Z. physik. Chem. 14: 317. 1894.
19. LEBEAU, P.   Compt. rend. 123: 818.   1896.
20. LEBLANC, M. and SACHSE, H.   Physik. Z. 32: 887.   1931.
21. MAGNUS, G.   Pogg. Ann. 104: 553.   1858.
22. MOISSAN, H.   Ann. chim. et phys. (5) 21: 386.   1880.
23. MOISSAN, H.   Compt. rend. 115: 1034.   1892.
24. PARKER, H. C. and PARKER, E. W.   J. Am. Chem. Soc. 46: 312.   1924.
25. SCHENK, R.   Ber. 39: 1506.   1906.
26. SPOONER, R. C. and WETMORE, F. E. W.   Can. J. Chem. 29: 777.   1951.
27. TICHANOWITSCH, M.   Chem. Zentr. (11) 6: 613.   1861.
28. WALDEN, P. and CENTNERSWER, M.   Bull. Acad. St. Petersburg, (5) 15: 17.   1902.
29. WIELAND, H.   Ber. B. 54: 1776.   1921.

PYRIDINE DERIVATIVES

PART V.* ON FLUORO-NITROPYRIDINES[1]

By W. Gruber

ABSTRACT

2-Fluoro-5-nitropyridine has been synthesized and its properties compared with 2,4-dinitro-fluorobenzene. Absorption spectra are given. The highly reactive compound was used to prepare well defined derivatives from alcohols, amines, and amino acids.

In conjunction with other studies in the pyridine series we were interested in the synthesis and properties of some fluoro-nitropyridines, which are 'structurally analogous' to the well known dinitro-fluorobenzenes.

The preparation of the 2- and 3-fluoropyridines from the amines has been effected by: (*a*) diazotation in 60% hydrofluoric acid (4,2), (*b*) decomposition of the fluoborates (Schiemann reaction) (9), (*c*) decomposition of the fluosilicates (1). We have obtained 2-fluoro-5-nitropyridine from 2-amino-5-nitropyridine in 20–30% yield by method (*a*); methods (*b*) and (*c*) gave only traces. However, attempts to obtain other fluoro-nitropyridines by these methods were unsuccessful. From 2-amino-3-nitropyridine only the 2-hydroxy derivative was obtained by methods (*a*) or (*b*) and 4-fluoro-3-nitropyridine was not obtained from the 4-amino derivative. The failure of 4-aminopyridine to give 4-fluoropyridine has been reported (9).

As the fluorine in 2-fluoro-5-nitropyridine (NFP) shows the expected high reactivity, some precautions are necessary in its isolation. It gave 2-methoxy-5-nitropyridine (4) with sodium methoxide, or, more slowly with 10% aqueous methanol. From NFP and *o*-toluidine, glycine ethylester or phenylalanine, the corresponding N-substituted 2-amino-5-nitropyridines were obtained. Though NFP had advantages over 2-chloro-5-nitropyridine, which gave no such derivative with glycine ester, it is inferior to 2,4-dinitrofluobenzene for the characterization of phenols (12): with low melting xylenols, NFP gave only oily ethers.

Ultraviolet Absorption Spectra

The comparison of 2-fluoro-5-nitropyridine with the (corresponding) 1-fluo-2,4-dinitrobenzene could not be made, since the latter shows only end-absorption. However, it was interesting to compare the spectra of the fluoropyridines with the fluoro-nitrobenzenes.

It is known (8) that introduction of fluorine has very little effect on the general shape of the pyridine curve; it produces only a slight bathochromic and hyperchromic shift. These shifts fit very well in the pattern proposed by Spiers and Wibaut (11) for halopyridines.

On the contrary, introduction of fluorine in nitrobenzene changes the shape of the absorption curve considerably (Fig. 1). Nitrobenzene shows one maximum at 255 mμ, which is also the sole maximum in the symmetrically substituted *p*-fluoro-nitrobenzene. In the ortho- and meta-compounds this maximum is shifted towards shorter wave lengths, and a second maximum occurs near 280 mμ.
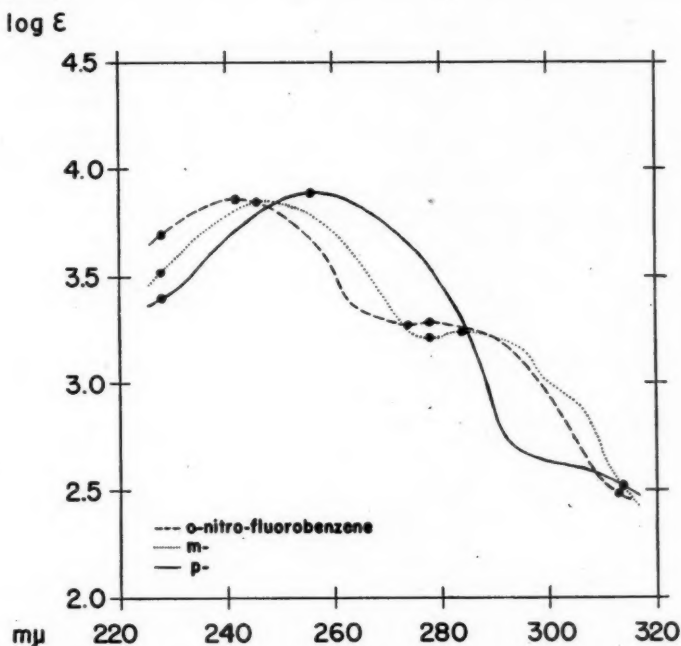
FIG. 1

2- and 4-Nitropyridines also show very distinctly a second maximum in the region of longer wave lengths, whereas this second maximum is absent in 3-nitropyridine (Fig. 2). However if the absorption spectra are measured in an unpolar solvent, e.g. trimethylpentane, instead of in alcohol, 3-nitropyridine also shows a second maximum.*

It is worth while noticing, that NFP shows nearly the same ultraviolet absorption curve as does 3-nitropyridine, the introduction of fluorine producing only a bathochromic effect (Fig. 3).

EXPERIMENTAL**

5-Nitro-2-fluoropyridine (NFP)

Of the several preparative methods tried, the following proved to be the most satisfactory. 2-Amino-5-nitropyridine (10.4 gm.) (3) was dissolved in

*The effect of the solvent on the absorption spectra of heterocyclic bases, e.g. pyridine, is discussed in (8).
**Melting points are corrected. Analyses are by A. Bernhardt, Mühlheim (Ruhr), Germany.

2-nitropyridine
3- (isooctane), ----(alcohol)
4-

Fig. 2

—— 5-nitro-2-fluoropyridine
---- 3-nitropyridine
········ 2,4-dinitro-fluorobenzene

Fig. 3

100 ml. of 60% hydrofluoric acid, cooled to 0°C., and 6.3 gm. sodium nitrite added in small portions to the well stirred solution. After standing overnight

at room temperature, the acid was neutralized with sodium bicarbonate, an excess of sodium bicarbonate added, and the mixture saturated with sodium chloride. The mixture was extracted continuously with ether for 12 hr., the solvent evaporated, and the residue, consisting of NFP and 2-hydroxy-5-nitropyridine, distilled *in vacuo*. The receiver was cooled with dry ice-acetone mixture. NFP is rather volatile, has a characteristic smell, and is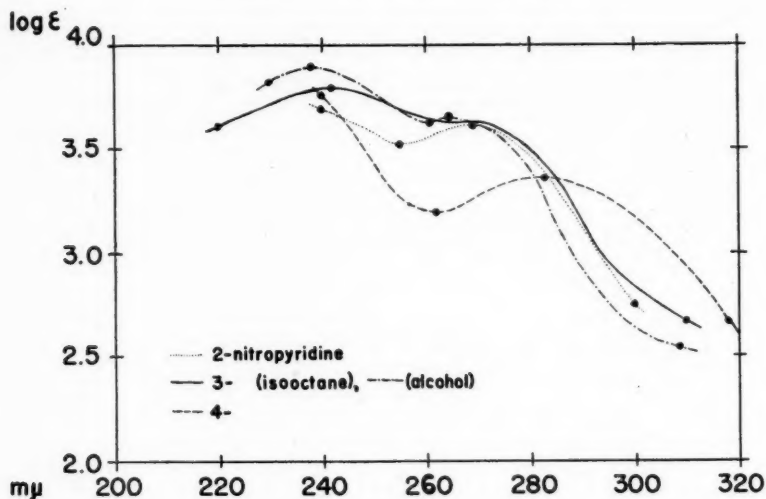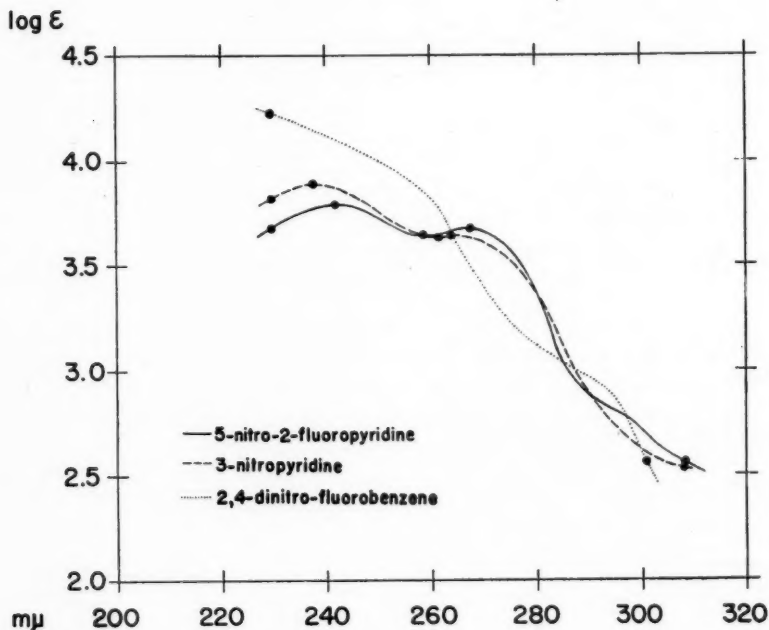 a typical lachrymator, even in low concentrations; it also has an irritating action on the skin, like 2,4-dinitro-fluobenzene. Yield 2.3 gm. (i.e. 22%), m.p. 19–21°C.; white prisms; b.p. 79–81°C. at 5–6 mm. Hg. Calc. for $C_5H_3FN_2O_2$: C, 42.26; H, 2.13; N, 19.72%. Found: C, 42.52; H, 2.01; N, 19.60%. $n_D^{23°} = 1.5258$; sp. gr.$\frac{23°}{23} = 1.410$; found: $R_D = 30.93$. Ultraviolet absorption in 2,2,4-trimethylpentane ($c = 0.00011$): λ_{max} 242 mμ (log $\epsilon = 3.78$); 268 mμ (log $\epsilon = 3.67$) (Fig. 3).

Attempts to prepare NFP by heating 2-chloro-5-nitropyridine with potassium fluoride in a nonpolar solvent, corresponding to the convenient synthesis of 2,4-dinitro-fluorobenzene (5), were unsuccessful.

5-Nitro-2-methoxypyridine

Sodium, 200 mgm. was dissolved in absolute methanol, (5 ml.) the solution was cooled to 10°C. and added to a cooled solution of 420 mgm. NFP in 3 ml. of absolute methanol. A violent reaction set in and was completed by heating the mixture on the steam bath for 30 min. After cooling, the mixture was poured into water and the precipitate collected on a Büchner funnel. After sublimation *in vacuo* (39 mm.), the yield was 425 mgm. (94%); m.p. 104–108°C. After recrystallization from diluted methanol, the m.p. was 109–110°C. The mixed m.p. with an authentic sample was not depressed.

A solution of 300 mgm. NFP in 8 ml. of dilute methanol (15% v/v) was kept for 12 hr. at room temperature, after which no more crystals precipitated. Yield of 5-nitro-2-methoxypyridine 15 mgm., m.p. 109–110°. Calc. for $C_6H_6N_2O_3$: N, 18.18; OCH_3, 20.14%. Found: N, 18.05; OCH_3, 20.20%.

N-(5-nitropyridyl-2)-o-toluidine

A mixture of 600 mgm. NFP and 600 mgm. *o*-toluidine was heated on the steam bath for two hours; the solid content of the flask was recrystallized from 70 ml. 10% hydrochloric acid with a little charcoal, and then twice from dilute alcohol; m.p. 137–139°C., mixed melting point with a sample prepared from 2-chloro-5-nitropyridine was not depressed. Yield almost quantitative. Calc. for $C_{12}H_{11}N_3O_2$: C, 62.87; H, 4.84%. Found: C, 63.12, 62.83; H, 4.74, 4.76%.

Ethyl N-(5-nitropyridyl-2)-aminoacetate

A solution of 250 mgm. of glycine ethyl ester hydrochloride and 336 mgm. of sodium bicarbonate in 5 ml. water was added to a solution of 284 mgm. of NFP in 10 ml. of ethanol. After standing at 5°C. for five hours the precipitation of white needles began. They were collected the next day and had a melting point of 140–145°C.; crude yield 425 mgm. After purification by recrystallization from dilute alcohol the melting point was 142–143°C. Calc. for $C_9H_{11}N_3O_4$: C, 48.00; H, 4.92; N, 18.66%. Found: C, 47.94; H, 5.00; N, 18.72%.

N-(5-nitropyridyl-2)-β-phenylalanine

Phenylalanine (330 mgm.) and sodium bicarbonate (336 mgm.) were dissolved in 15 ml. water and mixed with a solution of 284 mgm. NFP in 5 ml. alcohol. After 15 hr. at room temperature the solvents were removed *in vacuo* at 30°C., and the residue recrystallized several times from absolute methanol. Brownish-yellow plates, yield 291 mgm. (52%), m.p. 183–185°C. Calc. for $C_{14}H_{13}N_3O_4$: C, 58.53; H, 4.56; N, 14.63%. Found: C, 58.42; H, 4.63; N, 14.47%.

Ultraviolet Absorption Spectra

The fluoro-nitrobenzenes and dinitrobenzenes were prepared from the nitro-anilines in a Schiemann reaction according to Org. Synth., Coll. Vol. II, p. 225. The nitropyridines were prepared by oxidation of the aminopyridines with hydrogen peroxide in oleum (6, 7, 10). The spectra were measured in 2,2,4-trimethylpentane ('isooctane') unless otherwise stated.

o-Nitro-fluorobenzene b.p. 86–87°C. at 10–11 mm. Hg ($c = 0.00015$);

λ_{max}: 242 mμ (log ϵ = 3.86), 278 mμ (log ϵ = 3.27).

m-Nitro-fluorobenzene b.p. 53–54°C. at 1–2 mm. Hg. ($c = 0.00021$);

λ_{max}: 246 mμ (log ϵ = 3.87), 284 mμ (log ϵ = 3.23).

p-Nitro-fluorobenzene b.p. 86–88°C. at 12–14 mm. Hg ($c = 0.00021$);

λ_{max}: 256 mμ (log ϵ = 3.88).

2-Nitropyridine m.p. 70–71°C., in 95% ethanol ($c = 0.00014$);

λ_{max}: 269 mμ (log ϵ = 3.60).

3-Nitropyridine m.p. 35–36°C., ($c = 0.00014$);

λ_{max}: 238 mμ (log ϵ = 3.88), 264 mμ (log ϵ = 3.64). In 95% ethanol ($c = 0.00016$), λ_{max}: 242 mμ (log ϵ = 3.78).

4-Nitropyridine m.p. 49–51°C., in 95% ethanol ($c = 0.00013$):

λ_{max}: 282 mμ (log ϵ = 3.35).

ACKNOWLEDGMENT

REFERENCES

1. BEATY, R. D. and MUSGRAVE, W. K. R. J. Chem. Soc. 875. 1952.
2. BINZ, A. and RÄTH, C. Ann. 486: 95. 1931.
3. CALDWELL, W. T. and KORNFELD, E. C. J. Am. Chem. Soc. 64: 1695. 1942.
4. CHICHIBABIN, A. E. and RJAZANCEV, M. D. J. Russ. Phys. Chem. Soc. 47: 1571. 1915; J. Chem. Soc. 110: 224. 1915; Chem. Abstracts, 10: 2898. 1916.
5. COOK, G. H. and SAUNDERS, B. C. Biochem. J. (London), 41: 558. 1947.
6. KIRPAL, A. and BÖHM, W. Ber. 64: 767. 1931.
7. KIRPAL, A. and BÖHM, W. Ber. 65: 680. 1932.
8. MILLER, W. K., KNIGHT, S. B., and ROE, A. J. Am. Chem. Soc. 72: 1629. 1950.
9. ROE, A. and HAWKINS, G. F. J. Am. Chem. Soc. 69: 2443. 1947.
10. SCHICKH, O. v., BINZ, A., and SCHULZ, A. Ber. 69: 2593. 1936.
11. SPIERS, C. W. F. and WIBAUT, J. P. Rec. trav. chim. 56: 573. 1937.
12. ZAHN, H. and WÜRTZ, A. Z. anal. Chem. 134: 183. 1951.

SYNTHESIS, POTENTIOMETRIC TITRATIONS, AND SPECTRA OF PYRAZOLONES[1]

By Paul E. Gagnon, Jean L. Boivin[2], and René J. Paquin[3]

ABSTRACT

Monosubstituted benzoylacetic esters, obtained by condensation of n-alkyl halides with ethyl benzoylacetate, were reacted with hydrazine and phenylhydrazine to give 3-phenyl and 1,3-diphenyl 5-pyrazolones monosubstituted in position 4 by alkyl radicals R (R = H, $C_nH_{2n+1(n=1\ to\ 10)}$, and $C_6H_5CH_2$.). The dissociation constants of the pyrazolones were determined by potentiometric titrations. A study was made of the ultraviolet absorption spectra in both neutral and acid medium and of the infrared absorption spectra. X-ray powder diffraction patterns and data of the pyrazolones were obtained.

INTRODUCTION

The condensation of hydrazine and its monosubstituted derivatives with β-keto esters gives the corresponding hydrazone which, by elimination of ethanol, cyclizes into pyrazolones. Antipyrin (II) was thus prepared by methylation of 3-methyl-4-pyrazolone (I) which was obtained from ethyl acetoacetate and hydrazine (12).
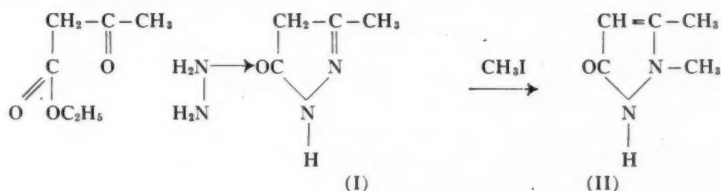
The main object of the present work was to synthesize and study the properties of 4-monosubstituted-3-phenyl-5-pyrazolones and 4-monosubstituted-1,3-diphenyl-5-pyrazolones obtained by condensation of hydrazine and phenylhydrazine with a homologous series of β-keto esters.

The starting esters used in the present work, the ethyl α-monosubstituted α-benzoylacetates (IV), were prepared by alkylation of ethyl benzoylacetate (III) with the required alkyl halide.
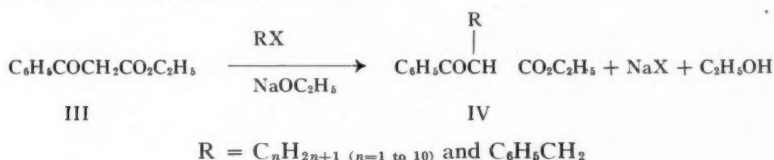
$$C_6H_5COCH_2CO_2C_2H_5 \xrightarrow[NaOC_2H_5]{RX} C_6H_5COCH^R CO_2C_2H_5 + NaX + C_2H_5OH$$

III   IV

$$R = C_nH_{2n+1\ (n=1\ to\ 10)}\ and\ C_6H_5CH_2$$

Several of these β-keto esters were reported previously (3, 15, 16). In the present investigation other esters of the homologous series were obtained in good yields, some dehydrobenzoyl acetic acid being isolated as a by-product in each case. The properties and analyses of the ethyl α-monosubstituted benzoylacetates prepared are given in Table I.

TABLE I

ETHYL α-SUBSTITUTED BENZOYLACETATES $C_6H_5COCH(R)CO_2C_2H_5$

R	B.p., °C.	Yield, %	$d25°C$	Formula	Analysis			
					Calculated		Found	
					C	H	C	H
C_5H_{11}	149–153 (2 mm.)	61	1.4980	$C_{16}H_{22}O_3$	73.28	8.40	73.52	8.47
C_6H_{13}	156–159 (2 mm.)	68	1.4952	$C_{17}H_{24}O_3$	73.91	8.69	74.33	9.00
C_7H_{15}	170–173 (2 mm.)	62	1.4939	$C_{18}H_{26}O_3$	74.48	8.97	74.38	9.11
C_8H_{17}	180–182 (2 mm.)	80	1.4928	$C_{19}H_{28}O_3$	75.00	9.21	74.93	9.32
C_9H_{19}	158–160 (0.4 mm.)	67	1.4909	$C_{20}H_{30}O_3$	75.47	9.43	75.30	9.24
$C_{10}H_{21}$	162–164 (0.2 mm.)	66	1.4997	$C_{21}H_{32}O_3$	75.89	9.63	75.57	9.58

The condensation of hydrazine with ethyl benzoylacetate (IV, R = H) to give 3-phenyl-5-pyrazolone (VI, R = H) was carried out by Curtius (4).

Similarly, 4-methyl-3-phenyl-5-pyrazolone (VI, R = CH₃) was prepared by Auwers and Mauss (2) from ethyl α-methyl benzoylacetate (IV, R = CH₃) and hydrazine hydrate.

Other 4-monosubstituted-3-phenyl-5-pyrazolones (VI) were prepared from the corresponding β-keto esters (IV) and hydrazine by modifying slightly the method used by Curtius, Auwers, and Mauss. The esters were refluxed with an excess of hydrazine hydrate and then heated under reduced pressure. The pyrazolones were isolated by dissolving the reaction product in alkali and precipitating with acetic acid. The hydrazones (V), presumably formed during the reaction, were not isolated.

$R = C_nH_{2n+1}$ (n=1 to 10) and $C_6H_5CH_2$
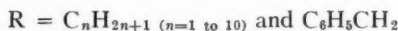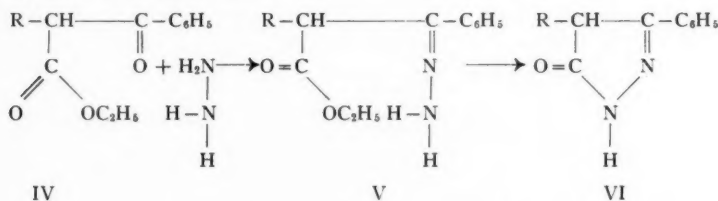
1,3-Diphenyl-5-pyrazolone (VII, R = H) was prepared by Knorr and Klotz (13) by heating a mixture of ethyl benzoylacetate (IV, R = H) and phenyl-hydrazine in ethanol.

A series of 4-monosubstituted-1,3-diphenyl-5-pyrazolones (VIII) was thus prepared by heating mixtures of substituted ethyl benzoylacetates (IV) with phenylhydrazine.

```
R—CH————C—C₆H₅        R—CH————C—C₆H₅        R—CH————C—C₆H₅
    |        ‖              |        ‖              |        ‖
O=C      O + H₂N —→ O=C         N      —→   O=C         N
    |        |              |        |              \      /
  OC₂H₅    H—N           OC₂H₅    H—N                 N
             |                      |                  |
            C₆H₅                   C₆H₅               C₆H₅

     IV                    VII                   VIII
```
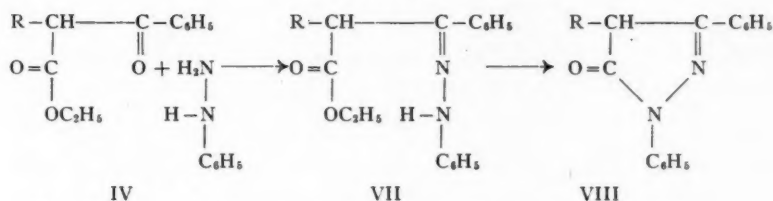
$$R = C_nH_{2n+1}\ (n=1\ to\ 10)\ and\ C_6H_5CH_2$$

The individual properties and analyses of all the pyrazolones prepared are given in Tables II and III.

TABLE II
4-Monosubstituted-3-phenyl-5-pyrazolones

R	M.p., °C.	Yield, %	Formula	Analysis Calculated C	H	N	Found C	H	N	Neutral Å	log E_m	Acid Å	log E_m
H*										2500	4.21	2500	4.28
CH₃**										2540	4.21	2520	4.12
C₂H₅	165–168	83	C₁₁H₁₂N₂O	70.21	6.38	14.89	69.84	6.53	14.80	2500	4.14	2440	4.18
C₃H₇	186–188	91	C₁₂H₁₄N₂O	71.28	6.93	13.86	71.19	6.93	13.63	2500	4.10	2440	4.12
C₄H₉	180–181	95	C₁₃H₁₆N₂O	72.22	7.41	12.96	72.38	7.46	12.95	2500	4.10	2500	4.10
C₅H₁₁	139–140	91	C₁₄H₁₈N₂O	73.04	7.82	12.18	73.00	7.73	12.25	2500	4.15	2460	4.13
C₆H₁₃	116–117	96	C₁₅H₂₀N₂O	73.77	8.19	11.48	73.66	8.05	11.48	2500	4.12	2480	4.17
C₇H₁₅	108–109	96	C₁₆H₂₂N₂O	74.42	8.52	10.85	74.31	8.47	10.82	2500	4.10	2480	4.06
C₈H₁₇	110–111	92	C₁₇H₂₄N₂O	75.00	8.83	10.28	75.28	9.08	10.10	2520	4.11	2440	4.11
C₉H₁₉	100–102	87	C₁₈H₂₆N₂O	75.52	9.09	9.79	75.26	9.14	9.84	2500	4.17	2420	4.09
C₁₀H₂₁	95–96	88	C₁₉H₂₈N₂O	76.00	9.33	9.33	76.34	9.45	9.24	2500	4.21	2480	4.07
C₆H₅CH₂	184–185	90	C₁₆H₁₄N₂O	76.80	5.60	11.20	76.66	5.49	11.13	2520	4.17	2500	4.09

* Curtius, T. J. prakt. Chem. 50: 515. 1894; Michaelis, A. and Rassmann, W. Ann. 352: 158. 1907.
** Auwers, K. and Mauss, H. J. prakt. Chem. 110: 206. 1925.

TABLE III
4-Monosubstituted-1,3-diphenyl-5-pyrazolones

R	M.p., °C.	Yield, %	Formula	Analysis Calculated C	H	N	Found C	H	N	Neutral Å	log E_m	Acid Å	log E_m
H*										2700	4.35	2700	4.35
CH₃	204–205	81	C₁₆H₁₄N₂O	76.80	5.59	11.20	77.02	5.33	11.22	3100 2500	4.09 4.57	3100 2500	3.78 4.29
C₂H₅	213–214	77	C₁₇H₁₆N₂O	77.28	6.06	10.60	77.95	5.57	10.64	3100 2500	3.80 4.32	3100 2520	3.81 4.30
C₃H₇	198–199	71	C₁₈H₁₈N₂O	77.70	6.47	10.07	77.77	6.16	9.93	3100 2480	3.81 4.31	3100 2520	3.76 4.24
C₄H₉	192–193	70	C₁₉H₂₀N₂O	78.09	6.89	9.59	78.77	6.89	9.60	3100 2500	3.90 4.39	3100 2520	3.73 4.19
C₅H₁₁	174–175	60	C₂₀H₂₂N₂O	78.43	7.19	9.15	78.83	7.12	9.26	3114 2530	3.88 4.33	3120 2520	3.87 4.32
C₆H₁₃	158–159	60	C₂₁H₂₄N₂O	78.75	7.50	8.75	79.16	7.18	8.92	3100 2520	3.85 4.29	3100 2520	3.81 4.30
C₇H₁₅	134–135	55	C₂₂H₂₆N₂O	79.04	7.78	8.38	79.20	7.60	8.52	3110 2540	4.08 4.54	3100 2510	4.15 4.61
C₈H₁₇	144–145	53	C₂₃H₂₈N₂O	79.31	8.05	8.05	79.48	7.95	8.02	3120 2540	4.15 4.55	3150 2520	4.13 4.56
C₉H₁₉	133–134	50	C₂₄H₃₀N₂O	79.56	8.29	7.74	79.23	8.02	7.84	3100 2520	3.79 4.27	3100 2520	3.79 4.25
C₁₀H₂₁	116–117	51	C₂₅H₃₂N₂O	79.80	8.51	7.44	80.26	8.33	7.32	3100 2500	3.82 4.32	3100 2500	3.77 4.27
C₆H₅CH₂	178–179	73	C₂₃H₁₈N₂O	80.98	5.52	8.59	80.81	5.41	8.75	2630	4.10	2630	4.13

* Knorr, L. and Klotz, C. Ber. 20: 2546. 1887.

Potentiometric Titrations

Pyrazolones may be considered as weak acids PYRH which dissociate into pyrazolone ions PYR⁻ (II) and protons H⁺.

$$PYRH + H_2O \rightleftharpoons PYR^- + H_3O^+$$
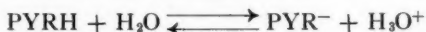
As previously reported (5) their dissociation constants were determined, with a good approximation, from the pH values of the midpoint of the flat portion of their titration curves.

All the 3-phenyl and 1,3-diphenyl-4-monosubstituted-5-pyrazolones give titration curves of the same shape (Figs. 1 and 2) and are less acidic in character than carbon dioxide.
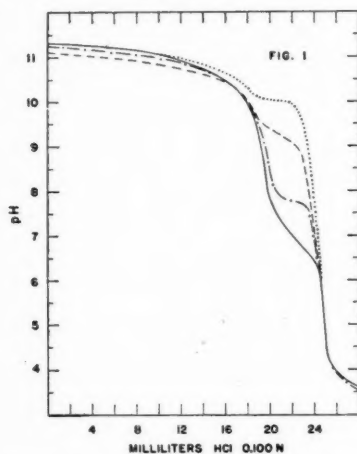
FIG. 1.   Potentiometric titration curves of:
——— 3-Phenyl-5-pyrazolone.   .... 4-Octyl-3-phenyl-5-pyrazolone.
– – – – 4-Heptyl-3-phenyl-5-pyrazolone.   –·–·–·– 4-Benzyl-3-phenyl-5-pyrazolone.
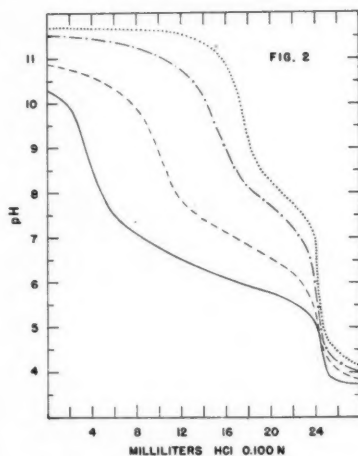
FIG. 2.   Potentiometric titration curves of:
——— 1,3-Diphenyl-5-pyrazolone.   .... 4-Heptyl-1,3-diphenyl-5-pyrazolone.
– – – – 4-Propyl-1,3-diphenyl-5-pyrazolone. –·–·–·– 4-Benzyl-1,3-diphenyl-5-pyrazolone.

The value of the pK_a in the case of the 4-monosubstituted-3-phenyl-5-pyrazolones shows a gradual increase (Table IV). For example, 3-phenyl-5-pyrazolone has a pK_a value of 7.4 and the corresponding 4-decyl pyrazolone has a value of 11.0. The other members of the series have pK_a values intermediate between these and it is possible to classify them, from the 4-propyl to the 4-decyl, as very weak acids since their dissociation constants are in the region 10^{-8} to 10^{-11}.

The 4-benzyl-3-phenyl-5-pyrazolone has a pK_a value of 7.7 and may therefore be classified in the group of weak acids, together with the unsubstituted and also the methyl and ethyl 3-phenyl-5-pyrazolones. It is of interest to note that the 4-benzyl substituted pyrazolone has a pK_a value close to that of the 4-methyl substituted pyrazolone indicating that they are acids of about the same strength.

TABLE IV
DISSOCIATION CONSTANTS OF 4-MONOSUBSTITUTED-5-PYRAZOLONES

Substituent	3-Phenyl		1,3-Diphenyl	
	Amount of substance, gm. $\times 10^2$	pK_a*	Amount of substance, gm. $\times 10^2$	pK_a
H	6.40	7.4	2.70	6.2
CH_3	6.96	7.6	5.46	7.8
C_2H_5	7.52	7.8	5.25	8.0
C_3H_7	8.08	8.0	5.11	7.0
C_4H_9	8.64	8.2	5.09	7.2
C_5H_{11}	9.20	8.4	5.05	7.3
C_6H_{13}	9.76	8.6	5.19	7.4
C_7H_{15}	10.32	9.2	5.73	8.0
C_8H_{17}	10.88	10.2	5.12	7.5
C_9H_{19}	11.44	10.6	5.16	7.2
$C_{10}H_{21}$	12.00	11.0	4.68	6.7
$C_6H_5CH_2$	10.00	7.7	3.19	7.6

* *As determined from the curves.*

The 4-monosubstituted-1,3-diphenyl-5-pyrazolones have pK_a value varying between 7 and 8 (Table IV). The unsubstituted pyrazolone is slightly more acidic as shown by its pK_a value of 6.2. The variation of the pK_a values for the homologous series shows a maximum value of 8.0 for the 4-ethyl and 4-heptyl compounds. Beyond this the values decrease regularly with the increase of the number of carbon atoms of the substituent.

Here again the 4-benzyl-1,3-diphenyl-5-pyrazolone has a pK_a value intermediate to that of the other compounds and as in the case of the 3-phenyl-5-pyrazolones it has an acidity very close to that of the corresponding methyl substituted compound.

If a comparison is made between the 3-phenyl and 1,3-diphenyl pyrazolones it is noted that the latter are slightly more acidic than the former. The unsubstituted members of both series show slightly more acidic properties than the rest of the series. This is especially true in the 1,3-diphenyl pyrazolone series where the pK_a value of the unsubstituted compound is 6.2 and that of the adjacent member in the series is 7.8. Comparing the 3-phenyl-5-pyrazolone with the 1,3-diphenyl-5-pyrazolone we note that the latter has a pK_a value of 6.2 as compared to 7.4 for the former. It is evident therefore that the diphenyl pyrazolone is more acidic than the monophenyl compound and since both molecules differ but by one phenyl group then this difference in acidity may be attributed to the effect of the phenyl group.

Ultraviolet Absorption Spectra

The ultraviolet absorption spectra of the pyrazolones were determined in neutral and acid solution. The results obtained are given in Tables II and III and shown graphically in Figs. 3 and 4.

A close inspection of the absorption curves shows that the spectra of the 4-monosubstituted-3-phenyl-5-pyrazolones (Fig. 3) are almost identical. In neutral solution, they all possess, in the 2500 Å region, a single absorption maximum of high intensity, log E_m varying from 4.10 to 4.21. In acid solution,
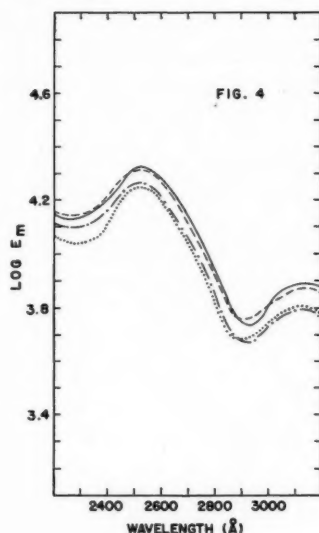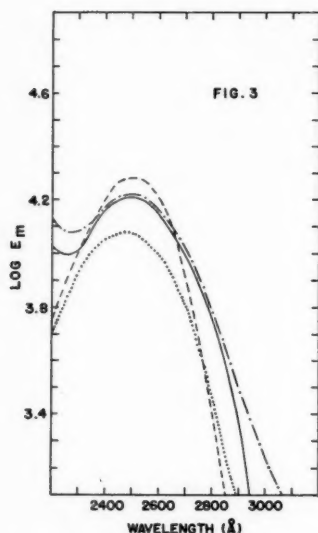
FIG. 3. Ultraviolet absorption spectrum of:
  3-Phenyl-5-pyrazolone: ———— in neutral solution; – – – – in acid solution.
  4-Decyl-3-phenyl-5-pyrazolone: –·–·–·–· in neutral solution; .... in acid solution.
FIG. 4. Ultraviolet absorption spectrum of:
  4-Amyl-1,3-diphenyl-5-pyrazolone: ———— in neutral solution; – – – – in acid solution.
  4-Nonyl-1,3-diphenyl-5-pyrazolone: –·–·–·–· in neutral solution; .... in acid solution.

the maxima are at slightly shorter wave lengths while the intensity remains nearly the same.

The 4-monosubstituted-3-phenyl-5-pyrazolones may exist under the following possible tautomeric forms:

$$R-CH-C-C_6H_5$$
$$O=C \quad N$$
$$N$$
$$H$$
IX

$$R-C=C-C_6H_5$$
$$O=C \quad N-H$$
$$N$$
$$H$$
X

$$R-C-C-C_6H_5$$
$$HO-C \quad N$$
$$N$$
$$H$$
XI
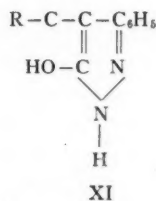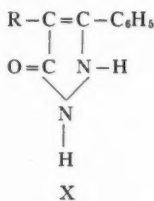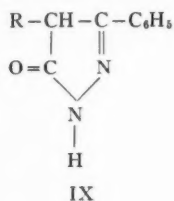
It has been reported that pyrazolones showing high intensity absorption maxima at short wave lengths have a double bond between two carbon atoms, whereas those with low intensity maxima at long wave lengths have a 2:3 double bond (6, 7, 9, 10). Shifts in the position of the maxima to longer or shorter wave lengths in acid solution were interpreted in terms of resonance effects (9). Small shifts in either direction may be due to a solvent effect, to the formation of a salt, or to a combination of several of these possibilities (18).

From these results one may assume that the 4-monosubstituted-3-phenyl-5-pyrazolones exist under structures X or XI, in neutral and acid solution,

since they possess a single high intensity maxima at short wave lengths and no appreciable shift occurs in acid media.

However, a subsequent study of the infrared absorption spectra of these pyrazolones seems to indicate that they possess the hydroxy form as shown by structure XI. This is of particular interest since previous work (8, 9) indicated that the hydroxy form existed only in alkaline solution.

4-Monoalkyl-1,3-diphenyl-5-pyrazolones, in which the position of the N-phenyl group is fixed by the method used to prepare the compound, may exist only under the following isomeric structures:

$$R-CH-C-C_6H_5 \qquad R-C=C-C_6H_5 \qquad R-C-C-C_6H_5$$

XII   XIII   XIV
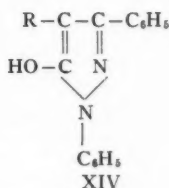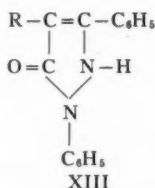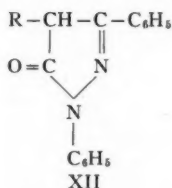
The 4-monoalkyl-1,3-diphenyl-5-pyrazolones (Fig. 4) exhibited two maxima in neutral solution, one of high intensity with log $E_m = 4.39$ at about 2500 Å and a second of low intensity, log E_m 3.91, in the longer wave length region at 3100 Å. In acid media the maxima were not shifted and the intensity remained nearly the same. The high intensity maximum at short wave length implied the presence of an ethylenic bond whereas the low intensity maxima at long wave lengths indicated a 2:3 double bond. From these results one may conclude that the 4-monoalkyl-1,3-diphenyl-5-pyrazolones may exist, in both neutral and acid media under the three structures XII, XIII, and XIV. Structures XIII and XIV may be discarded however since infrared absorption measurements show the presence of a $C=N$ bond and the absence of a hydroxyl group.

Infrared Absorption Spectra

The infrared absorption spectra of the pyrazolones were determined with a Perkin-Elmer spectrophotometer. The results obtained are given in Table V and some of the data are plotted in Figs. 5 and 6.

The 4-monosubstituted-3-phenyl-5-pyrazolones have absorption curves which are very similar. They show a band of relatively high intensity at about 1600 cm.$^{-1}$ and several other bands of smaller intensity in the double bond region, that is, between 1850 and 1470 cm^{-1}. In most of the cases, another weak band occurs in the hydrogen stretching region around 3300 cm^{-1}.

The most striking conclusion to be reached from these results is that apparently the $C=O$ group is not present, since its characteristic frequency at approximately 1700 cm.$^{-1}$ is absent. The absence of this functional group, however, offers a satisfactory explanation for the band at 3300 cm^{-1}. It is well known that pyrazolones can exist under the hydroxy form and, therefore, the band at 3300 cm.$^{-1}$ could be interpreted as the characteristic frequency of the hydroxyl group. This band, however, has but a small intensity and in some cases it occurs as an inflection point only. The 4-benzyl-3-phenyl-5-
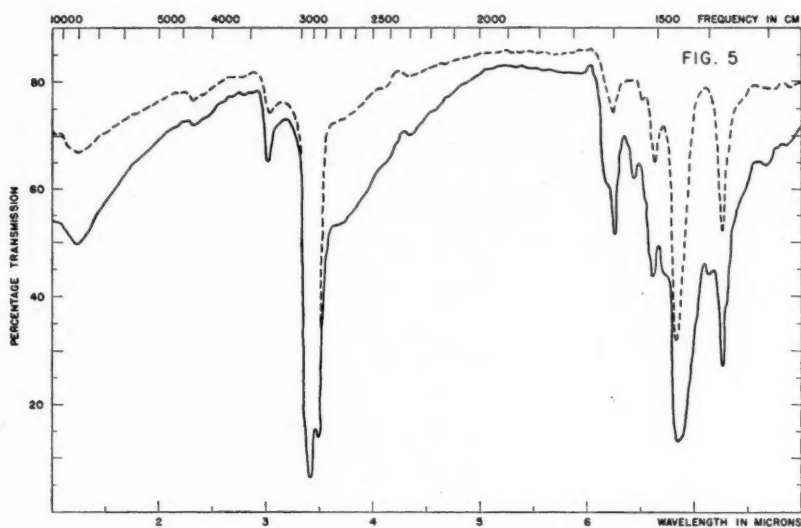
FIG. 5. Infrared absorption spectrum of:
- - - - 4-Octyl-3-phenyl-5-pyrazolone.
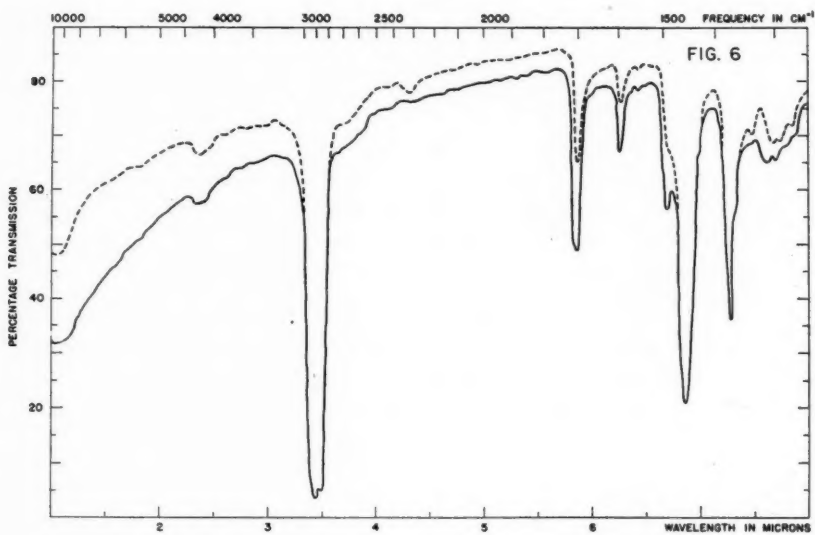——— 4-Benzyl-3-phenyl-5-pyrazolone.

FIG. 6. Infrared absorption spectrum of:
- - - - 4-Ethyl-1,3-diphenyl-5-pyrazolone.
——— 4-Heptyl-1,3-diphenyl-5-pyrazolone.

pyrazolone is an exception since it shows a band of relatively high intensity at 3300 cm^{-1}. This is in agreement with corresponding absorption in this region of another type of pyrazolone, the 4-benzyl-3-amino-5-pyrazolone. It must be noted that the NH frequency also falls in this region, but the absence of the C=O band offers a good indication for the correct assignment of the 3300 cm.$^{-1}$ band to the hydroxyl group.

The remainder of the spectrum is made up of several bands of small intensity. The fact that more than one band is observed in the double-bond region is a fair indication of the presence of conjugation. The most intense absorption in this region occurs at 1600 cm^{-1}. If we refer to the results obtained by Randal and his co-workers (17) then this band must be assigned to a cyclic C=N group. The above named authors reported the presence of such a band at about 1610 cm.$^{-1}$ for 3-methyl-5-pyrazolone. The other bands present in this region of the spectra have a very small intensity. They may be tentatively assigned to an ethylenic band or to characteristic phenyl and ring vibrations.

From these assignements, the 4-monosubstituted 3-phenyl-5-pyrazolones may be assumed to exist under structure XI, which is shown in the discussion of the ultraviolet spectra.

The infrared absorption spectra of the 4-monosubstituted-1,3-diphenyl-5-pyrazolones are similar and comparatively less complicated than those of the 3-phenyl-5-pyrazolones since they show but two absorption bands in the double-bond region. The 4-benzyl-1,3-diphenyl-5-pyrazolone is an exception since it shows but one band which is apparently resolved into a triplet with frequencies of 1635, 1615, and 1590 cm^{-1}.

A high intensity absorption band appears between 1700 cm.$^{-1}$ and 1710 cm^{-1}. Since this is the region in which the C=O group absorbs, this vibration can be attributed to this grouping. This is in accord with the vibration frequency of the C=O in cyclic compounds such as lactamus (17).

The other band, of slightly less intensity, occurs at a frequency of about 1600 cm^{-1}. This absorption occurs in the region characteristic of the C=N group. Randal and his co-workers (17) studied a number of cyclic derivatives such as thiazolidines, imidazolines, pyridines, and oxazolones, together with the 3-methyl-5-pyrazolone already mentioned, and they assigned the C=N vibration to the region between 1680 cm.$^{-1}$ and 1590 cm^{-1}. From these results the absorption band at 1600 cm.$^{-1}$ can be attributed to the presence of a cyclic C=N group.

The structure of the 4-monosubstituted-1,3-diphenyl-5-pyrazolones can therefore be represented as by formula XII, given in the ultraviolet section.

X-ray Powder Diffraction

The use of X-ray powder diffraction for analytical purposes has been extensively used to supplement other procedures. X-ray diffraction may be relied upon to provide a simple, rapid, and direct method of analysis. There are many analytical problems for which only X-ray diffraction can give the required results. This stems from the fact that X-ray diffraction patterns are characteristic of the compounds rather than of the elements or chemical groups present.

The success of this analytical method is dependent upon an adequate set of reference standards. This remains a fundamental limitation to the method since there are compounds for which crystallographic data are not yet available. The vast majority of published data (1, 11) have been limited to inorganic compounds, very few being for organic compounds.

X-ray powder diffraction patterns for organic compounds are much more complex and exhibit wider diffraction bands than do inorganic compounds. The success of this method for identifying individual members of a homologous series depends upon the extent to which an additional methylene group affects the powder pattern of a typical member of a series. This ability of the analytical method to distinguish between homologues was demonstrated for the anilides of the saturated aliphatic acids by Matthews and Michell (14) and later for the amides of these acids by Wurg and Sharples (19).

To our knowledge no data have been published on the X-ray powder diffraction of pyrazolones. The present work deals with the diffraction patterns of 4-monosubstituted-3-phenyl-5-pyrazolones and 4-monosubstituted-1,3-diphenyl-5-pyrazolones. The results obtained are given in Tables VI and VII and some of the patterns are shown in Figs. 7 to 10. As expected, the patterns are sufficiently different to allow distinction between the members of the homologous series and, therefore, offer a convenient method for the identification of the pyrazolones.

EXPERIMENTAL PART*

Ethyl α-Monosubstituted-α-benzoylacetate

Ethyl benzoylacetate (1.0 mole) was added to a cold solution of sodium ethoxide (0.5 mole, 300 ml. of absolute alcohol) and the mixture was refluxed for one hour. The required n-alkyl bromide (0.5 mole) was then slowly added to the boiling solution and the reaction mixture was refluxed until nearly neutral to moist litmus paper. The precipitated sodium bromide was filtered off and washed with ethanol. The alcoholic filtrate, concentrated under reduced pressure, was poured into cold water (500 ml.) acidified with hydrochloric acid (25 ml.). The viscous layer was decanted and the aqueous layer extracted three times with ether. The extracts were added to the viscous material. The resulting solution was washed with water three times and dried over anhydrous sodium sulphate. The ether was removed under reduced pressure and the residue was fractionated. The esters are listed, together with their boiling points, indices of refraction, and analyses in Table I.

4-Monosubstituted-3-phenyl-5-pyrazolones

Ethyl α-monosubstituted-α-benzoylacetate (0.02 mole) was added to an excess of hydrazine hydrate (0.06 mole) and the mixture was refluxed for five hours in a wax bath maintained at 115°C. The resulting viscous liquid was heated under reduced pressure (10 mm.) at 120 to 130°C. for three hours in order to remove the excess hydrazine hydrate together with the water and ethanol formed in the reaction. The solid obtained was cooled and dissolved

---

* *All melting points are uncorrected.*
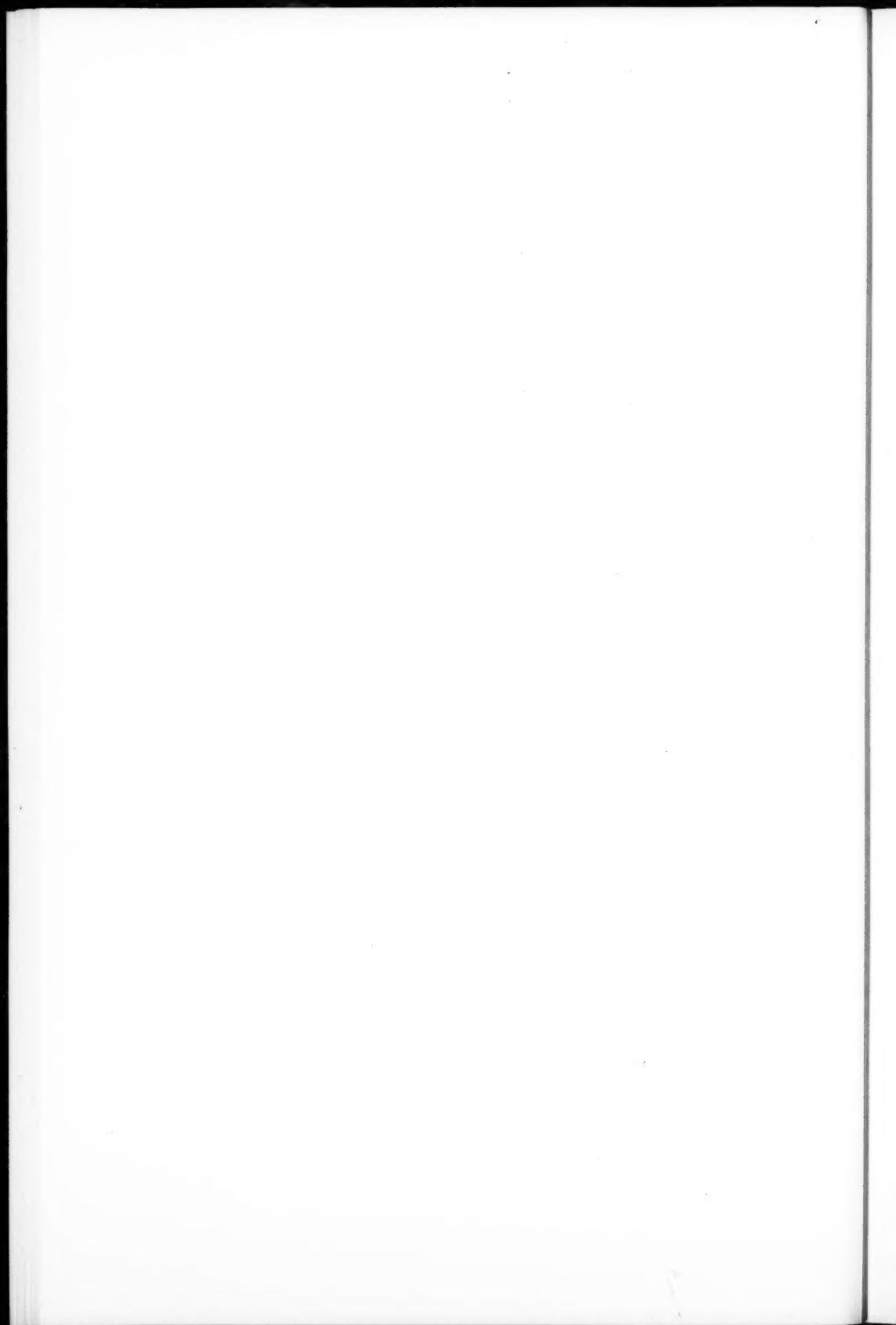
PLATE I

FIG. 7.   X-ray powder diffraction pattern of 3-phenyl-5-pyrazolone.
FIG. 8.   X-ray powder diffraction pattern of 4-propyl-3-phenyl-5-pyrazolone.
FIG. 9.   X-ray powder diffraction pattern of 4-methyl-1,3-diphenyl-5-pyrazolone.
FIG. 10.   X-ray powder diffraction pattern of 4-butyl-1,3-diphenyl-5-pyrazolone.

in sodium hydroxide (5%, 200 ml.). The solution was diluted with water (100 ml.) and washed with ether until the extracts were no longer colored. The alkaline solution was cooled and acidified with acetic acid (50%). The precipitate was filtered, washed with water, and dried. The product was purified by crystallization from ethanol, petroleum ether, or a mixture of the two. The pyrazolones are listed, together with their melting points, analyses, and ultraviolet absorption maxima in Table II. Their infrared absorption bands are given in Table V and their X-ray powder diffraction data in Table VI.

4-Monosubstituted-1,3-diphenyl-5-pyrazolones

A mixture of ethyl α-monosubstituted-α-benzoylacetate (0.01 mole) and phenylhydrazine (0.01 mole) was heated for four hours at 110 to 120°C. and for one hour at 180°C. The red viscous liquid obtained was cooled and dissolved in sodium hydroxide (10%, 100 ml.). The solution was diluted with water (100 ml.), filtered to remove the insoluble material, and washed with ether until the extracts were no longer colored. The alkaline solution was cooled to about 0°C. and acidified with acetic acid (50%). The precipitate was filtered, washed with water, and dried. The product was dissolved in ether and the ethereal solution washed with water three times and dried over anhydrous sodium sulphate. The ether was distilled off and the residue obtained was purified by crystallization from a small quantity of ethanol. The pyrazolones are listed together with their melting points, analyses, and ultraviolet absorption maxima in Table III. Their infrared absorption bands are given in Table V and their X-ray powder diffraction data in Table VII.

TABLE V

INFRARED ABSORPTION MAXIMA OF 4-MONOSUBSTITUTED-5-PYRAZOLONES

R	Absorption bands, cm.$^{-1}$												
	3-Phenyl								1,3-Diphenyl				
H	3150	1590	1565	1530	1500	1305	1285	1260	1710	1595		1320	1275
CH$_3$	3290	1595	1565	1530	1500	1305	1285	1258	1708	1600		1305	
C$_2$H$_5$	3200	1590	1565	1530	1500	1305	1285	1260	1705	1598	1305	1295	1275
C$_3$H$_7$		1600	1570	1535	1510	1300	1285	1265	1708	1600	1315	1300	1275
C$_4$H$_9$	3300	1600	1570	1535	1510	1305	1285	1265	1705	1595	1305	1295	1260
C$_5$H$_{11}$		1600	1565	1530	1510	1305	1275	1260	1712	1602	1320	1300	1280
C$_6$H$_{13}$	3300	1600	1570	1530	1508	1305	1285	1265	1710	1595	1305	1282	1260
C$_7$H$_{15}$	3300	1600	1570	1530	1500	1305	1285	1265	1705	1600	1315	1298	1280
C$_8$H$_{17}$	3330	1600	1570	1530	1505	1300	1285	1265	1708	1600	1310	1300	1275
C$_9$H$_{19}$		1600	1565	1555	1510	1300	1285	1265	1708	1600	1310	1295	1272
C$_{10}$H$_{21}$		1600	1575	1535	1510	1300	1290	1270	1708	1600	1315	1300	1275
C$_6$H$_5$CH$_2$	3310	1600		1555	1510	1300	1290	1270		1625 1615 1590	1325	1310	1270

Potentiometric Titrations

The potentiometric titrations were made by a method already described (5). The pyrazolones (4×10^{-4} mole) were dissolved in sodium hydroxide (0.1 N, 25 ml.). In the case of the 1,3-diphenyl-5-pyrazolones a small quantity of alco-

TABLE VI

X-RAY POWDER DIFFRACTION DATA OF 4-MONOSUBSTITUTED-3-PHENYL-5-PYRAZOLONES, $RC_9H_7N_2O$

R = H		CH_3		C_2H_5		C_3H_7		C_4H_9		C_5H_{11}		C_6H_{13}		C_7H_{15}		C_8H_{17}		C_9H_{19}		$C_{10}H_{21}$		$C_6H_5CH_2$	
d/n	I	d/n	I	d/n	I	d/n	I	d/n	I	d/n	I	d/n	I	d/n	I	d/n	I	d/n	I	d/n	I	d/n	I
10.5	4	8.7	6	13.3	8	12.2	8	12.9	5	11.0	6	11.5	5	15.7	5	16.6	5	16.8	10	18.7	7	13.2	3
5.40	5	7.0	4	10.0	2	9.9	2	10.1	2	8.1	3	8.2	3	9.9	1	9.4	2	15.1	6	16.5	7	8.3	1
4.69	1	6.33	4	6.7	8	7.5	4	8.2	1	6.6	2	6.8	2	7.9	5	7.5	1	7.1	4	13.1	5	7.40	3
4.45	2	5.54	2	5.81	1	7.0	4	7.5	1	5.93	2	6.05	1	7.2	2	7.1	5	5.63	3	10.2	2	6.30	3
4.16	10	5.02	10	5.39	4	6.45	4	6.9	5	5.24	4	5.37	2	6.5	5	6.05	3	5.11	10	8.7	3	5.42	5
3.58	3	4.78	6	4.98	1	5.65	2	5.56	5	4.90	5	5.04	5	5.50	5	5.65	5	4.39	10	6.65	3	4.93	3
3.43	3	4.61	8	4.54	8	5.23	1	5.27	2	4.35	4	4.55	3	4.97	2	5.26	1	4.14	10	5.63	5	4.66	7
3.24	3	4.03	10	4.24	8	4.96	6	4.83	5	4.14	10	4.32	10	4.71	5	4.81	5	3.55	5	5.12	5	4.35	10
3.12	2	3.65	10	4.03	10	4.72	1	4.48	4	3.92	2	4.03	8	4.34	10	4.57	5	3.29	1	4.73	5	4.03	8
2.86	1	3.53	2	3.70	8	4.43	10	4.30	4	3.58	6	3.80	9	4.17	7	4.45	5	2.81	2	4.40	10	3.53	5
2.71	2	3.40	5	3.46	4	4.27	8	4.10	5	3.22	6	3.33	8	3.89	8	4.22	10	2.46	1	4.14	4	3.27	5
2.62	1	3.25	5	3.27	4	3.87	10	3.86	7	2.86	4	2.85	3	3.74	10	4.05	1	8.67	1	3.97	4	2.68	2
2.51	3	2.97	4	2.99	2	3.64	5	3.44	3	2.72	3	2.58	1	3.52	5	3.95	10	8.38	1	3.76	5	2.22	1
2.41	1	2.88	2	2.84	1	3.29	5	3.24	10	2.61	3	2.04	1	3.37	3	3.57	5			3.49	3	1.92	1
2.33	1	2.79	3	2.51	1	3.01	4	3.05	4	2.49	2			3.24	3	3.30	3			3.30	2		
2.27	1	2.72	3	2.39	1	2.87	4	2.91	3	2.33	1			3.10	1	3.02	1			3.01	1		
2.10	2	2.54	1	2.01	1	2.66	1	2.76	3	2.20	2			2.76	2	2.81	1			2.82	4		
2.005	1	2.48	1			2.55	3	2.64	3					2.07	1	2.66	1			2.62	1		
1.945	2	2.37	1			2.37	2	2.54	3							2.40	1						
1.840	1	2.26	2			2.23	1	2.23	4														
1.780	1	2.165	1			2.10	4	2.13	2														
1.738	1	2.100	2			1.895	1	1.815	1														
1.121	1	2.050	1			1.822	1																
0.865	1	2.000	1			1.735	2																
0.839	1	1.781	2			1.683	1																

TABLE VII

X-RAY POWDER DIFFRACTION DATA OF 4-MONOSUBSTITUTED-1,3-DIPHENYL-5-PYRAZOLONES, RC₁₅H₁₁N₂O

R = H		CH₃		C₂H₅		C₃H₇		C₄H₉		C₅H₁₁		C₆H₁₃		C₇H₁₅		C₈H₁₇		C₉H₁₉		C₁₀H₂₁		C₆H₅CH₂	
d/n	I	d/n	I	d/n	I	d/n	I	d/n	I	d/n	I	d/n	I	d/n	I	d/n	I	d/n	I	d/n	I	d/n	I
9.5	8	10.6	10	10.1	10	10.4	9	10.4	10	10.5	9	9.8	1	10.5	10	10.8	10	11.3	10	13.5	8	11.4	5
8.4	8	7.4	10	7.5	10	7.9	10	8.5	10	9.0	10	8.6	10	9.1	1	10.3	10	10.4	10	12.1	10	8.9	10
7.0	9	6.8	10	7.2	10	7.3	3	7.4	2	8.0		7.9	2	8.3		8.6	3	7.6	9	9.3	8	7.1	2
5.9	9	6.3	9	5.3	9	6.7	3	6.3	9	7.5	9	7.4	1	6.9	8	7.4	5	7.1	7	8.7	10	6.7	1
5.6	7	6.1	10	4.94	9	6.0	1	6.0	3	6.5	2	7.0	1	6.2		6.9	5	6.6	2	8.3	2	5.9	9
5.2	9	5.18	9	3.92	9	5.7	3	5.5	3	6.1	2	6.7	1	5.9	1	5.5	1	5.9	4	7.8	9	5.6	7
4.91	7	4.55	9	3.77	7	5.2	9	5.21	3	5.7	2	6.4	1	5.6		5.31	9	5.6	4	5.8		5.4	8
4.22	9	4.13	9	3.53	10	4.67	3	4.91	4	5.2	8	5.7	4	5.4	2	4.79	9	5.4	7	5.3	9	5.1	8
4.14	7	3.89	2	3.35	9	4.32	9	4.57	3	4.85	10	5.2	3	5.2	2	4.34	1	4.91	4	5.0	9	4.86	6
3.99	8	3.79	10	3.16	1	4.04	3	4.28	7	4.35	4	4.69	6	4.94	1	4.20	7	4.40	4	4.8	1	4.69	8
3.60	10	3.63	2	3.02	1	3.73	9	4.06	4	4.16	4	4.24	2	4.64	9	4.05	8	4.06	1	4.6	5	4.56	8
3.32	8	3.56	3	2.86	1	3.58	8	3.91	8	4.05	4	4.12	9	4.15		3.79	7	3.89	3	4.4	1	4.37	5
3.19	8	3.35	3	2.59	1	3.45	8	3.71	8	3.75	8	3.81	8	4.05	1	3.58	7	3.61	2	4.2	9	4.18	9
2.99	5	3.27	3	2.48	1	2.86	8	3.58	8	3.61	7	3.58	7	3.74	7	3.46	8	3.52	1	4.0	9	4.05	10
2.80	5	3.15	1	2.26	1	2.60	1	3.37	9	3.43	7	3.44	6	3.58		3.26	1	3.35	1	3.8	5	3.91	2
2.54	5	3.05	1	2.22	1			3.29	8	3.30	1	3.14	6	3.43	1	2.83	1	3.26	1	3.7	3	3.75	8
2.32	1	2.89	1					3.13	7			2.88	6	3.17	7	2.11	1			3.6	9	3.64	8
		2.71	1					2.89	2					2.98						3.5	2	3.52	9
		2.58	1					2.82	4					2.82	1					3.4	2	3.32	7
		2.41	1					2.73	1					2.11	1					2.9	2	3.14	8
		2.26	1					2.03	1											2.6	1	3.07	8
		2.10	1																			2.69	2
		1.91	1																			2.57	1
		1.78	1																			2.52	4

hol was added to increase their solubility. The solution was diluted with water (200 ml.) and titrated with standard hydrochloric solution (0.1 N). The pH values were recorded with a Beckman pH meter, Model H 2. The results are given in Table IV and shown graphically in Figs. 1 and 2.

Ultraviolet Absorption Spectra

The ultraviolet absorption spectra of the pyrazolones were taken on a Beckman Spectrophotometer Model DU in the same way as previously described (9). The values obtained were plotted as log E_m against the wave lengths in Angstrom units. The solvents employed were ethanol (95%) and a solution of hydrochloric acid (0.01 N) in ethanol. The results are listed in Tables II and III and some of the data are plotted in Figs. 3 and 4.

Infrared Absorption Spectra

All the infrared absorption spectra of the pyrazolones were obtained with a Perkin-Elmer Model 21 double-beam null principle recording spectrophotometer. The pyrazolones were mulled in Nujol in an agate mortar until a uniform paste was obtained. The mulled samples were placed between two freshly polished rock salt plates and spread out into a uniform film by applying normal pressure. Visual observation of the sample through the plates quickly indicated whether a satisfactorily dispersed film had been obtained.

Infrared absorption spectra were then run and the resulting spectra interpreted. Over the whole range of the spectrum, from 10,000 to 650 cm.$^{-1}$, a given slit width was used for every wave length and these slit widths were the same for each pyrazolone. Only the portion of the spectra covering the range from 10,000 to 1250 cm.$^{-1}$ is given in Figs. 5 and 6. The curves all show the four specific bands of Nujol, a strong doublet at 2950 and 2850 cm.$^{-1}$ and two medium strong absorptions at 1460 and 1375 cm^{-1}. The other bands are given in Table V and have been discussed in the theoretical part.

X-ray Powder Diffraction

The pyrazolones were ground to a suitable state of subdivision in an agate mortar and mounted on Lindeman glass fibers with the aid of a little vaseline. The procedure was found adequate for the identification of the substances concerned.

The photographs were taken in a cylindrical camera having a diameter of 114.59 mm. All the samples were rotated during the 2.5 to 3.0 hr. exposure. The determinations were made on a North American Phillips diffraction unit with the copper Kα ($\lambda = 1.5387$ kx) radiation.

The values recorded in Tables VI and VII were determined from the patterns in the usual manner.

The calculated interplanar spacings are expressed in kx units. The corresponding intensities were determined visually and the values recorded are the relative intensities, the most intense line being taken as 10 units. Some of the patterns are shown in Figs. 7 to 10.

Research and Development Establishment and to Mr. F. Claisse of the Quebec Department of Mines for assistance with the infrared spectra and the X-ray diffraction measurements.

REFERENCES

1. AM. SOC. TESTING MATERIALS. X-Ray diffraction data index. A.S.T.M., Philadelphia, Pa. 1942.
2. AUWERS, K. and MAUSS, H. J. prakt. Chem. 110: 206. 1925.
3. BRESLOW, D. S. J. Am. Chem. Soc. 66: 1286. 1944.
4. CURTIUS, T. J. prakt. Chem. 50: 515. 1894.
5. GAGNON, P. E., BOIVIN, J. L., and BOIVIN, P. A. Can. J. Research, B, 28: 720. 1950.
6. GAGNON, P. E., BOIVIN, J. L., and BOIVIN, P. A. Can. J. Research, B, 29: 182. 1951.
7. GAGNON, P. E., BOIVIN, J. L., and CHISHOLM, A. Can. J. Chem. 30: 904. 1952.
8. GAGNON, P. E., BOIVIN, J. L., and GIGUÈRE, J. Can. J. Chem. 29: 328. 1951.
9. GAGNON, P. E., BOIVIN, J. L., and JONES, R. N. Can. J. Research, B, 27: 190. 1949.
10. GAGNON, P. E., NOLIN, B., and JONES, R. N. Can. J. Chem. 29: 843. 1951.
11. HANAWALT, J. D., RINN, H. W., and FREVEL, L. K. Ind. Eng. Chem. Anal. Ed. 10: 457. 1938.
12. KNORR, L. Ann. 238: 203. 1887.
13. KNORR, L. and KLOTZ, C. Ber. 20: 2546. 1887.
14. MATTHEWS, F. W. and MICHELL, J. H. Ind. Eng. Chem. Anal. Ed. 18: 662. 1946.
15. PERKIN, W. A., Jr. J. Chem. Soc. 45: 179. 1884.
16. PERKIN, W. A., Jr. and CALMAN, A. J. Chem. Soc. 49: 156. 1886.
17. RANDAL, H. M., FOWLER, R. G., FUSON, N., and DANGL, J. R. Infrared determination of organic structures. D. Van Nostrand Company, Inc., New York 1949. p. 222.
18. SCHIEBE, G. F.I.A.T. Review of German Science, 1939–1946. Vol. 35, p. 81. 1950.
19. WURZ, D. H. and SHARPLESS, N. E. Ind. Eng. Chem. Anal. Ed. 21: 1446. 1949.

THE ALPHA AND BETA 1,3,4,6-TETRAACETYL-D-GLUCOPYRANOSES AND THEIR CHLOROACETYL DERIVATIVES[1]

By R. U. Lemieux and G. Huber[2]

ABSTRACT

Reaction of 3,4,6-triacetyl-β-D-glucopyranosyl chloride with silver acetate in acetic acid gave 1,3,4,6-tetraacetyl-α-D-glucopyranose, m.p. 97–98°C., $[\alpha]_D$ +145° (chloroform). 3,4,6-Triacetyl-α-D-glucopyranosyl chloride, m.p. 93–94°C., $[\alpha]_D$ +185° (chloroform), prepared from the β-anomer by isomerization in acetone, with silver acetate in acetic acid gave 1,3,4,6-tetraacetyl-β-D-glucopyranose, m.p. 137–138°C., $[\alpha]_D$ +26° (chloroform). The structures of these glucose tetraacetates were established by the interconversion of chloroacetyl derivatives.

Our studies of the properties of the pentaacetylglucopyranoses (16, 17, 18) have established the strong activating effect of C2-acetoxy group participation in dissociation of the Cl to acetoxy group bond of the 1,2-*trans*-β-anomer. It was now of interest to examine the effect of altering the C2-substituent on the ease of dissociation and for this the anomeric 1,3,4,6-tetraacetyl-D-glucopyranoses were desirable starting materials.

In 1921, Brigl (5) reported the preparation of 2-trichloroacetyl-triacetyl-β-D-glucopyranosyl chloride (I) by reaction of pentaacetyl-β-D-glucopyranose with phosphorus pentachloride. Ammonia in ether was shown to preferentially remove the trichloroacetyl group to yield 3,4,6-triacetyl-β-D-glucopyranosyl chloride (II). The chloride (II) was shown to mutarotate in acetone solution to yield a strongly dextrorotatory sirupy product presumed to be the α-anomer (III). In re-examining these reactions we have found the yield of I to be much more reproducible and substantially increased by lengthening the reaction time from 2.5 hr. to 5 hr. and by adding carbon tetrachloride to hasten attainment of homogeneity. Further, we have crystallized III, and its chemical properties agree with the structure proposed by Brigl.

Later, Brigl (6) reported the preparation of triacetyl-D-glucosan ⟨1,5⟩ α ⟨1,2⟩ (Brigl's anhydride) (IV) by treating the β-chloride (II) with an excess of ammonia in dry benzene. Brigl (6) discovered that the anhydride (IV) reacts with methanol at room temperature to yield methyl 3,4,6-triacetyl-β-D-glucopyranoside (VII). Hardegger and de Pascual (10) found that reaction of the anhydride (IV) with acetic acid gave a glucose tetraacetate, m.p. 131°C., $[\alpha]_D$ +28° (chloroform), which was presumed to be 1,3,4,6-tetraacetyl-β-D-glucopyranose (VI). We have obtained the same substance, m.p. 137–138°C., $[\alpha]_D$ +26° (chloroform), in high yield by reaction of the 3,4,6-triacetyl-α-D-glucopyranosyl chloride (III) with silver acetate in acetic acid. Gakhokidze (8) has reported the preparation of 1,3,4,6-tetraacetyl-β-D-glucopyranose with melting point 138°C. The rotation

O—   O—   O—   O—
| | | |
ClCH   ClCH   ——————   HCCl   HC
| | | ⟍
HCOCOCCl₃ ——→   HCOH   ——→   HCOH   O
| | | ⟋
                                                     HC
I   II   III   IV

O—   O—   O—
| | |
HCOAc   AcOCH   CH₃OCH
| | |
HCOH   HCOH   HCOH

V   VI   VII

O—   O—   O—
| | |
HCOAc   AcOCH   CH₃OCH
| | |
HCOCOR   HCOCOR   HCOCOR

VIIIa, R = CH₂Cl ⇄ IXa, R = CH₂Cl ⌐— Xa, R = CH₂Cl
VIIIb, R = CHCl₂ ←— IXb, R = CHCl₂   Xb, R = CHCl₂
VIIIc, R = CCl₃   IXc, R = CCl₃   Xc, R = CCl₃
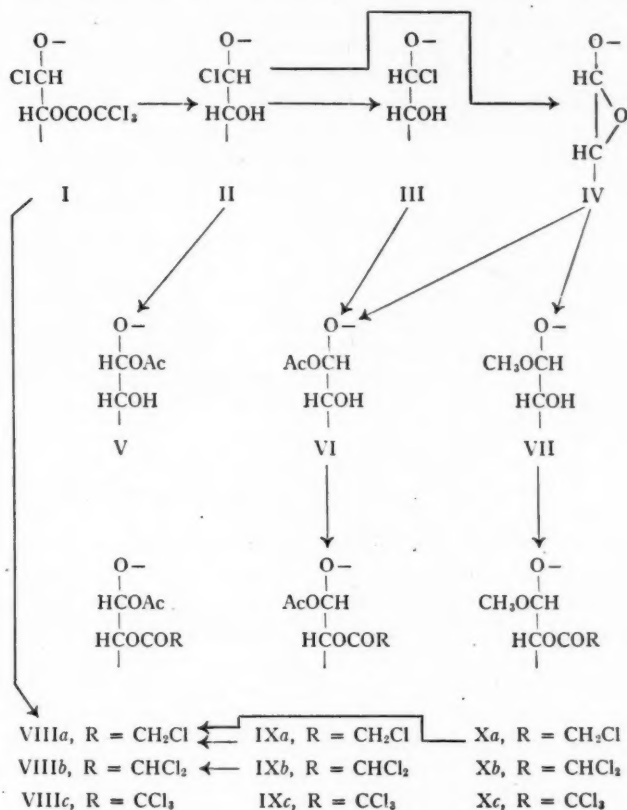
was not reported and an error may have been made (7, p. 40) in reporting the preparative procedure. Reaction of 3,4,6-triacetyl-β-D-glucopyranosyl chloride (II) with silver acetate in acetic acid gave 1,3,4,6-tetraacetyl-α-D-glucopyranose (V), m.p. 97–98°C., $[\alpha]_D$ +145° (chloroform), in high yield. The yield was much lower when ether was used as solvent. Proofs for the structures of these glucose tetraacetates (V and VI) are described below.

Trichloroacetylation of the α-tetraacetate (V) yielded a trichloroacetyl-tetraacetyl-α-D-glucose (VIIIc) which was identical to that obtained on reaction of 2-trichloroacetyl-triacetyl-β-D-glucopyranosyl chloride (I) with silver acetate in acetic acid. Therefore, the substance (V) must be 1,3,4,6-tetraacetyl-α-D-glucopyranose. Monochloroacetylation of V gave a product (VIIIa) which was also obtained by anomerization of the product from the monochloroacetylation of the β-tetraacetate (VI). Therefore, the latter substance (VI) must be 1,3,4,6-tetraacetyl-β-D-glucopyranose. These conclusions were substantiated in a variety of ways. Trichloroacetylation of VI yielded a

product (IX*c*) with the physical constants reported by Brigl (5) for 2-tri-chloroacetyl-tetraacetyl-β-D-glucopyranose. Dichloroacetylation of VI yielded 2-dichloroacetyl-tetraacetyl-β-D-glucopyranose (IX*b*) and anomerization of this product gave a substance identical to that (VIII*b*) obtained on dichloro-acetylation of the α-tetraacetate (V). Finally, the 2-monochloroacetyl-tetraacetyl-β-D-glucopyranose (IX*a*) was shown to be different to the mono-chloroacetyl-tetraacetyl-β-D-glucopyranoses which contain the monochloro-acetyl group at positions 1, 4, or 6. This precaution seemed warranted since acetyl migrations are known (12, 13) which involve positions 1, 2, 4, and 6 of the glucopyranose molecule.

The 2-monochloroacetyl, 2-dichloroacetyl, and 2-trichloroacetyl derivatives (X*a*, X*b*, and X*c*, respectively) of methyl 3,4,6-triacetyl-β-D-glucopyranoside were prepared (see Table I). The structure of the monochloroacetyl derivative (X*a*) was corroborated by acetolysis to the 2-monochloroacetyl-tetraacetyl-α-D-glucopyranose (VIII*a*).

THEORETICAL CONSIDERATIONS

Lemieux (16) has pointed out that participation of the C2-acetoxy group in replacement of the C1-acetoxy group of pentaacetyl-β-D-glucopyranose affords a reasonable account for the preferential chlorination of the C2-acetoxy group by phosphorus pentachloride to yield 2-trichloroacetyl-triacetyl-β-D-gluco-pyranosyl chloride (I). Abramovitch (1) has suggested that the preferential chlorination of the C2-acetoxy group may be due to the $-I$ effect of a chlorine atom at C1.

The formation of the 1,2-*cis*-α-anomer (VIII*c*) as the main product from the reaction of 2-trichloroacetyl-triacetyl-β-D-glucopyranosyl chloride (I) with silver acetate in acetic acid should be contrasted with the usual tendency for acetohalogenosugars to yield 1,2-*trans*-acetates under these reaction con-ditions (19). This result is in agreement with the conclusion (17) that the trichloroacetyl group has little tendency for participation in replacements at a neighboring carbon atom. Hickinbottom (14) has prepared α-glucosides by reaction of 2-trichloroacetyl-triacetyl-β-D-glucopyranosyl chloride (I) under the conditions of the Koenigs-Knorr reaction. The formation of the α-tetra-acetate (V) from the β-chloride (II) in 81% yield by reaction with silver acetate in acetic acid was to be expected on the basis of the conclusion reached by Winstein and Grunwald (20) that neighboring hydroxyl groups show little tendency for participation in replacement reactions. The formation of the β-tetraacetate (VI) from the α-chloride (III) in 79% yield under the same reaction conditions indicates that this reaction was also free of appreciable neighboring group participation. This result could not be predicted since evidence exists (2) that the C6-oxygen atom of glucose can participate in replacement reactions at the anomeric center. It is of interest to note that Hardegger and Montavon (11) have prepared ethyl α-D-isorhamnoside from 3,4-diacetyl-β-D-isorhamnosyl chloride and ethyl β-D-isorhamnoside from 3,4-diacetyl-α-D-isorhamnosyl chloride. The high yields of the Walden inversion products obtained in these reactions suggest that the transformations took

TABLE I

SOME DERIVATIVES OF D-GLUCOPYRANOSES

Compound	M.p., °C.	$[\alpha]_D^a$	$[M]_D$	A^b	B^b	% Carbon Calc.	% Carbon Found	% Hydrogen Calc.	% Hydrogen Found	Reference
Derivatives of tetraacetyl-D-glucopyranoses										
α-1,3,4,6- (V)	97–98	145°	50,500	±20,700	29,800	48.27	48.57	5.78	5.82	
β-1,3,4,6- (VI)	137–138	26	9000							c
α-2-Monochloroacetyl (VIIIa)	143–144	98	41,600	±18,700	22,900	45.23	45.19	4.98	5.01	
β-2-Monochloroacetyl (IXa)	118–118.5	9.8	4200				45.03		5.02	
α-2-Dichloroacetyl (VIIIb)	128–129	97	44,500	±18,800	25,700	42.00	41.87	4.38	4.39	
β-2-Dichloroacetyl (IXb)	134–135	15.3	6900				41.84		4.36	
α-2-Trichloroacetyl (VIIIc)	121–123	93	45,900	±18,600	27,400	38.92	39.08	3.88	3.89	d
β-2-Trichloroacetyl (IXc)	165–166	17.9	8800				38.99		3.88	e
β-1-Monochloroacetyl	134–134.5	−1.39				45.23	44.98	4.98	4.93	(4)
β-4-Monochloroacetyl	117–118	3				45.23	45.03	4.98	4.95	
β-6-Monochloroacetyl	145–145.5	10								
Derivatives of methyl triacetyl-β-D-glucopyranoside										
2-Monochloroacetyl (Xa)	97.5–98	−5.3				45.40	45.63	5.34	5.32	
2-Dichloroacetyl (Xb)	101–102	4.4				41.77	41.55	3.72	4.68	
2-Trichloroacetyl (Xc)	108.5–109	8				38.68	38.57	4.11	4.11	

aUnless otherwise stated the rotations were measured in chloroform, (c, 0.8–1 in the temperature range 22–26°C). bValues calculated on the basis of Hudson's rules of isorotation. cLit. (10), m.p. 131°C, $[\alpha]_D$ +28° (c, 1.3 in chloroform). dLit. (5), m.p. 120°C, $[\alpha]_D^{14}$ +101.5° (c, 2.5 in nitrobenzene). eLit. (5), m.p. 167°C, $[\alpha]_D^{16}$ +28.8° (c, 3 in nitrobenzene).

place by the S_N2 type of mechanism proposed by Isbell and Frush (15) for the reaction of α-acetobromoglucose with methanol in the presence of silver carbonate.

EXPERIMENTAL

Methods

The specific rotations were measured at room temperature, 22–26°C. The melting points are corrected.

2-Trichloroacetyl-triacetyl-β-D-glucopyranosyl Chloride (I) (5)

Pentaacetyl-β-D-glucopyranose, 78 gm., phosphorus pentachloride, 177 gm., and 40 ml. of carbon tetrachloride were heated under reflux for five hours. The mixture was evaporated in the vacuum of a water aspirator to a bath temperature of about 85°C. The sirupy residue was dissolved in 160 ml. of dry ether and the clarified solution was left overnight at −10°C. The crystalline deposit was washed first with 20 ml. of cold methanol then with 20 ml. of dry ether. The yield was 38 gm., 40%, of material, m.p. 132–138°C., $[\alpha]_D$ +14° (chloroform). After two recrystallizations from ether, the substance, $[\alpha]_D$ +8.9° (c, 1.4 in chloroform) melted at 140–142°C. Brigl (5) has reported m.p. 142°C., $[\alpha]_D$ +2.95° (c, 7.4 in benzene).

3,4,6-Triacetyl-α-D-glucopyranosyl Chloride

3,4,6-Triacetyl-β-D-glucopyranosyl chloride (5), 4.00 gm., was dissolved in 250 ml. of dry acetone. After four days at room temperature (5), the solution was evaporated *in vacuo* to sirup which was dissolved in ether. Hexane was added to near turbidity and the solution was left at 0°C. for several days. There was deposited 3.70 gm., 92.5% yield, of crystalline compound, m.p. 90–91.5°. Four recrystallizations from ether–hexane mixture raised the melting point to 93–94°C. with $[\alpha]_D$ +185° (c, 1.2 in chloroform). Calc. for $C_{12}H_{17}O_8Cl$: C, 44.38; H, 5.28; Cl, 10.9%. Found: C, 44.18; H, 5.22; Cl, 11.0%.

1,3,4,6-Tetraacetyl-α-D-glucopyranose (V)

3,4,6-Triacetyl-β-D-glucopyranosyl chloride (II), m.p. 156–158°C., $[\alpha]_D$ +28.7° (c, 1.1 in chloroform) (5), 1.95 gm., and silver acetate, 1.08 gm., were shaken with 20 ml. of acetic acid for six hours. The silver salts were removed by filtration and the acetic acid by distillation *in vacuo* to yield a sirup which was dissolved in a little ether. The solution was clarified and left overnight at −10°C. A crystalline product, m.p. 90–96°C., 1.40 gm., was formed. A second crop, 0.30 gm., was obtained from the mother liquor to raise the yield to 81%. The purified material is reported in Table I. Reaction of 3,4,6-triacetyl-β-D-glucopyranosyl chloride (II) 1 mM., with silver acetate, 3 mM., in 5 ml. ether for two hours gave the same material in 43% yield. Gakhokidze (8) has reported the use of silver carbonate instead of silver acetate under these conditions to yield 1,3,4,6-tetraacetyl-β-D-glucopyranose. It has been suggested (7, p. 40) that silver acetate was probably the reagent actually used. However, Gakhokidze's product melted at 138°C. and was probably of low specific rotation since he believed the substance to be a β-D-anomer.

1,3,4,6-Tetraacetyl-β-D-glucopyranose (VI) (10)

(a) The following reaction conditions are essentially those reported by Hardegger and de Pascual (10). Pure Brigl anhydride (IV), m.p. 59–60°C., [α]$_D$ +73° (c, 0.8 in chloroform), was prepared by the method of Gladding and Purves (9). The anhydride, 5.8 gm., was dissolved at 20°C. in 50 ml. of pure acetic acid. After five hours, the acetic acid was removed by distillation *in vacuo* at 30°C. The sirupy product crystallized from ether at −10°C. to yield 5.2 gm., 74%, of product, m.p. 128–130°C. Several recrystallizations from ethanol gave a pure substance, m.p. 136–137°C., [α]$_D$ +26° (c, 0.8 in chloroform). Hardegger and de Pascual have reported, m.p. 131°C., [α]$_D$ +28° (c, 1.3 in chloroform).

(b) A mixture of 650 mgm. 3,4,6-triacetyl-α-D-glucopyranosyl chloride, 350 mgm. silver acetate and 10 ml. of acetic acid was shaken at room temperature for six hours. Benzene, 10 ml., was added, the silver salts were removed by filtration, and the filtrate was evaporated *in vacuo* to a crystalline residue. The substance was dissolved in ether and hexane was added to turbidity. On standing at 0°C., 550 mgm., 79% yield, of a crystalline substance, m.p. 133–134°C., was deposited. Five recrystallizations from ethanol–hexane mixture raised the melting point to 137–138°C., [α]$_D$ +26° (c, 0.9 in chloroform). The substance did not depress the melting point of the above described preparation and gave the same monochloroacetyl derivative (IXa).

Methyl 3,4,6-Triacetyl-β-D-glucopyranoside (VII)

This substance, m.p. 94–95°C., [α]$_D$ +19° (c, 1 in chloroform), was prepared in the manner described by Gladding and Purves (9).

Monochloroacetylations

The glucose derivative, 4 mM., was dissolved in 15 ml. of dry benzene and 2 ml. of dry pyridine. Monochloroacetic anhydride, 10 mM., was added to the solution cooled to 0°C. After one hour, the mixture was left at room temperature for two hours. Chloroform, 50 ml., was added and the solution washed twice with ice-cold 20% hydrochloric acid, once with cold water, and finally with aqueous sodium bicarbonate solution. The colorless chloroform solution was evaporated *in vacuo* to a sirupy residue which was crystallized from ethanol. The yields of crude crystalline product were in the range 85–95%. The purified products from the monochloroacetylations of IV, V, VI, 1,2,3,6-tetraacetyl-β-D-glucopyranose (13) and 1,2,3,4-tetraacetyl-β-D-glucopyranose (13) are reported in Table I.

Dichloroacetylations

Dichloroacetyl chloride, b.p. 107–108°C., n_D^{25} 1.481, was used as acylating agent. The reaction conditions were essentially the same as described above for the monochloroacetylations. The reaction mixtures developed a dark reddish brown coloration. Consequently, the chloroform extract, freed from pyridine, was decolorized by percolation through Magnesol before concentration. The yields of crude crystalline product were in the range 75–80%. The purified compounds derived from IV, V, and VI are reported in Table I.

Trichloroacetylations

Trichloroacetyl chloride, b.p. 116–118°C., n_D^{25} 1.468, was used as acylating agent and the reaction conditions were essentially as described above for the monochloroacetylations. The yields of crude crystalline product were in the range 80–95%. The purified derivatives obtained from IV, V, and VI are reported in Table I.

Anomerizations and Acetolyses

The substance, 1 mM., was dissolved in 10 ml. of 50· 50 acetic acid – acetic anhydride mixture 0.5 M with respect to sulphuric acid (3). The solution was kept at 25°C. for the specified time and then poured into ice-water mixture which contained sufficient sodium acetate to combine with the sulphuric acid. In each case, a crystalline precipitate formed on allowing the solution to stand overnight at 4°C.

2-Monochloroacetyl-tetraacetyl-β-D-glucopyranose (IXa), 0.425 gm., after 7.5 hr. reaction time gave 0.32 gm., 78%, of material, m.p. 138–139°C. After several recrystallizations from ethanol the melting point was 142–144°C. This melting point was not depressed by admixture of the 2-monochloroacetyl-tetraacetyl-α-D-glucopyranose (VIIIa).

Acetolysis of methyl 2-monochloroacetyl-triacetyl-β-D-glucopyranoside (Xa), 400 mgm., for 6.5 hr. gave 0.21 gm., 48%, of material, m.p. 138–140°C. and this melting point was not depressed by 2-monochloroacetyl-tetraacetyl-α-D-glucopyranose (VIIIa).

2-Dichloroacetyl-tetraacetyl-β-D-glucopyranose (IXb), 460 mgm., after 24 hr. reaction time gave 300 mgm., 65%, of material, m.p. 114–120°C. Several recrystallizations from ethanol raised the melting point to 127–129°C. and this melting point was unchanged by 2-dichloroacetyl-tetraacetyl-α-D-glucopyranose (VIIIb).

2-Trichloroacetyl-tetraacetyl-α-D-glucopyranose

2-Trichloroacetyl-triacetyl-β-D-glucopyranosyl chloride (I), 4.7 gm., was shaken with silver acetate, 1.8 gm., in 100 ml. of acetic acid for 14 hr. at room temperature. The product, isolated in the usual manner, was crystallized from ethanol to yield 4.8 gm., 82%, of material, m.p. 114–118°C. After several recrystallizations from ether, the melting point was 120–122°C. and $[\alpha]_D$ +93° (c, 0.8 in chloroform). The melting point was not changed by admixture of 2-trichloroacetyl-tetraacetyl-α-D-glucopyranose (VIIIc) (see Table I).

REFERENCES

1. ABRAMOVITCH, R. A. J. Chem. Soc. 2996. 1951.
2. BARDOLPH, M. P. and COLEMAN, G. H. J. Org. Chem. 15: 169. 1950.
3. BONNER, W. A. J. Am. Chem. Soc. 73: 2659. 1951.
4. BRASS, K. and KURZ, E. Ber. 66: 442. 1933.
5. BRIGL, P. Z. physiol. Chem. (Hoppe-Seyler's), 116: 1. 1921.
6. BRIGL, P. Z. physiol. Chem. (Hoppe-Seyler's), 122: 245. 1922.

7. EVANS, W. L., REYNOLDS, D. D., and TALLEY, E. A.   *In* Advances in carbohydrate chemistry. Vol. 6. *Edited by* C. S. Hudson and S. M. Cantor. Academic Press Inc., New York.   1951.
8. GAKHOKIDZE, A. M.   J. Gen. Chem. (U.S.S.R.) 11: 117.   1941.
9. GLADDING, E. K. and PURVES, C. B.   J. Am. Chem. Soc. 66: 153.   1944.
10. HARDEGGER, E. and DE PASCUAL, J.   Helv. Chim. Acta, 31: 281.   1948.
11. HARDEGGER, E. and MONTAVON, R. M.   Helv. Chim. Acta, 30: 632.   1947.
12. HAWORTH, W. N., HIRST, E. L., and TEECE, E. G.   J. Chem. Soc. 1405.   1930; 2858.   1931.
13. HELFERICH, B. and KLEIN, W.   Ann. 455: 173.   1927.
14. HICKINBOTTOM, W. J.   J. Chem. Soc. 1676.   1929.
15. ISBELL, H. S. and FRUSH, H. L.   J. Research Natl. Bur. Standards, 43: 161.   1949.
16. LEMIEUX, R. U.   Can. J. Chem. 29: 1079.   1951.
17. LEMIEUX, R. U. and BRICE, C.   Can. J. Chem. 30: 295.   1952.
18. LEMIEUX, R. U. and SHYLUK, W. P.   Can. J. Chem. 31: 528.   1953.
19. TIPSON, R. S.   J. Biol. Chem. 130: 55.   1939.
20. WINSTEIN, S. and GRUNWALD, E.   J. Am. Chem. Soc. 70: 828.   1948.

THE TAUTOMERISM OF 2-NITRAMINOPYRIDINES[1]

By Alfred Taurins and Silvio J. Viron[2]

ABSTRACT

The nitration of 2-amino-4,6-dimethylpyridine with a mixture of nitric and sulphuric acids gives 4,6-dimethyl-2-nitramino-5-nitropyridine (III). 2-Nitraminopyridine (I), 4-methyl-2-nitraminopyridine (II), and (III) produce with diazomethane methyl derivatives of their tautomeric nitramino and nitrimino forms. Diazoethane gives with (I) both the expected ethyl derivatives. However, from (II) only the ethyl derivative of the nitramino form has been obtained. Diazopropane produces with (I) or (II) the propyl derivatives of the nitramino forms only. The resonance structures of the two tautomeric forms of 2-nitraminopyridine have been advanced.

INTRODUCTION

The study of nitraminopyridines (2–8, 10, 11, 13) was started by Tschitschibabin in 1914 with the nitration of 2-aminopyridine and its derivatives using a mixture of nitric and sulphuric acids as the nitrating agent.

Two of the chemical properties of 2-nitraminopyridines are of great interest; firstly, their ability to rearrange into 2-amino-3-nitro-, and 2-amino-5-nitropyridines by the action of concentrated sulphuric acid at moderate temperature, and secondly, their acidic nature. The acidic nature of 2-nitraminopyridines is associated with the mobility of the hydrogen atom of the nitramino group and formation of tautomeric nitramino (IA) and nitrimino (IB) forms.

Tschitschibabin and his co-workers studied the tautomerism of 2-nitraminopyridines by methylation with dimethyl and diethyl sulphate in alkaline solution. From 2-nitraminopyridine he obtained only alkyl derivatives of the nitrimino form (12). However, 5-nitro-2-nitraminopyridine (9) and 3,5-dibromo-2-nitraminopyridine (10) on methylation gave methyl derivatives of both the nitramino and nitrimino forms.

Although the methylated derivatives of both tautomeric forms of 2-nitraminopyridines in most cases were obtained, no actual proof of the original structure of these compounds was presented, because dimethyl sulphate actually methylated the sodium salt of these compounds in which 2-nitraminopyridines existed in the form of anions. Therefore we decided to investigate the direct alkylation of the three 2-nitraminopyridines with diazomethane, diazoethane, and diazopropane.

DISCUSSION

Several resonating structures can be assigned to both of the tautomeric forms of 2-nitraminopyridine, taking into account the mobility of the unshared electron pairs of both nitrogen atoms and π-electrons of the pyridine ring (Chart I). The consideration of the resonance hybrid structures (IA) and (IB)
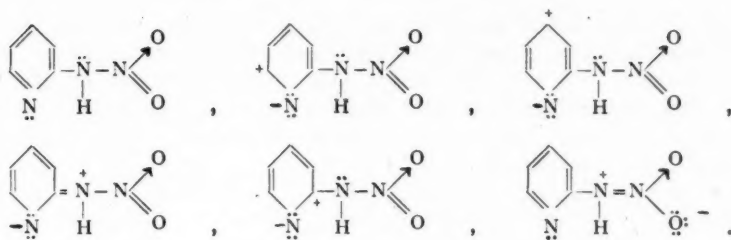
(IA) 2-Nitraminopyridine
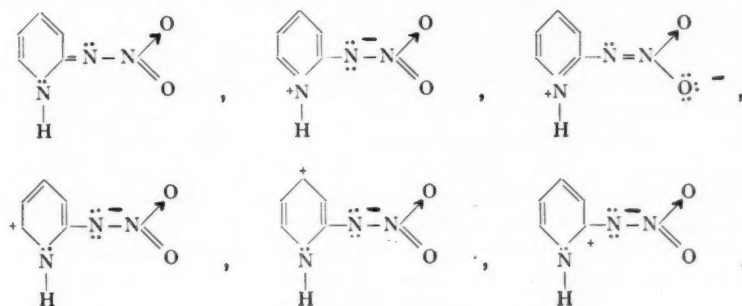
(IB) 2-Nitriminopyridine

CHART I. The electronic structure of 2-nitraminopyridine.

IV: R=CH₃
X: R=C₂H₅

V

VIII

VI: R=CH₃
XI: R=C₂H₅
XIII: R=C₃H₇

II: R=H
VII: R=CH₃
XII: R=C₂H₅
XIV: R=C₃H₇

III: R=H
IX: R=CH₃
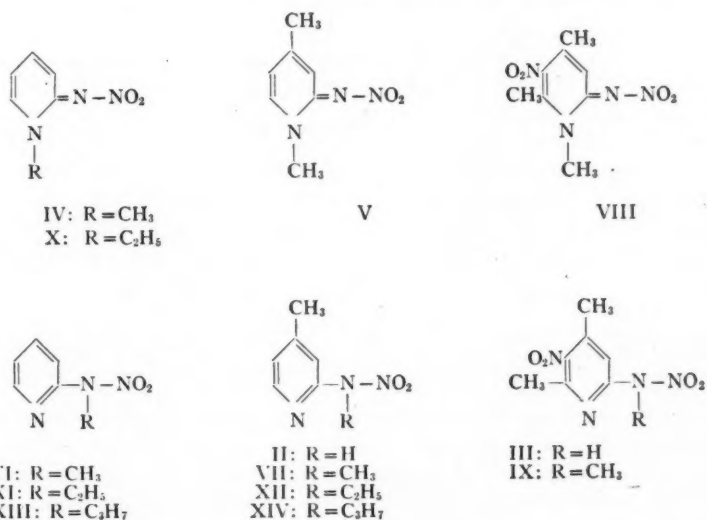
CHART II

reveals that both of them must be approximately of the same stability because the competitive $-M$ effects of the nitro group and pyridine nitrogen atom favor the existence of equal number of resonance structures of each tautomeric form. Therefore it seems reasonable to predict that the alkylating agents like diazomethane would produce alkyl derivatives of both nitrimino and nitramino forms of 2-nitraminopyridine.

The methylation of 2-nitraminopyridine (I) with diazomethane in ether yielded an ether-insoluble and an ether-soluble product. The ether-insoluble product proved to be 1,2-dihydro-1-methyl-2-nitriminopyridine (IV) as evidenced by its conversion to 1-methyl-2(IH)pyridone and nitrous oxide with hot alkali and by its identity with the product described by Tschitschibabin (12).

The oily ether-soluble product was soluble in dilute hydrochloric acid and formed a crystalline mercuric chloride double salt, but not a picrate. It must be 2-(1′-methylnitramino)pyridine (VI).

The methylation of 4-methyl-2-nitraminopyridine (II) and 4,6-dimethyl-2-nitramino-5-nitropyridine (III) with diazomethane also gave in each case the two methyl derivatives (V), (VIII) and (VII), (IX) respectively. However, unlike the methyl derivatives (VI) and (VII), 4,6-dimethyl-2-(1′-methylnitramino)-5-nitropyridine (IX) was not soluble in hydrochloric acid.

While the ethylation of 2-nitraminopyridine (I) with diazoethane in ether also gave ethyl derivatives of both tautomeric forms (X) and (XI), the propylation of (I) with diazopropane in ether produced only the ether-soluble propyl derivative of the nitramino form (XIII).

The ethylation and propylation of 4-methyl-2-nitraminopyridine (II) with the reagents mentioned above yielded only the derivatives (XII) and (XIV) of the nitramino forms, isolated as the mercuric chloride salts.

In the nitration of 2-amino-4,6-dimethylpyridine it was surprising to find that the reaction product contained a nitro group on the ring as well as the nitramino group in the two position. It is not known conclusively whether the nitro group occupies the three or five position. But from the behavior of such compounds as 2-nitraminopyridine and 4-methyl-2-nitraminopyridine which yield the 5-nitro derivatives predominantly when isomerized with sulphuric acid it seems very probable that the nitration product contains the nitro group in five position and can be named as 4-6-dimethyl-2-nitramino-5-nitropyridine (III).

EXPERIMENTAL

4,6-Dimethyl-2-nitramino-5-nitropyridine (III)

Sulphuric acid (40 ml.) was added dropwise to 44 ml. of 90–95% nitric acid at the temperature below 5°. Forty grams of 2-amino-4,6-dimethylpyridine were dissolved in 70 ml. of concentrated sulphuric acid while the flask was cooled in an ice bath. This solution was added carefully to the nitrating mixture at the temperature below 5°. After complete addition, the mixture was allowed to stand with constant stirring for three hours and then poured onto 100 gm. of crushed ice. The precipitate which separated had a distinct

yellow color and after filtration and drying weighed 27.9 gm. (57.5%). It was recrystallized twice from ethanol and obtained in the form of yellow plates melting at 174–175° (decomp.).

Anal. Calc. for $C_7H_8N_4O_4$: C, 39.62; H, 3.78; N, 26.41%.

Found: C, 40.05; H, 3.90; N, 26.40%.

Methylation of 2-Nitraminopyridine

(a) *1,2-Dihydro-1-methyl-2-nitriminopyridine* (IV)

To the solution of diazomethane in 40 ml. ether prepared from 20 gm. of methylnitrosourea was added portionwise 7 gm. of (I). The reaction was allowed to proceed with occasional shaking until gassing had ceased. The reddish insoluble product after filtration and drying weighed 4.3 gm. (55.8%). After recrystallization from ethanol it melted at 156–157°. A mixed melting point with a sample of (IV) prepared by interaction of dimethylsulphate on (I) showed no depression.

(b) *2- (1'-Methyl)-nitraminopyridine* (VI)

The ether filtrate from the previous reaction was added to 50 ml. of dilute hydrochloric acid (1:1) and shaken. The acid layer was separated and rendered alkaline with sodium carbonate depositing a dark colored oil. The oil was extracted with two 25 ml. portions of ether and the ether distilled off on a steam bath. An attempt to distill the residual oil at 0.5 mm. pressure resulted in an explosion. The oil obtained from a second run was dissolved in 5 ml. of ethanol and added to 15 ml. of saturated solution of mercuric chloride in 95% ethanol. A crystalline mercuric chloride salt was deposited. The yield was 2.6 gm. (11.6%). The product crystallized from water into gleaming white plates, m.p. 151.5–152°.

Anal Calc. for $C_6H_7N_3O_2HgCl_2$: C, 16.98; H, 1.65; N, 9.91%.

Found: C, 17.35; H, 1.62; N, 9.84%.

Methylation of 4-Methyl-2-nitraminopyridine (II)

(a) *1,2-Dihydro-1,4-dimethyl-2-nitriminopyridine* (V)

Seven grams of (II) was methylated with a solution of diazomethane in ether. The insoluble reaction product (3.9 gm.) was recrystallized twice from ethanol and had a melting point 161–162°.

Anal. Calc. for $C_7H_9N_3O_2$: C, 50.30; H, 5.37; N, 25.15%.

Found: C, 49.92; H, 5.32; N, 25.37%.

The substance (V) was readily decomposed by warming with a dilute solution of potassium hydroxide with the evolution of nitrous oxide.

(b) *2-(1'-Methyl)-nitramino-4-methylpyridine* (VII)

The ethereal filtrate was shaken with 50 ml. of dilute hydrochloric acid (1:1) in a separatory funnel. The acid layer was separated and neutralized with sodium carbonate. Extraction with 25 ml. of ether followed by distillation of the ether on a steam bath yielded an oily residue. Half of it was added to 50 ml. of saturated solution of mercuric chloride in ethanol with the deposition

of 1.7 gm. of a salt. The obtained mercuric chloride salt crystallized from water into long, fibrous white crystals, melting at 146–147°.

Anal. Calc. for $C_7H_9N_3O_2HgCl_2$: C, 19.62; H, 2.10; N, 9.81%.

Found: C, 19.19; H, 2.19; N, 9.39%.

The other half of the oil was added to 10 ml. of a saturated solution of picric acid in ethanol. The precipitate (picrate of VII) was recrystallized from acetone and alcohol. It formed yellow crystals which melted at 92–93°.

Anal. Calc. for $C_{13}H_{12}N_6O_9$: C, 41.91; H, 3.03; N, 21.21%.

Found: C, 42.05; H, 3.15; N, 20.56%.

Methylation of 4,6-Dimethyl-2-nitramino-5-nitropyridine (III)

(a) 1,2-Dihydro-2-nitrimino-5-nitro-1,4,6-trimethylpyridine (VIII)

Four grams of (III) was allowed to react with a solution of diazomethane in ether prepared from 15 gm. of methylnitrosourea. After gassing had ceased the brownish insoluble substance was collected on a filter and dried. The yield was 0.7 gm. After two recrystallizations from ethanol, the melting point of (VIII) was 213–214°.

Anal. Calc. for $C_8H_{10}N_4O_4$: C, 42.48; H, 4.43; N, 24.77%.

Found: C, 42.86; H, 4.68; N, 24.35%.

(b) 4,6-Dimethyl-2-(1'-methyl)-nitramino-5-nitropyridine (IX)

The ethereal filtrate was extracted with 50 ml. of hydrochloric acid (1:1) and the acid layer separated. No basic product could be isolated from this solution after neutralization with sodium carbonate. The ether solution remaining after the hydrochloric acid extraction was distilled on a steam bath to an oil which deposited crystals after standing for two days. Five milliliters of ethanol was added to facilitate filtration. The product weighed 0.9 gm. (18.9%). It was recrystallized from ethanol and obtained in the form of white crystals which melted at 104–105°.

Anal. Calc. for $C_8H_{10}N_4O_4$: C, 42.48; H, 4.43; N, 24.47%.

Found: C, 43.11; H, 4.10; N, 24.35%.

Interaction of Diazoethane with (I) and (II)

(a) 1,2-Dihydro-1-ethyl-2-nitriminopyridine (X)

Seven grams of (I) was added to the diazoethane solution in ether prepared from 25 gm. of ethyl nitrosourethane. The solution slowly took on a deep red color and the solid started to dissolve. After gassing had ceased the insoluble product was filtered and dried. It weighed 1.8 gm. After two recrystallizations from ethanol the melting point was 126–127° (identical with the melting point reported in the literature (12)). It liberated nitrous oxide on being warmed with dilute potassium hydroxide solution.

(b) 2-(1'-Ethyl)-nitraminopyridine (XI)

The ether filtrate was treated in the same manner as the filtrate from the methylation of (I). The oil obtained in this procedure formed a mercuric chloride salt which weighed 1.8 gm. It was recrystallized from 50% ethanol

and obtained in the form of gleaming white plates melting at 125.5–126°.

Anal. Calc. for $C_7H_9O_2N_3HgCl_2$: C, 19.62; H, 2.10; N, 9.81%.

Found: C, 19.48; H, 2.25; N, 9.76%.

(c) 2-(1'-Ethyl)-nitramino-4-methylpyridine (XII)

A solution of diazoethane was allowed to react with 7 gm. of (II). After the reaction was complete *no* insoluble product remained. From the ethereal solution the reaction product (XII) was isolated as mercuric chloride salt. It was recrystallized from 50% ethanol into long, white, fibrous needles melting at 131–132°.

Anal. Calc. for $C_8H_{11}N_3O_2HgCl_2$: C, 21.24; H, 2.41; N, 9.28%.

Found: C, 21.71; H, 2.67; N, 9.76%.

Interaction of Diazopropane with (I) and (II)

(a) 2-(1'-Propyl)-nitraminopyridine (XIII)

In the reaction of the solution of diazopropane prepared from 30 gm. of undistilled propyl nitrosourethane with 7 gm. of (I) *no* insoluble product remained. A mercuric chloride salt was obtained (1.2 gm.) when the usual procedure for its isolation was followed. It was recrystallized from 50% ethanol and had a melting point 122.5–123.5°.

Anal. Calc. for $C_8H_{11}N_3O_2HgCl_2$: C, 21.24; H, 2.41; N, 9.28%.

Found: C, 21.33; H, 2.70; N, 9.6%.

(b) 2-(1'-Propyl)-nitramino-4-methylpyridine (XIV)

The reaction of diazopropane with (II) gave no insoluble product. As usual an oil was obtained which formed a mercuric chloride salt, which after recrystallization from 75% ethanol melted at 88–89°.

Anal. Calc. for $C_9H_{13}N_3O_2HgCl_2$: C, 23.18; H, 2.78; N, 9.01%.

Found: C, 23.57; H, 2.88; N, 9.02%.

ACKNOWLEDGMENT

REFERENCES

1. FISCHER, O. J. prakt. Chem. 93: 363. 1916.
2. HALL, A. and VANDER WERF, C. J. Am. Chem. Soc. 73: 4466. 1951.
3. RÄTH, C. and PRANGE, G. Ann. 467: 1. 1928.
4. SEIDE, O. J. Russ. Phys. Chem. Soc. 50: 534. 1918.
5. SEIDE, O. Ber. 57: 791. 1924.
6. SEIDE, O. Ber. 57: 1802. 1924.
7. TSCHITSCHIBABIN, A. E. J. Russ. Phys. Chem. Soc. 46: 1236. 1914.
8. TSCHITSCHIBABIN, A. E. and BYLINKIN, I. G. J. Russ. Phys. Chem. Soc. 50: 471. 1918.
9. TSCHITSCHIBABIN, A. E. and KIRSSANOW, A. W. Ber. 61: 1223. 1928.
10. TSCHITSCHIBABIN, A. E. and KIRSSANOW, A. W. Ber. 61: 1236. 1928.
11. TSCHITSCHIBABIN, A. E. and KONOWALOWA, R. A. Ber. 58: 1712. 1925.
12. TSCHITSCHIBABIN, A. E. and MENSCHIKOW, G. P. Ber. 58: 406. 1925.
13. TSCHITSCHIBABIN, A. E. and RASORENOW, B. J. Russ. Phys. Chem. Soc. 47: 1286. 1915.
14. TSCHITSCHIBABIN, A. E. and WIDONOWA, M. S. J. Russ. Phys. Chem. Soc. 53: 238. 1921.

BIOCHEMISTRY OF THE USTILAGINALES

IX. THE β-D-CELLOBIOSIDE UNITS OF THE USTILAGIC ACIDS[1]

By R. U. Lemieux, J. A. Thorn,[2] and H. F. Bauer[3]

ABSTRACT

The two D-glucose residues in the two main components of the ustilagic acid mixture are shown to be present as β-D-cellobiopyranoside units.

The glucoustilic acid mixture (6) was completely methylated by standard procedures for methylation and the product was subjected to methanolysis followed by hydrolysis to yield a mixture of methyl derivatives of D-glucose and the ustilic acids (7). The presence in the hydrolyzate of only tri-O- and tetra-O-methyl derivatives of D-glucose was established by paper partition chromatography. Semimicro amounts of the two fractions were obtained by preparative paper partition chromatography (13). Since the fractions crystallized readily and completely, there could be no doubt that each fraction contained only one component. The compounds were characterized as 2,3,6-tri-O-methyl-D-glucose and 2,3,4,6-tetra-O-methyl-D-glucose by the preparation of suitable derivatives. Quantitative estimations showed the glucose derivatives to be present, within experimental error, in equimolar amounts. The mixture of partially methylated ustilic acids isolated from the hydrolyzate possessed the composition expected for a mixture of mono-O-methylustilic acid A and di-O-methylustilic acid B. Therefore, both the ustilagic acids A and B possessed disaccharide units which were derived either from D-cellobiose or D-maltose.

The A and B components of the glucoustilic acid mixture must be present in the same proportion as are the ustilic acids A and B in the ustilic acid mixture. The ustilic acid mixture has been shown (7) to contain about 70% ustilic acid A and about 30% ustilic acid B. The molar rotations for the mixtures listed in Table I were calculated on this basis. Thus, the possible presence in these mixtures of a small amount of impurities (8) was disregarded.

Acetylation of methyl glucoustilate mixture yielded a crystalline mixture of the acetyl derivatives with molar rotation −25,100 in chloroform. Several recrystallizations of this substance gave pure methyl octa-O-acetylglucoustilate A with molar rotation −25,200 in chloroform. Since the lactol carbon atoms of glucose derivatives make a strong contribution to molar rotation (about ±25,000) (4), these rotations show conclusively that the corresponding anomeric centers in the glucoustilic acids A and B are of the same configuration.

The molar rotations of acetylated glycosides of same configuration derived from a sugar and optically inactive alcohols are well-known to be remarkably constant in value. On this basis, a comparison of the molar rotation of the

TABLE I
THE MOLAR ROTATIONS OF GLUCOUSTILIC ACID DERIVATIVES AND RELATED SUBSTANCES

Substance	$[M]_D^{23-26}$ (chloroform)	References
Di-O-acetyl methyl ustilate A	$+200°$	
Tri-O-acetyl methyl ustilate B	$+4600$	
Acetylated methyl ustilate mixture	$+2000$	
Methyl octa-O-acetyl glucoustilate A	$-25,200$	
Acetylated methyl glucoustilate mixture	$-25,100$	
Octa-O-acetyl-β-D-cellobiose	-9900	4
Octa-O-acetyl-α-D-cellobiose	$+27,800$	4
Octa-O-acetyl-β-D-maltose	$+42,500$	4
Octa-O-acetyl-α-D-maltose	$+83,000$	4

acetylated methyl glucoustilate mixture with the molar rotations of the α- and β-octa-O-acetyl derivatives of D-cellobiose and D-maltose (see Table I) would lead to the conclusion that the contribution to the rotation made by the optically active methyl ustilate portions would be $-50,000$ or greater (numerically) should the acetylated methyl glucoustilates possess α-D-cellobiose, β-D-maltose, or α-D-maltose residues. Since such a strong levorotation is exceedingly unlikely for residues derived from the weakly dextrorotatory acetylated methyl ustilates (see Table I), the optical rotatory data strongly suggested that the glucoustilic acids are β-D-cellobiosides. Chemical evidence was obtained which substantiated these conclusions. Acetolysis of the methyl glucoustilate mixture yielded octa-O-acetyl-α-D-cellobiose (1, p. 124). Therefore, the glucoustilic acids are definitely cellobiosides. It is well established (14) that hepta-O-acetyl-β-D-cellobiopyranosides usually can be isomerized to the α-anomers. Treatment of the levorotatory methyl octa-O-acetylglucoustilate A, $[M]_D$ $-25,200$, with boron trifluoride in chloroform solution (9) gave a dextrorotatory isomer, $[M]_D$ $+24,200$. These molar rotations are in excellent agreement with the values expected for anomeric cellobiopyranosides on the basis of Hudson's rules of isorotation (4). Therefore, the reaction must have effected a *beta* to *alpha* isomerization. Since the glucosidic union which joins the glucose residues in acetylated cellobiosides is known to be highly resistant to anomerization (10), the reaction must have involved the cellobiosyl to ustilic acid bond. Therefore, the glucoustilic acids must be β-D-cellobiopyranosides and their structures can be represented by the formulas I(a) and I(b).
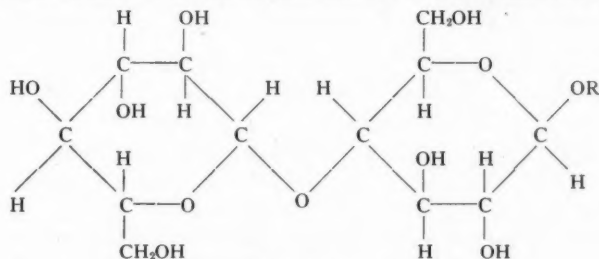
I(a). Glucoustilic acid A, R = $C_{16}H_{31}O_3$.
I(b). Glucoustilic acid B, R = $C_{16}H_{31}O_4$.

Although cellobiose can be considered to be a repeating unit of such substances as cellulose and lichenin, it appears that the ustilagic acids comprise the first *true* cellobiosides of biological origin to be characterized.

EXPERIMENTAL

Methylation of Glucoustilic Acid Mixture

Ustilagic acid (6), 25 gm., was methylated with dimethyl sulphate, 90 ml., and 30% sodium hydroxide, 210 ml., in the usual way. The acidified reaction mixture was extracted with ether to yield 22.4 gm. of a partially methylated derivative. After two further methylations using methyl iodide, 100 ml., and silver oxide, 75 gm., the yield was 19.4 gm. of partially crystalline material which contained 36.5% methoxyl groups. The methoxyl group content calculated for a mixture of 70% nona-O-methylglucoustilate A and 30% deca-O-methylglucoustilate B is 38.5%.

Quantitative Estimation of Tri-O- and Tetra-O-methyl-D-glucoses

The fully methylated glucoustilic acid, 100 mgm., was heated for six hours in a sealed tube at 100°C. with 2 ml. of 5% methanolic hydrogen chloride. The solution was evaporated to dryness under reduced pressure and the residue was heated at 100°C. with 2 ml. of 10% hydrochloric acid for three hours. The hydrochloric acid was destroyed by the addition of an excess of an ethereal solution of diazomethane. The ether was removed by evaporation and the aqueous residue was filtered. The filter was washed with water to yield 25 ml. of filtrate.

Inspection of the solution by paper partition chromatography with butanol–ethanol–water (3) as developing phase showed only two reducing components detectable by the aniline phthalate reagent. The R_f values indicated the presence of a tri- and a tetra-O-methyl-D-glucose.

A portion of the solution, 150 cmm., was developed on a sheet of Whatman 1 paper in the usual way as a 20 cm. streak across the paper. After the resultant bands were located by use of spots developed simultaneously, the zones were cut out and the methylglucoses eluted with water (2). The amounts of tri- and tetra-O-methyl-D-glucoses were determined by use of the anthrone reaction (2, 12). The blank was made up from the eluate of a strip of filter paper of equal area taken from the same chromatogram but which contained no reducing sugar. The transmission readings were compared to standard curves prepared from pure samples of 2,3,6-tri-O-methyl and 2,3,4,6-tetra-O-methyl-D-glucose. The ratio of tri- to tetra-O-methylglucose was 0.91. The yields were about 70% of theory.

Hydrolysis of Fully Methylated Glucoustilic Acid Mixture

The methylated glucoustilic acid mixture, 5 gm., was heated under reflux with 50 ml. of 5% methanolic hydrogen chloride for 17 hr. The solution was added to 100 ml. of water and extracted several times with chloroform. After it was dried with sodium sulphate, the solution was evaporated to an oil. A solution of the material in 25 ml. of ethanol and 10 ml. of N potassium hydroxide was refluxed for half an hour. After neutralization with hydrochloric acid,

the solution was evaporated to near dryness. The residue was stirred with sodium sulphate to yield a solid which was extracted with chloroform. Evaporation of the chloroform gave 1.7 gm. of the methylated glucoses. The residue from the extraction was dissolved in hot water, the solution was made strongly acid with hydrochloric acid and extracted with chloroform. Evaporation gave 1.75 gm. of a crystalline mixture of methylated ustilic acids, m.p. 41–55°C. After several recrystallizations from acetone the material melted at 56–70°C. Calc. for a mixture containing 60% mono-O-methylustilic acid A and 40% di-O-methylustilic acid B: neutral equiv., 314; OCH$_3$, 13.8%. Found: neutral equiv., 313; OCH$_3$, 13.8%.

The methylated glucose fraction, 400 mgm., was hydrolyzed by heating at 100°C. with 8 ml. of 10% hydrochloric acid for three hours. The solution was neutralized with diazomethane and evaporated to about a 2 ml. volume. The two methylated glucose components were separated by paper chromatography on a preparative scale (13) and characterized as follows.

2,3,4,6-Tetra-O-methyl-α-D-glucose

The tetra-O-methyl-D-glucose fraction crystallized at once on seeding with an authentic sample of 2,3,4,6-tetra-O-methyl-D-glucose. After two recrystallizations from petroleum ether, the material, $[\alpha]_D$ +102 ⟶ +84° (c, 1 in water), melted at 95.5°C. (with some melting from 81°C.). These constants are in agreement with the published values (5) for 2,3,4,6-tetra-O-methyl-α D-glucose. The anilide derivative (15) melted at 137–139°C. and did not depress the melting point of an authentic sample of the same melting point.

2,3,6-Tri-O-methyl-D-glucose

The tri-O-methyl-D-glucose fraction crystallized on standing several days. A 10 mgm. sample was heated for three minutes on the steam bath with 0.5 ml. of pyridine and 20 mgm. of p-nitrobenzoyl chloride. Water was added, the sirup was triturated with sodium bicarbonate solution, washed with water, and dried *in vacuo*. A chloroform extract was treated with charcoal, filtered, and evaporated to yield a crystalline residue which was recrystallized from 0.8 ml. of methanol. The substance possessed the specific rotation and did not depress the melting point of 1,4-di-O-p-nitrobenzoyl-2,3,6-tri-O-methyl-D-glucose, m.p. 190°C., $[\alpha]_D$ −32 (c, 0.2 in chloroform).

Acetylated Methyl Glucoustilate Mixture

A solution of glucoustilic acid in methanol was treated with an excess of diazomethane. Addition of petroleum ether precipitated the methyl glucoustilate mixture in quantitative yield. The material was heated at 100°C. for three hours with sodium acetate and acetic anhydride. The acetyl derivative crystallized on shaking the acetylation mixture with cold water. The yield of crude material, m.p. 94–95.5°C., $[\alpha]_D$ −25.6° (c, 4.3 in chloroform), was quantitative. Calc. for a mixture containing 70% methyl octa-O-acetylglucoustilate A and 30% methyl nona-O-acetylglucoustilate B: methoxyl, 3.17; acetyl, 36.5%. Found: methoxyl, 3.21; acetyl, 35.2%.

Methyl Octa-O-acetylglucoustilate A

The mixture of acetylated methyl glucoustilates was recrystallized once from benzene – petroleum ether, three times from isopropanol, and finally three times from isopropanol – petroleum ether. The yield was 7 gm. of a substance which had reached constant physical properties, m.p. 108–109.5°C., $[\alpha]_D$ −27° (c, 2.3 in chloroform). Calc. for $C_{45}H_{70}O_{22}$: C, 56.12; H, 7.32%. Found: C, 56.10; H, 7.35%. Methanolysis of a sample and alkaline hydrolysis of the methyl ustilate fraction thus formed (7) to yield ustilic acid gave a substance, m.p. 110–111°C., after one crystallization from ethanol. This melting point was unchanged by admixture with ustilic acid A of the same melting point. When the melting of ustilic acid A is observed with a heating stage microscope, a transformation in crystal form is observed at 102–103°C.

Methyl Di-O-acetylustilate A

Pure methyl ustilate A (7) was acetylated with acetic anhydride and sodium acetate in the usual manner. The crystalline product was recrystallized from ethanol. The substance melted at 26–27°C. and $[\alpha]_D$ +0.6 (c, 4.3 in chloroform). Calc. for $C_{17}H_{32}O_4$ $(COCH_3)_2$: acetyl, 22.3%. Found: acetyl, 23.2%.

Methyl Tri-O-acetylustilate B

Acetylation of pure methyl ustilate B (7) as described above gave a sirup which resisted crystallization. The material, $[\alpha]_D$ +10.5° (c, 4 in chloroform), for analysis was distilled at a bath temperature of 170–180°C. at 10^{-3} mm. Calc. for $C_{17}H_{31}O_5(COCH_3)_3$: acetyl, 29.0%. Found: acetyl, 29.3%.

Acetylated Methyl Ustilate Mixture

Acetylation of purified methyl ustilate mixture (7) as described above gave a sirupy product, $[\alpha]_D$ +4.9° (c, 1.9 in chloroform). Calc. for a mixture containing 70% methyl di-O-acetylustilate A and 30% methyl tri-O-acetylustilate B: acetyl, 24.3%. Found: acetyl, 23.8%.

Octa-O-acetyl-α-D-cellobiose

The methyl glucoustilate mixture, 0.50 gm., was cooled with 1.4 ml. acetic anhydride in an ice–salt mixture. Concentrated sulphuric acid, 0.28 ml., was added to 0.60 ml. acetic anhydride cooled in the ice–salt mixture. The mixtures were combined (1, p. 124) and shaken at room temperature until solution was complete. The next day crystallization was initiated by scratching and after 2.5 days reaction time the crystals were collected, washed with ether, and recrystallized from ethanol. The yield was 20 mgm., m.p. 220–222°C. Recrystallization from ethanol raised the melting point to 226.5–228°C. and $[\alpha]_D$ +42° (c, 0.7 in chloroform). The substance did not depress the melting point of an authentic sample of octa-O-acetyl-α-D-cellobiose prepared by acetolysis of cellulose (1).

Anomerization of Methyl Octa-O-acetylustilate A

Methyl octa-O-acetylglucoustilate A, $[\alpha]_D$ −27° (chloroform), 2.90 gm., was dissolved in 50 ml. of pure chloroform and the solution was saturated with boron trifluoride. After 48 hr. at room temperature, the mixture was shaken

with aqueous bicarbonate solution. The chloroform was washed with water, dried, and evaporated to a solid which was recrystallized from ethanol–petroleum ether mixture. The substance, 1.30 gm., $[\alpha]_D$ +8° (chloroform) was shown to be heterogeneous by chromatography on a 5:1 Magnesol-Celite column (11). The material, 1.00 gm., was treated again under the above conditions for anomerization except that the reaction time was 24 hr. The product was recrystallized from ethanol–petroleum ether mixture to yield 0.70 gm. of material, $[\alpha]_D$ +22.6° (chloroform). The substance, 100 mgm., in 2 ml. of benzene was added to the top of 140 × 35 mm. (in diam.) column of 5 parts Magnesol to 1 part Celite (11), and the chromatogram was developed with 1500 ml. of 100:1 benzene to ethanol mixture. A band was located on the extruded column by streaking with 1% potassium permanganate in 2.5 N sodium hydroxide which extended from 3 mm. to 25 mm. from the top of the column. Elution with warm acetone and crystallization from ethanol gave 50 mgm. of material, m.p. 103–105°C., $[\alpha]_D$ +25.2° (c, 1.5 in chloroform). Calc. for $C_{29}H_{46}O_{14}(COCH_3)_8$: C, 56.12; H, 7.32; acetyl, 35.8%. Found: C, 56.22; H, 7.36; acetyl, 36.1%.

ACKNOWLEDGMENTS

REFERENCES

1. BRAUN, G. *In* Organic syntheses. Coll. Vol. II. *Edited by* A. H. Blatt. John Wiley and Sons, Inc., New York. 1946.
2. DIMLER, R. J., SCHAEFER, W. C., WISE, C. S., and RIST, C. E. Anal. Chem. 24: 1411. 1952.
3. HIRST, E. L. and JONES, J. K. N. Discussions Faraday Soc. 7: 271. 1949.
4. HUDSON, C. S. Sci. Papers U.S. Bur. Standards, 21(533): 241. 1926.
5. IRVINE, J. C. and OLDHAM, J. W. H. J. Chem. Soc. 1744. 1921.
6. LEMIEUX, R. U. Can. J. Chem. 29: 415. 1951.
7. LEMIEUX, R. U. Can. J. Chem. 31: 396. 1953.
8. LEMIEUX, R. U. and CHARANDUK, R. Can. J. Chem. 29: 759. 1951.
9. LINDBERG, B. Acta Chem. Scand. 2: 426. 1948.
10. LINDBERG, B. Acta Chem. Scand. 3: 1355. 1949.
11. McNEELY, W. H., BINKLEY, W. W., and WOLFROM, M. L. J. Am. Chem. Soc. 67: 527. 1945.
12. MORRIS, D. L. Science, 107: 254. 1948.
13. MUELLER, J. H. Science, 112: 405. 1950.
14. PACSU, E. J. Am. Chem. Soc. 52: 2571. 1930.
15. PRINGSHEIM, H. and STEINGROEVER, A. Ber. 59: 1001. 1926.

A CONVENIENT SYNTHESIS OF DL-ORNITHINE[1]

By Roger Gaudry

ABSTRACT

DL-Ornithine is readily prepared in a 68% yield by condensing 3-bromopropyl-phthalimide with ethyl acetamidocyanoacetate and by hydrolyzing the resulting 2-acetamido-2-carbethoxy-5-phthalimidovaleronitrile into DL-ornithine, isolated as the monohydrochloride. 3-Bromopropylphthalimide is obtained in a 57% yield from 3-aminopropanol by reaction with phthalic anhydride, followed by phosphorus tribromide.

INTRODUCTION

Many syntheses of DL-ornithine are recorded in the literature (2) but few of them are suitable for the preparation of this amino acid in important quantities.

In 1945, Albertson and Archer (1) published a satisfactory synthesis of DL-ornithine from the condensation product of acrylonitrile and ethyl acetamido-malonate. This method requires a high pressure hydrogenation to transform ethyl 2-acetamido-2-carbethoxy-4-cyanobutyrate into 3-acetamido-3-carbethoxy-piperidone, a compound which gives ornithine upon acid hydrolysis.

We have investigated the preparation of DL-ornithine from the commercially available 3-aminopropanol (I). By using an adaptation of the procedure recently described in Organic Syntheses (4) for the preparation of 2-bromoethylphthalimide, 3-aminopropanol is easily transformed into 3-bromopropylphthalimide (II). It is not necessary to isolate the intermediate 3-hydroxypropylphthalimide.

The condensation of 3-bromopropylphthalimide with ethyl acetamidocyano-acetate in the presence of sodium ethylate gives the readily isolated 2-carbe-
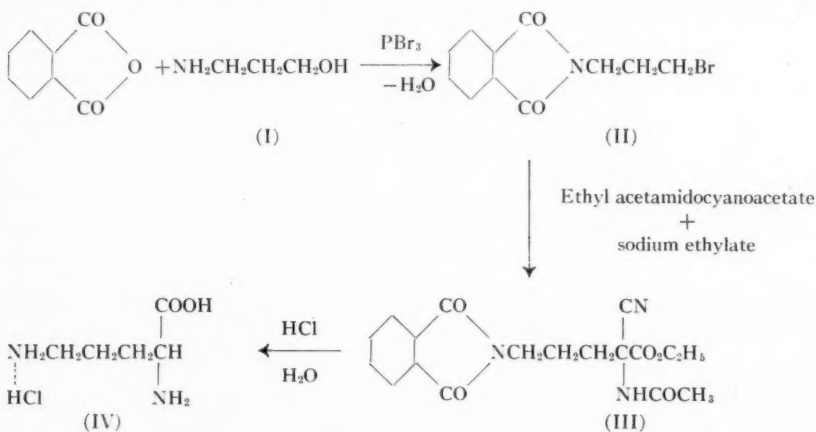
1060

thoxy-2-acetamido-5-phthalimidovaleronitrile (III) in an 80% yield. Acid hydrolysis of this product gives 86% of DL-ornithine (IV), isolated as the mono-hydrochloride, bringing the over-all yield calculated from ethyl acetamido-cyanoacetate to 68%.

The use of 3-chloropropylphthalimide instead of the corresponding bromo compound is not to be recommended because its preparation, using phosphorus trichloride or thionyl chloride, gives a lower yield of a product which is more difficult to purify, and also a lower yield of the condensation product with ethyl acetamidocyanoacetate. Ethyl acetamidomalonate was also found to be less satisfactory than ethyl acetamidocyanoacetate because its condensation product with 3-bromopropylphthalimide is not as easily isolated as 2-car-bethoxy-2-acetamido-5-phthalimidovaleronitrile.

This method of synthesis is derived from the old method of Sörensen (5) with the following differences: (*1*) 3-Bromopropylphthalimide is prepared from 3-aminopropanol instead of potassium phthalimide and trimethylene dibromide (3). (*2*) Ethyl phthalimidomalonate is replaced by the much more convenient ethyl acetamidocyanoacetate. (*3*) The direct, one-step hydrolysis with hydrochloric acid allows the easiest isolation of DL-ornithine as the monohydrochloride.

EXPERIMENTAL

3-Bromopropylphthalimide (II)

(To be carried out in a well ventilated fume cupboard). In a one liter, round bottom flask are placed 148 gm. (one mole) of finely ground phthalic anhydride. Seventy-five grams (one mole) of 3-aminopropanol are added rapidly. After the spontaneous reaction has stopped, any lumps of unreacted phthalic anhydride are broken up with a glass rod or a spatula, and the flask is rotated gently by hand until a clear solution is obtained. While still hot, the flask is placed on a boiling water bath, and is fitted with a good reflux condenser. Seventy-two milliliters of freshly distilled phosphorus tribromide are now added in small portions, either through the condenser or by means of a small separatory funnel attached to a connecting tube placed between the flask and the condenser. A first portion of 15 to 20 ml. is added, and the flask is shaken gently and heated on the water bath until the reaction starts. The rest is then added in portions of approximately 10 ml., while being shaken gently and allowed enough time between each addition for the vigorous reaction to take place. When the addition of phosphorus tribromide is completed, the mixture is heated on the water bath for one additional hour, 100 ml. of ethyl alcohol are added to the hot, viscous liquid, and the solution is poured into a large volume of well stirred ice water containing broken ice. The alcohol prevents the too rapid solidification and the formation of large, hard lumps while the product is being poured into ice water. After standing overnight in the cold, the precipitate is filtered in a large Buechner funnel, and thoroughly washed with cold water until the filtrate is but faintly acidic, and allowed to dry. At this stage, the yield of crude product is approximately 200 gm. It is recrystallized from 200 ml. of ethanol. The yield of the first crop is 149 gm.

A second crop of 5 to 6 gm. is obtained by concentrating the alcoholic filtrate to one third of its volume. Total yield: 154 gm., 57.5%. M.p.*: 74°C. (lit.: 72°–73° (3)). Calc. for $C_{11}H_{10}O_2NBr$: Br, 29.85%. N, 5.22%. Found: Br, 29.69%. N, 5.46%.

2-Acetamido-2-carbethoxy-5-phthalimidovaleronitrile (III)

In a one liter, three neck, round bottom flask, fitted with a mechanical stirrer, and a reflux condenser with a calcium chloride tube, are placed 500 ml. of absolute ethanol. Metallic sodium (11.5 gm., 0.5 mole) is dissolved in it. Eighty-five grams (0.5 mole) of ethyl acetamidocyanoacetate are now added. The mixture is stirred at room temperature for 15 min. and is treated with 134 gm. (0.5 mole) of dry, powdered 3-bromopropylphthalimide. The flask is placed in a water bath, and the mixture is stirred continuously while the temperature is kept at 50°C. for 24 hr. and then raised and kept at 80°C. for a second 24 hr. period. When 3-bromopropylphthalimide is first added to the cold alcoholic solution, it does not dissolve, but after the mixture has been kept at 50°C. for a few minutes, the dissolution becomes complete. After a little while, a precipitate begins to appear, which keeps increasing slowly as the reaction takes place. The mixture is then cooled by replacing the hot water bath with ice water. The precipitate is filtered on a Buechner funnel, washed with two 50 ml. portions of cold ethanol, and allowed to dry. Yield: 142 gm., 79.5%. M.p.: 210°. Calc. for $C_{18}H_{19}O_5N_3$: N, 11.76%. Found: N, 11.85%. The product can be recrystallized from a very large volume of ethanol in which it is only sparingly soluble, but the melting point and analytical results remain unchanged.

DL-Ornithine Monohydrochloride (IV)

In a two liter, wide neck, round bottom flask, fitted with a good reflux condenser, are placed 500 ml. of concentrated hydrochloric acid and 500 ml. of water, and the solution is heated up to the boiling point. The condenser is removed, and 118 gm. of 2-acetamido-2-carbethoxy-5-phthalimidovaleronitrile are added to the hot solution, in five or six portions, allowing enough time between each addition for the product to dissolve almost completely. Excessive foaming occurs if the portions added are too large or if the previous ones have not yet dissolved. The solution is then boiled under reflux for five hours. After standing overnight in the cold, the precipitate of phthalic acid is filtered on a Buechner funnel, washed on the filter with two 50 ml. portions of ice water, and discarded. The filtrate and washings are evaporated to dryness in vacuo. The residue is dissolved in 200 ml. of water, 45 ml. of concentrated ammonium hydroxide are added, and the solution is again taken to dryness in vacuo. Eight hundred milliliters of methanol are added to the residue, and the mixture is mechanically stirred at room temperature for one hour. The precipitate is filtered on a Buechner funnel, transferred to a beaker, and again mechanically stirred for one hour with a fresh 500 ml. portion of methanol, to dissolve any remaining ammonium chloride. The insoluble DL-ornithine monohydrochloride is filtered in a Buechner funnel, washed on the filter with two

---

* Melting points are uncorrected.

50 ml. portions of methanol and allowed to dry. Yield: 50.6 gm., 90.8%. M.p.: 222°. (lit.: 225° (1)). Calc. for $C_5H_{13}O_2N_2Cl$: N, 16.61%. Found: N, 16.47%. The product is readily recrystallized, with a loss of 5 to 6%, by dissolving it in 200 ml. of boiling water and adding 400 ml. of ethanol. Found: N, 16.63%. M.p.: 227°. The over-all yield of analytically pure DL-ornithine monohydrochloride calculated from ethyl acetamidocyanoacetate is 68%. DL-Ornithine dipicrate: M.p.: 199°, unaffected by mixture with an authentic sample.

ACKNOWLEDGMENTS

REFERENCES

1. ALBERTSON, N. F. and ARCHER, S. J. Am. Chem. Soc. 67: 2043. 1945.
2. ARCHER, S. Amino acids and proteins. *Edited by* David M. Greenberg. Charles C. Thomas, Publisher, Springfield, Illinois. 1951. p. 153.
3. GABRIEL, S. and WEINER, J. Ber. 21: 2671. 1888.
4. SOINE, T. O. and BUCHDAHL, M. R. Org. Syntheses, 32: 18. 1952.
5. SÖRENSEN, S. P. L. Z. f. physiol. Chem. (Hoppe-Seyler's), 44: 448. 1905.

THE REDUCTION OF AROMATIC NITRO COMPOUNDS
BY MAGNESIUM AND METHYL ALCOHOL[1]

By Karl F. Keirstead

ABSTRACT

A study has been made of the reduction of substituted nitro compounds by magnesium in methyl alcohol. Some nitro compounds smoothly reduce to the corresponding azoxy compounds, while others yield a complex mixture of azo, azoxy, and other compounds. An investigation has been made of the various factors affecting the velocity of the reaction and the relative proportion of the products. An attempt is made to clarify the various reactions taking place.

The only reference found in the literature to the use of magnesium and methyl alcohol for the reduction of aromatic nitro compounds is a paper by Zechmeister and Rom (16). It is claimed that this method produced excellent yields of azoxy compounds from methyl, chloro, or bromo substituted nitrobenzenes, although azo compounds were present in certain reduction mixtures.

Since the reduction takes place under essentially neutral conditions, it was of interest to investigate the use of this method for the reduction of substituted nitro compounds that undergo hydrolysis, cleavage, or some similar reaction in the strong alkaline solution employed when azoxy compounds are prepared using dextrose or sodium arsenite (6).

First attempts in this study to prepare either the azo or azoxy compound from any of the compounds mentioned above failed completely. It was later established that this failure was due to the use of a stainless steel stirrer. This effect was confirmed by the addition of stainless steel turnings to a well stirred mixture of short pieces of magnesium ribbon in methyl alcohol. No visible evolution of gas took place during forty minutes. In a duplicate mixture a vigorous reaction was evident in the absence of turnings after one minute. This initial difficulty prompted a closer study of both the reaction between magnesium and methyl alcohol [I], and the reaction between magnesium, methyl alcohol, and the nitro compound [I, II, III].

$$Mg + 2CH_3OH \rightarrow Mg(OCH_3)_2 + 2(H) \tag{I}$$

$$2H_2O + Mg(OCH_3)_2 \rightarrow Mg(OH)_2 + 2CH_3OH \tag{III}$$
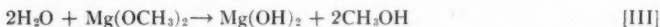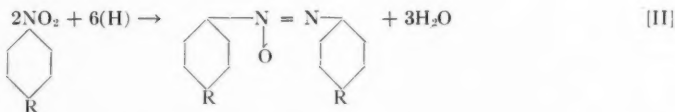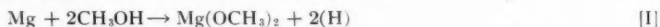
For the purpose of the present discussion, the reactions taking place in a mixture of methyl alcohol, magnesium, and an aromatic nitro compound may be considered separately as follows:

I. Reaction between magnesium and the methyl alcohol.

1064

II. Effect of the nitro compound on the reaction between the magnesium and the alcohol.

III. Reduction of the nitro compound by hydrogen and by magnesium methylate.

IV. Reduction of the azoxy compound by magnesium methylate.

I. *Reaction Between Magnesium and Methyl Alcohol*

The effect of various factors on the reaction between magnesium and methyl alcohol was studied both by the disappearance of the magnesium (Table I and Fig. 4) and by the evolution of hydrogen (Figs. 1–3).

TABLE I

LOSS OF WEIGHT OF MAGNESIUM UNDER CERTAIN CONDITIONS

Run No.	Magnesium	Magnesium reacted, mgm.	Methyl alcohol, % water[a,b]	Stirring
1	Polished ribbon[c]	31.3	0.01	Magnetic stirrer
2	Same	6.7	0.07	Same
3	Turnings	7.9	0.01	Same
4	Same	3.1	0.07	Same
5	Polished ribbon	17.4	0.01	Shaker
6	Turnings	3.5	0.01	Same
7*	Polished ribbon	88.0 87.0 91.5	0.01	Magnetic stirrer

Time, 15 min.; temperature, 23°–25°C.; alcohol, 25 ml.
Added 0.0533 gm. 4-chloronitrobenzene.
[a]Determined by Karl Fisher method.
[b]Per cent by weight.
[c]All magnesium ribbon used throughout was prepared immediately before use by polishing with fine emery cloth.

It may be seen by reference to Table I that the velocity of the reaction between magnesium and methyl alcohol depends on the following factors:

(a) Condition of the magnesium surface.

The polished magnesium ribbon reacts four to five times as fast as magnesium turnings in the presence of 0.01% water.

(b) Degree of agitation.

Rapid stirring increases the velocity by a factor of approximately two.

(c) Amount of moisture in the methanol.

As shown in Run 1 and 2, an increase in moisture content from 0.01% to 0.07% reduces the amount of magnesium dissolved from 31.3 mgm. to 6.7 mgm. in the same time. The effect of moisture has also been observed in the presence of the nitro compound. The addition of 1 ml. of water to 250 ml. methyl

alcohol (0.02% water) containing 0.02 mole of the aromatic nitro compound increases the reaction time from 30 min. to two–seven hours depending on the nitro compound used.

The effect of the form of the magnesium is again shown in Fig. 1. An inspection of Curves 2 and 3 shows that the magnesium ribbon reacts about
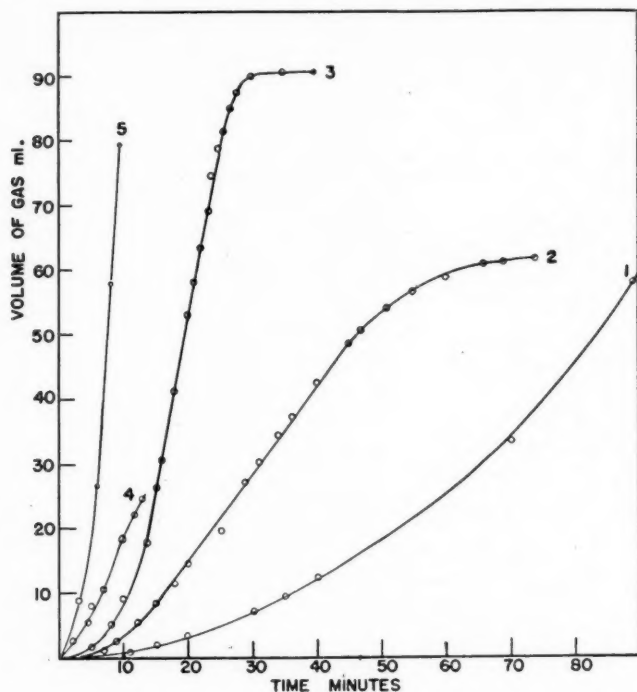
FIG. 1. Effect of water and ethyl iodide on velocity of reaction: Curve 1—Magnesium powder (0.086 gm.) in methyl alcohol (25 ml.). Water content 0.014%. Curve 2—Magnesium powder (0.0752 gm.) in methyl alcohol (25 ml.). Water content 0.007%. Curve 3—Magnesium ribbon (0.0804 gm.) in methyl alcohol (25 ml.). Water content 0.007%. Curve 4—Magnesium powder (0.0987 gm.) and ethyl iodide (0.0660 gm.) in methyl alcohol (25 ml.). Water content 0.007%. Curve 5—Magnesium ribbon (0.0799 gm.) and ethyl iodide (0.3230 gm.) in methyl alcohol (25 ml.). Temperature 25° ± 0.5°C.; rapid stirring with magnetic stirrer.

four times as fast as the magnesium powder in alcohol containing the same amount of water (0.007%). An approximate comparison of the reaction rates of magnesium ribbon, turnings, and powder in alcohol can be made more readily from the present data by estimating the weight of magnesium powder reacting in the first 15 min. (Curve 1). The volume of hydrogen produced is about 3 ml. (25°C. and 760 mm.) which corresponds to approximately 1.5 mgm. magnesium. This weight can be compared with 7.9 mgm. and 31.3 mgm. for turnings and ribbon respectively in alcohol of approximately the same water content (0.01%).

If all the magnesium surfaces were chemically identical, the velocity of the reaction would be a function of the surface area. Since, however, the velocity of the reaction appears to decrease with increased surface area of the magnesium, it may be concluded that the difference in the reaction rates of polished ribbon, turnings, and powder is due mostly to the presence of an oxide or a hydroxide coating on the turnings and the powder.

The effect of small amounts of moisture in the alcohol on the velocity of the reaction between the magnesium and the alcohol has already been mentioned. This inhibition effect appears to be out of proportion to the small amount of water present. Considering again Runs 1 and 2 (Table I), it may be seen that the amounts of water present in the 0.01% and the 0.07% alcohol are respectively 2.0 mgm. and 13.9 mgm. Thus an increase of 11.9 mgm. of water is accompanied by a reduction of 24.6 mgm. of magnesium entering the reaction. Two alternative explanations account for the effect of the water. Firstly, the water may combine with the magnesium, be adsorbed on the surface, or otherwise tend to block contact between the magnesium and the alcohol. The second alternative would involve the combination of the water with magnesium methylate to form magnesium hydroxide [III]. Even with the most efficient stirring, the concentration of the magnesium methylate could be expected to be greater near the magnesium surface. The reaction of water with this layer would produce a layer of magnesium hydroxide in colloidal or powder form that would tend to block reaction between magnesium and the methyl alcohol.

II. *Effect of the Nitro Compound on the Reaction Between the Magnesium and the Alcohol*

In the presence of an aromatic nitro compound a marked increase in the reaction rate is noted. The result of a typical experiment is given in Run 7, (Table I). The reaction rate has increased about three times by the addition of 0.0533 gm. 4-chloronitrobenzene. It may be seen that the effect is quite reproducible under the experimental conditions employed.

On the other hand, when a smaller amount of alcohol or when a less soluble nitro compound is used, it becomes more difficult to obtain a reproducible measure of the reaction rate. Under such conditions an adherent coating on the magnesium may result in an apparent increase in weight for a given piece of magnesium. This coating appears to be related to an unusually large increase in viscosity of the mixture.

In an attempt to account for characteristic viscosity changes that were observed during the preparation of a typical azoxy compound, measurements were carried out with a Fisher Electroviscometer. During the reaction between magnesium, 2,5-dichloronitrobenzene, and methyl alcohol, an initial increase in viscosity took place during the first 10 min. after which a decrease took place. However, this viscosity maximum was not observed in the following: (*a*) magnesium methylate, 2,5-dichloronitrobenzene, and methyl alcohol; (*b*) magnesium reacting with methyl alcohol.

It is apparent that the viscosity changes taking place during the reduction must be due to a substance not present in mixture (*a*) or mixture (*b*). An

inspection of reactions [I–III] immediately suggests that the viscosity changes depend on the formation of water which reacts with magnesium methylate to produce colloidal magnesium hydroxide.

The aging of the colloidal magnesium hydroxide might then result in a decrease in viscosity. One might expect the magnesium hydroxide on formation to be rather heavily solvated with methyl alcohol. The loss of this alcohol of solvation would result in a reduction of viscosity. One would suspect that the coating on the magnesium is insoluble magnesium hydroxide, the final stage in the aging of the colloidal magnesium hydroxide. One would further conclude that the beneficial result of rapid stirring during the preparation of the azoxy compound is due largely to the partial removal of a thick coating of magnesium hydroxide from the surface of the magnesium.

The over-all rate of the magnesium reaction with methyl alcohol in the presence of a nitro compound is then the result of two effects: activation by the nitro compound and inhibition by water initially present or produced by the reduction of the nitro compound.

In an attempt to account for the activation of the reaction by the nitro compound it was of interest to consider the possibility that the nitro compound formed an intermediate with the magnesium. This approach was suggested by the work of Vishnyakov (13) who made a detailed study of the reaction between magnesium and methyl alcohol.

The following claims made by Vishnyakov are of interest:

(a) Magnesium (powder) reacts with alcohols only when other substances which activate this reaction are present.

b) The first portions of the gas formed are rich in hydrocarbons, the total gas corresponding closely to the equation,

$$2R'OH + Mg \rightarrow Mg(OR')_2 + H_2. \tag{IV}$$

(c) With small amounts of RX (the activator, an alkyl halide) the reaction starts only after an induction period; with relatively larger amounts of Mg and RX the reaction begins quickly and exhibits two velocity maxima during its course.

Since the results of Vishnyakov are available to the present author in abstract form only, it was considered advisable to repeat some of the work reported.

The first point of variance is in the claim that the magnesium reacts only in the presence of an activator. Reference has already been made to the reaction of magnesium powder with methyl alcohol (Curves 1 and 2, Fig. 1). However, the activation of the reaction by an alkyl halide can be readily observed by comparing Curves 2 and 4, Fig. 1.

Vishnyakov suggests the following reactions to account for the hydrocarbon formation and for the activation by the alkyl halide.

$$RX + Mg \rightarrow RMgX \tag{V}$$

$$RMgX + R'OH \rightarrow R'OMgX + RH \tag{VI}$$

The initial sharp velocity maximum at the end of 10 min. was attributed to the initial formation of R'OMgX which in turn was thought to activate the reaction of the alcohol with the magnesium.

In an attempt to verify the presence of the maximum described by Vishnyakov eight reactions were carried out. In each case the weight of magnesium powder was 0.07–0.09 gm. The amount of ethyl iodide was varied successively from 1.9 gm., Run 1 to 0.02 gm., Run 8. Two typical results are shown in Fig. 2. The induction period described by Vishnyakov was not evident in any
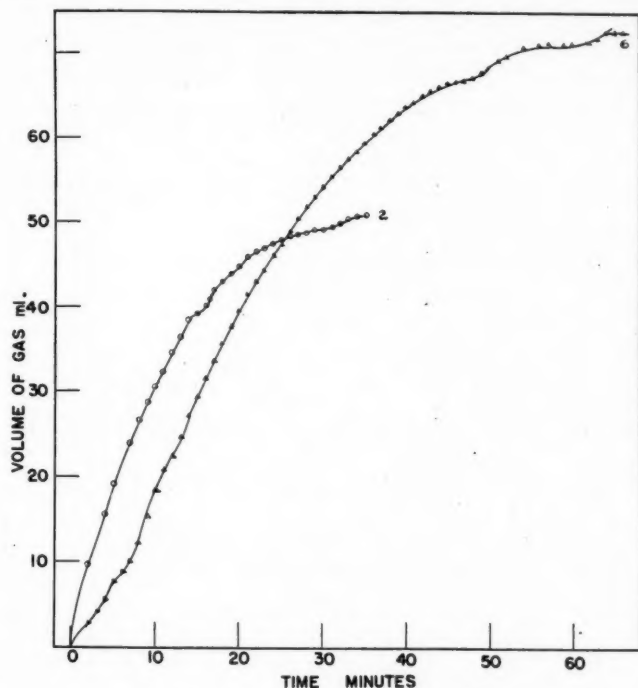
FIG. 2. Magnesium powder reacting with methyl alcohol in presence of ethyl iodide: Run 2. Magnesium powder (0.0718 gm.) and ethyl iodide (1.9224 gm.) in methyl alcohol. Run 6. Magnesium powder (0.0987 gm.) and ethyl iodide (0.0660 gm.) in methyl alcohol.

plot. The existence of velocity maxima is equally in doubt. Indeed, except for the greater velocity, the curve for magnesium powder in the presence of ethyl iodide, (Run 2, Fig. 2) does not differ greatly from the curve for magnesium alone, (Curve 2, Fig. 1).

Evidence for the occurrence of reactions involving the ethyl iodide has been found in connection with the analysis of the gas produced. This gas was examined both by infrared and by a mass spectrometer. After the usual precautions for background and a blank on the methyl alcohol, 10% ethane and 15% ethylene were found.

According to the mechanism proposed by Vishnyakov the only hydrocarbon would be ethane. The presence of both ethane and ethylene makes it more likely that the significant reaction is a disproportionation.

$$C_2H_5I + C_2H_5MgI \rightarrow C_2H_4 + C_2H_6 + MgI_2 \qquad \text{[VII]}$$
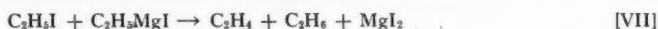
One would conclude then that the apparent activation of the reaction between magnesium and methyl alcohol in the presence of ethyl iodide is the result of a side reaction whereby magnesium is initially consumed at a greater rate and whereby the volume of gas produced is greater than would otherwise be expected.

The activation effect produced by the addition of a nitro compound is shown in Curves 2 and 3, Fig. 3. The curves so produced resemble the plot resulting
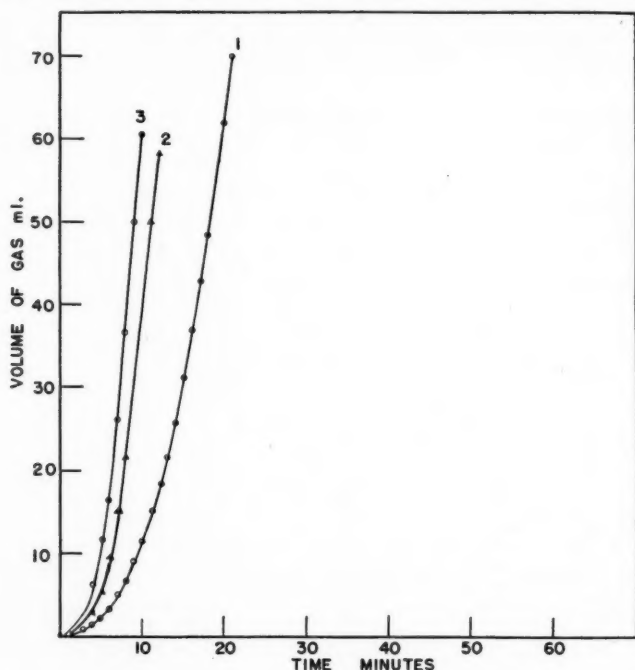
FIG. 3. Effect of 2,5-dichloronitrobenzene on reaction between magnesium ribbon and methyl alcohol: Curve 1—Polished magnesium ribbon in methyl alcohol. Curve 2—Polished magnesium ribbon and 2,5-dichloronitrobenzene (0.03 gm.) in methyl alcohol. Curve 3—Polished magnesium ribbon and 2,5-dichloronitrobenzene (0.01 gm.) in methyl alcohol.

from the activation by ethyl iodide (Curve 3, Fig. 1). Since these curves are similar to the curve for magnesium alone (Curve 3, Fig. 1) except for a shorter induction period, no useful conclusions can be drawn from these data concerning the mechanism of the activation by the nitro compound.

The presence of an intermediate compound was suggested at one stage in the work by the appearance of a highly colored substance during the reduction

of 2,5-dichloronitrobenzene. The bright violet color formed during the first 10 min. changed later to a muddy brown. Other characteristic color changes were observed during other reductions. Efforts to isolate a possible intermediate were unsuccessful. It was later concluded that the color changes were mostly the results of adsorption of the reaction products on the colloidal magnesium hydroxide formed in the course of the reaction. As the chemical and physical properties of the magnesium hydroxide change during the reaction corresponding changes occur in the color of the adsorbed substances.

Considerable effort was spent in an attempt to relate the loss in weight of the magnesium in a fixed time (15 min.) to the weight of the nitro compound present (4-chloronitrobenzene and 4-nitroanisole). The results for 4-nitroanisole are shown in Fig. 4. Similar results were found for 4-chloronitrobenzene.
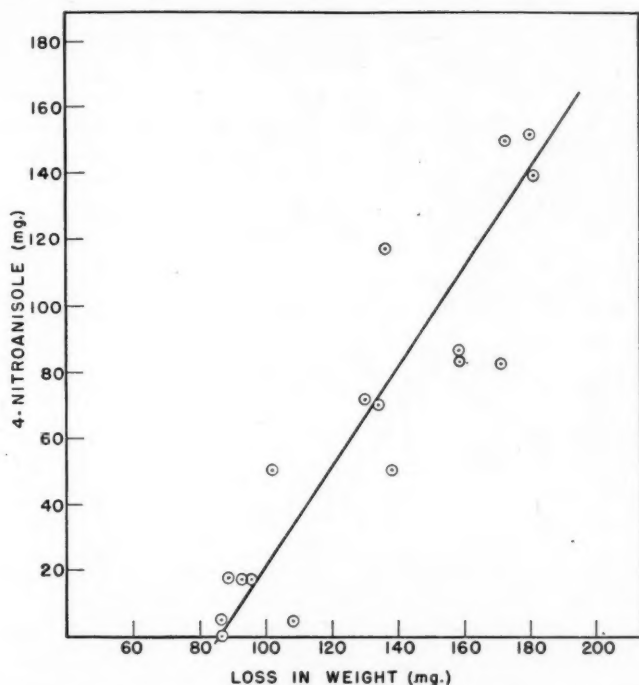
Fig. 4. Loss of weight of magnesium in solution of 4-nitroanisole and methyl alcohol (25 ml.), 15 min.

The preparation of the surface and small variations in moisture content of the alcohol are the chief factors affecting reproducibility of the results. The results show an almost linear relationship between the weight of the nitro compound and the weight of magnesium reacting in a given time.

While the mechanism by which the reaction between the magnesium and the alcohol is activated by the nitro compound remains somewhat obscure, some

conclusions can be drawn from the data shown in Fig. 4. It is likely that the apparent linear relationship between the nitro compound and the weight of the magnesium consumed is the over-all result of several factors of which the most important are the actual activation effect together with the inhibition effect due to the water produced in the reaction. If the activation continued throughout the reaction and were in fact a function of the concentration of the nitro compound, the activation effect would decrease with time as the concentration of the nitro compound decreased. The over-all reaction rate would as a result show a marked decrease with time under the influence of a diminishing activation together with an increasing inhibition due to the water produced. Since the reaction is uniform, the hypothesis that the activation is equally effective during the whole time must be rejected. It may be concluded, then, that the activation effect of the nitro compound is most important during the first part of the reaction. Reference to Fig. 3 shows that in the absence of a nitro compound the curve for the reaction is linear after about 10 min. while in the presence of the nitro compound the curve for the reaction is linear after about three minutes. The most logical assumption appears to be that the activation produced by the nitro compound is related to the role of a depolarizer in the corrosion of a metal.

III. *Reduction of an Aromatic Nitro Compound by Magnesium and Methyl Alcohol*

It is interesting to compare reduction by magnesium and methyl alcohol with reduction by sodium methylate. According to Klinger (8) the latter reaction is:

$$4C_6H_5NO_2 + 3CH_3ONa \rightarrow 2(C_6H_5N)_2O + 3HCOONa + 3H_2O. \qquad [VIII]$$
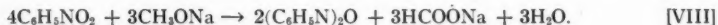
Fry and Bowman (4) suggested that the mechanism involved first a reaction between the sodium methylate and water to form methyl alcohol and sodium hydroxide. A subsequent reaction between sodium hydroxide and methyl alcohol was thought to produce hydrogen which is the active agent.

In contrast to the above reaction [VIII] magnesium methylate was found to have a minor effect on the reduction of a nitro compound. Several days are required to produce an appreciable amount of reduction of the nitro compound whereas in the mixture of magnesium and methyl alcohol the reduction is complete in 30 min.

The conclusion that the hydrogen produced by the reaction between magnesium and the methyl alcohol is the active agent is supported by the volume of gas (1.3 moles) disappearing in the presence of the nitro compound (1 mole). The reduction of the nitro compound (1 mole) to the corresponding azoxy compound requires 1.5 moles.

IV. *Reduction of the Azoxy Compound by Magnesium Methylate*

Zechmeister and Rom (16) mentioned the presence of an azo compound in certain mixtures obtained when preparing an azoxy compound by the action of magnesium and methyl alcohol. It is likely that the azo compounds were

produced by the reduction of the azoxy compound by the magnesium methylate. It has been found that a pure azoxy compound undergoes some reduction after being in contact for several hours with a solution of magnesium methylate in methyl alcohol.

RESULTS AND EXPERIMENTAL PROCEDURE

The results obtained from the reduction of 12 nitro compounds on a preparative scale are shown in Table II. The yields from Experiments 1–4 confirm in a general way the results reported by Zechmeister and Rom (16). The reduction of the remaining nitro compounds by this method is reported for the first time. For the purpose of the present study, the compounds were identified by their melting points. It should be mentioned that all reactions recorded in Table II were carried out under the same experimental procedure as given for Experiment I in the experimental part.

It has already been shown that the azoxy compound may be reduced to the azo compound by magnesium methylate in methyl alcohol. It would therefore appear that the latter reaction might be inhibited by reducing the concentration of magnesium methylate in the reaction mixture. Reference to Reaction III shows that this effect can be brought about by the addition of a small amount of water to the reaction mixture. With this experimental modification, the yield of 2,2′,5,5′-tetrachloroazoxybenzene was raised from 3.7% (Expt. 7, Table II) to 35%. Similarly the yield of 2,2′-dimethyl-3,3′-dichloroazoxybenzene was raised from 52% (Expt. 10, Table II) to 68%.

Reference to the experimental part shows that the addition of water to a mixture of 2,5-dichloronitrobenzene, magnesium, and methyl alcohol reduced the reaction temperature from the usual reflux temperature to about 30°C. It may be argued that the improved yield was the result of the lower temperature rather than the smaller concentration of the magnesium methylate. The latter possibility was tested by carrying out a similar experiment at 30°C. without addition of water. The product of the reaction was a complex mixture from which no pure azoxy compound was obtained after fractional crystallization involving 15 fractions.

Inspection of Table II shows that no azoxy compound could be isolated from certain reduction mixtures. In agreement with experience, unsuccessful reductions were prominent with ortho substituted compounds, while on the other hand, the method appears to be promising for the reduction of nitroanilines where the amino group is protected by an acetyl group. Few methods exist for the reduction of nitroanilines to the corresponding azoxy compound. Since many such reductions are carried out in strong alkaline solution (3, 6), it is likely that an acetyl group would be rapidly lost by hydrolysis.

A certain similarity appears to exist in the properties of the unknown component found in reduction mixtures where the azoxy compound is absent or present in small yield. This component, usually a bright yellow or brown, was highly soluble in alcohol but unlike a tar could not be removed by treatment with activated charcoal or chromatographic alumina. No amines were found in the reduction mixtures.

TABLE II

REDUCTION OF SOME NITROBENZENE COMPOUNDS BY MAGNESIUM AND ABSOLUTE METHYL ALCOHOL.

Expt. No.	Substituent	Recovery, %	Reagents			Azoxy compound			Azo			Comments
			Nitro comp., moles	Mg, moles	CH₃OH, ml.	M.p.* found, °C.	Gm.	Conversion, %	M.p.* found, °C.	Gm.	Conversion, %	
1	4-Chloro	10.0	0.02	0.12	125	155.5–6.5^a	0.94	39.2	183–4^k	0.76	33.6	
2	Same	..	"	..	"	"	1.40	58.3	..	0.77	34.0	
3	3-Bromo	11.8	0.04	0.12	300	110–111^b	3.3	61.0	—	0	0	
4	4-Bromo	46.0	0.04	0.12	300	173–3.5^c	3.7	98.0	—	0	0	
5	3-Iodo	0	0.02	0.12	300	117–118^d	1.9	42	—	0	0	
6	4-Iodo	0	0.02	0.12	300	202–203.5^e	1.1	37	188–9^l	0.19	6	2.1 gm. crude product
7	2,5-Dichloro	0	0.02	0.12	125	146–7^f	0.124	3.7	—	0	0	2.19 gm. crude product, m.p. 135°–137°C.
8	3,4-Dichloro	0	0.016	0.12	125	138–9^g	0.46	17	—			
9	2,4-Dichloro	0	0.02	0.12	125	130.5^h	0.13	3.8	164–5^m	0.08	2.5	2.0 gm. crude product, m.p. 119°–120°C.
10	2-Methyl-3-chloro	0	0.02	0.12	125	121.3^i	1.5	52.0	—	0	0	
11	4-Acetamino	0	0.02	0.12	125	273–4^j	1.5	41.0	—	0	0	
12	3-Acetamino	0	0.016	0.10	250	254–5^n	0.615	30.0	—	0	0	
13	4-Methoxy	0	0.022	0.11	250	114°	0.605	21.0	—			

*All melting points were checked against reliable standards.

†Further identified by conversion to the corresponding diaminoazoxy compounds.

No azoxy or azo compound could be found in the reaction mixture of the following: 2-nitroiodobenzene, 4-aminonitrobenzene, 2-nitroanisole, 3-nitroanisole, 3-nitrobenzaldehyde.

^{a}Ref. (7), 155–6°C.
^{b}Ref. (1), 109–10°C.
^{c}Ref. (14), 175°C.
^{d}Ref. (10), 118–9°C.
^{e}Ref. (5), 119.0–9.5°C.

^{f}Ref. (2), 147°C.
^{g}Ref. (3), 137–138°C.
^{h}Ref. (12), 126–7°C.
^{i}Ref. (6), 122–3°C.
^{j}Ref. (11), 275°C.

^{k}Ref. (15), 185–6°C.
^{l}Ref. (2), 188–9°C.
^{m}Ref. (17), 161–2°C.
^{n}Ref. (10), 254°C.
^{o}Ref. (9), 116°C.

MATERIALS

Canadian Industries Limited reagent anhydrous absolute synthetic methyl alcohol Grade A-1 was used throughout. When first taken from the drum the alcohol contained 0.01% moisture. Alcohol containing 0.007% moisture was obtained by reaction with magnesium followed by slow distillation through an efficient column. The magnesium ribbon, turnings, and powder were Baker and Adamson, purified.

EXPERIMENTAL

Reaction of Magnesium with Methyl Alcohol as Measured by the Evolution of Gas (Curve 2, Fig. 1)

Magnesium powder (0.0752 gm.) was added to methyl alcohol (25 ml., 0.007% water). Magnetic stirring was used. A water bath maintained the temperature at $25° \pm 0.5°$. The gas evolved was measured in the gas burette of Fisher Orsat precision model gas analyzer with the volume of gas evolved balanced against atmosphere pressure and read at one minute intervals.

Hydrogen Consumed in the Presence of 4-Chloronitrobenzene

(a) Polished magnesium ribbon (0.0800 gm.) in methyl alcohol (25 ml.) produced 66.9 ml. gas (0° C. and 760 mm.).

(b) Polished magnesium ribbon (0.0800 gm.) in methyl alcohol (25 ml.) containing 4-chloronitrobenzene (0.1028 gm.) produced 48.5 ml. gas (0° C. and 760 mm.).

Gas consumed $= 66.9 - 48.5 = 18.4$ ml. for 1 mole 4-chloronitrobenzene
$$= (18.4 \times 157.5)/0.1028 \text{ ml.}$$
$$= 1.26 \text{ moles gas}/ 1 \text{ mole 4-chloronitrobenzene.}$$

Viscosity Changes During Reduction of 2,5-Dichloronitrobenzene by Magnesium and Methyl Alcohol

2,5-Dichloronitrobenzene (2.6 gm.) was dissolved in methyl alcohol (150 ml.). To this solution was added freshly polished magnesium ribbon (2.37 gm.) cut into small pieces. The viscosity changes were followed by a Fisher electro-viscometer. The speed of the rotation of the spindle was checked at intervals by a stroboscope. The temperature was $24° \pm 0.5°$ C. The relative viscosity was as follows: 130 sec.–7.0; 224 sec.–8.2; 415 sec.–12.0; 488 sec.–13.5; 552 sec.–12.7; 780 sec.–11.0; 980 sec.–10.2.

Analysis of the Gas Produced by the Reaction Between Magnesium Powder, Ethyl Iodide, and Methyl Alcohol

Magnesium powder (0.1675 gm.), ethyl iodide (1.7032 gm.), and methyl alcohol (25 ml.) were allowed to react. The gas was collected over mercury. Analysis by a mass spectrograph gave the following approximate results: methyl alcohol, 20%; ethane, 10%; ethylene, 15%; hydrogen, 55%. Suitable correction was made for background. The calibration for methyl alcohol was taken from a run on a pure sample while those for ethane and ethylene were taken from the average of several American Petroleum Institute spectrograms. The presence of ethylene was confirmed by infrared analysis of the same sample.

Reduction of 2,5-Dichloronitrobenzene by Magnesium Methylate

Polished magnesium ribbon (2.9 gm.) was added to redistilled methyl alcohol (250 ml.). When all the magnesium had dissolved, 2,5-dichloronitrobenzene (3.8 gm.) was added to the hot solution. The mixture was allowed to stand for three days at room temperature and then diluted with water, acidified with hydrochloric acid, and then steam distilled. 2,5-Dichloronitrobenzene (2.3 gm., m.p. 52° C.) was recovered from the steam distillate. A small quantity of a product remained. Recrystallization produced a few milligrams of 2,2′,5,5′-tetrachloroazoxybenzene (m.p. 145° C.).

Reduction of 2,2′,5,5′-Tetrachloroazoxybenzene by Magnesium Methylate

2,2′,5,5′-Tetrachloroazoxybenzene (1 gm., m.p. 145° C.) was added to a freshly prepared solution of magnesium methylate and allowed to stand for several hours. The recovered product, melting at 142°–143°, was separated into four fractions melting respectively at 145°–146° C., 144°–145° C., 145°–146° C., and 184°–186° C. The last fraction is the reduction product, 2,2′,5,5′-tetrachloroazobenzene.

Reduction of 4-Chloronitrobenzene by Magnesium and Methyl Alcohol (Expt. 1, Table II)

4-Chloronitrobenzene (3.15 gm., 0.02 mole) was dissolved in redistilled methyl alcohol (125 ml.) in a 250-ml., three-necked flask provided with a reflux condenser and a pyrex stirrer with a mercury seal. Magnesium turnings or short pieces of polished ribbon (2.9 gm., 0.12 mole) were added to the solution. A rapid reaction set in and the alcohol reached the boiling point within 10 min. After the solution of the magnesium was complete, the mixture was heated at reflux temperature for two hours. It was diluted with water, neutralized with hydrochloric acid to dissolve the magnesium hydroxide, and then steam distilled. In the distillate was unchanged 4-chloronitrobenzene (0.3 gm.). The product remaining was dissolved in alcohol and separated by fractional crystallization into 4,4′-dichloroazoxybenzene (1.4 gm., m.p. 155.5°–156.5° C.) and 4.4′-dichloroazobenzene (0.77 gm., m.p. 183°–184° C.).

Reduction of 2,5-Dichloronitrobenzene by Magnesium and Methyl Alcohol in the Presence of Water

Water (1 ml.) was added to 2,5-dichloronitrobenzene (3.8 gm., 0.02 mole) dissolved in methyl alcohol (0.06% water) in a 250-ml., three-necked flask provided with a reflux condenser and a pyrex stirrer with a mercury seal. Freshly polished magnesium ribbon (2.9 gm., 0.12 mole) cut into small pieces was added. The reaction began at once but the temperature did not exceed 31° C. At the end of 30 min., water (1 ml.) was again added and after two hours the temperature was raised to 45°. At the end of five hours the reaction was complete.

The mixture, after being diluted with water and neutralized with hydrochloric acid to dissolve the magnesium hydroxide, was steam distilled. In the distillate was unchanged 2,5-dichloronitrobenzene (1.2 gm.). The residue from the steam distillation was dissolved in methyl alcohol and treated with Norite.

Fractional crystallization of the product gave 2,2′,5,5′-tetrachloroazoxyben-zene (m.p. 144°–145° C.). The yield was 0.7878 gm. or 35% calculated on the 2,5-dichloronitrobenzene converted.

ACKNOWLEDGMENT

REFERENCES

1. BAMBERGER, E. and RENAULD, E. Ber. 30: 2278. 1897.
2. DE CRAUW, T. Rec. trav. chim. 50: 782. 1931.
3. DAINS, F. B. and KENYON, W. O. J. Am. Chem. Soc. 53: 2357. 1931.
4. FRY, H. S. and BOWMAN, P. E. J. Am. Chem. Soc. 52: 1531. 1930.
5. GABRIEL, S. Ber. 9: 1408. 1876.
6. GAUDRY, R. and KEIRSTEAD, K. F. Can. J. Research, B. 27: 894. 1949.
7. HEUMAN, K. Ber. 5: 911. 1872.
8. KLINGER, H. Ber. 15: 866. 1882.
9. LEHMANN, O. Ber. 23: 1740. 1890.
10. MELDOLA and ANDREWS, J. Chem. Soc. 69: 9. 1896.
11. MIXTER, W. G. Am. Chem. J. 5: 1. 1883. *In* Beilstein's Handbuch der organischen Chemie. 16: 655. 1933.
12. VAN DE LANDE, L. M. F. Rec. trav. chim. 51: 110. 1932.
13. VISHNYAKOV, M. N. J. Gen. Chem. (U.S.S.R.), 6: 107–28. 1936. *Abstracted in* Chem. Abstracts, 30: 5179. 1936.
14. WERIGO, A. Ann. 165: 198. 1873.
15. WILLGERODT. Ber. 14: 2636. 1881.
16. ZECHMEISTER, L. and ROM, P. Ann. 468: 117–32. 1928.
17. ZINCKE, T. and KUCHENBECKER, A. Ann. 330:53. 1904.

CONSTRUCTION AND USE OF A
SEMIMICRO LIGHT-SCATTERING APPARATUS[1]

By D. A. I. Goring

ABSTRACT

A light-scattering apparatus requiring only 4 ml. of liquid was designed and built. The device has permitted the measurement of intensity for angles between $37\frac{1}{2}°$ and $135°$ to the incident beam. In this range the unpolarized, horizontal, and vertical components of the light emitted from a solution of fluorescein were constant to within $\pm0.2\%$, 0.4%, and 0.6% respectively. The apparatus was calibrated with a suspension of Ludox colloidal silica which absorbed no light for $\lambda = 3800$ Å to 6000 Å. The suspension was found to possess all the properties of a Rayleigh scattering system except randomness. This condition was achieved by extrapolating the light-scattering and spectrophotometric functions to zero concentration when computing the calibration factor. The molecular weight of a sample of sodium carrageenate, determined by the method of Zimm, was 1,700,000. The distribution of intensity at zero concentration fell between that for stiff rods and polydisperse coils.

INTRODUCTION

No description has yet been published of a light-scattering apparatus specifically designed for a small volume of liquid. The present device evolved directly from an earlier model briefly described in a previous publication (10).

Construction of a geometric photometer similar to that of Brice, Halwer, and Speiser (1) was not attempted; the precise optical system required would be difficult to combine with a small cell volume and a continuous observation of the angular variation of intensity. Instead the apparatus was calibrated with a liquid the turbidity of which was measured spectrophotometrically. Provided a suitable calibrating liquid is chosen this method has been shown to give reliable values of the molecular weight (10).

To illustrate the use of the device a measurement of particle size has been given for the polysaccharide, carrageenin. The molecular weight, M, was determined from the usual equation

[1]
$$H\left(\frac{c}{\tau}\right)_{c=0} = \frac{1}{M}$$

where τ is defined as the turbidity, due to scattering alone, which the solution would show if the particles obeyed the Rayleigh law and therefore produced a symmetrical distribution of intensity. In Eq. [1] c is the concentration and the constant H has the usual significance.

Since the polysaccharide solution showed a large dissymmetry of scattering the more accurate method of Zimm (17) was used. The intensity of scatter, I_θ, was measured for different values of the angle, θ, defined by the direction of scattering and the transmitted beam. A graph of c/I_θ vs. $\sin^2\frac{1}{2}\theta + \kappa c$ was drawn where κ was a constant chosen to separate the distribution of intensity

for each concentration. The value of $\left(\dfrac{c}{I_\theta}\right)_{\substack{\theta=0 \\ c=0}}$ was found by extrapolation. The value of $(c/\tau)_{c=0}$ was obtained from

[2] $$\left(\frac{c}{\tau}\right)_{c=0} = C\left(\frac{c}{I_\theta}\right)_{\substack{\theta=0 \\ c=0}}$$

where C was the calibration factor determined with a Ludox suspension. To obtain M, $(c/\tau)_{c=0}$ was substituted in Eq. [1].

The distribution of intensity at $c = 0$ was computed from the Zimm plot and was compared with theoretical distributions predicted for spheres, coils, and rods.

THE LIGHT-SCATTERING APPARATUS

A photograph and a plan of the light-scattering apparatus are shown in Figs. 1 and 2 respectively.
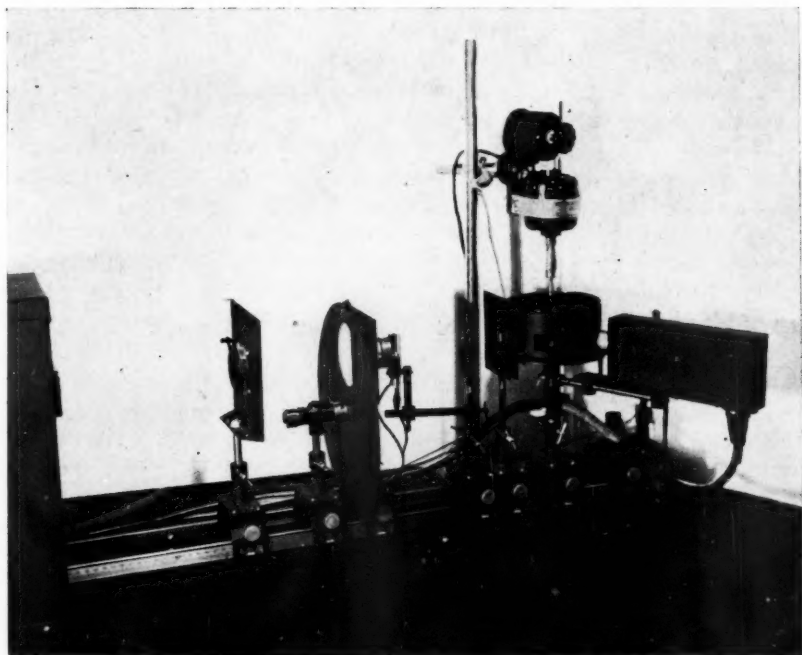
FIG. 1. Photograph of the light-scattering apparatus.

Light from source B was focused on slit C. An image of C was produced by lens E in the center of the scattering cell Q. Scattered light from the center of Q was focused by lens T through slit U on photomultiplier tube V.

The components for the primary beam (A → P) were mounted on a 125 cm. optical bench. The cell was immersed in a cylindrical water bath, K, which
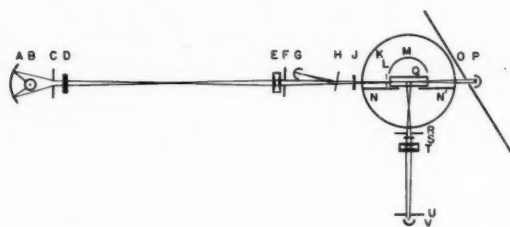
Fig. 2. Plan of the light-scattering apparatus. The letters corresponding to various parts are referred to in the text.

rested on a circular table mounted on the optical bench. The components for the scattered beam (R → V) were mounted on a rotatable arm centered below the table.

Light Source

The light source was a General Electric AH-4 mercury arc. Current to the lamp was drawn from the 110 v. mains and stabilized with a 500 w. Sola constant-voltage transformer. The operating current was adjusted to the recommended value of 0.9 amp. by means of a Variac transformer. After the lamp had been running 15 min, variations in the current were less than 0.5%.

As shown in Fig. 2, a concave spherical mirror, A, with a radius of curvature of 64 mm. focused an image of the lamp on slit C. The mirror proved more effective than a condensing lens for increasing the incident intensity.

A filter, D, in the incident beam gave monochromatic light. Wratten filters 77A and 76 were used for the 5461 Å and the 4358 Å lines respectively.

The lamp, mirror, and slit were enclosed in a ventilated, light-proof housing with filter D covering the opening for the incident beam.

The Incident Beam

To reduce the size of the beam in the cell, the distance between slit C and lens E was approximately twice that between the center of the cell, Q, and lens E. Slit C was 8 mm. high by 3 mm. wide, making the dimensions of the incident beam in the cell 4 mm. high by 1.5 mm. wide.

Lens E was a Schneider-Zenir f 4.5, with a focal length of 150 mm. A rectangular stop, F, set the convergence in the horizontal and vertical planes at 2.5° and 8° respectively.

The incident beam entered the water bath, K, through a cylindrical surface. To counteract the convergence produced in the horizontal plane, a planoconcavo cylindrical spectacle lens, J, was set adjacent to the entrance window. A sharp image of slit C was thereby produced in the scattering cell.

After traversing the scattering cell, the incident beam passed through a baffle O on to a phototube P. Comparative measurements of the transmitted intensity were made with P in order to compute the decrease in intensity of the incident beam on traversing the half-length of the cell. A correction for the decrease was applied to the intensity. This correction is important when colored solutions are studied (10).

Fluctuations in incident intensity were measured by a phototube, G, on to which was focused light reflected from a microscope cover glass, H, set at 7° to the incident beam. No polarization was found in the incident light after passage through the cover glass. During an experiment the variation in lamp intensity measured at G was less than 1%, so that for routine work the monitor was removed from the apparatus and was only used when highest accuracy was desired.

The Cell and Water Bath

The cylindrical water bath (K in Fig. 2) was a pyrex crystallizing dish, 125 mm. in diameter, selected visually to be free from optical aberration. As shown in Fig. 3, the position of the bath on the table was adjusted by three centering screws.
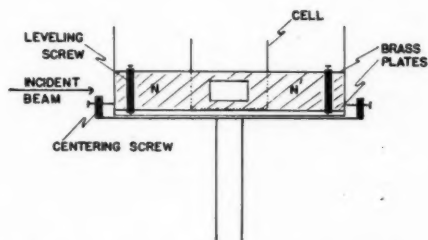
FIG. 3. Section of the table and cylindrical water bath showing the position of the cell and the baffle NN'.

Two brass plates, held 24 mm. apart by three pillars, fitted exactly into the dish and supported the cell and the baffles L, M, and NN'. The cell fitted closely through a rectangular hole cut in the center of the upper plate and a rectangular recess in the lower plate. Leveling screws were fitted through the pillars separating the plates. If desired, the temperature of the water bath could be controlled by flat coils of copper tubing above the top plate and below the bottom plate.

The cells were made of optical glass* 2 mm. thick and had inside dimensions of length, height, and width equal to 40 mm., 50 mm., and 5 mm. respectively. With 4 ml. of liquid in the cell the height of the meniscus cleared the top of the incident beam by 6 mm.

The system of baffles is shown in Figs. 2 and 3. The baffle NN' shielded from the photomultiplier tube the path of the incident beam through the bath and the ends of the cell. The scattered light was viewed through a rectangular hole, 12 mm. high and 19.5 mm. wide in NN'. The size of the hole and position of the baffle were chosen to permit unbroken passage of the scattered beam between $\theta = 37\frac{1}{2}°$ and $\theta = 135°$.

A semicircular baffle, M (Fig. 2), was placed behind the cell to prevent reflections from the back of the water bath entering the photomultiplier. A plate, L, with a rectangular hole, 7.5 mm. high by 2.5 mm. wide, was set in the path of the incident beam near the cell. This baffle stopped any diffuse light

*Cells were supplied in pyrex and soft glass by the Pyrocell Manufacturing Co.

from entering the cell. Baffles and bath were painted flat black; small windows were left clear for the primary beam and scattered light.

The Scattered Beam

The distance between slit U and lens T (Fig. 2) was twice the distance between the center of the scattering volume and T. Slit U was 12 mm. high by 6 mm. wide and therefore the area in the cell from which scattered light was received was 6 mm. high by 3 mm. wide. The position of lens T was adjusted so that an image of U (obtained by substituting a galvanometer lamp for the photomultiplier tube) was in sharp focus in the center of the cell. A rectangular stop, R, reduced the convergence to 8° in the vertical plane and to 3° in the horizontal plane.

Lens T was a Schneider-Componar f-4.5, with a focal length of 50 mm. As in the incident beam, a plano-concavo cylindrical spectacle lens, S, was included to counteract the convergence of the water bath and thereby to permit a sharp image of slit U in the center of the scattering cell. Therefore the scattering volume was defined by the height (4 mm.) and width (1.5 mm.) of the incident beam and the width (3 mm.) of the image of U in the cell.

From an angular scale on the edge of the table, the direction of the analyzing arm was determined. To prevent stray light entering the photomultiplier, the components S → V of the analyzing arm were enclosed in a light-proof box with stop R as the only opening.

The photomultiplier was an R.C.A. 1P21 phototube. A potential of 90 v. was maintained across the dynodes and between the anode and dynode 9 a potential of 45 v. was used. Dry cells were found to be a stable and reliable source of power.

The output of the photomultiplier was read directly on a d'Arsonval galvanometer and the sensitivity was controlled with an Ayrton shunt. Dark currents were 0.004 μamp. The additional output for I_{90} from a dust-free solution of 0.1 M sodium acetate was 0.004 μamp. which corresponded to 10 mm. on the galvanometer scale. Thus the sensitivity was adequate even for the extremely small intensity scattered by 0.1 M aqueous sodium acetate.

Correction and Normalizing Factors

It was necessary to apply several factors and small corrections to the data.

(1) *Variations in intensity and sensitivity.*—The galvanometer deflection for the light scattered was divided by the deflection for the 90° intensity from a plastic block. Thus variations in the intensity of the lamp or in the sensitivity of the photomultiplier were accurately compensated. The block was machined from a piece of Lucite which was four years old. It was kept in the dark and the scatter from it was assumed constant.

(2) *Change in scattering volume.*—For any position of the analyzing arm the scattering volume was assumed to be a right parallelapiped. A factor, sin θ, was applied to the observed intensity to allow for increase in the scattering volume for angles other than 90°.

(3) *The horizontal component.*—Unpolarized light was used in the incident beam and therefore the scattered light contained a horizontal component pro-

portional to $\cos^2 \theta$. To normalize the intensity it is usual to apply the factor $1/(1 + \cos^2 \theta)$. The 1P21 photomultiplier tube was found to be 1.013 times more sensitive to vertically than to horizontally polarized light. The normalizing factor used was, therefore, $1/(1 + 0.987 \cos^2 \theta)$.

(4) *Depolarization.*—The depolarization, ρ, was measured by means of a polaroid placed in the scattered beam in the 90° position. When the value of ρ was significant (> 0.005) the molecular weight was multiplied by the factor $(6 - 7\rho)/(6 + 6\rho)$ (Ref. 6).

(5) *Dark current.*—With the photomultiplier in circuit, a shutter was placed across the incident beam and the galvanometer set at zero. On illuminating the solution the deflection obtained was due only to the light scattered. By this method a direct measurement of the dark current was unnecessary.

(6) *Refractive index corrections.*—If liquids of different refractive indices are used in the scattering cell, correction must be made for the change in (a) the scattering volume (8) and (b) the size of the cone of light received by the lens T (Fig. 2) on the analyzing arm (8, 10). Only dilute aqueous solutions were used in the present work; it was assumed that the refractive index remained constant thereby precluding the necessity of a correction.

(7) *Scatter of solvent.*—Intensities for the solvent were measured and subtracted from those for the solution.

(8) *Reflection.*—As pointed out by Sheffer and Hyde (14) the reflection in a *backward direction* from flat surfaces at the end of the cell can alter the distribution when a large dissymmetry exists. In the present device the two water–glass interfaces produced a back reflection of 0.8% of the incident beam which was assumed negligible.

Testing the Apparatus

The symmetry of the apparatus was tested by observing the distribution of intensity emitted by a solution of 1 mgm. per liter of fluorescein in 0.1 M sodium acetate solution. Using an unpolarized incident beam, measurements were made of the unpolarized and the vertically and horizontally polarized components of the fluorescence. With fluorescein, the intensity of fluorescence is equal in all directions and therefore the factor $1/(1 + 0.987 \cos^2 \theta)$ was not applied; the intensity was corrected by the factor, $\sin \theta$, for the change in scattering volume and the horizontal component was multiplied by the factor 1.013.

As shown in Fig. 4, I_θ was constant within $\pm 0.2\%$ for the unpolarized light. The horizontal and vertical components were constant within $\pm 0.4\%$ and $\pm 0.6\%$ respectively. This result showed that the apparatus was set up in a symmetrical manner and that the correction for the variation of the scattering volume with θ was accurate.

As a final test for absence of secondary reflections the distribution of intensity scattered by a 0.1 M aqueous solution of sodium acetate was measured. In Fig. 5 the unpolarized and horizontally and vertically polarized components of the envelope are given: for comparison, the unpolarized envelope of a phosphate buffer obtained with the apparatus described by Goring and Johnson (10) is given also.
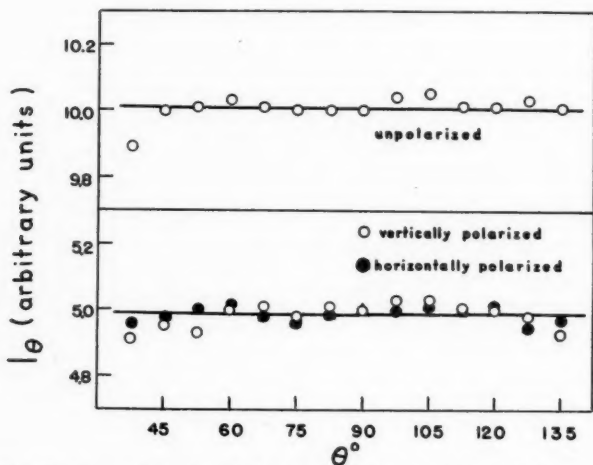
FIG. 4. Distribution of intensity of light emitted by a solution of 1 mgm. per liter of fluorescein in 0.1 M sodium acetate solution. The scale of the ordinate was chosen to magnify the errors.
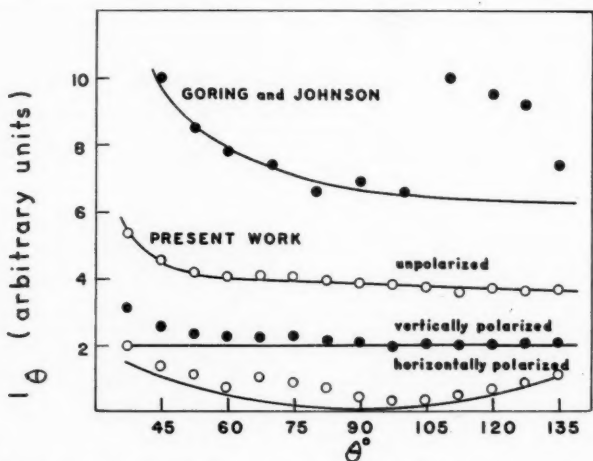

FIG. 5. Unpolarized and vertically and horizontally polarized components for a 0.1 M solution of sodium acetate; and on the same absolute scale the envelope of a phosphate buffer (pH = 7.7; I = 0.05) determined by Goring and Johnson on the previous apparatus (10).

As shown in Fig. 5, the absence of large irregularities for the distributions obtained with the present device indicated that secondary reflections were almost completely eliminated. There was a small anomalous increase in the horizontal component for $\theta = 67\frac{1}{2}°$ to $\theta = 90°$. This effect was reproducible and was probably due to minute reflections from various parts of the instrument. Comparison of the unpolarized distribution with the previously obtained envelope showed a marked improvement in regularity. The difference in absolute intensities was not significant since different solutions were used.

Calibration

The apparatus was calibrated with suspensions of Ludox colloidal silica the turbidities of which were determined spectrophotometrically. Ludox has been used by Tietze and Neurath (15) and is recommended by Oster (12) as a calibrating solution. An electron micrograph of its particles (Fig. 6) shows a fairly
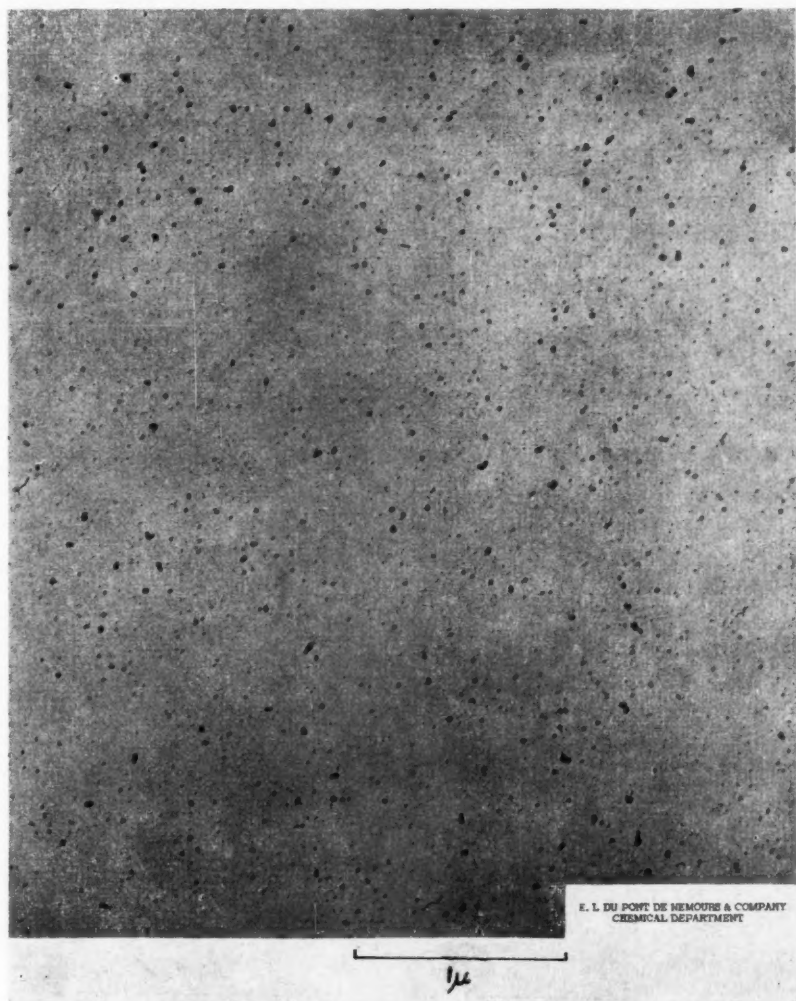
FIG. 6.   An electron micrograph of Ludox particles (reproduced by kind permission of Mr. J. M. Rule of DuPont).

uniform particle size with an average diameter of about 200 Å. Such a suspension would approximate to a simple Rayleigh system and therefore would be a

good calibrating liquid provided there was no absorption of light and the total dissipation in the transmitted beam was due to scattering alone.

For a given solution in which c, M, and the interaction constant, B, do not vary, the light-scattering equation (6) may be written

$$[3] \qquad\qquad \frac{\lambda^4 \tau}{(n_0 dn/dc)^2} = \text{constant}$$

where λ is the wave length of the incident beam, n_0 is the refractive index of the solvent, and dn/dc is the refractive index increment. If the solution is a Rayleigh scattering system showing no absorption, the spectrophotometrically determined values of τ should give a constant value of $\lambda^4 \tau/(n_0\, dn/dc)^2$ for a range of wave lengths.

To test the constancy of $\lambda^4 \tau/(n_0\, dn/dc)^2$ for Ludox,* the variation of τ, n_0, and dn/dc with λ was required. The variation of τ was measured with a Beckman DU spectrophotometer using 5 cm. cells. A tungsten filament was used as a source. A vertical slit, 2 mm. wide by 10 mm. high, was set in front of the photocell on the spectrophotometer. The slit was 8 cm. from the center of the 5 cm. cell. The area of the slit was 1/500 the area of the spherical surface containing the slit about the center of the 5 cm. cell. Thus a relatively negligible quantity of light scattered at low angles to the beam could enter the slit and reach the photocell. Although the slit decreased the sensitivity of the instrument, an accurate balance could be obtained for all wave lengths from 3800 Å to 6000 Å with a spread of 20 Å in the wave length of the monochromator beam.

The change of n_0 with λ was assumed to be the same as that for water. The refractive index increment was measured at 4358 Å and 5461 Å with a Bellingham and Stanley critical angle refractometer; the values of dn/dc at different wave lengths were obtained by assuming a linear variation of dn/dc with λ. The error involved in this assumption was small since dn/dc for Ludox decreased by only 1.5% from $\lambda = 4358$ Å to $\lambda = 5461$ Å.

The graph of $\lambda^4 \tau/(n_0\, dn/dc)^2$ vs. λ for a Ludox suspension is given in Fig. 7. The value of $\lambda^4 \tau/(n_0\, dn/dc)^2$ is constant to within $\pm 1.2\%$. The small regular increase at the higher wave lengths would result if a nonlinearity existed in the relationship between dn/dc and λ.

A series of four Ludox suspensions of concentrations from 7% to 1.8% (by dry weight) were used to determine the calibration factor. The turbidity of each was measured in the Beckman at the wave length of the highest intensity emitted from the green line of the mercury arc. From the graph of c/τ vs. c shown in Fig. 8 $(c/\tau)_{c=0}$ was obtained.

A distribution of scattered intensity for each of these concentrations was measured in the light-scattering apparatus. The data were represented as a Zimm plot part of which is shown in Fig. 9. The $\theta = 0$ and $c = 0$ lines extrapolated to a common intercept to give $\left(\dfrac{c}{I_\theta}\right)_{\substack{\theta=0 \\ c=0}}$.

Kindly donated by Mr. J. M. Rule of Du Pont de Nemours, Delaware.
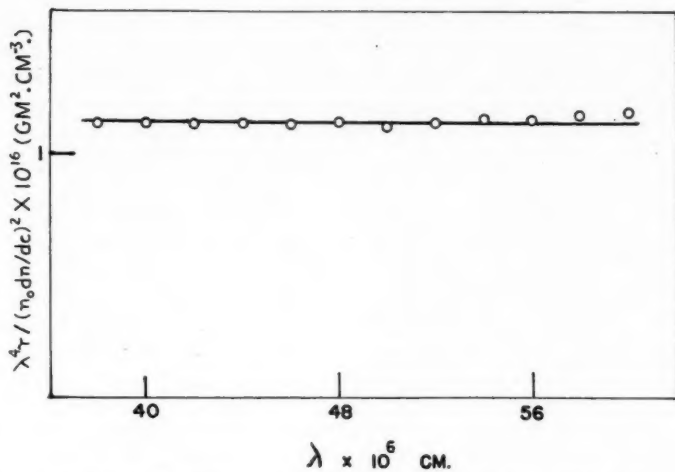
FIG. 7. $\lambda^4 \tau / (n_0 \, dn/dc)^2$ vs. λ for a 7% suspension of Ludox colloidal silica.
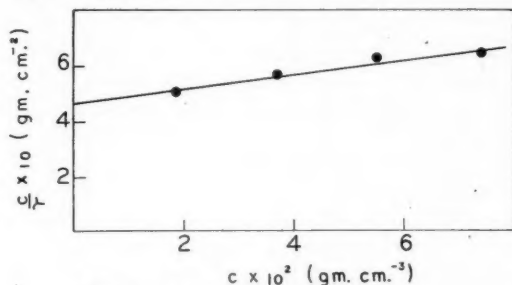
FIG. 8. c/τ vs. c for Ludox suspensions.
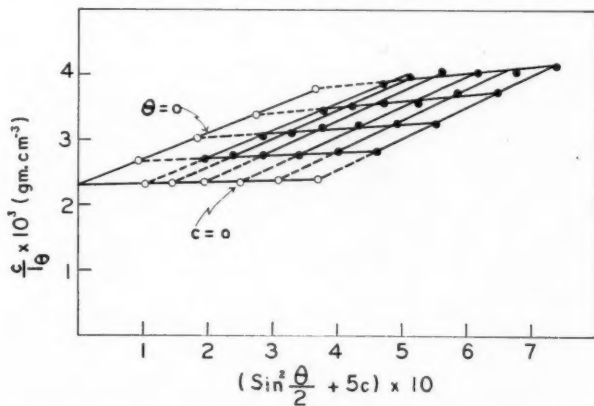
FIG. 9. Zimm plot for Ludox. The range of concentration was from 7.4×10^{-2} to 1.8×10^{-2} gm.cm.$^{-3}$; the range of θ was from $37\frac{1}{2}°$ to $75°$.

It was necessary to make a small adjustment to allow for the dissymmetry. The turbidity in Eq. [1] used for computing M is taken as that which the solution would have had if interference had not caused a decrease of scatter in the backwards direction. Therefore, in calibrating, the relationship between τ and I_θ should be that for a Rayleigh system. If a dissymmetry exists, the value of $\left(\frac{c}{I_\theta}\right)_{\substack{\theta=0\\c=0}}$ will be smaller than that for an ideal system having the observed $(c/\tau)_{c=0}$. By a graphical integration it was found that for spheres showing a small dissymmetry, the error can be corrected by using

$$\frac{1}{2}\left[\left(\frac{c}{I_\theta}\right)_{\substack{\theta=0\\c=0}} + \left(\frac{c}{I_\theta}\right)_{\substack{\theta=180\\c=0}}\right]$$

instead of $\left(\frac{c}{I_\theta}\right)_{\substack{\theta=0\\c=0}}$. The calibration factor, C, was then obtained from

[4]
$$\left(\frac{c}{\tau}\right)_{c=0} = \frac{C}{2}\left[\left(\frac{c}{I_\theta}\right)_{\substack{\theta=0\\c=0}} + \left(\frac{c}{I_\theta}\right)_{\substack{\theta=180\\c=0}}\right].$$

The value of C was decreased 4.2% by this correction for dissymmetry.

MOLECULAR WEIGHT OF CARRAGEENIN

Sodium carrageenate was prepared from Irish moss by aqueous extraction and dialysis (2, 16). For light-scattering the polysaccharide was dissolved in acetate buffer (pH = 5.5; I = 0.05) made up by the method of Green (11). Dilutions were made in the cell. Motes were removed by centrifuging in stainless steel cups at 27,000 g. for 20 min. Ultrafiltration (9) was not successful because the polysaccharide clogged the filter.

The Zimm plot is given in Fig. 10. From $\theta = 135°$ to $\theta = 75°$ readings were taken every 15°; from 75° to $37\frac{1}{2}°$ readings were taken every $7\frac{1}{2}°$ to facilitate extrapolation to $\theta = 0$. For constant angle, c/I_θ varied linearly with c and the
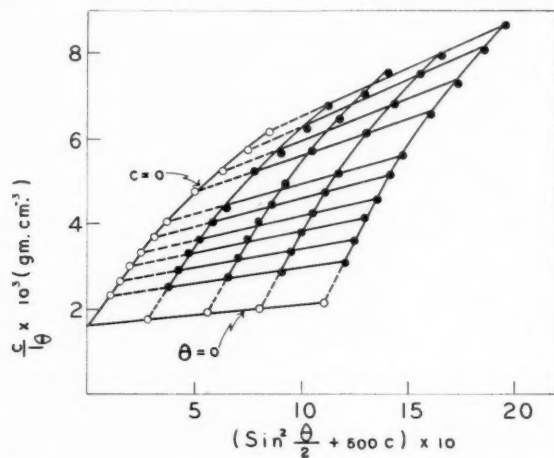
Fig. 10. Zimm plot for sodium carrageenate in sodium acetate buffer (pH = 5.5; I = 0.05). The range of concentration was from 2.2×10^{-3} to 0.6×10^{-3} gm.cm.$^{-3}$; the range of θ was from $37\frac{1}{2}°$ to 135°.

best straight line between the four points at different concentrations was used for extrapolation. The variation of c/I_θ with $\sin^2\frac{1}{2}\theta$ at constant concentration showed a curvature for higher values of θ. From $\theta = 67\frac{1}{2}$ to $\theta = 37\frac{1}{2}$ the graph was essentially linear and extrapolation of these five points was used to determine $(c/I_\theta)_{\theta=0}$.

The extrapolations of the curves for $\theta = 0$ and $c = 0$ gave a common intercept for $\left(\dfrac{c}{I_\theta}\right)_{\substack{\theta=0 \\ c=0}}$ which equalled 0.0016. From this value and the calibration factor, $(c/\tau)_{c=0}$ was 0.31 gm. cm.$^{-2}$. The refractive index increment for sodium carrageenate was found to be 0.131 gm.$^{-1}$ cm.^{3} from which H was computed. By substituting these results in Eq. [1] a molecular weight of 1,700,000 ($\pm$100,000) was obtained.

DISCUSSION

Performance

In several ways the present apparatus was superior to its predecessor (10). It required only 4 ml. whereas in the previous model a volume of 15 ml. was necessary. It was more stable and sensitive and could be used over a wider range of angular distribution. Also, as shown in Fig. 5, it was freer from secondary reflections.

It was anticipated that reflection from the flat sides of the cell would distort the distribution. From Fresnel's laws it was computed that for $\theta = 37\frac{1}{2}°$, 4.1% of the light is reflected back from the two glass–water interfaces. For $\theta = 90°$, the intensity of reflection is 0.8%. Thus, a distribution of intensity should show an appreciable decrease for angles away from the 90° position.

Because of the long, narrow shape of the scattering cell, this error was compensated by a similar reflection from the back of the cell. The effect is illustrated in Fig. 11. A secondary scattering volume may be defined as the volume emitting light which, when reflected from the back of the cell, is received by the analyzing arm. If the incident beam is assumed to be parallel and the width
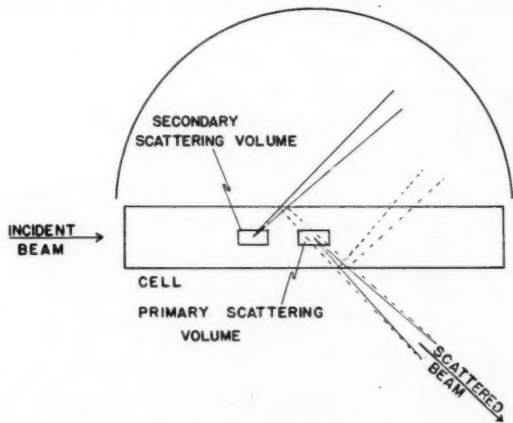
FIG. 11. Illustrating the manner in which part of the light scattered in the secondary scattering volume is reflected from the back of the cell and reinforces the main scattered beam.

of the cell (5 mm.) is small compared with the distance between the scattering volume and lens T (90 mm., see Fig. 2) the primary and secondary scattering volumes are the same size. Thus the reflected light received by the analyzing arm from the secondary scattering volume will be similar in intensity and composition to the light lost from the primary scattering volume due to back reflection. This compensation occurred in the present apparatus since I_θ was found constant for the range of angles studied as shown in Fig. 4.

The incomplete removal of motes was assumed to cause the dissymmetry found in the distribution for 0.1 M sodium acetate (Fig. 5). Alternate causes were (a) diffuse secondary reflections at angles near the incident beam or (b) a dissymmetry in the solution itself. In any case the intensity was very small in comparison with that scattered by the solutions of carrageenin (I_{90} for a buffer was $I_{90}/100$ for a 0.3% solution of sodium carrageenate) and any error was further reduced by subtraction.

It is interesting to note that, as shown in Fig. 5, the vertically and horizontally polarized components for the sodium acetate solution were approximately a Rayleigh distribution. The turbidity was 2.17×10^{-5} cm.$^{-1}$; this value equals that for a 0.1% solution of a protein having a molecular weight of 6000.

Calibration

The turbidity of the calibrating solution should be related to intensity of scatter in the unique manner defined by the Rayleigh equation. Therefore the scatterers should be small, random, and isotropic. The further condition of nonabsorption is imposed because the turbidity is determined spectrophotometrically.

The constancy of $\lambda^4\tau/(n_0\,dn/dc)^2$ for the Ludox suspension (Fig. 7) indicated that no absorption of light occurred in the range of wave lengths from 3800 Å to 6000 Å. The depolarization was small (0.007) showing negligible anisotropy. From the Zimm plot (Fig. 9) I_{45}/I_{135} was 1.06. Thus the envelope was almost symmetrical indicating that the particle size was small enough to give a near approximation to Rayleigh scattering; the error involved was eliminated by the correction mentioned earlier.

Randomness could not be assumed since concentrations as high as 0.074 gm. cm.$^{-3}$ were used. The slope of $(c/I_\theta)_{\theta=0}$ vs. c in Fig. 9 showed that intermolecular interaction occurred. However, from the Zimm plot the limiting relationship between $\left(\dfrac{c}{\tau}\right)_{c=0}$ and $\left(\dfrac{c}{I_\theta}\right)_{\substack{\theta=0\\c=0}}$ was obtained in which the scatterers were completely random. This was the main advantage of the extrapolation method.

It was interesting to compare the extrapolation method of calibration with the more usual technique based on a determination of the 90° intensity.* For each concentration of Ludox, C_{90} was calculated from

[5]
$$\frac{1}{\tau} = C_{90} \times \frac{1}{I_{90}}.$$

*With the 90° method of calibration it is more accurate not to apply a dissymmetry factor since, for a suspension of spheres showing a small dissymmetry, I_{90} is a good approximation to the constant value of I_θ for the ideal system of equivalent turbidity. The earlier apparatus (10) was calibrated by the 90° method and a correction for dissymmetry was made. The discrepancy observed in the calibrating factors for different solutions was probably due in part to this error.

If each calibrating solution obeyed the Rayleigh law, the C_{90} values should be constant and equal to C determined by the extrapolation method. As shown in Fig. 12, C_{90} increased from 162 to 181 cm. when c decreased from 0.074 to 0.018 gm. cm.$^{-3}$. The variation in C_{90} may have been due to inapplicability of the Rayleigh equation at high concentration because of nonrandom-
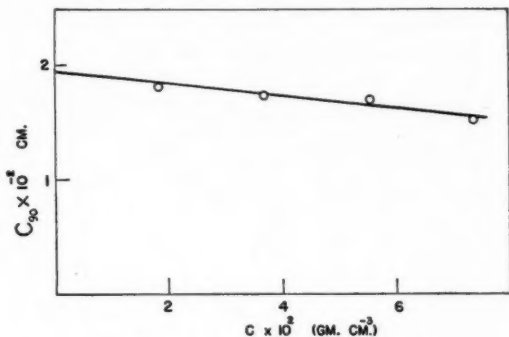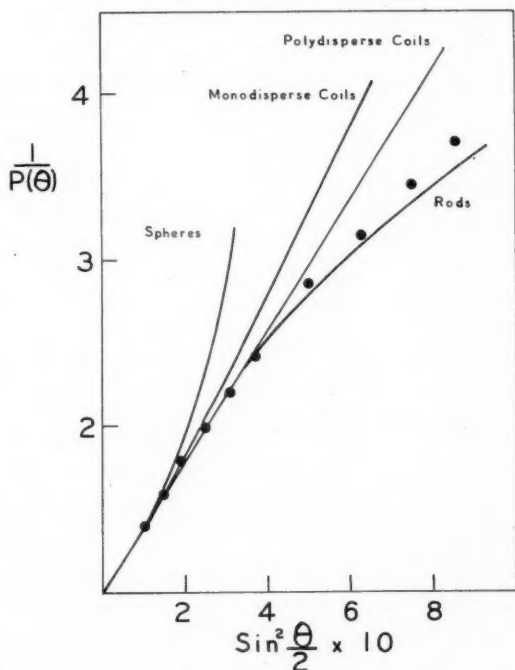
FIG. 12. C_{90} vs. c for Ludox solutions.

FIG. 13. Graph of $1/P(\theta)$ vs. $\sin^2\frac{1}{2}\theta$. The points are for sodium carrageenate derived from the data in Fig. 10. The lines are computed for various shapes from the figures published by Doty and Steiner (7).

ness. In Fig. 12, $(C_{90})_{c=0}$ was 194 cm. in good agreement with the factor 195 cm. obtained by the extrapolation method.

Molecular Size and Shape of Carrageenin

The molecular weight of 1,700,000 was higher than the values of 100,000 to 500,000 reported by Cook, Rose, and Colvin (3) for samples of carrageenin of various degrees of degradation. The higher value may have resulted from a milder extraction of the polysaccharide in the present work.

As noted by Doty and Bunce (5) and by Peterlin (13) the angular distribution of intensity can indicate the shape and characteristic dimension of the molecule. In Fig. 13 the distribution at $c = 0$ is given as $1/P(\theta)$ vs. $\sin^2\frac{1}{2}\theta$. The data are compared with theoretical curves for various shapes computed from the figures published by Doty and Steiner (7).

The distribution was nearest to that for a stiff rod; the length of the rod was 3700 Å. Peterlin (13) has shown that for a chain in which the orientation from link to link is not random, the graph of $1/P(\theta)$ vs. $\sin^2\frac{1}{2}\theta$ approaches that of a stiff rod. The carrageenin molecule is believed to contain one branch point for every 10 hexose residues (4) and therefore a straight chain configuration is unlikely. However an extended branched structure, flexible in its major axis, could give the observed distribution.

It is always possible that the shape of the envelope was distorted by a small concentration of heavy aggregates not removed by centrifuging. Thus more detailed interpretation is postponed until the dispersion in particle size has been determined.

ACKNOWLEDGMENTS

REFERENCES

1. Brice, B. A., Halwer, M., and Speiser, R.　J. Am. Optical Soc. 40: 768.　1950.
2. Butler, M. R.　Biochem. J. (London), 28: 759.　1934.
3. Cook, W. H., Rose, R. C., and Colvin, J. R.　Biochem. et Biophys. Acta, 8: 595. 1952.
4. Dillon, T. and O'Colla, P.　Proc. Roy. Irish Acad. B, 54: 51.　1951.
5. Doty, P. and Bunce, B. H.　J. Am. Chem. Soc. 74: 5029.　1952.
6. Doty, P. and Edsall, J. T.　Advances in Protein Chem. 6: 35.　1951.
7. Doty, P. and Steiner, R. F.　J. Chem. Phys. 18: 1211.　1950.
8. Edsall, J. T., Edelhoch, H., Lontie, R., and Morrison, P. R.　J. Am. Chem. Soc. 72: 4641.　1950.
9. Goring, D. A. I. and Johnson, P.　J. Chem. Soc. 33.　1952.
10. Goring, D. A. I. and Johnson, P.　Trans. Faraday Soc. 48: 367.　1952.
11. Green, A. A.　J. Am. Chem. Soc. 55: 2331.　1933.
12. Oster, G.　J. Polymer Sci. 6: 525.　1952.
13. Peterlin, A.　Nature, 171: 259.　1953.
14. Sheffer, H. and Hyde, J. C.　Can. J. Chem. 30: 817.　1952.
15. Tietze, F. and Neurath, H.　J. Biol. Chem. 194: 1.　1952.
16. Young, E. G. and Rice, F. A. H.　J. Biol. Chem. 164: 35.　1946.
17. Zimm, B. H.　J. Chem. Phys. 16: 1099.　1948.

STUDIES ON THE GLYCOPROTEINS OF THE DOMESTIC FOWL

I. A MODIFICATION OF THE METHOD OF ELSON AND MORGAN FOR THE DETERMINATION OF HEXOSAMINE, AND ITS APPLICABILITY TO TISSUE HYDROLYZATES[1]

By P. A. Anastassiadis and R. H. Common

ABSTRACT

The method of Elson and Morgan for the determination of hexosamine has been studied spectrophotometrically with the object of applying the method to the analysis of tissue hydrolyzates. It has been shown that it is possible by appropriate blanks to correct for interference due to humin. It has been found necessary (a) to increase the strength of the buffer solution in order to stablize the pH and, in extreme cases, first to neutralize the dried hydrolyzate; and (b) to increase the amount of acetylacetone. These modifications also reduce interference by hydroxyproline to a minimum. The use of an appropriate excess of acetylacetone was found to depress the formation of the secondary chromogen during acetylation. A procedure based on these findings is proposed for the direct determination of hexosamine in acid hydrolyzates of tissues.

INTRODUCTION

The colorimetric method of Elson and Morgan (2) for the determination of hexosamine depends on acetylation of the hexosamine with acetylacetone in the presence of sodium carbonate. This treatment is said to yield a pyrrole derivative. On treating the solution with excess ethanolic hydrochloric acid containing p-dimethylaminobenzaldehyde (Ehrlich reagent), the pyrrole derivative yields a red color. Subsequent workers, including Immers and Vaseur (5), have noted that the red solutions display an absorption peak in the region 530 mμ to 535 mμ (vide also Fig. 4 in the present paper). Elson and Morgan reported interference by indole compounds, but stated that these yield a color with Ehrlich reagent also when the acetylation step is omitted. Various workers have sought to apply the Elson and Morgan method directly to tissue hydrolyzates. Some (8) have removed excess hydrochloric acid from hydrolyzates by neutralization with sodium hydroxide; others (3, 6) have preferred drying the hydrolyzate in vacuo over solid sodium hydroxide. Most workers, however, have reported erratic results. Ogston et al. (7) suggested that this might be due in part to loss of acetylacetone by evaporation during acetylation; they, therefore, recommended carrying out the acetylation under reflux. Johnston et al. (6) have preferred to obviate such loss by acetylating in sealed glass tubes at 100° C. The effects of varying the time of acetylation and concentration of the acetylating medium have also been studied. Both Blix (1) and Immers and Vaseur (5) have favored a stronger concentration than that originally recommended by Elson and Morgan (2). Schloss (9) studied the effect of varying pH on the acetylation and demonstrated that at least two chromogens are produced. It has been shown also that sugars and sugar – amino acid mixtures interfere seriously, and this again hampers the application of the method to biological material (4, 5).

The present communication deals with a further attempt to apply the method directly to tissue hydrolyzates. Since the ultimate object of the work has been an investigation of the distribution of mucopolysaccharide material in the tissues of the fowl, most of the studies on tissues reported in the present paper were made using avian oviduct, a tissue likely to contain appreciable amounts of hexosamine.

EXPERIMENTAL

Interference of Colored Material Formed During Hydrolysis with the Colorimetric Determination of Hexosamine

In order to study this interference, samples of freeze-dried avian oviduct were hydrolyzed with 25 times their fresh weight of 4 N hydrochloric acid for hours at 100° C. in sealed glass tubes. The hydrolyzates were light brown in color; small amounts only of insoluble humin were formed. For the purpose of studying interference, this small amount of insoluble humin was not removed. The acid was then removed *in vacuo* over solid sodium hydroxide, and the residue taken up in water. Acetylation and color development were performed as suggested by Johnston *et al.* (6), and the final solution after the color reaction was diluted so that each milliliter corresponded to 10 mgm. fresh tissue.

The light absorption curves of these solutions were measured in a Beckman DU spectrophotometer. The average values for such curves are presented in Fig. 1. The curves did not display any distinct peak around 530 mμ to 535 mμ.
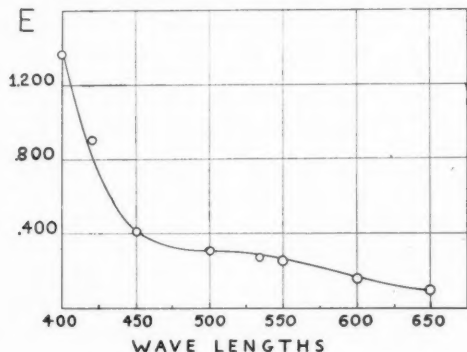
FIG. 1.   Light absorption curve of acetylated tissue hydrolyzates treated with *p*-dimethylaminobenzaldehyde.

Size of sample: 10 mgm. fresh tissue per ml. of final solution.

Acetylating medium: 0.083 M sodium carbonate and 0.66% acetylacetone. (Level of Elson and Morgan and of Johnston *et al.*)

Even in this region, most of the absorbency appeared to be irrelevant and in all probability was due to colored material formed during hydrolysis (e.g. humin) and acetylation.

In order to study the absorbency due to the products of hydrolysis of protein and to reaction of such products of hydrolysis during acetylation, the foregoing analytical procedure was also performed on samples of casein

(Champlain Chemical Company). Casein was chosen as a protein known to be very low in hexosamine. At the same time absorption curves were prepared using a solution of hexosamine only. The results are summarized in Table I.

TABLE I

COMPARISON OF LIGHT ABSORPTION BY TISSUE HYDROLYZATES AND CASEIN HYDROLYZATES WITH THE LIGHT ABSORPTION BY GLUCOSAMINE IN THE COLORIMETRIC METHOD OF ELSON AND MORGAN

	Extinctions (1 cm. cell)				
	450 mμ	500 mμ	535 mμ	550 mμ	600 mμ
a. Tissue hydrolyzates (11 samples)	0.390	0.298	0.269	0.238	0.133
b. Casein hydrolyzates (4 samples) recalculated to same extinction at 450 mμ as tissue hydrolyzates	0.390	0.251	0.185	0.162	0.091
c. Difference of (a) and (b)	0.000	0.047	0.084	0.076	0.042
d. Standard hexosamine solution (extinctions recalculated to basis of 0.084 at 535 mμ)	0.014	0.049	0.084	0.069	0.049

The light absorption curve for hexosamine alone displayed low absorbency in the region 450 mμ (*vide* Fig. 4 for typical hexosamine absorption curve). On the other hand, at 450 mμ the absorbencies of tissue and casein hydrolyzates were falling off from high values in the near ultraviolet. In order to facilitate comparisons, the extinctions for the casein hydrolyzates were recalculated to give the same extinction at 450 mμ as was given by the tissue hydrolyzates, and these values are presented in Table I, line (b). The difference, (c), between (a) and (b) in Table I might then be expected to provide some measure of the hexosamine in the tissue hydrolyzates, i.e. the values obtained by difference as above ought to display some degree of correspondence with the values obtained for hexosamine only. A comparison of the values in line (c) with those in line (d) of Table I shows that the values obtained by difference did in fact correspond to a curve of the same shape as that obtained with hexosamine only. Hence this preliminary work suggested that it might be possible by suitable choice of blanks to arrive at corrections for the irrelevant absorptions.

Accordingly, tissue samples were hydrolyzed and treated as follows, color development being carried out as before:—

A. Acetylated hydrolyzate plus Ehrlich reagent.
Read against complete reagent blank.

B. Acetylated hydrolyzate treated as was A, but with the p-dimethyl-aminobenzaldehyde omitted from the Ehrlich reagent.
Read against blank of water plus acetylacetone.

C. Acetylated hydrolyzate plus Ehrlich reagent.
Read against hydrolyzate similarly treated but with the p-dimethyl-aminobenzaldehyde omitted from the Ehrlich reagent.

D. Water plus acetylacetone plus Ehrlich reagent.

Read against similar solution but with the p-dimethylaminobenzalde-hyde omitted from the Ehrlich reagent.

Standard. Glucosamine solution acetylated and treated with Ehrlich reagent.

Read against complete reagent blank.

The experimental data are summarized in Table II.

TABLE II

COMPARISON OF ESTIMATES OF LIGHT ABSORPTION DUE TO HEXOSAMINE IN PROTEIN HYDROLYZ-ATES ANALYZED BY METHOD OF ELSON AND MORGAN WITH LIGHT ABSORPTION OBTAINED USING GLUCOSAMINE SOLUTIONS

	No. of analyses	Extinction (1 cm. cell)							
		400 mμ	420 mμ	450 mμ	500 mμ	535 mμ	550 mμ	600 mμ	650 mμ
A	11	1.287	0.900	0.390	0.298	0.269	0.238	0.133	0.087
B	11	0.654	0.529	0.397	0.238	0.166	0.146	0.097	0.070
"Hexosamine a"	—	0.633	0.471	–0.007	0.060	0.103	0.088	0.036	0.017
C	11	1.445	0.484	0.018	0.072	0.120	0.113	0.042	0.022
D	11	0.833	0.122	0.006	0.010	0.018	0.019	0.006	0.002
"Hexosamine b"	—	0.622	0.369	0.012	0.062	0.102	0.094	0.036	0.019
Standard hexosamine	12	0.061	0.060	0.016	0.058	0.103	0.081	0.037	0.005
Difference curve from Table I			—	0.000	0.047	0.084	0.076	0.042	—

The difference (A − B) is also reported as "Hexosamine a" and the differ-ence (C − D) as "Hexosamine b".

A satisfactory feature of the results presented in Table II is that the values for "Hexosamine a" agreed rather closely with the values for "Hexosamine b", and that both sets of values agreed closely with the curve for hexosamine. This agreement suggested that no serious interference from side reactions had taken place over the range 450 mμ to 650 mμ, and that the use of the cor-rection blank was justifiable.

The next step was to study whether the use of large samples of hydrolyzate would give proportionate increases in the extinction attributable to hexosamine when the foregoing corrections were applied. It was found that the increases in extinction were not proportional. As will be shown below, this failure to attain proportionality was due to lowering of the pH by the larger samples, the intensity of the color maximum being sensitive to pH.

The Sensitivity of the Acetylation of Hexosamine to pH and the Effect of Dried Hydrolyzates on the pH of the Acetylating Medium

The dependence of the acetylation step upon close control of pH became apparent in the course of experiments undertaken to compare extinctions obtained with casein plus known amounts of hexosamine with the extinctions obtained with hexosamine alone.

The determinations were carried out as described above, the acetylations being performed in a solution 0.083 M as to sodium carbonate and 0.66% as to

acetylacetone, i.e. the levels used by Elson and Morgan (2) and by Johnston et al. (6).

The extinction maxima for hexosamine were calculated from the following relation:—

$$EM = Et_{530} - Eu_{530} - \tfrac{1}{2}[Et_{600} - Eu_{600}] - \tfrac{1}{2}[Et_{450} - Eu_{450}]$$

where EM = extinction maximum for hexosamine

Et = extinction of sample treated with Ehrlich reagent

Eu = extinction of sample not treated with Ehrlich reagent

Subscript numerals = wave length in $m\mu$.

The results are presented in Table III. Recoveries of the added hexosamine were irregular and low. Attempts to improve recoveries by increasing the

TABLE III

RECOVERIES OF HEXOSAMINE HYDROCHLORIDE (H.H.) ADDED TO CASEIN AND WITH USE OF WEAK ACETYLATING MEDIUM (0.083 M SODIUM CARBONATE AND 0.66% ACETYLACETONE)

Material, weight per ml. of final solution	Number of samples	Extinction at 535 mμ, corrected for irrelevant absorptions				Recovery, %
		Casein hydro-lyzate	Casein hydro-lyzate +H.H.	Column 4–3	Standard H.H.	
2 mgm. casein + 20 μgm. H.H.	2	0.055	0.095	0.040	0.309	12.9
2 mgm. casein + 30 μgm. H.H.	2	0.055	0.114	0.059	0.611	9.7
4 mgm. casein + 20 μgm. H.H.	2	0.052	0.076	0.024	0.306	7.8

amounts of acetylacetone were unsuccessful, but suggested the desirability of studying the control of pH, because an increase of the amount of acetylacetone without a simultaneous increase of the carbonate content of the acetylating medium led to lowered "recoveries".

Accordingly, series of determinations of extinction of hexosamine solutions were carried out where constant levels of acetylacetone (0.66% of the acetylating medium) and of total carbonate (0.083 M) were employed, but where the pH was adjusted to various values by hydrochloric acid. The pH was measured before and after acetylation, but the change was always less than 0.02 pH units.

A representative series of results is presented in Fig. 2. Maximal extinction at 530 mμ was realized within the narrow range of pH 9.2 to pH 9.6. The intensity of the color fell off rapidly below pH 9.0 and above pH 10.5. Schloss (9) has also noted that the color maximum is only realized within a narrow range of pH.

In view of the narrow pH range for maximal color development, it was decided to study the possibility of stabilizing the pH during acetylation by using a more strongly buffered medium. The influence of buffer concentration on the Elson and Morgan reaction was examined in the first place with hexosamine alone. The concentrations of sodium carbonate and acetylacetone were increased simultaneously so that the acetylation mixture before reaction
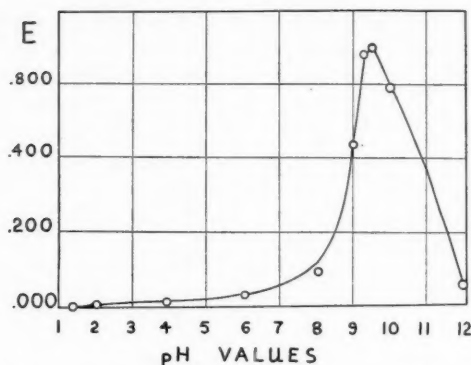
Fig. 2. Effect of the pH during acetylation on the intensity of the color given by the reaction of the acetylated hexosamine with *p*-dimethylaminobenzaldehyde.
Extinction at 530 mμ of 20 μgm. hexosamine hydrochloride per 1 ml. final solution.
Acetylating medium: 0.083 M sodium carbonate plus 0.66% acetylacetone.

had a pH = 9.5 approx. The results are summarized in Fig. 3. The extinction increased as the level of acetylacetone in the reaction mixture increased from 0.66% (the level used by Elson and Morgan) to 1.8%. Between 1.8% and 3% the extinction remained relatively steady, but above 3.0% the extinction began to fall off. Working levels of 1.83% acetylacetone and 0.33 M sodium carbonate were selected provisionally. Similar concentrations were adopted by Immers and Vaseur (5) in order to reduce interference by sugar – amino acid interactions.

Recoveries of hexosamine added to casein or to tissue hydrolyzates and obtained by the use of the more strongly buffered acetylation medium are presented in Tables IV and V. Recoveries were improved quantitatively (comparison of recoveries in Tables III and IV) when the stronger buffer was used. However, reproducibility was found still to be erratic, not only as between
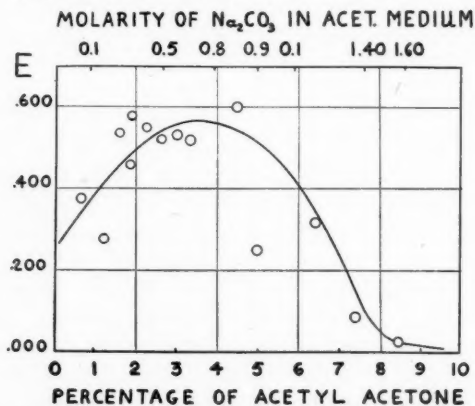
Fig. 3. Effect of acetylacetone buffer concentration on the intensity of the color at the iso-pH 9.50. [The value of the molarity of Na₂CO₂ following 0.9 should read 1.0, not 0.1]

TABLE IV

RECOVERIES OF HEXOSAMINE HYDROCHLORIDE (H.H.) ADDED TO CASEIN AND WITH USE OF STRONG ACETYLATING MEDIUM (0.33 M SODIUM CARBONATE AND 1.83% ACETYLACETONE)

Material, weight per ml. of final solution	Number of samples	Extinction at 535 mμ, corrected for irrelevant absorptions				Recovery, %
		Casein hydro-lyzate	Casein hydro-lyzate +H.H.	Column 4-3	Standard H.H.	
0.43 mgm. casein +13.3 μgm. H.H.	3	0.075	0.583	0.508	0.428	118.7
1 mgm. casein +10 μgm. H.H.	1	0.211	0.544	0.333	0.365	91.2
2 mgm. casein +10 μgm. H.H.	1	0.336	0.715	0.379	0.365	103.8

TABLE V

RECOVERIES OF HEXOSAMINE HYDROCHLORIDE (H.H.) ADDED TO TISSUES AND ACETYLATED IN A STRONG MEDIUM (0.33 M SODIUM CARBONATE AND 1.83% ACETYLACETONE)

Material, weight per ml. of final solution	Number of samples	Extinction at 535 mμ corrected for irrelevant absorptions				Recovery, %
		Tissue hydro-lyzate	Tissue hydro-lyzate +H.H.	Column 4-3	Standard H.H.	
0.45 mgm. tissue +11 μgm. H.H.	4	0.276	0.567	0.291	0.344	84.6
1.00 mgm. tissue +10 μgm. H.H.	3	0.506	0.816	0.310	0.297	104.4
2.00 mgm. tissue +16.7 μgm. H.H.	3	0.849	1.594	0.745	0.548	135.9

different levels of acetylacetone (*vide* Table IV) but also as between different determinations on one and the same sample (results not shown here).

Effect of Acetylacetone Concentration on Relative Development of Chromogens Formed During Acetylation

Schloss (9) has shown that at least two chromogens are formed by the acetylation of hexosamine with acetylacetone, and that the optimal conditions for development of their color maxima differ rather widely. Schloss found that one chromogen gave a color maximum at 530 mμ when the acetylation time was one hour and time of the color reaction was a few minutes; a second chromogen gave a color maximum at 512 mμ when time of acetylation was 20 min. and the time of color reaction was 24 hr. Thus the original Elson and Morgan method appears to have been based principally on the color given by the first chromogen. Schloss suggested that the second chromogen might afford a more satisfactory basis for the determination of hexosamine. It seemed probable, therefore, that modification of the acetylation conditions so as to restrict chromogen development to one chromogen only might contribute to improved reproducibility and proportionality between extinction and amount of hexo-

samine present. Experiments showed that an increase of the acetylacetone concentration led to substantial elimination of formation of the second chromogen.

The results of a series of measurements obtained by increasing the acetyl-acetone concentration *without* changing the buffering capacity of the acetylating medium are given in Table VI. With a color reaction time of one hour, the

TABLE VI

EFFECT OF ACETYLACETONE CONCENTRATION ON THE RELATIVE YIELD OF THE TWO CHROMOGENS
Concentration of sodium carbonate in the acetylating medium:—0.33 M;
hexosamine hydrochloride per ml. final solution:—13.5 μgm.

Acetylacetone concentration in the acetylating medium		Extinction due to hexosamine HCl		Ratio of extinction at 512 mμ to extinction at 530 mμ
%	pH	At 530 mμ after 1 hr. color reaction	At 512 mμ after 24 hr. color reaction	
3.03	9.25	0.714	0.373	0.522
2.27	9.41	0.739	0.440	0.595
1.97	9.51	0.664	0.428	0.645
1.72	9.60	0.740	0.510	0.689
1.30	9.70	0.665	0.516	0.776
1.10	9.81	0.550	0.505	0.918
0.89	9.90	0.561	0.540	0.963
0.49	10.18	0.240	0.374	1.558

extinction at 530 mμ increased steadily with increasing amounts of acetyl-acetone, whereas with a color reaction time of 24 hr. the extinction at 512 mμ decreased as acetylacetone concentration increased.

The effect became clearer on studying the complete absorption curves (*vide* Fig. 4). The lowest pair of curves shows that there was not any displacement of the maximum towards lower wave lengths when the time of color reaction was prolonged to 24 hr. and the concentration of acetylacetone was highest. The intermediate pair of curves showed no appreciable displacement. The highest pair of curves shows that the lowest concentration of acetyl-acetone resulted in a marked displacement of the maximum towards 512 mμ when the color reaction was prolonged for 24 hr. These observations were confirmed in a further series of experiments where an acetylation time of 20 min. was used for the purpose of emphasizing development of color from the second chromogen, and of 1 hr. for the purpose of emphasizing color development from the first chromogen.

Neither series of experiments, however, showed whether the results were due to the change of pH or to the change in acetylacetone concentration *per se.* Accordingly, experiments were made in which the sodium carbonate concentration was further increased, so as to maintain the pH at or slightly above pH 9.5, although the concentration of acetylacetone was also further increased. The results are presented in Table VII. Development of the second chromogen was almost completely absent at pH 9.7 when the medium contained 7.8% acetylacetone. At pH 9.9, and with a relatively high concentration (viz. 5.2%)
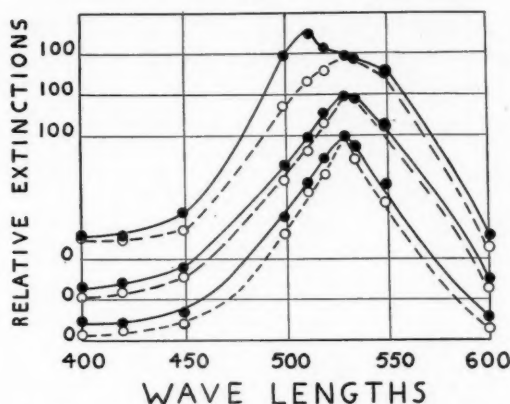
FIG. 4. Effect of acetylacetone concentration on the development of the two chromogens formed during the acetylation of hexosamine. 100 = Extinction at 530 mμ.
Acetylating medium buffered with 0.33 M sodium carbonate.
Lowest pair of curves: acetylacetone concentration 3.03%, pH 9.25.
Intermediate pair of curves: acetylacetone concentration 2.27%, pH 9.41.
Highest pair of curves: acetylacetone concentration 0.89%, pH 9.90.
Broken lines: extinction curves after 1 hr. color reaction.
Full lines: extinction curves after 24 hr. color reaction.

acetylacetone, formation of the second chromogen was almost completely suppressed. This is of interest in view of the fact that formation of the second chromogen is relatively favored at pH 9.9 with low concentrations of acetyl-acetone (9). The results strongly suggest that formation of the second chromogen was depressed by increasing the acetylacetone concentration, and that this effect took place whether the acetylation was performed (*a*) in a solution

TABLE VII

EXTINCTION OF HEXOSAMINE HYDROCHLORIDE (H.H.)ACETYLATED IN 0.5 M SODIUM CARBONATE BUFFER MEDIUM WITH DIFFERENT CONCENTRATIONS OF ACETYLACETONE

Acetyl-acetone concen-tration, %	pH values	Concentration of H.H.μgm./ml. final solution	Extinction values							
			20 min. acetylation				1 hr. acetylation			
			1 hr. color reaction		24 hr. color reaction		1 hr. color reaction		24 hr. color reaction	
			512 mμ	530 mμ	512 mμ	530 mμ	512 mμ	530 mμ	512 mμ	530 mμ
7.83	9.60	6.7	0.262	0.355	0.204	0.263	0.314	0.425	0.572	0.337
		13.4	0.561	0.753	0.428	0.552	0.640	0.850	0.522	0.652
		20.0	0.842	1.150	0.628	0.810	0.944	1.290	0.758	0.961
5.21	9.90	6.7	0.263	0.345	0.246	0.275	0.325	0.430	0.313	0.355
		13.4	0.480	0.615	0.440	0.490	0.642	0.848	0.600	0.698
		20.0	0.815	1.070	0.722	0.822	0.915	1.200	0.842	0.960

buffered with a constant amount of sodium carbonate, and therefore at a lower pH, or (*b*) in a solution where the sodium carbonate was increased simultaneously with the acetylacetone, so as to keep the pH constant. Furthermore, increase of acetylacetone tended to give improved proportionality between extinction and hexosamine concentration. Notwithstanding these improve-

ments, reproducibility was not completely satisfactory. This may be exemplified by the following results for 16 separate determinations of hexosamine alone at each of two levels of concentration.

Hexosamine taken per ml. final solution, μgm.	Average extinction of hexosamine (1 cm. cell) and its standard error	Coefficient of variation
4	0.270 ± 0.010	14.2
10	0.599 ± 0.012	8.2

The average ratio (Extinction of 4 μgm. hexosamine × 2.5)/(Extinction of 10 μgm. hexosamine) for 16 separate determinations was found to be 1.139 ± 0.044 and the percentage of standard deviation on the average ratio (coefficient of variation) was 15.4%.

The foregoing results support the recommendation given below that at least six aliquots from each hydrolysis should be run in order to reduce error from variability.

Interference by Hydroxyproline and its Elimination

Interference by sugar – amino acid interactions has been studied by Immers and Vaseur (5) and by Horowitz *et al* (4). Immers and Vaseur pointed out the possibility of making a rough correction for this interference by heating the hydrolyzate solution with sodium carbonate alone in absence of acetylacetone and then applying the color reaction. Experiments in this laboratory support this view.

Possible interference by hydroxyproline does not seem to have been mentioned in the literature. Preliminary experiments in this laboratory showed that hydroxyproline gave about 2% as much color at 530 mμ in the Elson and Morgan reaction as did an isomolecular amount of hexosamine. Even this small interference might be appreciable when analyzing collagenous tissues of high hydroxyproline content. The absorption curve for hydroxyproline in the reaction was found to exhibit a maximum at 550 mμ; the height of the peak increased with increasing time of the color reaction and at the same time moved towards longer wave lengths (*vide* Fig. 5). Fortunately, increasing the concentration of acetylacetone also reduces the extinction at 550 mμ due to the presence of hydroxyproline. Hence the proposed increase of the concentration of acetylacetone also reduces this interference by four-fifths, i.e. to values at which it is negligible in practice. This is also evident from the results presented in Fig. 5.

Application of (a) Correction Blanks, (b) Increased Buffering Capacity of Acetylation Medium, and (c) Increased Amount of Acetylacetone to Determinations of Hexosamine in Tissue Hydrolyzates

Tissue hydrolyzates (hen's oviduct) were dried over solid sodium hydroxide *in vacuo* and dissolved in water. The pH of the solutions ranged from pH 1.70 to pH 1.80. The effects of varying the size of sample on the pH of the acetyla-
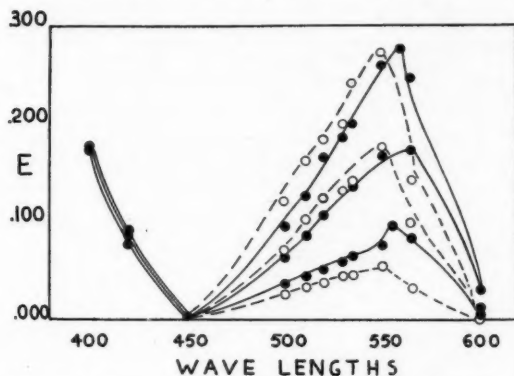
FIG. 5. Effect of acetylacetone concentration and time of color reaction on the extinction curve of the color given by acetylated hydroxyproline plus p-dimethylaminobenzaldehyde.
Hydroxyproline concentration 600 μgm. per ml. final solution.
Acetylating medium buffered with 0.33 M sodium carbonate.
Lower pair of curves: acetylacetone concentration 3.03%.
Intermediate pair of curves: acetylacetone concentration 1.93%.
Highest pair of curves: acetylacetone concentration 0.50%.
Broken lines: extinction curves after 1 hr. color reaction.
Full lines: extinction curves after 24 hr. color reaction.

tion mixture are illustrated in Table VIII. It will be noted that 0.50 M sodium carbonate maintained the pH of the acetylating mixture at a sufficiently steady level for a useful range of size of tissue hydrolyzate samples (to a level as high as 2 mgm. per ml. of acetylating medium).

The corresponding extinctions of the color reaction, corrected for presence of humin as described above ("hexosamine extinction"), are presented in Table IX. Improved consistency of results was attained as the acetylacetone concentration was increased. The proportionality between extinction and amount

TABLE VIII
EFFECT OF THE SIZE OF TISSUE SAMPLES ON THE pH OF ACETYLATION

Size of the samples (dried tissue)		Acetylating medium*			
Wt. per ml. of the acetylating medium	Wt. per ml. of final solution	0.66/0.085/9.50	1.88/0.33/9.60	2.47/0.50/9.62	—/0.50/11.02
		pH after acetylation			
0.0 mgm.	0.00 mgm.	9.31	9.61	9.62	10.69
2.2 "	0.67 "	8.58	9.51	9.59	10.70
4.4 "	1.34 "	8.08	9.39	9.49	10.50
6.6 "	2.10 "	7.70	9.21	9.41	—
Hexosamine HCl 22 μgm.	6.70 μgm.	9.31	9.62	9.63	10.90

*The first number indicates percentage of acetylacetone, the second molarity of sodium carbonate, and the third the pH of the acetylating medium.

TABLE IX

EFFECT OF THE ACETYLATING MEDIUM ON THE PROPORTIONALITY BETWEEN SIZE OF TISSUE
SAMPLES AND HEXOSAMINE EXTINCTION

Size of sample (dried tissues), wt. per ml. of acetylating medium	Acetylating media*			
	0.66/0.085/9.50	1.88/0.33/9.60	2.47/0.50/9.62	—/0.50/11.02
	Hexosamine extinctions			
2.2 mgm. tissue	0.292	0.442	0.479	
4.4 " "	0.267	0.790	0.874	0.014
6.6 " "	0.239	1.070	1.242	0.030
2.2 mgm. tissue +22 μgm. H.H.	0.440	0.638	0.741	0.021
4.4 mgm. tissue +44 μgm. H.H.	0.421	1.248	1.372	0.063
6.6 mgm. tissue +66 μgm. H.H.	0.378	—	1.905	—
22 μgm. hexosamine HCl (H.H.)	0.360	0.354	0.426	0.004

The first number indicates percentage of acetylacetone; the second molarity of sodium carbonate, and the third the pH of the acetylating medium.

of hexosamine, although by no means perfect, was better than that obtained previously, and suggested that the proposed modifications would enable the Elson and Morgan method to give useful results on tissue hydrolyzates.

The average ratio (Extinction of A mgm. tissues $\times$ 2.5)/(Extinction of 2.5 $\times$ A mgm. tissues) for 17 separate determinations on different samples of hen's oviducts was found to be 1.063 $\pm$ 0.059. Consequently, the standard deviation expressed as a percentage of the average ratio was 22.9% as compared with a value of 14.8% for determinations of hexosamine alone. The weight of tissue A taken for the above 17 determinations was of the order of 2 mgm. The close approximation of the average value of ratio of tissues (1.063) to the average value of ratio of hexosamine alone (1.139) suggests that, for the level of tissues hydrolyzates used in these determinations, the effect of the dried hyrdolyzate on the pH of the strongly buffered acetylating medium had little influence on the depression of the extinction.

Relatively large samples must be taken for acetylation whenever the tissue is low in hexosamine. It may then be advisable carefully to adjust the pH of the solution of dried hydrolyzate to pH 9.5 before proceeding with the acetylation. Appropriate experiments showed that, provided this neutralization is carried out slowly and with continual mixing using sodium hydroxide, no appreciable deamination of hexosamine takes place.

SUGGESTED PROCEDURE

The following procedure is recommended on the basis of the work described above.

Reagents

    (a) Hydrochloric acid 4 N.

    (b) Acetylacetone, Eastman Kodak, 4% in 0.75 M sodium carbonate and made immediately before use.

(c) Sodium carbonate, 0.75 M in water.

(d) Ehrlich's reagent:—0.8 gm. p-dimethylaminobenzaldehyde is dissolved in 30 ml. aldehyde-free ethanol and 30 ml. hydrochloric acid, reagent grade, is added. Store in refrigerator in amber bottle with ground glass stopper. The p-dimethylaminobenzaldehyde should be purified by recrystallization from solution in hydrochloric acid by addition of saturated sodium acetate solution. The recrystallization should be performed immediately before the Ehrlich reagent is made up. The Ehrlich reagent should not exhibit any absorbency at 530 mμ.

(e) Alcoholic hydrochloric acid:—30 ml. aldehyde-free ethanol plus 30 ml. hydrochloric acid conc.

(f) Standard hexosamine:—

Stock solution; 1 gm. glucosamine hydrochloride dissolved and made to 100 ml. in water. Store in a 250 ml. flask in the deep freeze.

Working standard; thaw out stock standard and dilute 1 ml. to 100 ml. in water. Replace stock solution in deep freeze.

Procedure

Hydrolyze samples of tissue containing approximately 500 μgm. hexosamine with 5 ml. 4 N hydrochloric acid by heating in sealed pyrex tubes 13 mm. $\times$ 100 mm. for four hours in a boiling water bath. If quantities greater than 0.1 gm. dry matter are necessary in order to have hexosamine in amounts of the order of 500 μgm., then larger quantities of hydrochloric acid should be used in larger tubes.

Open the tubes and remove the acid by evaporation at low pressure over solid sodium hydroxide. Care is necessary to avoid a reduction of the pressure to a level lower than the vapor pressure of the 4 N hydrochloric acid at the maximal prevailing temperature, otherwise the sample may spurt on boiling.

Add 5 ml. of water and dissolve the residue, using a stirring rod. If insoluble humin has been formed, remove this by centrifuging.

For each analysis the determination is made at two levels of concentration of hydrolyzate (H) and two levels of concentration of standard (S) are set up at the same time, together with the necessary blanks (Bl). Set up these sub-samples in fifteen 5-ml. glass stoppered pyrex volumetric flasks according to the following scheme:—

Quantities in ml.	H_1	Bl_1	H_2	Bl_2	H_3	Bl_3	S_1	S_2	Bl_4
No. of flasks set up	3	1	3	1	1	1	2	2	1
Hydrolyzate solution	0.2	0.2	0.5	0.5	0.5	0.5	—	—	—
Hexosamine standard	—	—	—	—	—	—	0.2	0.5	—
Water	0.3	0.3	—	—	—	—	0.3	—	0.5
Acetylacetone in sodium carbonate	1.0	1.0	1.0	1.0	—	—	1.0	1.0	1.0
Sodium carbonate	—	—	—	—	1.0	1.0	—	—	—

Close the flasks firmly by turning the ground glass stoppers and immobilize them with the help of rubber stoppers or otherwise in a wire basket. Immerse the basket in a constant level boiling water bath so arranged that the level of the water is 1 cm. lower than the tops of the volumetric flasks. Leave the flasks in the boiling water bath for one hour. Cool the flasks in ice-water for 10 min. Add 3 ml. aldehyde-free alcohol to each flask and mix well. Warm the flasks in a water bath at 37°C. for three minutes.

Now add 0.5 ml. Ehrlich reagent to flasks H_1, H_2, H_3, S_1, S_2, and Bl_4, and add 0.5 ml. alcoholic hydrochloric acid to flasks Bl_1, Bl_2, Bl_3.

Make up the flasks to 5 ml. by addition of alcohol, mix well, and leave them in a water bath at 37°C. for 60 min.

Read the extinctions at 530 mμ of the sets of solution H_1, H_2, and H_3 against their corresponding blanks.

Correct the values of H_1 and H_2 for any extinction in H_3.

If flask H_3 displays a substantial extinction (i.e. if it be more than one-tenth of the extinction of H_2), this indicates serious interferences by combination of sugars and amino acids and by indole compounds.

The extinctions of the standards are read against Bl_4.

If the extinctions for H_1 and H_2 per microgram display appreciable and systematic divergences, much larger than the average divergence of the standard, then the analysis should be repeated with careful adjustment of the solution of dried hydrolyzate to pH 9.5 by means of 1.0 N sodium hydroxide before proceeding with the subsequent steps.

It is most important that the flasks to be used for correction for sugar and amino acid interference (i.e. H_3 and Bl_3) be not in the slightest degree contaminated with acetylacetone. For this reason the manipulation and heating of these flasks is preferably carried out apart from the other flasks.

In this procedure the acetylation is carried out in stoppered 5 ml. Pyrex flasks and not in sealed glass tubes.

The investigation described in this paper was based on acetylation in sealed glass tubes, but towards the end of the work it was found that the acetylation could equally well be carried out in sufficiently securely stoppered 5 ml. volumetric flasks, which are capable of withstanding the pressure developed. Their use has the advantage of avoiding a troublesome sealing and transfer, while retaining the advantages of acetylating in a closed vessel.

DISCUSSION

The difficulty experienced in obtaining adequate reproducibility of results seems to be due to the following circumstances. Firstly, whereas the amino group of hexosamine is readily split off by heating in alkaline solution (10), the acetylation of hexosamine cannot be carried out except in hot alkaline solution. Secondly, the acetylation of hexosamine does not yield a unique product; not all the products of acetylation are chromogenic and the relationship between the two main chromogenic products varies with the pH, the acetylacetone concentration, and the strength of the buffer, and there are also indications that the acetylation products are not particularly stable.

Thirdly, the acetylation reaction can only be carried out with the free amino group of hexosamine. The amino group must be freed by acid hydrolysis since alkaline hydrolysis would destroy hexosamine. Subsequent neutralization with alkali introduces the danger of localized decomposition of hexosamine. Removal of excess acid from the hydrolyzates by drying is consequently the only alternative, but this also leaves the amino acids as the acid salts. The results of the present study strongly suggest that the first and second of these circumstances may be overcome by increasing the amount of acetylacetone, and the third by increasing the buffering capacity of the acetylating medium.

Where it is necessary to neutralize the solution of dried hydrolyzate, care is necessary in bringing the reaction to pH 9.5 lest there be local decomposition of hexosamine.

The stronger concentrations of acetylacetone and buffer have the further advantage of affording an excess of acetylating agent such that the eventual acetylation of amino and hydroxy groups of amino acids and carbohydrate does not lower the yield of acetylated hexosamine. Acetylation of the samples in the strong acetylacetone buffer medium has been shown also to restrict the hydroxyproline interference and the possibility of correcting for interference by the sugars — amino acid reactions.

Strict standardization of the procedure and a number of replicates in the stage subsequent to hydrolysis are regarded as essential if reasonably reliable results are to be secured.

REFERENCES

1. Blix, G. Acta Chem. Scand. 2: 467–473, 1948. *Abstracted in* Chem. Abstracts, 43: 6269. 1949.
2. Elson, L. A. and Morgan, W. T. Biochem. J. (London), 27: 1824–1828. 1933.
3. Hadidian, Z. and Pirie, N. W. Biochem. J. (London), 42: 260–265. 1948.
4. Horowitz, H. N., Ikawa, M., and Fling, M. Arch. Biochem. 25: 226–229. 1950.
5. Immers, J. and Vaseur, E. Nature, 165: 898–899. 1950.
6. Johnston, J. P., Ogston, A. G., and Stanner, J. E. Analyst, 76: 88–89. 1951.
7. Ogston, A. G. and Staniez, J. E. Biochem. J. (London), 46: 364–376. 1950.
8. Palmer, J. W., Smyth, E. M., and Meyer, K. J. Biol. Chem. 119: 491–500. 1937.
9. Schloss, B. Anal. Chem. 23: 1321–1325. 1951.
10. Tracey, M. V. Biochem. J. (London), 52: 265–267. 1952.

THE USE OF A DIFFUSION CLOUD CHAMBER TO CHARACTERIZE CONDENSATION NUCLEI[1,2]

By Daphne Schiff, H. I. Schiff,[3] and P. R. Gendron

ABSTRACT

The original Langsdorf diffusion cloud chamber has been modified so that the temperature gradient obtained can be controlled. The supersaturations thus produced can be calculated from a diffusion equation. The effectiveness of various inorganic nuclei in causing condensation in this supersaturated vapor has been studied.

INTRODUCTION

It is generally believed that the efficiency of a nucleus in causing condensation of water vapor is governed solely by particle size. However, until now no experimental investigation has been undertaken to ascertain the role played by other physical or chemical properties. By characterizing nuclei according to the degree of supersaturation which they will tolerate, it was hoped that the property responsible for nucleation power would become evident.

A diffusion cloud chamber was used for this work, since it will produce a gradient of supersaturation. The diffusion cloud chamber was first described by Langsdorf (3) who used it to study ion tracks in a medium of air supersaturated with methanol vapor. Schiff and Gendron (5) later modified the apparatus so that the temperature gradient obtained could be regulated. The present paper deals with a similar cloud chamber in which conditions are even more carefully controlled. The temperature gradient can be measured and from a suitable diffusion equation the resulting supersaturations present in the chamber may be calculated.

EXPERIMENTAL

Fig. 1 is a diagram of the cloud chamber used. The vapor was supplied by heating the liquid in the evaporator E at a constant temperature (as indicated by T_3) by means of a nichrome heating element H_2, wound around the outside of the evaporator. This evaporator had a large surface area to ensure that the vapor depleted by cloud formation was continuously renewed. The level in the evaporator was maintained constant by the reservoir R. To prevent spray droplets from entering the chamber the top wall was kept independently hot by means of a ring heater, H_1, soldered to the top of the chamber. Thermocouple T_1 indicated the temperature of the chamber ceiling. To facilitate cleaning and assembly the upper portion of the chamber was made in two sections bolted together and rendered leak-tight with a Teflon gasket.
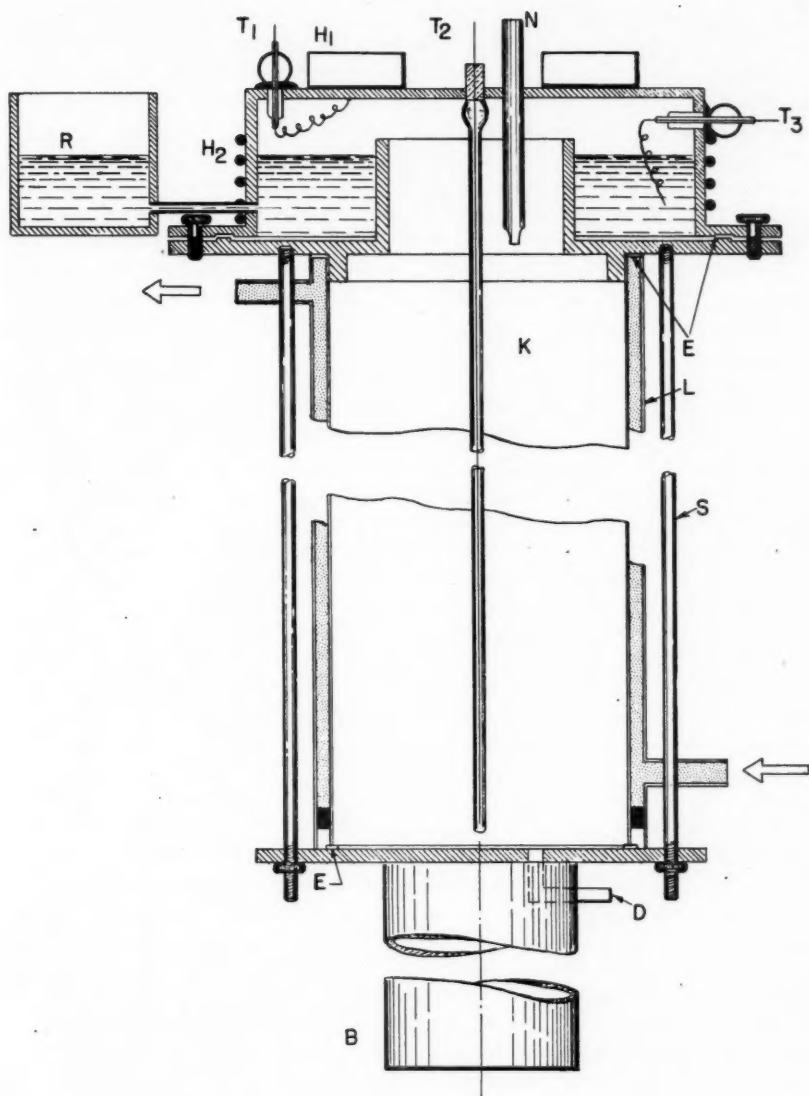
FIG. 1.

The floor of the chamber is cooled by immersing the 6 in. brass rod B in a dewar flask containing a freezing mixture of dry ice and acetone. The condensate may be removed from the floor through the drain tube D. The top and bottom parts of the chamber are made of nickel coated brass and are held together by four threaded rods.

The sensitive portion of the chamber K is constructed of a 10 in. length of Corning electrically conducting glass, 60 mm. in diameter. A temperature gradient was produced along this tubing by allowing a low viscosity, high flash point, water white oil with a constant initial temperature to flow at a constant rate between the glass jacket L and the electrically conducting glass, through which a constant current was passed. The chamber was made airtight by pressing the glass tube between teflon gaskets E, placed below the evaporator and above the cold floor. It was easy to dismantle and clean the chamber so that spurious condensation caused by contamination could be avoided. The outer jacket was separated from the chamber by a rubber gasket. The temperature at any height in the center of the chamber could be measured by raising or lowering thermocouple T_2 in the pyrex tube. N was a brass tube through which nuclei were added to the chamber.

To start an experiment, the oil, heated in a constant temperature bath, entered the jacket at a temperature of about 60°C. The rate of flow of the oil and the current in the chamber wall were regulated so that the oil was about 90° at the top. H_1 and H_2 were controlled so that the water in the evaporator was at 90–95°C. and the ceiling was approximately the same. The brass rod B was immersed about one-half inch in a freezing mixture. These conditions were kept constant for about four hours until a steady state was reached. By this time any foreign particles in the enclosed air which caused condensation had fallen to the floor and the temperature gradient as measured in the center of the chamber by T_2 was constant. Also a cloud caused by the self nucleation of the water vapor is about 2 cm. from the floor. That is, the water vapor produced at the top of the chamber had diffused downwards becoming more and more supersaturated until it reached the critical point at which self nucleation occurred. A gradient of supersaturation was thus present in the chamber.

When these conditions were established, a few cubic centimeters of the nuclei were injected from a heated syringe into the top of the chamber slowly. The tube N was constructed so that the particles were injected horizontally. These particles could not be seen until they caused condensation of the water vapor. When viewed with a parallel beam of light at an angle of 120° this condensation was easily visible especially after the particles had fallen some distance and had time to grow. The upper limit of the cloud was ascertained by gradually moving the light upward until the cloud was no longer evident. Then thermocouple T_2 was moved to this height and the temperature at which condensation apparently initiates was recorded. The number of nuclei injected was sufficient to keep the height of the cloud constant for at least 10 min. It took at least an hour for all the cloud particles to settle out but then more nuclei could be added and a new estimate of the cloud height made.

The salt to be studied was coated evenly on the chromel nuclei coil. This was done by repeatedly dipping the coil in a solution or, in the case of insoluble compounds, a slurry of the salt. The wire was then heated in a flask in a stream of clean dry air and a few cubic centimeters of this air taken with the syringe for nucleating the chamber. An extensive study by electron micro-

graphs of the nuclei produced (1) has shown that their size and monodispersity vary with the current in the coil and the rate of flow of the carrier air. Although the size and monodispersity of the nuclei used did not affect the height of the cloud, they affected its visibility. Consequently, for each salt used various conditions of nuclei production were tried until the one giving the most distinct cloud was found. Then an electron micrograph was made of these nuclei so that their size would be known accurately.

The flux of water vapor in the chamber was measured at the end of each day by melting the ice collected on the floor and allowing it to drain through D into a graduated cylinder.

RESULTS

In Table I are given the results for the six types of nuclei used. The temperature of the cloud top is given in column 3 and the temperature of the water evaporator is given in column 2. The last column shows the supersaturation of water vapor corresponding to these clouds.

TABLE I

Nucleus	Water, °C.	Cloud top, °C.	S	Nucleus	Water, °C.	Cloud top, °C.	S
NaCl	91.5	89	1.09	AgI	92	82.5	1.15
	93.5	92	1.04		92	91	1.06
	93	90	1.08		92	85.5	1.12
	93.5	93	1.02		91.5	85.5	1.12
	92.5	91	1.06		91.5	84	1.14
	93	90.5	1.07		91	83	1.14
	91	89	1.09		93	85	1.13
CaCl₂	91	91	1.06	MnCl₂	91.5	90	1.07
	91.5	91.5	1.05		91.5	91.5	1.05
	91	89	1.09		92	89.5	1.08
	91.5	92	1.04		93.5	92	1.04
CuSO₄	93	87	1.11		93	90	1.07
	92	90	1.08		93	89	1.09
	92	86	1.12		93	90.5	1.07
	91	85	1.13		93.5	91.5	1.05
	91	85	1.13	LiCl	92	93.5	1.01
	94.5	90	1.08		93	93	1.02
	94	87	1.11		93	93.5	1.01
	94	85	1.13		93	93	1.02
	94	85	1.13		93	93.5	1.01
	94	86.5	1.12				
	93.5	89	1.09				
	92	90	1.08				

The flux measured for several eight hour periods averaged 14 ± 0.4 cc./eight hours, that is 1.75×10^{-5} cc./cm.^{2} cross section/sec.

The calculations of the degree of supersaturation existing at cloud formation were made from the following considerations. It is necessary to know both the vapor pressure and the saturation pressure at that point. Direct experimental measurements of the vapor pressure cannot be made, however, without either disturbing the system or involving very elaborate techniques. Langsdorf (3)

treated this problem theoretically for his cloud chamber. By considering the energy flux he obtained an expression for the temperature distribution in the chamber. Upon introducing this distribution into the Kuusinen equations (2) for mass flux he derived an expression for the degree of supersaturation as a function of the distance from the chamber floor. His expression however, includes the energy flux, which is difficult to determine, and the thermal conductivity coefficient of the gas to which no unique value can be given since the coefficient is a complex function of both the temperature and composition. An additional criticism arises out of his neglect of self-nucleation which certainly exists in his chamber and which provides an additional mechanism for mass transfer. In a more recent paper Shutt (6) also used the Kuusinen equations but was primarily concerned with the conditions inside the cloud.

By taking advantage of our ability to determine the temperature distribution experimentally we have been able to obviate the need of knowing the energy flux and thermal conductivity coefficient. If we also assume that we can apply Kuusinen's one dimensional, isothermal, diffusion equations we get:

[1] $$c_2 = w\,D_2 - (k\,D_2/x)$$

[2] where $$\dot{w} = c_1 v_1 + c_2 v_2,$$

c_1 and c_2 are the mass flux and v_1 and v_2 are the partial specific volumes of water vapor and air respectively,

D_2 is the concentration of the air,

k is the diffusion coefficient of water in air,

x is the distance from the bottom of the chamber.

Since there is no flux of air $c_2 = 0$. Substituting [2] into [1] and using the perfect gas law value for D_2 we get:

$$0 = c_1 v_1 p_2 - (k\,dp_2/dx)$$

where p_2 is the partial pressure of air.

But $$v_1 = RT/M_1 p_0$$

where M_1 is the molecular weight of water vapor and p_0 is the pressure in the chamber $= 1$ atm. and then

$$0 = \frac{c_1 RT\,p_2}{M_1 p_0} - k\,\frac{dp_2}{dx}.$$

Now the variation of k with temperature and pressure can be represented as:

$$k = \frac{k_0}{p_0}\frac{(T)^{1+\alpha}}{T_0}$$

where T_0 is the temperature of the self-nucleated cloud at which k equals k_0 and α is a constant.

Making this substitution we get:

$$0 = \frac{c_1 RT\,p_2}{M_1} - k_0\frac{(T)^{1+\alpha}}{T_0}\frac{dp_2}{dx}.$$

Upon rearranging:

$$\frac{dp_2}{p_2} = \frac{c_1 R \ (T_0)^{1+\alpha}}{M_1 k_0} \frac{dx}{T_\alpha}.$$

For water in air α can be taken as unity.

Integrating between the conditions at the self-nucleated cloud ($p_2{}^0$, x_0) and any point in the chamber (p_2, x) then gives:

$$\ln \frac{p_2}{p_2{}^0} = \frac{c_1 R T_0{}^2}{M k_0} \int_{z_0}^{z} \frac{dx}{T}.$$

For our experiments $c_1 = 1.75 \times 10^{-5}$ cc. cm.$^{-2}$ sec.$^{-1}$
$R = 82.06$ cc. atm. mole^{-1} deg.$^{-1}$
$M = 18$ gm. mole^{-1}
$k_0 = 0.219$ cm.^{2} atm. sec.$^{-1}$
$T_0 = 333°$A.

The integral was evaluated by measuring the area under the temperature distribution curve. The equation thus gives a value for the partial pressure of air and hence the partial pressure of water vapor at any point in the chamber. The degree of supersaturation was then obtained as the ratio of the calculated pressure to the saturation pressure of water at that temperature (Fig. 2).
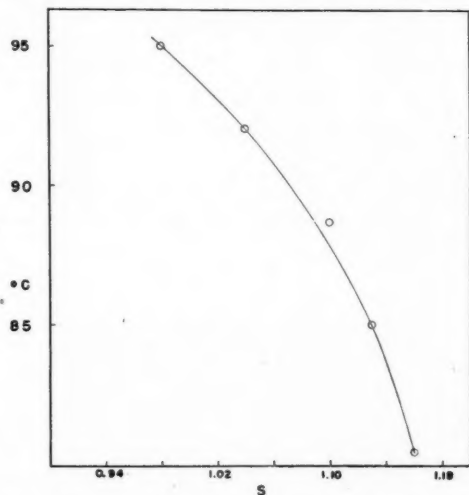
FIG. 2.   Supersaturation ratio as a function of temperature.

In practice, the temperature distribution in the chamber did not vary markedly from experiment to experiment so only one representative curve of $1/T$ (°A) vs. height was used for evaluation of the integral (Fig. 3). The error in S introduced by this simplification was at the most 1%.

The water evaporator was not always at the same temperature. However this temperature does not come into our equation and only affects S in so far
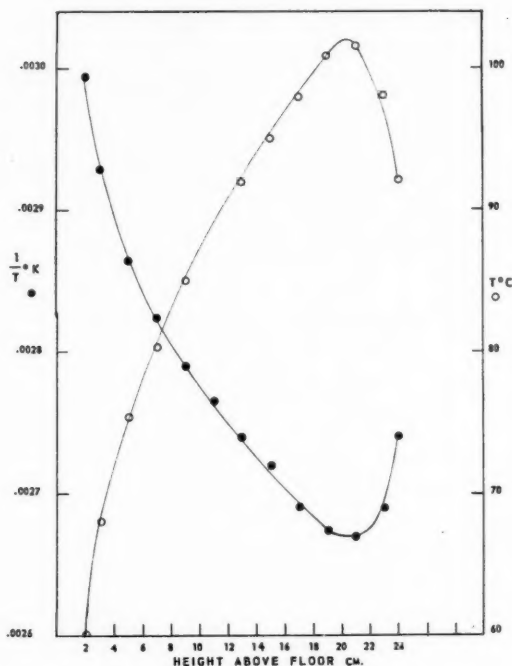
FIG. 3.   Temperature distribution in the chamber.

as it changes T_0. T_0 had an average value of 60°C. and this was used in the calculations. It is estimated that the use of this average value for T_0 may cause S to be in error by 4%. Table II was obtained by averaging the values of S in Table I.

TABLE II

Nucleus	Supersaturation
LiCl	$1.02 \pm .01$
NaCl	$1.06 \pm .02$
CaCl$_2$	$1.06 \pm .02$
MnCl$_2$	$1.07 \pm .01$
CuSO$_4$	$1.11 \pm .02$
AgI	$1.12 \pm .02$

Again, if variations of the flux are taken into account the resulting variation in supersaturation is at the most 2%.

Summarizing, the total maximum variation in the supersaturation values caused by variations in the flux, the temperature of the self-nucleated cloud, and the temperature distribution are 7%. However this error will occur consistently for each salt investigated and therefore will not affect their relative differences.

Fig. 4 is taken from the electron micrographs and shows the variation of size of the NaCl nuclei with temperature of the coil. The magnification used is 40,000. These sizes did not affect the height of the cloud but only its visibility.

Fig. 5 shows comparative size of the six nuclei used. From the magnification (40,000) the minimum size of each nucleus was above 10^{-6} cm.
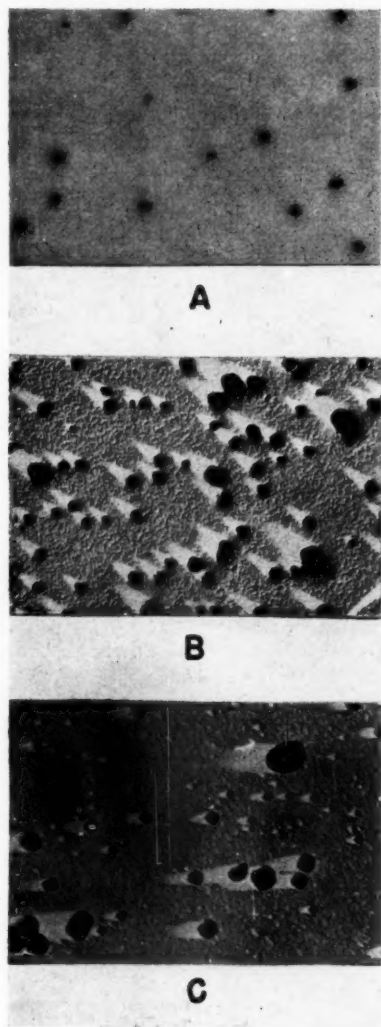
FIG. 4.   NaCl nuclei (40,000 ×).
A. 330°C.   B. 410°C.   C. 470°C.
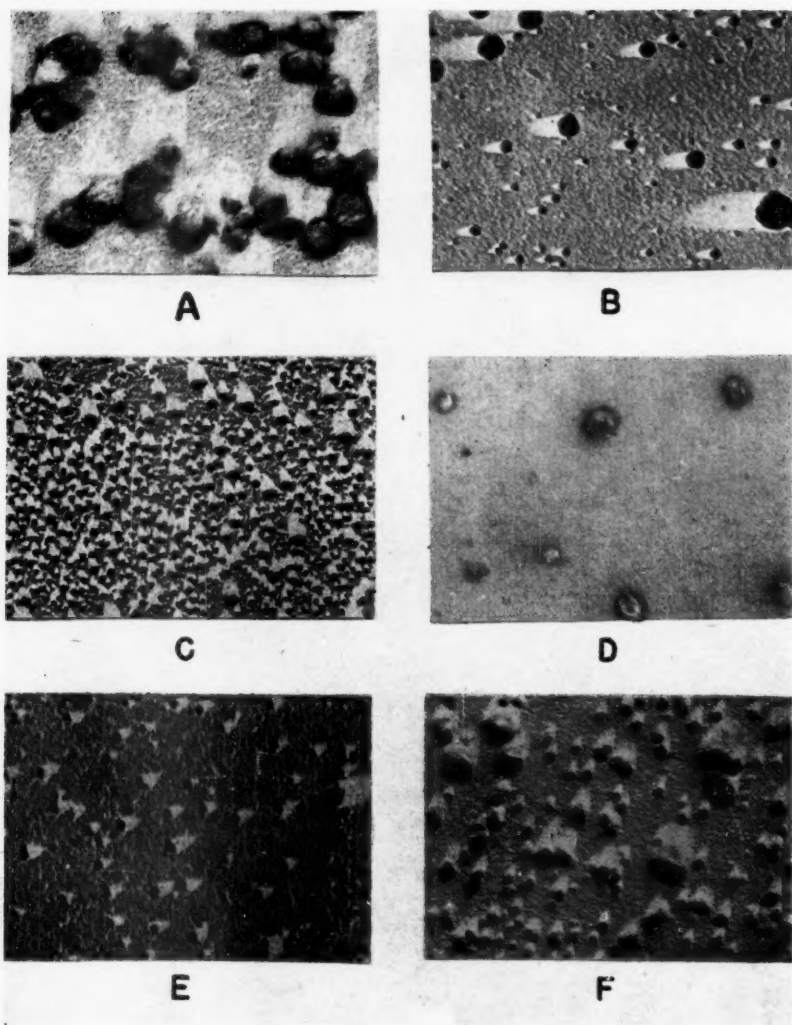
Fig. 5.   Condensation nuclei (40,000 ×).
          A. LiCl   C. CuSO₄   E. AgI
          B. NaCl   D. CaCl₂   F. MnCl₂

DISCUSSION

The results in Table II indicate that there is a total of a 10% difference in the supersaturations that these nuclei will tolerate. The average deviations, shown in the table, which, we feel are a measure of the reducability of these values, are at the most 2%. Therefore the difference in nucleating efficiency is

a real one. This difference was also found, but in a qualitative manner, in the original diffusion cloud chamber (5).

In our experiments, this difference is independent of particle size. According to Pound's theory of heterogeneous nucleation (4), the nucleation rate is not affected by particles greater than 10^{-7} cm. The electron micrographs indicate that the minimum size of particles used in our experiments was of the order of 10^{-6} cm. so we were operating well out of the critical size range. In fact, this was proved since the height of the cloud did not vary for the three very different sizes of NaCl shown in Fig. 4.

This difference in nucleating efficiency does not seem to be explained by any of the more obvious physical and chemical properties of these compounds such as solubility, crystal structure, hygroscopicity, and the like. The only order observed is that the nucleation power varies as the weight of the cation used. This might lead to many properties such as density and charge to mass ratio. A more extensive list of compounds would have to be studied before the property responsible for nucleation efficiency was clearly defined.

As already stated, the assumptions involved in developing and applying our diffusion equation may alter the absolute values that we have given for the supersaturation tolerances of these nuclei. However, we feel that the *differences* indicated are real and significant. The diffusion cloud chamber is an effective way of measuring such differences in nucleating efficiency.

ACKNOWLEDGMENTS

REFERENCES

1. BISSONNETTE, F. M.Sc. Thesis, University of Montreal, Montreal, Que. 1953.
2. KUUSINEN, K. Ann. d. Physik 24: 445. 1935.
3. LANGSDORF, A. Rev. Sci. Instr. 10: 91. 1939.
4. POUND, E. M. Report No. 1. Contract #AF 19(122)-185. U.S. Air Force Material Command.
5. SCHIFF, D. and GENDRON, P. R. J. Colloid Sci. 6: 495. 1951.
6. SHUTT, R. P. Rev. Sci. Instr. 22: 730. 1951.

THE ELECTRODE BEHAVIOR OF COPPER[1]

By A. K. WIEBE AND C. A. WINKLER

ABSTRACT

Potentials ranging from −0.063 volt to +0.044 volt were observed for freshly prepared copper electrodes in sulphuric acid. The potential was dependent upon concentration of the electrolyte, the gas with which the electrolyte was saturated, the nature of the electrode surface, and the intensity of the stirring. The rate of potential decay was influenced by the nature of the dissolved gas and concentration of the electrolyte. When current was passed for the first time across a freshly prepared electrode face, the potential build-up was nonlinear, but subsequent passage of current gave a linear build-up of potential. The apparent capacitance at a copper cathode increased with the time allowed for the potential to decay after current had been passed. It was also dependent upon the current used to measure it, and appeared to be somewhat affected by the area of the cathode. Reliable estimates of the surface areas of the electrodes appeared to be possible from the times required for the electrodes to reach maximum potentials.

INTRODUCTION

Potential change and rates of potential change associated with overvoltage phenomena have often been interpreted in terms of a parallel mesh of resistance and capacitance at or near the electrode surface (cf. 4). Earlier work in this laboratory (8) with copper and silver electrodes appeared to support this view. Two distinct types of potential build-up curves were observed, one of which (the initial curve) was tentatively associated with the deposition of a close-packed monatomic film of hydrogen on the electrode surface and the other with the charging of a condenser.

The results of recent studies with electrodes of mercury (9) and platinum (10) made it desirable to reinvestigate the electrode behavior of copper.

EXPERIMENTAL AND RESULTS

The cathode ray oscilloscope unit and Leeds and Northrup type K potentiometer arrangement used have been described in previous papers from this laboratory (5,7–10). The electrolytic cell and experimental methods were also essentially similar.

The copper electrodes were prepared by cementing turned plugs into a small female ground joint, using a solution of lucite in chloroform as the cement. The female joint was sealed to a larger male joint which fitted into the cell. Experiments showed that electrodes prepared in this way gave the same results as those in which seepage of electrolyte between the metal and glass was prevented with a small pressure of hydrogen gas behind the electrode. The electrode face was ground until a uniform surface was obtained. The electrode cross section was 0.37 cm^2.

All potential measurements were made as before, with reference to a saturated calomel electrode.

As with platinum (10), the potential of a freshly prepared copper electrode immersed in hydrogen saturated electrolyte approached a steady state value (zero potential) from more positive potentials, but at a much slower rate (curve I, Fig. 1A). With platinum, the zero potential in hydrogen saturated
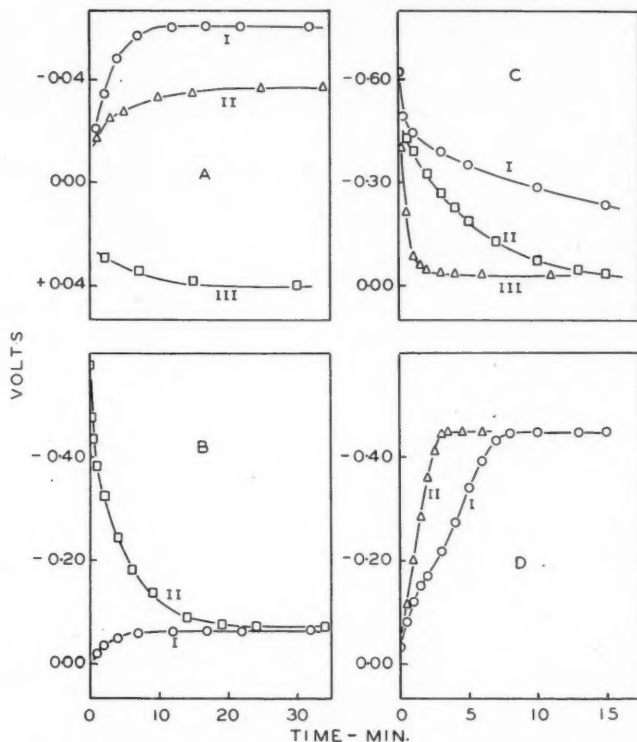

FIG. 1.   A. Potential behavior of a copper cathode in $N/5$ sulphuric acid.
Curve   I: Electrolyte saturated with hydrogen.
Curve   II: Electrolyte saturated with nitrogen.
Curve III: Electrolyte saturated with oxygen.
B. Potential–time curves for a copper cathode in $N/5$ sulphuric acid saturated with hydrogen.
Curve   I: Attainment of steady state (zero) potential.
Curve   II: Potential decay.
C. Potential decay curves for a copper cathode in electrolytes of different acid concentrations, saturated with nitrogen.
Curve   I: $N/1000$ sulphuric acid.
Curve   II: $N/100$ sulphuric acid.
Curve III: $N/5$ sulphuric acid.
D. Potential build-up curves for a copper cathode in $N/5$ sulphuric acid saturated with nitrogen (solutions unstirred).
Curve   I: Initial curve on a fresh copper surface prepared by grinding with No. 225 optical compound and water on glass. The electrode was left in contact with the solution for 130 min. before switching on the current.
Curve   II: Subsequent curve obtained after allowing the potential to decay from the maximum of Curve I.

electrolyte was steady within 30 sec. of immersion, whereas 15 to 20 min. were required with a copper electrode.

In electrolyte saturated with nitrogen, copper, like platinum, gave a negative change of potential which was complete in about 20 min., and attained a steady state potential more positive than in electrolyte saturated with hydrogen (curve II, Fig. 1A). The behavior of copper in oxygen saturated electrolyte was also similar to that of platinum, with the potential changing to a more positive value with time. The steady state potential was considerably more positive than in electrolyte saturated with either nitrogen or hydrogen (curve III, Fig. 1A).

The zero potential of a copper cathode immersed in $N/5$ sulphuric acid saturated with hydrogen was -0.063 volt, while that of a similar electrode immersed in oxygen saturated electrolyte was $+0.04$ volt. In marked contrast, the electrode potentials of mercury (9) and of platinum (10) were changed by about one volt when electrolyte saturated with oxygen replaced a hydrogen saturated electrolyte.

The potentials of copper electrodes varied with (i) the concentration of the electrolyte, (ii) the gas with which the electrolyte was saturated, (iii) the nature of the electrode surface, and (iv) the intensity of stirring (Table I).

TABLE I
ZERO POTENTIALS AT COPPER ELECTRODES

Sol'n.	Sol'n. sat'd with gas	Potential		Cathode surface ground with:
		Sol'n. stirred	Sol'n. unstirred	
$N/5$ H_2SO_4	H_2	-0.063 ± 0.003		No. 225 optical compound and water on glass
As above	N_2	-0.050 ± 0.003	-0.035 ± 0.005	As above
As above	N_2	-0.033 ± 0.003	-0.024 ± 0.004	120 Mesh emery and water on glass
$N/100$ H_2SO_4	N_2		-0.010	No. 225 optical compound and water on glass
$N/1000$ H_2SO_4	N_2	-0.016	-0.010	As above
$4N$ H_2SO_4	N_2		-0.044	As above
$N/5$ H_2SO_4	O_2	$+0.044$	$+0.032$	As above

However, as these potential effects were small, a study of zero potentials would seem to be of little value for the elucidation of the cathode reactions involved.

Potential decay curves were obtained as before (9), by allowing the potential to decay on open circuit after current had been passed until the maximum value of the overvoltage had been reached.

The potential of a copper cathode immersed in $N/5$ sulphuric acid saturated with hydrogen decayed to a value identical with the steady state potential observed under similar conditions (Fig. 1B). This would seem to indicate that the copper surface was in the same condition at the end of the decay process as it was when the zero potential was measured (before flow of current).

Potential decay curves at copper cathodes were influenced by the nature of the dissolved gas and the concentration of the electrolyte. The decay process in $N/5$ sulphuric acid saturated with nitrogen (curve III, Fig. 1C) was complete in much less time than that in hydrogen saturated electrolyte of the same concentration (curve II, Fig. 1B). In nitrogen saturated solution, the potential decayed at a markedly slower rate as the concentration of the electrolyte was reduced (Fig. 1C). The rates of potential decay in $4N$ and $N/5$ sulphuric acid were approximately equal.

As with mercury (9) and platinum (10) two types of potential build-up curves could be distinguished for copper cathodes. An initial potential build-up curve, obtained when current was passed for the first time across the face of a freshly prepared electrode, was nonlinear throughout. On the other hand, when the current was switched on after the potential was allowed to decay on open circuit from the maximum of the initial curve, the subsequent curve was linear and reached the maximum potential in a much shorter period of time.

As with platinum, the initial and subsequent potential build-up curves at a copper cathode immersed in hydrogen saturated electrolyte were essentially identical unless the initial curve was obtained within 15–20 min. after the electrode was introduced into the electrolyte. In electrolyte saturated with nitrogen, the initial curve (curve 1, Fig. 1D) was independent of the time of immersion of the electrode (prior to switching on the current).

This electrode behavior would seem to indicate that on a copper surface, as on platinum, molecular hydrogen in solution is adsorbed as a monatomic film. The electrode behavior of the two metals appears to differ mainly in the rate of dissociation and adsorption of hydrogen, as indicated by the time required for the zero potential to reach a steady value. The dissociation and subsequent adsorption of hydrogen as a monatomic film at a platinum surface appears to be essentially complete in about 30 sec., whereas with copper the process apparently requires 15 to 20 min. (curve 1, Fig. 1A). This comparatively slow rate of dissociation and adsorption at a copper surface would seem to indicate that the forces between hydrogen and copper atoms are weaker than those existing between hydrogen and platinum atoms.

The initial potential build-up curves on cathodes of mercury (9) and of platinum (10) were taken to be associated with the deposition of a monatomic film of hydrogen on the electrode surfaces such that each surface atom of mercury or of platinum accommodated one atom of hydrogen when the potential reached a maximum. The time required for the potential to reach a maximum with a given current was designated t_{max} and it was shown that the application of Faraday's laws to the charge passed in the interval t_{max} may provide a convenient method of measuring the surface areas of platinum electrodes.

The true area of a copper electrode is unknown, so that the number of surface copper atoms cannot be calculated as with mercury (9). Moreover, since stable oxides of indefinite thickness tend to form on a copper surface, the current reversing techniques used with platinum (10) cannot be successfully applied at a copper electrode. As a result, there is no direct evidence that at t_{max} each

surface atom of copper accommodates one atom of hydrogen. However, it is interesting to compare areas obtained by application of Faraday's laws to the quantity of charge passed in the interval t_{max}, with those given by apparent capacitance measurements. The values of t_{max} were taken directly from the initial potential build-up curves. A value of 5.2 Å^2 was calculated for the effective area of a copper atom, on the assumption that the atoms in solid copper are close-packed. The apparent capacitance of copper cathodes was determined from the rate of potential change in the linear sections of the subsequent potential build-up curves. From these measurements the areas of the electrodes could be calculated by the Bowden–Rideal method (3), assuming a capacitance of 20 microcoulombs per volt cm.^{2} at a uniplanar surface (2, 5,6).

Areas of copper cathodes determined by the Bowden–Rideal method decreased with time of immersion in $N/5$ sulphuric acid as shown in Fig. 2. The
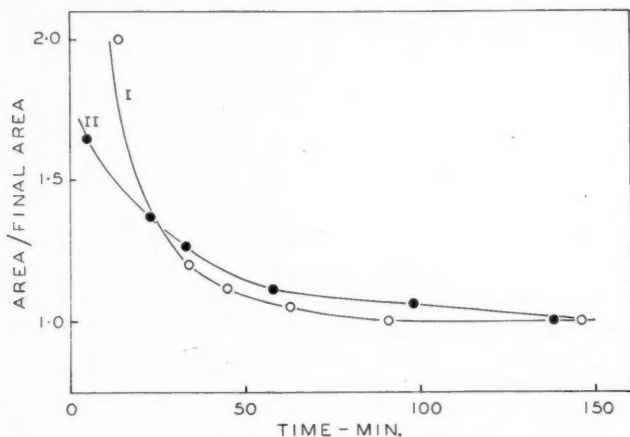
FIG. 2.   Change in area of copper cathodes with time, in $N/5$ sulphuric acid saturated with nitrogen.
          Curve I: Electrode surface ground with 120 mesh emery and water on glass.
          Curve II: Electrode surface ground with No. 225 optical compound and water on glass.

initial change was quite rapid but appeared to be complete in about two hours. Thus, after the copper cathodes had been allowed to age for two to three hours, experiments were made to determine how the apparent capacitance was related to the current used in the measurements and to the period of potential decay prior to the switching on of the current.

The apparent capacitance at a copper cathode immersed in $N/5$ sulphuric acid increased with the time allowed for the potential to decay after current had been passed (Table II). The recorded increase in apparent capacitance corresponds to a decrease in the slope of the subsequent build-up curves. This behavior, although less pronounced, is identical with that observed at a mercury cathode with initial potentials of about −0.61 volt (9). As with mercury

TABLE II

Time of potential decay, min.	Apparent capacitance, microcoulombs/volt
1	310
2	440
3	410
4	440
6	450
8	460
10	470
15	480
20	510
30	520
60	510

Note: The electrode surface was ground with No. 225 optical compound and water on glass. The current used for capacitance measurements was 4.36×10^{-5} amp.

cathodes, the linear rate of potential build-up might be expected to increase with the time allowed for the potential to decay if it were the result of a true capacitance.

The apparent capacitance also varied with the current used to measure it (Fig. 3). The observed minima in the values of apparent capacitance, in
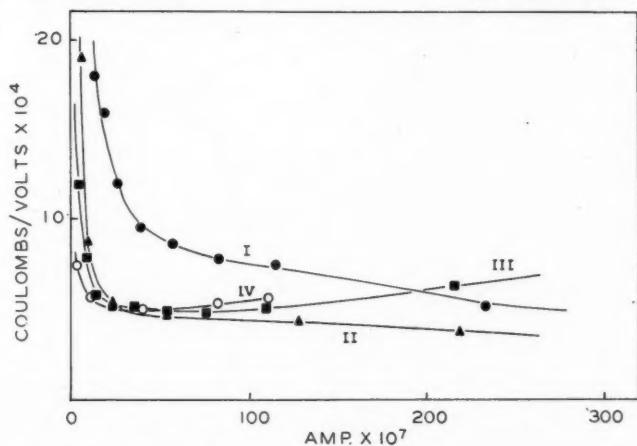
FIG. 3.   Relation between apparent capacitance and current at a copper cathode in nitrogen
saturated electrolytes.
Curve   I: $4\ N$ sulphuric acid.
Curve   II: $N/5$ sulphuric acid.
Curve III: $N/100$ sulphuric acid.
Curve IV: $N/1000$ sulphuric acid.
Electrode surfaces ground with No. 225 optical compound and water on glass.

$N/100$ and $N/1000$ acid, corresponding to maxima in the rates of potential build-up, would seem to indicate that at least two separate reactions occurred, the rates of which were altered to a different extent by change in the current.

Insufficient evidence is available to propose a definite mechanism but possibly adsorption–desorption equilibria are involved (1), together with reactions of the type

$$H^+ (ads) + e \longrightarrow H (ads).$$
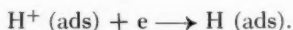
For copper electrodes ground with No. 225 optical compound and allowed to age for two hours in $N/5$ H_2SO_4 saturated with nitrogen before switching on the current, surface areas determined by rate of potential build-up agreed well with those determined from the charge passed during t_{max}, over a range of current of $4.19 \times 10^{-5} - 3.03 \times 10^{-6}$ amp. The values of apparent capacitance presented in the last column of Table III were obtained by dividing the total apparent capacitance by the area estimated from the quantity of charge passed in t_{max} (i.e. by hydrogen packing). When similar experiments were made with electrodes ground with 120 mesh emery and water on glass (Table IV), the areas measured by the two methods differed by a factor of about four. Furthermore, the total apparent capacitance for electrodes ground with 120 mesh emery (Table IV) was only slightly larger than for electrodes ground with No. 225 optical compound (Table III) whereas measurements by hydrogen packing showed the former surfaces to have almost six times the area of the latter.

TABLE III

AREA BY H PACKING COMPARED WITH AREAS BY RATE OF POTENTIAL BUILD-UP

	Area by H packing			Area by rate of potential build-up		Apparent capacitance	
				Area		Microcoulombs/volt	
I, amp. $\times 10^6$	t_{max}, min.	Area, cm.^{2}	$\times$ Planar	Cm.^{2}	Total	Per cm.^{2}
41.9	2.7	22.0	63	23.4	460	21
17.5	6.4	21.8	57	21.2	410	19
17.5	3.0	10.3	60	22.2	430	42
17.4	7.7	26.0	59	21.8	440	17
17.4	6.3	21.4	79	29.2	580	27
17.2	7.3	24.4	56	20.8	420	17
8.05	10.4	16.4	58	21.4	440	27
5.56	9.0	10.0	53	19.6	390	39
5.56	11.0	12.0	60	22.5	440	37
5.55	24.5	26.6	78	28.6	530	22
5.40	19.5	20.8	71	26.3	520	25
3.03	39.0	22.8	60	22.2	460	20
Average		19.5		23.3	460	26

Note: Apparent area of the cathode = 0.37 cm.^{2}
The cathodes were ground with No. 225 optical compound.
Current used for the area measurements by rate of potential build-up = 4.2×10^{-5} amp.

This would indicate that the apparent capacitance is affected to some extent by the area of the cathode but that the relation is by no means linear. Hence, the Bowden–Rideal method would seem to be of doubtful value for the estimation of true surface areas of electrodes.

Since the Bowden–Rideal method did not appear to give a reliable estimate of true surface areas, it seemed possible that the observed change of area with

TABLE IV
AREAS BY HYDROGEN PACKING COMPARED WITH AREAS BY RATE OF POTENTIAL BUILD-UP

Area by hydrogen packing			Area by rate of potential build-up		Apparent capacitance	
			Area		Microcoulombs/volt	
I, amp. $\times 10^5$	t_{max}, min.	Area, cm.^{2}	$\times$ Planar	cm.^{2}	Total	Per cm.^{2}
19.8	2.5	96	47	17	350	3.7
11.2	5.8	130	80	30	600	4.7
7.18	8.1	114	86	32	650	5.7
4.20	15.8	130	69	26	510	3.9
2.34	19	87	76	28	570	6.5
1.25	47	114	75	28	560	4.8
Average		112		27	540	4.9

Note: Apparent area of cathode = 0.37 cm.^{2}
The cathodes were ground with 120 mesh emery and water on glass.
Current used for area measurements by rate of potential build-up = 4×10^{-5} amp.

time of aging (Fig. 2) might also be apparent rather than real. To examine this possibility, the current was switched on 10 min. after the introduction of the copper electrodes into nitrogen saturated electrolyte. Areas by the Bowden–Rideal method were then determined immediately following t_{max}. For electrodes ground with No. 225 optical compound (Table V), the Bowden–Rideal

TABLE V
AREAS BY H PACKING COMPARED WITH AREAS BY RATE OF POTENTIAL BUILD-UP ($N/5$ H_2SO_4)

Area by H packing			Area by rate of potential build-up		Apparent capacitance	
			Area		Microcoulombs/volt	
I, amp. $\times 10^5$	t_{max}, min.	Area, cm.^{2}	$\times$ Planar	Cm.^{2}	Total	Per cm.^{2}
4.38	3.7	31.7	87	32	640	20
2.55	6.2	30.8	93	34	690	22
2.55	5.9	29.0	98	36	730	25
2.55	6.4	31.8	88	33	650	20
Average		30.9		34	680	22

Note: Current used for areas by rate of potential build-up = 2.55×10^{-5} amp.
The cathode surfaces were ground with No. 225 optical compound and water on glass.

measurements were made 20 min. after the time of immersion. For electrodes ground with 120 mesh emery (Table VI), 25–28 min. elapsed between the time the electrodes were introduced into the electrolyte and the time the Bowden–Rideal measurements were made. The values of apparent capacitance per cm.^{2} obtained for electrodes that were aged for 10 min. (Tables V and VI) were in reasonable agreement with those obtained on similarly prepared electrodes that had been allowed to age for two hours (Tables III and IV). The apparent capacitance per cm.^{2} appeared to increase slightly as the area decreased. Hence, the Bowden–Rideal method appears to give a fairly reliable indication of changes of area, although the magnitude of the change may be somewhat underestimated.

TABLE VI

AREAS BY H PACKING COMPARED WITH AREAS BY RATE OF POTENTIAL BUILD-UP ($N/5$ H_2SO_4)

Area by H packing			Area by rate of potential build-up		Apparent capacitance	
			Area		Microcoulombs/volt	
I, amp. $\times 10^4$	t_{max}, min.	Area, cm.^{2}	$\times$ Planar	Cm.^{2}	Total	Per cm.^{2};
1.14	11.0	244	123	46	910	3.9
1.14	11.4	254	121	45	900	3.5
1.15	8.7	195	95	35	700	3.6
1.15	11.7	262	122	45	900	3.5
Average		236		43	850	3.6

Note: Current used for areas by rate of potential build-up = 1.14 $\times$ 10⁻⁴ amp.
The cathode surfaces were ground with 120 mesh emery and water on glass.

Cathode areas determined from the charge passed in time t_{max} in $N/100$ sulphuric acid (Table VII) and in $N/5$ sulphuric acid (Table V) were in good agreement. It would seem, therefore, that this quantity of charge is independent of the acid concentration and is a function of the cathode surface area only. Thus the application of Faraday's laws to the product It_{max} appears to provide a method of determining the true surface area of an electrode.

TABLE VII

AREAS BY H PACKING IN $N/100$ H_2SO_4 SAT'D. WITH N_2

Time of aging in sol'n., min.	Current, amp. $\times 10^5$	t_{max}, min.	Area, cm.^{2}
45	2.63	5.9	30
10	2.68	6.5	34
10	2.73	7.0	37
10	2.70	6.6	34
10	2.70	6.2	33
Average			33.5

Note: The cathodes were prepared by grinding with No. 225 optical compound and water on a glass surface.

REFERENCES

1. BAERG, A. and WINKLER, C. A.   Can. J. Chem. 31: 521.   1953.
2. BOWDEN, F. P. and GREW, K. E. W.   Discussions Faraday Soc. 1: 91.   1947.
3. BOWDEN, F. P. and RIDEAL, E. K.   Proc. Roy. Soc. (London), A, 120: 59.   1928.
4. HICKLING, A.   Quarterly Revs. (London), 3: 95.   1949.
5. HUTCHEON, A. T. and WINKLER, C. A.   Can. J. Research, B. 27: 353.   1949.
6. PROSKURNIN, M. and FRUMKIN, A.   Trans. Faraday Soc. 31: 110.   1935.
7. ROXBURGH, J. M. and WINKLER, C. A.   Can. J. Research, B, 28: 383.   1950.
8. WIEBE, A. K., GAUVIN, W., and WINKLER, C. A.   Can. J. Chem. 29: 301.   1951.
9. WIEBE, A. K. and WINKLER, C. A.   Can. J. Chem. 31: 306.   1953.
10. WIEBE, A. K. and WINKLER, C. A.   Can. J. Chem. 31: 665.   1953.

THE REACTION OF CYANOGEN BROMIDE WITH THE SODIUM SALTS OF CARBOXYLIC ACIDS

I. THE REACTION OF CYANOGEN BROMIDE WITH SODIUM BENZOATE[1]

By D. E. Douglas, Jean Eccles,[2] and Anne E. Almond[3]

ABSTRACT

The main products of the reaction of cyanogen bromide with sodium benzoate at 250° to 300°C. are carbon dioxide, benzonitrile, and sodium bromide. Tracer studies have shown that the carbon of the carbon dioxide is derived almost entirely from the cyanogen bromide.

Zappi and Bouso (3) have investigated the reaction of cyanogen chloride with the sodium salts of several carboxylic acids, both aliphatic and aromatic, at 200 to 300°C. to form the corresponding nitriles:

$$RCOONa + ClCN \rightarrow NaCl + CO_2 + RCN.$$
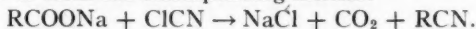
Since good yields of nitriles were obtained they proposed this reaction as a method of synthesis of these compounds.

The corresponding reaction of cyanogen bromide with the sodium salts of various carboxylic acids is being investigated because of its potential application in the synthesis of labelled molecules. By the use of carbon-14-labelled reactants, it has been found that, depending on the carboxylic acid employed, the carbon of the product carbon dioxide may be derived from the carboxyl group or the cyanogen bromide. With sodium acetate and propionate the carbon dioxide carbon originates in the carboxyl group (1).

In this paper, the reaction of cyanogen bromide with sodium benzoate is described. Data are presented to show that in this case the carbon dioxide is derived almost entirely from the cyanogen bromide. Observations on the reaction of cyanogen bromide with the sodium salts of homologous fatty acids will be published later.

EXPERIMENTAL

Cyanogen bromide-C^{14} was prepared from aqueous sodium cyanide-C^{14} and bromine by a vacuum-line modification of the method Graf *et al.* (2). Benzoic acid-carboxyl-C^{14} was prepared by carbonation of phenylmagnesium bromide by standard vacuum-line procedure.

Reaction of Cyanogen Bromide with Sodium Benzoate

The apparatus (Fig. 1) consisted of a tube for the cyanogen bromide connected by a ground joint and stopcock to a U tube with a by-pass between its arms. The U tube was joined through a glass spiral to a vacuum manifold with an attached mercury manometer. A weighed sample (one to two millimoles)
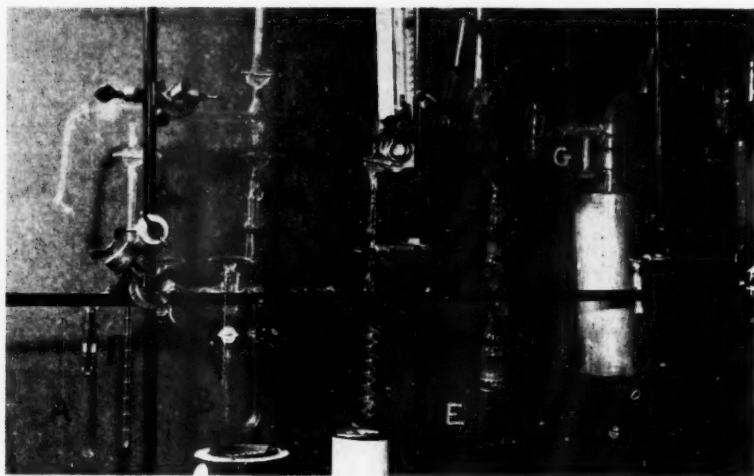
Fig. 1.   Vacuum reaction apparatus.

A—Tube to contain cyanogen bromide.
B—U tube.

C—Electrically heated Wood's metal bath.
D—Spiral trap.

E—Carbon dioxide absorption trap.
F—Graduated tube for estimating yield of nitrile.
M—Mercury manometer.
G—Vacuum manifold.

of sodium benzoate was suspended on a mixture of 0.5 gm. each of powdered glass and ignited fuller's earth by evaporating an aqueous slurry of the three materials with stirring. The dried powder was confined to the bottom of the U tube with two plugs of glass wool. The bottom of the U tube was immersed in an electrically heated Wood's metal bath controlled by a Powerstat transformer.

An excess of cyanogen bromide was weighed into the glass stoppered tube, which was then connected to the apparatus, and surrounded by a bath of liquid nitrogen. The whole train was evacuated by means of a fore-pump and mercury diffusion pump. The glass spiral was cooled with liquid nitrogen, and the cyanogen bromide was allowed to volatilize and pass slowly through the contents of the U tube. The process took between 10 and 20 min. No significant pressure change occurred during reaction. The contents of the spiral were later fractionated. Carbon dioxide and unreacted cyanogen bromide were frozen into a trap containing excess 0.5 N sodium hydroxide (or, 0.2 N sodium sulphide saturated with barium hydroxide when active cyanogen bromide was reactant). The nitrile was condensed with a liquid nitrogen bath into a graduated tube. A varying amount of white or brownish crystalline material condensed in the cooler part of the exit of the U tube during the reaction.

Treatment of the Reaction Products

Barium hydroxide solution in a slight excess was added to the heated solution of carbonate in sodium hydroxide from the carbon dioxide trap, and the precipitate of barium carbonate was filtered, dried, weighed, and counted.

For final activity determination, a sample of the carbonate was decomposed with lactic acid in a vacuum transfer apparatus, and the carbon dioxide reconverted to barium carbonate. A small amount of activity was usually found in the filtrate from the first precipitation.

When the carbon dioxide was absorbed in 0.2 M sodium sulphide saturated with barium hydroxide, the barium carbonate was filtered off, weighed, and counted and a sample was decomposed with lactic acid and reconverted to barium carbonate as described above. An aliquot of the original filtrate, which contained the excess cyanogen bromide-C^{14} from the reaction as thiocyanate, was counted.

The nitrile was washed from the graduated tube with ethanol into a bomb tube and hydrolyzed by heating with an excess of 2 N sodium hydroxide. Benzoic acid was recovered by acidification of an aqueous solution of the sodium salt with hydrochloric acid, and recrystallized from hot water. M.p. 121.5°–122°C.; mixed m.p. with authentic benzoic acid 121–122°C.

To confirm the identification of the reaction product as benzonitrile. in experiment No. 5 the nitrile was divided into two portions one of which was hydrolyzed as described above. The other portion in dry ether was added to an excess of lithium aluminum hydride in the same solvent. After a few hours, the mixture was decomposed with water, and a few drops of saturated sodium hydroxide added. The solution was extracted continuously with ether. A crystalline hydrochloride formed on passing hydrogen chloride into the dried ether extract. The chloride content of this compound, determined by titration with mercuric nitrate was in good agreement with the theoretical value for benzylamine hydrochloride. Calc. for $C_7H_{10}N$: Cl, 24.7; found: Cl, 24.55.

A sample of the crystalline material from the exit side of the U tube of the train (experiment No. 5) was recrystallized from toluene-cyclohexane. After sublimation, it melted at 100–104°C. By hydrolysis with concentrated hydrochloric acid at 220°–230°C., benzoic acid was obtained, with a specific activity of 249 counts/min./mgm. as compared with 253 counts/min./mgm. for the starting material. This material probably consisted of benzamide and kyaphenin, the trimer of benzonitrile, both of which yield benzoic acid under the hydrolytic conditions employed. Kyaphenin has been identified among the products of the reaction of cyanogen chloride with sodium benzoate (3).

Sodium bromide was identified in the nonvolatile residue remaining in the bottom of the U tube by extracting the fuller's earth and glass with water and precipitating bromide as the silver salt with silver nitrate.

Counting was carried out with a helium flow-type windowless counter and an Atomic Instrument Model 101-A scaler. Corrections were applied for self-absorption in the various substances counted.

RESULTS AND DISCUSSION

Data for several typical experiments are given in Tables I and II. Owing to the difficulty of obtaining reproducible conditions in heterogeneous pyrolytic reactions of this type, there is considerable variation in the experimental results. Specific activity data show conclusively that the carbon of the product

TABLE I

DATA FOR THE REACTION OF SODIUM BENZOATE-CARBOXYL-C^{14} WITH CYANOGEN BROMIDE

Expt. no.	Temp., °C.	Specific activity of original C_6H_5COOH, counts/min./mmole	Specific activity C_6H_5COOH from hydrolyzate, counts/min./mmole	Specific activity of $BaCO_3$, counts/min./mmole	Per cent yield of $BaCO_3$	Per cent yield of C_6H_5
2	280–285	160,600	139,900	4240	72.2	47
4	296–297	39,500	28,500	356	68.1	35
5	284–288	30,450	32,170*	197	77.8	34

*Benzylamine hydrochloride obtained by reduction of the benzonitrile had a specific activity of 25,400 counts/min./mmole.

TABLE II

DATA FOR THE REACTION OF SODIUM BENZOATE WITH CYANOGEN BROMIDE-C^{14}

Expt. no.	Temp., °C.	Specific activity of CNBr, counts/min./mmole	Specific activity of $BaCO_3$, counts/min./mmole	Per cent yield of $BaCO_3$	Specific activity of C_6H_5-COOH from hydrolyzate, counts/min./mmole	Per cent activity recovered as $BaCO_3$ and thiocynate	Per cent yield of C_6H_5CN
6	289	314,600	267,900	86.7	9,060	74.5	20
7	296–302	314,600	272,800	49.5	490	50.1	46

carbon dioxide is derived almost entirely from the cyanogen bromide. The presence of low activity in the barium carbonate when carboxyl-labelled sodium benzoate is a reactant (Table I) and in the recovered benzoic acid when cyanogen bromide alone is labelled (Table II) reveals that a small fraction of the carbon dioxide has its origin in the carboxyl group, probably through a simultaneously occurring alternate reaction yielding the same end products. The occurrence of a side reaction of this type also could explain the trend towards lower activity per millimole of the active product as compared with the active reactant, but this difference may include errors in correcting for self-absorption in the different materials counted.

In the absence of sufficient data on the reaction of cyanogen bromide with sodium salts of other carboxylic acids, a mechanism explaining the derivation of the carbon dioxide from cyanogen bromide is difficult to postulate. At the temperatures employed (250–300°C.), cyanogen bromide should be largely dissociated into CN radicals and bromine atoms, and it is almost certain that a free radical heterogeneous reaction takes place.

Further work should make possible a correlation of the genesis of the carbon dioxide with the general behavior of the carboxyl group of various acids, and thus suggest a mechanism for this reaction.

ACKNOWLEDGMENT

REFERENCES

1. DOUGLAS, D. E. and ALMOND, A. E. Unpublished results.
2. GRAF, S., ENGELMAN, M., GILLESPIE, H. B., and GRAF, A. M. Cancer Research, 11, 338–392. 1951.
3. ZAPPI, E. and BOUSO, O. Ann. asoc. quim. Argentina, 35: 137–148. 1947.

FATTY ACIDS OF FILBERT OIL AND NASTURTIUM SEED OIL[1]

By Mary J. Chisholm and C. Y. Hopkins

ABSTRACT

The fatty acids of a sample of filbert kernel oil (*Corylus avellana* L.) were examined by means of ester distillation and low-temperature crystallization. Stearic, oleic, and linoleic acids were identified but eicosenoic acid was not found although earlier workers had reported its presence in considerable amount in samples from the same species. Nasturtium seed oil (*Tropaeolum majus* L. var.), examined in the same way, was found to contain about 20% of 11-eicosenoic acid. An estimate is given of the fatty acid composition of the two oils.

INTRODUCTION

During a study of the occurrence of *n*-eicosenoic acid in plants, attention was drawn to a report of its presence in substantial amount in the oil of filbert kernels (4). This genus (*Corylus*) had been studied by earlier workers without yielding evidence of the presence of eicosenoic acid (3, 9). Accordingly, a new examination of filbert oil was undertaken to determine its value as a source of the acid in question.

The occurrence of eicosenoic acid in the seed oils of several Cruciferae species has been well established (2, 7, 8). The chief component acid in these oils is docosenoic (erucic) acid and it is evident that oils containing a fairly large proportion of docosenoic acid are likely to contain an appreciable amount of eicosenoic acid as well. An apparent exception was nasturtium seed oil (*Tropaeolum*), which was reported to consist almost entirely of oleic and erucic acids (6), with small amounts of saturated and linoleic acids. It seemed desirable, therefore, to reinvestigate this oil also.

EXPERIMENTAL

A. *Filbert Oil*

Filberts were purchased locally and were identified as *Corylus avellana* L. var. Barcelona. The kernels (555 gm.) were crushed and extracted by petroleum ether, yielding 354 gm. of bright yellow oil (63.7%). The oil had iodine value 88.1, saponification value 192.3, and unsaponifiable matter 0.5%. It was converted to methyl esters directly by methanol with dry hydrogen chloride as catalyst. A portion of the mixed methyl esters (308 gm.) was distilled through a heated column, packed with metal rings, at a pressure of 0.1 mm. or less. The distillation data are given in Table I.

The course of the distillation showed that the fatty acids were predominantly 18 carbons in chain length. There was no evidence of a C_{20} fraction. The residue was so small as to signify a very small content of C_{20} or C_{22} acids, if any.

A portion of fraction 1 was saponified. The mixed acids had equivalent weight 274, indicating a mixture of C_{16} and C_{18} acids. The remainder of the fraction (19 gm.) was fractionally crystallized from acetone, giving 11 gm. of solid esters, iodine value 3.6; 5.0 gm. of liquid esters, iodine value 85; and 2.3 gm. of liquid esters, iodine value 117.

TABLE I
DISTILLATION OF METHYL ESTERS OF FILBERT OIL

Fraction	Vapor temp., °C. (approx.)	Wt. of fraction, gm.	Iodine value	$n_D^{25°}$
1	100–110	24.0	42.2	1.4448
2	110–115	24.2	85.5	1.4505
3	115–116	38.4	93.0	1.4515
4	116–117	14.4	98.9	1.4515
5	117–119	41.6	98.8	1.4515
6	119–120	43.4	93.9	1.4515
7	120–121	42.5	92.7	1.4515
8	121–123	40.2	91.3	1.4512
9	123–126	12.7	89.2	1.4510
	(Residue distilled from smaller flask)			
10	124–126	16.4	83.5	1.4508
11	(a)	1.5	—	1.4520
Residue	—	6.0	—	—

(a) *Portion obtained by rinsing the column packing.*

Fraction 4 was fractionally crystallized from acetone. The most soluble portion (1.7 gm.) was subjected to the hexabromide test but failed to show evidence of linolenic acid.

On crystallizing 20 gm. of fraction 5 from acetone at −35°, methyl stearate, m.p. 37.5–38° was obtained (0.3 gm.). Succeeding lots of crystals had iodine value 86.7 (13 gm.), 87.7 (2.7 gm.), and 153 (2.7 gm.). The methyl stearate, after hydrolysis and crystallization, gave stearic acid, m.p. 69.2–69.8°, equivalent weight 284.2.

The portion of iodine value 86.7 was oxidized by alkaline permanganate giving dihydroxystearic acid, m.p. 129.5–130.5° alone and mixed with an authentic sample. Thus this fraction contained ordinary oleic acid.

The portion of iodine value 153 was oxidized similarly and the solid product was recrystallized from ethyl acetate. It melted at 172–173°, alone and mixed with an authentic sample of tetrahydroxystearic acid, proving the presence of linoleic acid in the fraction.

The mixed acids of fraction 9 had equivalent weight 284. Crystallization of 9 gm. of the esters from acetone gave 1.7 gm. of iodine value 68, 4.0 gm. of iodine value 86, and 1.9 gm. of iodine value 112.5. The middle portion gave dihydroxystearic acid on oxidation, m.p. 129–130°, alone and mixed with an authentic sample.

Fraction 11 (1.5 gm.) also gave dihydroxystearic acid on oxidation.

The residue was saponified and separated from the unsaponifiable matter. The mixed acids had iodine value 72.7, equivalent weight 297. Upon recrystallizing from acetone, the products were as follows:

Temp. of cryst'n., °C.	Yield, gm.	M.p., °C.	Equivalent weight	Iodine value
0°	0.35	64–66°	333	
−40°	0.4	Semisolid	296	
Filtrate	3.1	—	293	85.3

The solid portion apparently contains one or more of the higher saturated acids (C > 18). The portion from the filtrate was oxidized by permanganate, freed of saturated acids, and crystallized from ethyl acetate and finally from ethanol, giving dihydroxystearic acid, m.p. 129–130°. Its identity was confirmed by mixed melting point. Accordingly, the major unsaturated acid, even in the residue, is oleic acid. Oleic was identified as the principal acid also in fractions 5, 9, and 11.

Estimation of the fatty acid composition from the above data gives the following percentages: palmitic 3, stearic 4, higher saturated acids, less than 1, oleic 82, linoleic 11.

B. *Nasturtium Oil*

Nasturtium seed (4.5 kilograms) was purchased from a local seed house. It was the ordinary dwarf garden variety, stated by Bailey (1) to be a variety of *Tropaeolum majus* L.

The husks were removed by abrading and aspirating. The seeds were ground further and extracted by petroleum ether, yielding 318 gm. of oil (7%). The oil had iodine value 74.5, saponification value 158.7, and unsaponifiable matter 3.8%. A portion of the mixed methyl esters (270 gm.) was distilled *in vacuo* as described in part A for filbert oil (Table II).

TABLE II
DISTILLATION OF METHYL ESTERS OF NASTURTIUM SEED OIL

Fraction	Vapor temp., °C. (approx.)		Wt. of fraction, (gm.)	Iodine value	$n_D^{25°}$
1	(a)	115–140	8.1	65.2	1.4510
2		140–142	10.0	100.7	1.4529
3		142–151	4.8	93.9	1.4529
4		151–157	4.7	80.0	1.4530
5		157–158	12.8	78.2	1.4529
6		158–160	15.0	78.2	1.4529
7		160–162	9.7	76.8	1.4529
8	(b)	137–140	9.6	76.9	1.4530
9		140–148	13.1	75.1	1.4537
10		148	12.4	72.5	1.4540
11		148–149	40.0	71.9	1.4541
12		149–153	53.5	71.9	1.4540
13		153–155	29.4	71.8	1.4541
14		155–160	7.4	70.9	1.4541
15		160–162	4.4	70.0	1.4542
16	(c)		5.0	62.2	1.4598
Residue			30.0		

(a) *Pressure 0.5 mm.*
(b) *Pressure reduced to 0.1 mm.*
(c) *Portion obtained by rinsing the column packing.*

By plotting iodine number and refractive index of each fraction against the aggregate amount of distillate (Fig. 1), it is seen that there is a small proportion of C_{18} esters (chiefly in fractions 1–4), a larger amount of C_{20} esters (fractions 5–8) and a still larger amount of C_{22} esters. The peak in the iodine value curve occurs in the fractions containing methyl linoleate.
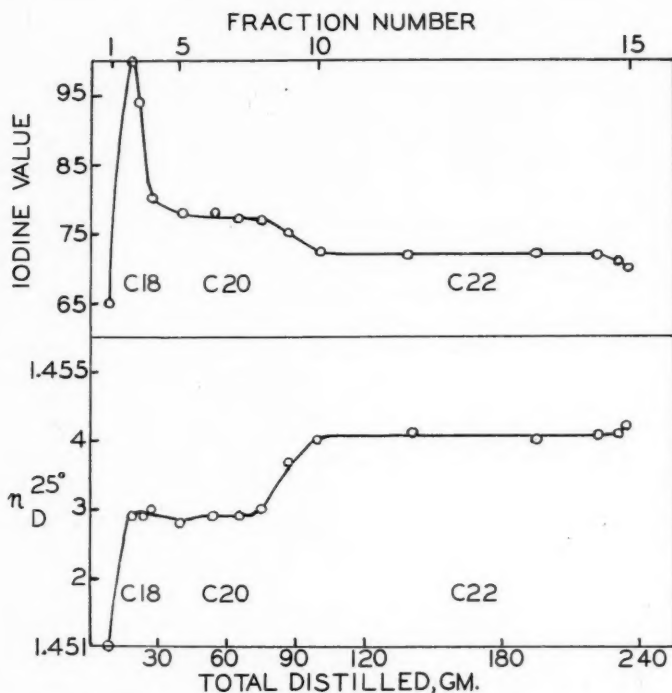
FIG. 1.   Methyl esters of nasturtium seed oil. Constants of successive fractions plotted against aggregate weight of distillate.

Fraction 1 was crystallized from acetone and gave 2.2 gm. of solid esters, iodine value 5.7. Upon hydrolysis to acids, this portion had m.p. 62–64° and equivalent weight 269, indicating that it is a mixture of palmitic and stearic acids.

Fraction 2 gave 0.3 gm. of solid acids and the remainder evidently consisted of oleic and linoleic acids.

Fraction 6 (iodine value 78.2) was fractionally crystallized from acetone, with the following results:

Fraction	Temp. of cryst'n., °C.	Yield, gm.	Iodine value
6–1	−24°	0.5	74.5
6–2	−30°	6.7	77.8
6–3	−45°	5.3	77.7
6–4	Filtrate	1.2	80.3

Fractions 6–2 and 6–3 were united and hydrolyzed. The resulting acid was crystallized from acetone at −12° and gave 5.0 gm. of eicosenoic acid, m.p. 24°. (Found, iodine value 81.5, equivalent weight 310.6; $C_{20}H_{38}O_2$ requires

iodine value 81.7, equivalent weight 310.5). Hydroxylation of the acid by permanganate gave dihydroxyeicosanoic acid, m.p. 129–130°. The melting point was unchanged on admixture with 11,12-dihydroxyeicosanoic acid prepared from jojoba oil.

Cleavage of the dihydroxy acid by periodate gave nonaldehyde (the semi-carbazone melted at 99–100°) and 10-aldehydodecanoic acid (the semicar-bazone melted at 160–161°). The melting points were unchanged in admixture with authentic samples. The original acid is therefore 11-eicosenoic acid.

Fraction 16 and the residue were combined, saponified, and freed from unsaponifiable matter. The acids (22 gm.) had iodine value 70.7 (erucic acid has iodine value 75.0). They were crystallized from acetone as follows:

Fraction	Temp. of cryst'n., °C.	Yield, gm.	Iodine value
R1	−10°	10.6	69.5
R2	−37°	4.3	72.2
R3	−50°	2.1	73.4
R4	Filtrate	2.5	69.8

Fraction R1 melted at 30–35° and its equivalent weight was 341. It was recrystallized as follows:

Fraction	Temp. of cryst'n., °C.	Yield, gm.	Properties
R11	4°	1.0	M.p. 69–71°
R12	−50°	8.0	I.V. 72.2
R13	Filtrate	0.3	Equiv. wt. 337 I.V. 71.1

R11 is evidently a saturated acid. After recrystallization, the equivalent weight was 360, indicating a mixture of behenic and lignoceric acids. R12 is almost pure docosenoic acid. Upon hydroxylation by permanganate it gave 13,14-dihydroxybehenic acid, m.p. 130–130.5° alone and mixed with an authentic sample, showing that the original material was erucic acid.

Tetracosenoic acid may be present in R2 and R3 but if so, it constitutes a relatively small proportion of the total acids.

From these data, the percentage composition of the fatty acids is estimated as follows: palmitic 0.5, stearic 0.5, higher saturated acids 1, oleic 7, linoleic 2, eicosenoic 20, erucic 69.

DISCUSSION

A. Filbert oil from nuts grown in Europe was examined by Schuette and Chang in 1933 (9) and by Bertram in 1936 (3). These authors carried out a partial separation of the fatty acids but neither found positive evidence of acids higher than C_{18}. Fang and Bullis (1949) extracted the oil from two varieties of North American filberts and carried out a distillation of the methyl esters (4). Calculations based on the saponification number of the ester frac-

tions indicated that the fatty acids of the Barcelona variety contained 21% of eicosenoic acid and that the Du Chilly variety contained 15%. However, the acid was not isolated or identified.

The present study of oil from a sample of the Barcelona variety has not confirmed the presence of eicosenoic acid, although the procedure is the same as that employed for the identification of the acid in other oils, in amounts from 3 to 20% of the total acids (7, 8). It is judged, therefore, that the content of eicosenoic acid in our sample is much less than the 21% reported by Fang and Bullis. The possibility of as much as one per cent of this acid being present is not entirely excluded but it is believed that any greater amount would have been detected.

The oil therefore contains the common octadecoic acids, oleic and linoleic, which constitute about 93% of the total; the remaining acids are saturated. These values agree well with those of Bertram (3) and show that the oil is similar to olive oil in composition.

B. Nasturtium seed oil (*Tropaeolum majus*) was shown by Gadamer to have erucic acid as its chief constituent (5) and this was confirmed in 1926 by Sudborough and co-workers (10). A further study of oil from a dwarf variety was made in 1938 by Hilditch and Meara (6), including the distillation of a small volume of the methyl esters. They reported the presence of oleic, linoleic, and erucic acids, along with a little saturated acid, and placed the content of erucic acid at 81.8% of the total fatty acids.

In the present work, also with the dwarf variety, 11-eicosenoic acid has been isolated and identified. The amount is substantial and is estimated as 20% of the total acids. This is the highest proportion yet found in a glyceride oil from plants. However, the low content of oil in the seed (7%) renders it unsuitable as a source of eicosenoic acid in quantity. The content of oleic and erucic acids in the oil is calculated to be somewhat lower than that reported by Hilditch and Meara but the total content of monoenoic acids is about the same (96%). Saturated acids are present in unusually small amount.

Although the main purpose of this work was to determine the presence or absence of eicosenoic acid in the two oils, the data are sufficient for a rough estimate of the fatty acid compositions, excluding some minor components which may be present in amounts less than one per cent (Table III).

TABLE III
ESTIMATED FATTY ACID COMPOSITION

Acid	Per cent of total fatty acids	
	Filbert oil	Nasturtium seed oil
Palmitic	3	0.5
Stearic	4	0.5
Higher saturated acids	<1	1
Oleic	82	7
Eicosenoic		20
Erucic		69
Linoleic	11	2

REFERENCES

1. BAILEY, L. H.   Manual of cultivated plants. The Macmillan Company, New York. 1949.
     p. 602.
2. BALIGA, M. N. and HILDITCH, T. P.   J. Soc. Chem. Ind. (London), 67: 258.   1948.
3. BERTRAM, S. H.   Öle, Fette, Wachse, Seife, Kosmetik. No. 14: 2.   1936.
4. FANG, S. C. and BULLIS, D. E.   J. Am. Oil Chemists' Soc. 26: 512.   1949.
5. GADAMER, J.   Arch. Pharm. 237: 471.   1899.
6. HILDITCH, T. P. and MEARA, M. L.   J. Chem. Soc. 1608.   1938.
7. HOPKINS, C. Y.   Can. J. Research, B, 24: 211.   1946.
8. HOPKINS, C. Y.   Unpublished work.
9. SCHUETTE, H. A. and CHANG, C. Y.   J. Am. Chem. Soc. 55: 3333.   1933.
10. SUDBOROUGH, J. J., WATSON, H. E., and AYYAR, P. R.   J. Indian Inst. Sci. A, 9: 65.   1926.

DINITRO-ISOBUTYLPHENOL AND DINITRO-ISOAMYLPHENOL[1]

By G. G. S. Dutton, T. I. Briggs,[2] and E. Merler

ABSTRACT

An unequivocal synthesis of ortho- and para-isobutyl and isoamyl phenols by the method of Klages is described. The resulting phenols were nitrated and characterized as their amine salts. The nitrophenols were prepared as part of a program for testing potential herbicides.

INTRODUCTION

It has been generally accepted that branching an alkyl side chain in a phenol lowers its phenol coefficient (6, 17). This has also proved to be true in the case of dinitroalkyl phenols as far as their herbicidal activity is concerned, with the exception of the ortho-(sec-butyl) isomer (5). In view of this apparent anomaly we desired to extend our previous work on the synthesis of dinitro-n-alkyl phenols (8) to isomers containing sec-alkyl groups.

Since rearrangements are known to occur when alcohols are condensed with an aromatic nucleus (10) we have preferred to use a modification of the method of Klages (11) whereby the desired alkyl group may be built up by reacting a methoxycarbonyl compound with a Grignard reagent. The resulting alcohol may then be dehydrated, the substituted ethylene hydrogenated, and on replacing the methoxyl group by hydroxyl the required phenol is obtained.

Since the isobutyl and isoamyl compounds were also needed for testing as herbicides the preparation of these phenols by the method of Klages and their subsequent nitration is described in this paper. A later communication will extend the use of this method to the preparation of sec-amyl and sec-hexyl phenols.

EXPERIMENTAL*

2-Isobutylphenol

(a) *2-Methyl-1-(o-methoxyphenyl)-1-propanol*

A Grignard reagent was prepared in the usual manner in an atmosphere of nitrogen using magnesium (37 gm., 1.5 moles), ether (250 cc.), and isopropyl bromide (196 gm., 1.5 moles) dissolved in ether (350 cc.). The reagent thus formed was treated with 2-methoxybenzaldehyde (102 gm., 0.75 mole) in ether (100 cc.) at 0°C. with vigorous stirring and then refluxed for five hours. The cooled solution was then slowly poured onto cracked ice and ammonium chloride. The ether layer was separated, washed, and dried. A small portion was evaporated and gave a negative test with 2,4-dinitrophenylhydrazine. Removal of the solvent from the main portion and distillation of the residual

oil under vacuum gave 2-methyl-1-(o-methoxyphenyl)-1-propanol (98 gm., 73%) as a clear liquid boiling at 96°C. (1 mm.) and having n_D^{19}, 1.5235. Literature (12) b.p. 133°C. (14 mm.) and n_D^{16}, 1.524. Anal. calc. for $C_{11}H_{16}O_2$: OCH_3, 17.21%. Found: OCH_3, 17.30%. *Phenylurethane* m.p. 148°C. (from carbon tetrachloride). Anal. calc. for $C_{17}H_{21}NO_3$: N, 4.68; OCH_3, 10.36%. Found: N, 4.76; OCH_3, 10.30%.

(b) *2-Methyl-1-(o-methoxyphenyl)-1-propene*

2-Methyl-1-(o-methoxyphenyl)-1-propanol (5 gm.) was refluxed three hours with 20% sulphuric acid. There was thus obtained 2-methyl-1-(o-methoxy phenyl)-1-propene (4 gm., 90%) having b.p. 77°C. (1 mm.) and n_D^{23}, 1.5435. Literature (12) b.p. 109°C. (14 mm.) and n_D^{17}, 1.545. Anal. calc. for $C_{11}H_{14}O$: OCH_3, 19.13%. Found: OCH_3, 17.88, 17.80%. *Nitrosylchloride*, obtained in poor yield, m.p. 129°C. Anal. calc. for $C_{11}H_{14}ClNO_2$: N, 6.61%. Found: N, 7.00%.

(c) *2-Isobutylanisole*

2-Methyl-1-(o-methoxyphenyl)-1-propene (21 gm.) was dissolved in 95% ethanol (25 cc.) and Raney nickel catalyst added (about 5 gm.). Hydrogenation was carried out in an Aminco microhydrogenator at 500 p.s.i. and 50°C. yielding 2-isobutylanisole (16 gm., 76%) boiling at 55°C. (0.1 mm.) and having n_D^{25}, 1.5005. Anal. calc. for $C_{11}H_{16}O$: OCH_3 18.89%. Found: OCH_3, 18.40, 18.45%. The *sulphonamide* m.p. 103°C. was prepared by treating the alkylanisole with chlorosulphonic acid and ammonia according to the method of Huntress and Carten (9). Anal. calc. for $C_{17}H_{17}NO_3S$: N, 5.76, OCH_3, 12.75%. Found: N, 5.71; OCH_3, 12.62%.

(d) *2-Isobutylphenol*

2-Isobutylanisole (9 gm.) was treated with pyridine hydrobromide (11.5 gm.) and glacial acetic acid (1.3 cc.) and the whole heated under reflux at 200°C. for five hours (15). The cooled mixture was then poured into water and the organic layer extracted with ether. The ether layer was successively washed with dilute hydrochloric acid, sodium bicarbonate solution, and water. After drying and removal of solvent, fractionation gave a quantitative yield of 2-isobutylphenol b.p. 51°C. (0.01 mm.) and n_D^{24}, 1.5171. Literature (3) b.p. 86°C. (6 mm.). Anal. calc. for $C_{10}H_{14}O$: C, 80.0; H, 9.33%. Found: C, 79.8, 79.7; H, 9.24, 9.24%. *3,5-Dinitrobenzoate* m.p. 84°C. Anal. calc. for $C_{17}H_{16}N_2O_6$: N, 8.13%. Found: N, 8.09%.

4-Isobutylphenol

(a) *2-Methyl-1-(p-methoxyphenyl)-1-propanol*

By means of a Grignard reaction from isopropyl bromide and anisaldehyde there was obtained 2-methyl-1-(p-methoxyphenyl)-1-propanol (67%) boiling at 103°C. (1 mm.) and having n_D^{24}, 1.5215. Literature (16) b.p. 157°C. (21 mm.) and n_D^{20}, 1.5210. Anal. calc. for $C_{11}H_{16}O_2$: OCH_3, 17.21%. Found OCH_3, 17.40%. Phenylurethane m.p. 77°C. Literature (16) 82°C. Anal. calc. for $C_{17}H_{21}NO_3$: N, 4.68%. Found: N, 4.58%.

(b) 2-Methyl-1-(p-methoxyphenyl)-1-propene

The above carbinol was dehydrated with 20% sulphuric acid to give 2-methyl-1-(p-methoxyphenyl)-1-propene (71%) boiling at 81°C. (1 mm.) and having n_D^{24}, 1.5470. Literature (4) b.p. 118°C. (15 mm.). Anal. calc. for $C_{11}H_{14}O$: OCH_3, 19.13%. Found: OCH_3, 18.90%. The *nitrosyl chloride*, obtained in very poor yield, melted at 133°C. Anal. calc. for $C_{11}H_{14}ClNO_2$: N, 6.61%. Found: N, 6.53%.

(c) 4-Isobutylanisole

The ethylene obtained above was hydrogenated as before, yielding 4-isobutylanisole (72%) boiling at 68°C. (1 mm.) and having n_D^{25}, 1.4975. Literature (4) b.p. 123°C. (15 mm.) and n_D^{24}, 1.4980 (19). Anal. calc. for $C_{11}H_{16}O$: OCH_3, 18.89%. Found: OCH_3, 18.95, 18.88%. The *sulphonamide* m.p. 205°C., was obtained in poor yield. Anal. calc. for $C_{11}H_{17}NO_3S$: N, 5.76%. Found: N, 5.65%.

(d) 4-Isobutylphenol

4-Isobutylanisole was demethylated as before yielding 4-isobutylphenol (75%) boiling at 60°C. (0.01 mm.). On standing the oil solidified and recrystallization gave the pure phenol m.p. 52°C. This phenol was first reported as a solid by Barber and Haslewood (2) who give m.p. 51–52°C. Anal. calc. for $C_{10}H_{14}O$: C, 80.0; H, 9.33%. Found: C, 80.0, 80.1; H, 9.36, 9.30%. *3,5-Dinitrobenzoate* m.p. 131°C. Anal. calc. for $C_{17}H_{16}N_2O_6$: N, 8.13%. Found: N, 8.08%.

2-Isoamylphenol

(a) 3-Methyl-1-(o-methoxyphenyl)-1-butanol

By means of a Grignard reaction from isobutyl bromide and 2-methoxybenzaldehyde there was obtained the impure alcohol as a tan colored solid. Recrystallization from benzene – petroleum ether (30–60°C.) yielded pure *3-methyl-1-(o-methoxyphenyl)-1-butanol* as a white solid melting at 73°C. (Attempted distillation caused dehydration.) Anal. calc. for $C_{12}H_{18}O_2$: OCH_3, 15.97%. Found: OCH_3, 15.93, 15.95%. *Phenylurethane* m.p. 107°C. Anal. calc. for $C_{18}H_{23}NO_3$: N, 4.47; OCH_3, 9.90%. Found: N, 4.40; OCH_3, 9.90, 9.92%.

(b) 3-Methyl-1-(o-methoxyphenyl)-1-butene

The above carbinol was dehydrated as before yielding *3-methyl-1-(o-methoxyphenyl)-1-butene* (50%) boiling at 82°C. (1 mm.) and having n_D^{18}, 1.5430. Anal. calc. for $C_{12}H_{16}O$: OCH_3, 17.60%. Found: OCH_3, 17.51, 17.55%. The *nitrosyl chloride*, obtained in good yield, melted at 137°C. Anal. calc. for $C_{12}H_{16}ClNO_2$: N, 5.79; OCH_3, 12.80%. Found: N, 5.98; OCH_3, 12.67, 12.61%.

(c) 2-Isoamylanisole

The ethylene obtained above was hydrogenated giving a quantitative yield of 2-isoamylanisole b.p. 75°C. (0.5 mm.) and n_D^{18}, 1.4995. Anal. calc. for $C_{12}H_{18}O$: OCH_3, 17.40%. Found: OCH_3, 17.43, 17.37%. *Sulphonamide* m.p. 113°C. Anal. calc. for $C_{12}H_{19}NO_3S$: N, 5.44; OCH_3, 12.06%. Found: N, 5.37; OCH_3, 12.09%.

TABLE I
DINITRO-ISOBUTYL AND ISOAMYL PHENOLS AND THEIR AMINE SALTS*

Dinitrophenol	B.p., °C. (0.1 mm.)	Yield, %	Piperidine salt				Morpholine salt				Cyclohexylamine salts			
			Formula	M.p., °C.	Nitrogen, % Calc.	Found	Formula	M.p., °C.	Nitrogen, % Calc.	Found	Formula	M.p., °C.	Nitrogen, % Calc.	Found
4,6-Dinitro-2-isobutyl**	130	66	$C_{15}H_{23}N_3O_5$	187	12.92	12.84	$C_{14}H_{21}N_3O_6$	168	12.84	12.84	$C_{16}H_{23}N_3O_5$	193	12.38	12.39
2,6-Dinitro-4-isobutyl	143	55	$C_{15}H_{23}N_3O_5$	189	12.92	12.95	$C_{14}H_{21}N_3O_6$	164	12.84	12.82	$C_{16}H_{23}N_3O_5$	192	12.38	12.32
4,6-Dinitro-2-isoamyl**	140	57	$C_{16}H_{25}N_3O_5$	167	12.39	12.48	$C_{15}H_{23}N_3O_6$	190	12.32	12.29	$C_{17}H_{27}N_3O_5$	188	11.90	11.89
2,6-Dinitro-4-isoamyl	154	55	$C_{16}H_{25}N_3O_5$	176	12.39	12.47	$C_{15}H_{23}N_3O_6$	169	12.32	12.32	$C_{17}H_{27}N_3O_5$	185	11.90	11.94

*All the salts are yellow, orange, or red.
**Ref. (13).

(d) 2-Isoamylphenol

2-Isoamylanisole was demethylated giving a quantitative yield of 2-iso-amylphenol b.p. 64°C. (0.01 mm.) and n_D^{24}, 1.5120. Anal. calc. for $C_{11}H_{16}O$: C, 80.5; H, 9.82%. Found: C, 80.2, 80.4; H, 9.70, 9.71%. *3,5-Dinitrobenzoate* m.p. 92°C. Anal. calc. for $C_{18}H_{18}N_2O_6$: N, 7.82%. Found: N, 7.75%.

4-Isoamylphenol

(a) 3-Methyl-1-(p-methoxyphenyl)-1-butanol

By means of a Grignard reaction from isobutyl bromide and anisaldehyde there was obtained 3-methyl-1-(*p*-methoxyphenyl)-1-butanol in crude form as an oil (60 gm., 68%). Attempted distillation caused obvious dehydration. It was not possible to obtain a phenylurethane.

(b) 3-Methyl-1-(p-methoxyphenyl)-1-butene

The above carbinol was dehydrated giving *3-methyl-1-(p-methoxyphenyl)-1-butene*, in high yield, boiling at 91°C. (1 mm.) and having n_D^{27}, 1.5390. Anal. calc. for $C_{12}H_{16}O$: OCH_3, 17.60%. Found: OCH_3, 17.43, 17.43%. The *nitrosyl chloride* was obtained in good yield, m.p. 153°C. Anal. calc. for $C_{12}H_{16}ClNO_2$: N, 5.79; OCH_3, 12.80%. Found: N, 5.74; OCH_3, 12.16, 12.08%.

(c) 4-Isoamylanisole

3-Methyl-1-(*p*-methoxyphenyl)-1-butene (75 gm.) was hydrogenated in the usual way and gave 4-isoamylanisole (58 gm., 78%) boiling at 78°C. (1 mm.) and having n_D^{27}, 1.4940. The literature (1) gives b.p. 121°C. (14 mm.) and n_D^{22}, 1.4995 (19). Anal. calc. for $C_{12}H_{18}O$: OCH_3, 17.40%. Found: OCH_3, 17.50, 17.50%. The *sulphonamide* was obtained in good yield and melted at 103°C. Anal. calc. for $C_{12}H_{19}NO_3S$: N, 5.45; OCH_3, 12.06%. Found: N, 5.51; OCH_3, 12.09, 12.05%.

(d) 4-Isoamylphenol

4-Isoamylanisole (34 gm.) was demethylated as described above and yielded 4-isoamylphenol (29 gm., 94%) as an oil boiling at 68°C. (0.01 mm.) and having n_D^{25}, 1.5060. The literature (14) gives b.p. 245–250°C. (760 mm.) and n_D^{27}, 1.505. Anal. calc. for $C_{11}H_{16}O$: C, 80.5; H, 9.82%. Found: C, 80.3, 80.3; H, 9.80, 9.59%. The *3,5-dinitro-benzoate* melted at 124°C. Anal. calc. for $C_{18}H_{18}N_2O_6$: N, 7.82%. Found: N, 7.80%.

Nitration of the Phenols

The four phenols described above were then nitrated in the usual manner and the dinitrophenols thus formed were characterized as their piperidine, morpholine, and cyclohexylamine salts as described in an earlier communication (7). The relevant data are summarized in Table I.

REFERENCES

1. BARANGER, P. M. Bull. soc. chim. France, 49: 1213. 1931.
2. BARBER, M. and HASLEWOOD, G. A. D. Biochem. J. 39: 285. 1945.
3. BARTZ, Q. R., MILLER, R. F., and ADAMS, R. J. Am. Chem. Soc. 57: 371. 1935.
4. BRAZIDEC, E. LE. Bull. soc. chim. France, 31: 255. 1922.
5. CRAFTS, A. S. Science, 101: 417. 1945.
6. DOHME, A. R. L., COX, E. H., and MILLER, E. J. Am. Chem. Soc. 48: 1688. 1926.
7. DUTTON, G. G. S., BRIGGS, T. I., BROWN, B. R., and HILLMAN, M. E. D. Can. J. Chem. 31: 685. 1953.
8. DUTTON, G. G. S., BRIGGS, T. I., BROWN, B. R., and POWELL, R. K. Can. J. Chem. 31: 837. 1953.
9. HUNTRESS, E. H., and CARTEN, F. H. J. Am. Chem. Soc. 62: 603. 1940.
10. HUSTON, R. C. and KAYE, I. A. J. Am. Chem. Soc. 64: 1576. 1942.
11. KLAGES, A. Ber. 37: 3987. 1904.
12. LEVY, J. and PERNOT, R. Bull. soc. chim. France, 49: 1721. 1931.
13. MILLS, L. E. and FAYERWEATHER, B. L. U.S. Patent No. 2,192,197. 1940.
14. NAZAROVA, Z. M. J. Gen. Chem. (U.S.S.R.), 8: 1336. 1938. *Abstracted in* Chem. Abstracts, 33: 4214[8]. 1939.
15. PREY, V. Ber. 74: 1219. 1941.
16. SUSA, A. Ann. chim. 14: 73. 1940.
17. SUTER, C. M. Chem. Rev. 28: 269. 1941.
18. TIFFENEAU, M. and LEVY, J. Bull. soc. chim. France, 39: 776. 1926.
19. TSUKERVANIK, I. P. and TAMBOVTSEVA, V. D. Bull. univétat Asie centrale, 22: 221. 1938. *Abstracted in* Chem. Abstracts, 34: 4729[2]. 1940.

INTERACTION OF KETO- AND TERTIARY AMINO-FUNCTION IN MEDIUM RINGS[1, 2]

By Edward H. Mottus,[3] Hans Schwarz,[4] and Léo Marion

ABSTRACT

The ultraviolet and infrared absorption spectra of protopine and some of its derivatives have been studied. The interaction between a keto group and a tertiary nitrogen in a 10-membered ring is illustrated by the study of these spectra. On the basis of these studies a quaternary carbinolamine structure (V) is suggested for protopine and cryptopine salts. Some of the reactions of protopine, cryptopine, and vomicine are discussed.

Medium rings containing both tertiary amino- and carbonyl-function have been found to occur in nature in the alkaloids protopine (I), cryptopine[5], and vomicine (II). Perkin (6), in his studies on the structure of protopine and cryptopine, noted that reactions without analogy occurred. Many of the reactions in the chemistry of vomicine could not be explained by Huisgen, Wieland, and Eder (5) on the basis of Robinson's (1) structure without assuming some kind of unusual interaction between the carbonyl and the tertiary amine function.
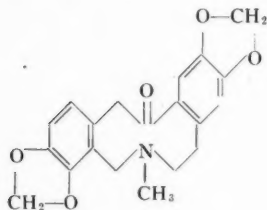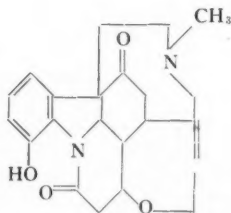
I   II

In order to study the interaction of the carbonyl- with the tertiary amino-function we measured the ultraviolet and infrared spectra of protopine and some of its derivatives. Protopine (I) was chosen since it contained a 10-membered ring which offered possibilities for interaction between the keto-

and the amino-function. Since the keto group is conjugated with an aromatic system, any change in the electronic configuration of the carbonyl should change the ultraviolet absorption. Furthermore, because of the absence of methoxyls in protopine it should be possible to determine the formation of a methoxy group in a derivative without difficulty.

The spectra of I, its perchlorate, and its methiodide were chosen as examples. The ultraviolet absorption of I would be expected to be a composite of the two chromophoric systems present in the molecule. Fig. 1 shows that such is not
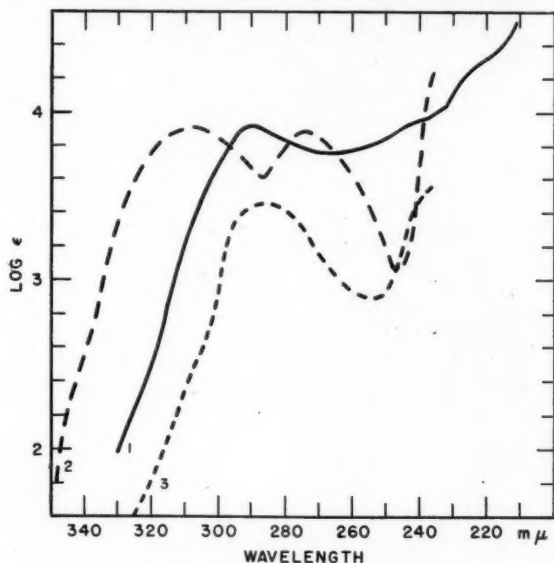
Fig. 1.   Ultraviolet spectra in alcohol, curve 1, protopine; curve 2, α-ketodihydrosafrol (spectrum copied from Ref. (4)); curve 3, dihydrosafrol (spectrum copied from Ref. (4)).

the case. To obtain the protopine curve the absorption due to the α-ketodi-hydrosafrol portion of I should be shifted to shorter wave lengths. This would be the case if in I either the keto group is not in the plane of the benzene ring or there is interaction between the keto- and the amino-function. A study of the Fisher-Taylor-Hirschfelder model of I indicates that it could exist in three forms. One is energetically improbable since the two aromatic nuclei would lie one on top of the other. The second possibility (Fig. 2) shows that the nitrogen and the carbonyl oxygen are very close resulting in a repulsion tending to force the carbonyl out of the plane of the benzene ring. By inverting the nitrogen of the second form, the third form (Fig. 3) is obtained in which the carbonyl is very nearly in the plane of the benzene ring, and there is a facile approach of the nitrogen to the carbonyl carbon. Bond formation between the nitrogen and the carbonyl would then be possible without any further steric change so that an effect similar to that of intramolecular hydrogen bonding (III (a)) might be expected (III (b)).
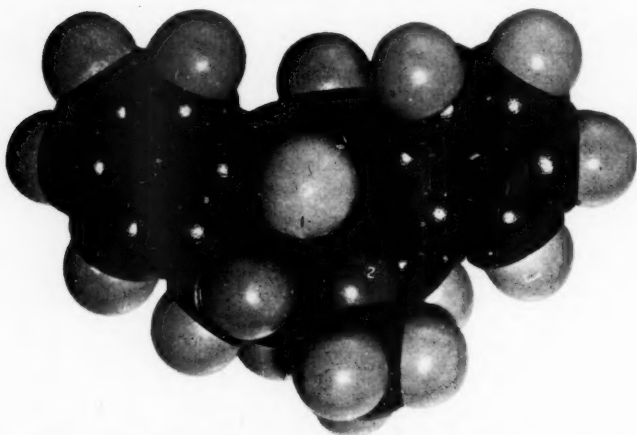
FIG. 2.   Photograph of Fisher-Taylor-Hirschfelder model of form 2 of protopine (shown without methylene-dioxy groups); 1, oxygen atom; 2, nitrogen atom.
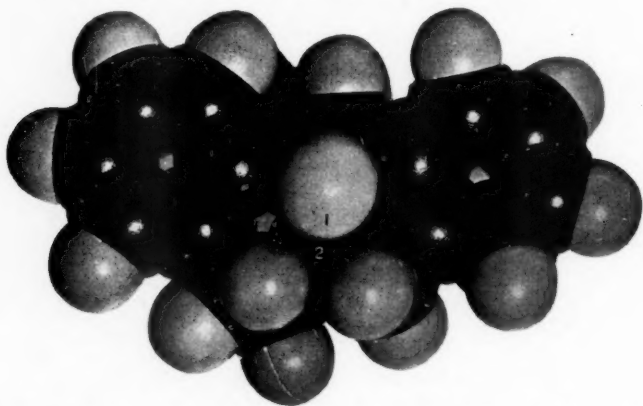
FIG. 3.   Photograph of Fisher-Taylor-Hirschfelder model of form 3 of protopine (shown without methylene-dioxy groups); 1, oxygen atom; 2, nitrogen atom.

Both of the possible forms of protopine would be expected to explain the hypsochromic shift observed in the ultraviolet spectrum. However, the effect on the carbonyl band in the infrared is different which allows us to differen-

$$\underset{}{>}\overset{\delta+}{C} = \overset{\delta-}{O} \ldots \overset{\delta+}{H} - \overset{\delta-}{O} - \qquad\qquad \underset{\underset{\underset{C}{|}}{\overset{..\,\delta-}{N}}}{>}\overset{\delta+}{C} = \overset{\delta-}{O}$$

(a)   (b)

III
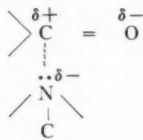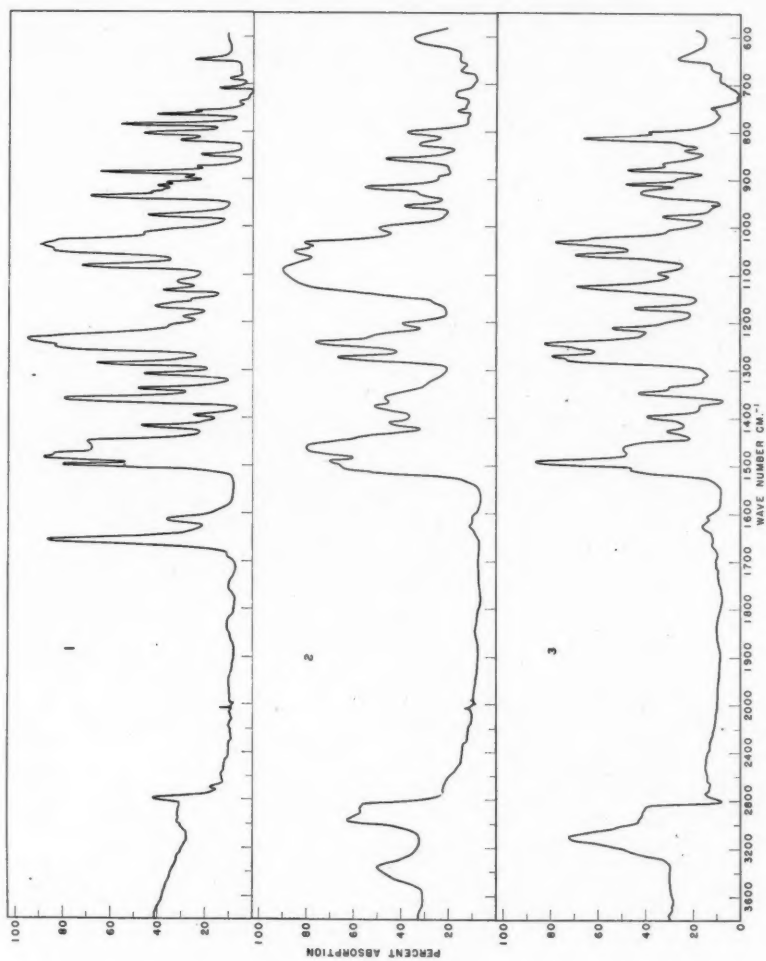
FIG. 4. Infrared spectra in nujol mulls, curve 1, protopine; curve 2, protopine perchlorate; curve 3, protopine methiodide.

tiate between the two forms. Loss of conjugation (form 2) should result in a shift to higher frequency. "Nitrogen bonding"[6] (form 3, III(b)) on the other hand results in absorption at lower wave numbers. Since the carbonyl peak in the infrared spectrum of protopine (1658 cm.$^{-1}$, Fig. 4, curve 1) is lower than that of acetophenone (1690 cm.$^{-1}$) we believe that the third form is favored and we therefore propose IV for protopine[7].
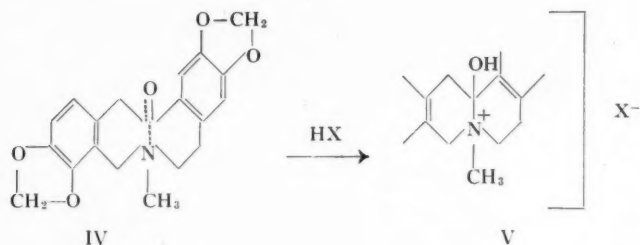
In this form the nitrogen will be quite inert since it is pretty well buried in the molecule. (Protopine does not give a methiodide at 42°; for the preparation of this derivative, heating for 10 hr. at 100° in a sealed tube is necessary (6).)
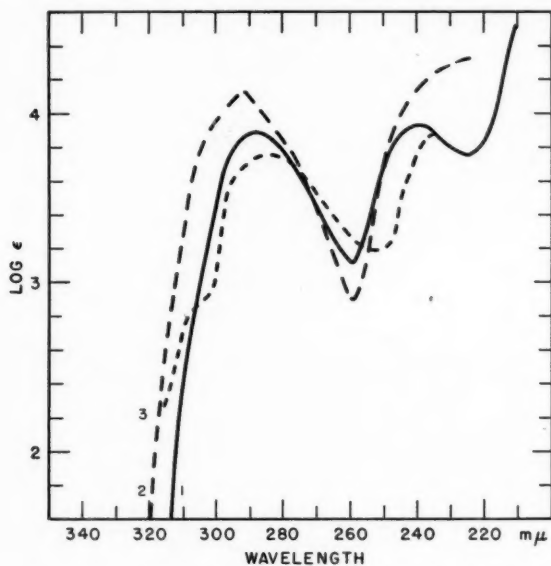
Fig. 5. Ultraviolet spectra in alcohol, curve 1, protopine salt (as hydrochloride); curve 2, diisosafrol (spectrum copied from Ref. (4)); curve 3, two moles of dihydrosafrol (curve calculated from Ref. (4)).

[6] *In analogy to hydrogen bonding we suggest the term "nitrogen bonding" for this similar effect.*

[7] *It is proposed that the structure of vomicine and its salts is modified in the same way.*

A salt of protopine derived from structure IV has structure V, which is in agreement with our findings. The infrared spectrum of protopine perchlorate shows the strong band at 3385 cm.$^{-1}$ indicating the presence of an OH group[8] and no absorption in the carbonyl region (Fig. 4, curve 2). The molecular absorption (E) in the ultraviolet of V is in close agreement with the molecular absorption of diisosafrol (VI) and the sum of the molecular absorptions of two moles of dihydrosafrol (VII) (Fig. 5).

VI   VII
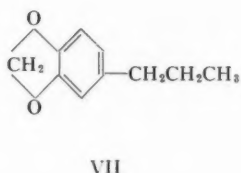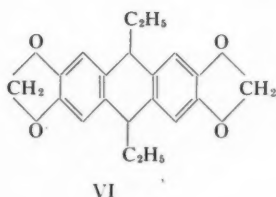
The methiodide derived from IV would be expected to contain a methoxyl and an N-methyl. This agrees very well with the infrared spectrum taken in a nujol mull, which shows neither OH nor carbonyl band (Fig. 4, curve 3).

(a)   (b)   (c)
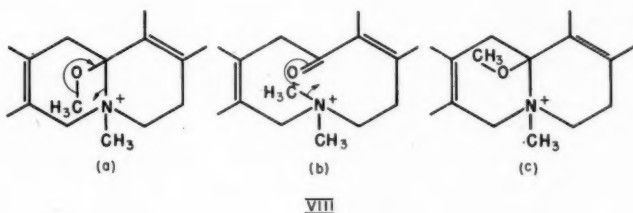
VIII

From the study of the models of I (Figs. 2 and 3) it becomes clear that the methiodide could exist in three different forms, two derived from the model in Fig. 2 (VIIIa, 1 O-CH$_3$; 1 N-CH$_3$ and VIIIb, 2 N-CH$_3$), and one derived from the model in Fig. 3 (VIIIc, 1 O-CH$_3$; 1 N-CH$_3$). In crystalline form either VIIIa or VIIIc or both are present (see above). In solution, however, the equilibrium

$$\overline{VIIIc} \rightleftharpoons \overline{VIIIa} \rightleftharpoons \overline{VIIIb}$$

is more likely.

Of the two equilibria involved, one $\overline{VIIIc} \rightleftharpoons \overline{VIIIa}$ is an inversion of the nitrogen. The other, $\overline{VIIIa} \rightleftharpoons \overline{VIIIb}$ does not involve an actual migration of the methyl group but only a change in the binding electrons as can be deduced from Fig. 2 (and represented by arrows in formula VIII). This is supported by the ultraviolet spectrum of the methiodide which is intermediate between

[8] *The enol form is not considered since, if this enol were the predominant form in acid solution the ultraviolet spectrum of a salt should resemble that of a correspondingly substituted stilbene derivative, and this has not been found to be the case (see spectra in Ref. 7).*
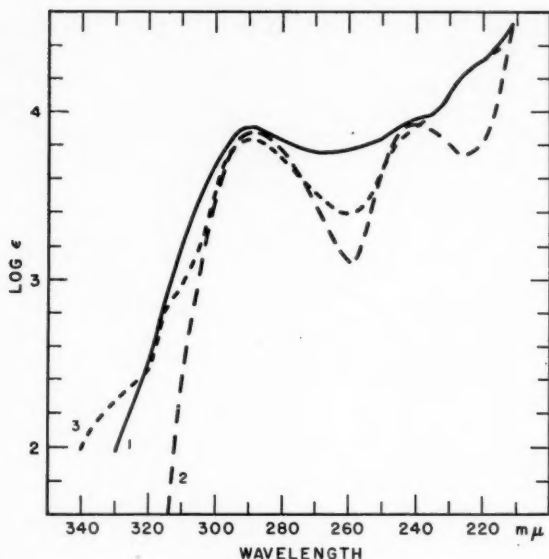
FIG. 6.   Ultraviolet spectra in alcohol, curve 1, protopine; curve 2, protopine salt (as hydrochloride); curve 3, protopine methiodide.

that of protopine and that of its salt. Under the conditions of a Zeisel determination Form VIII(b) only seems to be present (no OCH$_3$; 2 N-CH$_3$). Huisgen et al. (5) came to the same conclusions: methyl vomicinium salts (no OCH$_3$; 2 N-CH$_3$) on reduction with sodium amalgam gave rise to methylvomicine (1 OCH$_3$; 1 N-CH$_3$).

These new observations throw some light on many of the unusual reactions observed with vomicine and cryptopine derivatives. They are in agreement with Huisgen, Wieland, and Eder's (5) explanations for the reactions of vomicine except that whereas these authors call the quaternary form a canonical form (mesomeric grenzform) we consider it as the form present in all salts of vomicine. All reactions in acidic solution are therefore carried out with the quaternary form.

The quaternary form V for protopine and cryptopine in acid media helps to interpret some of the unusual reactions observed by Perkin (6). For example, the formation of isocryptopine and isoprotopine salts is simply a dehydration of V rather than a rearrangement of the enol as proposed by Perkin.
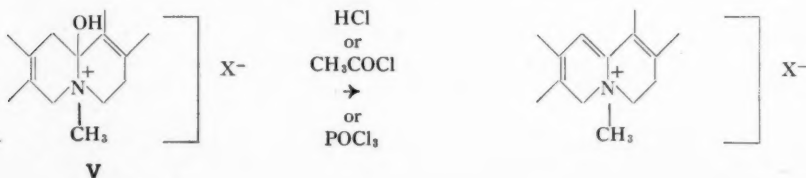
The reaction of protopine and cryptopine in acid solution with sodium amalgam was found by Perkin to give the dihydro-compounds. This is more likely an Emde degradation rather than the reduction of the carbonyl.

EXPERIMENTAL

Spectra

The ultraviolet spectra were determined with a Beckmann Spectrophotometer Model DU. The infrared spectra were all taken in nujol mulls with a Perkin-Elmer double beam infrared Recording Spectrophotometer, Model 21.

Protopine Perchlorate

To protopine, dissolved in dilute acetic acid, was added perchloric acid. The perchlorate, recrystallized from water, melted at 321–322°. Calc. for $C_{20}H_{19}O_5N \cdot HClO_4$: C, 52.93; H, 4.43; N, 3.09. Found: C, 53.00; H, 4.46; N, 3.33%.

Protopine Methiodide

The methiodide was made according to Perkin (6). Calc. for $C_{20}H_{19}O_5N \cdot CH_3I$: N, 2.83; 2 N-$CH_3$, 6.07. Found: N, 3.01; N-CH_3, 6.25; OCH_3, 0.0.

ACKNOWLEDGMENTS

The authors express their gratitude to Dr. H. J. Bernstein of the National Research Laboratories for revealing discussions, and to Mr. R. Lauzon and Dr. R. N. Jones, also of these laboratories, for the determination of the infrared spectra.

REFERENCES

1. BAILEY, A. S. and ROBINSON, R. Nature, 161: 433. 1948.
2. BROWN, H. C., FLETCHER, R. S., and JOHANNESEN, R. B. J. Am. Chem. Soc. 73: 212. 1951.
3. HENRY, T. A. The plant alkaloids. 4th ed. J. and A. Churchill Ltd., London. 1944. p. 294.
4. HILLMER, A. and SCHORNING, P. Z. physik. Chem. A, 168: 81. 1934.
5. HUISGEN, R., WIELAND, H., and EDER, H. Ann. 561: 193. 1948.
6. PERKIN, W. H. JR. J. Chem. Soc. 109: 815. 1916; 115: 713. 1919.
7. WESSELY, F., BAUER, A., CHWALA, CH., PLAICHINGER I., and SCHÖNBECK, R. Monatsh. 79: 596. 1948.

CANADIAN JOURNAL OF CHEMISTRY

Notice to Contributors

GENERAL: Manuscripts should be typewritten, double spaced, and the **original and one extra copy** submitted. Style, arrangement, spelling, and abbreviations should conform to the usage of this Journal. Names of all simple compounds, rather than their formulas, should be used in the text. Greek letters or unusual signs should be written plainly or explained by marginal notes. Superscripts and subscripts must be legible and carefully placed. Manuscripts should be carefully checked before being submitted, to reduce the need for changes after the type has been set. If authors require changes to be made after the type is set, they will be charged for changes that are considered to be excessive. **All pages, whether text, figures, or tables, should be numbered.**

ABSTRACT: **An abstract of not more than about 200 words, indicating the scope of the work and the principal findings, is required.**

ILLUSTRATIONS:

(i) *Line Drawings*: All lines should be of sufficient thickness to reproduce well. Drawings should be carefully made with India ink on white drawing paper, blue tracing linen, or co-ordinate paper **ruled in blue only**; any co-ordinate lines that are to appear in the reproduction should be ruled in black ink. Paper ruled in **green, yellow, or red should not be used** unless it is desired to have all the co-ordinate lines show. Lettering and numerals should be neatly done in India ink preferably with a stencil (**do not use typewriting**) and be of such size that they will be legible and not less than one millimeter in height when reproduced in a cut three inches wide. All experimental points should be carefully drawn with instruments. Illustrations need not be more than two or three times the size of the desired reproduction, but the ratio of height to width should conform with that of the type page. **The original drawings and one set of small but clear photographic copies are to be submitted.**

(ii) *Photographs*: Prints should be made on glossy paper, with strong contrasts; they should be trimmed to remove all extraneous material so that essential features only are shown. Photographs should be submitted **in duplicate**; if they are to be reproduced in groups, one set should be so arranged and mounted on cardboard with rubber cement; the duplicate set should be unmounted.

(iii) *General*: **The author's name, title of paper, and figure number should be written in the lower left hand corner (outside the illustration proper) of the sheets on which the illustrations appear.** Captions should not be written on the illustrations, but typed together at the end of the manuscript. All figures (including each figure of the plates) should be numbered consecutively from 1 up (arabic numerals). **Each figure should be referred to in the text.** If authors desire to alter a cut, they will be charged for the new cut.

TABLES: Each table should be typed on a separate sheet. Titles should be given for all tables, which should be numbered in roman numerals. Column heads should be brief and textual matter in tables confined to a minimum. **Each table should be referred to in the text.**

REFERENCES: **These should be listed alphabetically by authors' names, numbered in that order, and placed at the end of the paper.** The form of literature citation should be that used in this Journal. **Titles of papers should not be given.** The first page only of the references cited should be given. **All citations should be checked with the original articles.** Each citation should be referred to in the text by means of the key number.

REPRINTS: A total of 50 reprints of each paper, without covers, are supplied free to the authors. Additional reprints will be supplied according to a prescribed schedule of charges. On request, covers can be supplied at cost.

Approximate charges for reprints may be calculated from the number of printed pages, obtained by multiplying by 0.6 the number of manuscript pages (double-spaced typewritten sheets, 8½ in. by 11 in.) and making allowance for space occupied by line drawings and half-tones (not inserts). The cost per page is tabulated at the back of the reprint request form sent with the galley.

Contents